



**Ontario Geological Survey  
Open File Report 6091**

**Geological Synthesis  
of the Highway 101 Area,  
East of Matheson, Ontario**

**2002**





ONTARIO GEOLOGICAL SURVEY

Open File Report 6091

Geological Synthesis of the Highway 101 Area, East of Matheson, Ontario

by

B.R. Berger

2002

Parts of this publication may be quoted if credit is given. It is recommended that reference to this publication be made in the following form:

Berger, B.R. 2002. Geological synthesis of the highway 101 area, east of Matheson, Ontario; Ontario Geological Survey, Open File Report 6091, 124p.

© Queen's Printer for Ontario, 2002



© Queen's Printer for Ontario, 2002.

Open File Reports of the Ontario Geological Survey are available for viewing at the Mines Library in Sudbury, at the Mines and Minerals Information Centre in Toronto, and at the regional Mines and Minerals office whose district includes the area covered by the report (see below).

Copies can be purchased at Publication Sales and the office whose district includes the area covered by the report. Although a particular report may not be in stock at locations other than the Publication Sales office in Sudbury, they can generally be obtained within 3 working days. All telephone, fax, mail and e-mail orders should be directed to the Publication Sales office in Sudbury. Use of VISA or MasterCard ensures the fastest possible service. Cheques or money orders should be made payable to the *Minister of Finance*.

Mines and Minerals Information Centre (MMIC) Macdonald Block, Room M2-17 900 Bay St. Toronto, Ontario M7A 1C3	Tel: (416) 314-3800 1-800-665-4480(toll free inside Ontario)
Mines Library 933 Ramsey Lake Road, Level A3 Sudbury, Ontario P3E 6B5	Tel: (705) 670-5615
Publication Sales 933 Ramsey Lake Rd., Level A3 Sudbury, Ontario P3E 6B5	Tel: (705) 670-5691(local) 1-888-415-9845(toll-free) Fax: (705) 670-5770 E-mail: pubsales@ndm.gov.on.ca

#### **Regional Mines and Minerals Offices:**

Kenora - Suite 104, 810 Robertson St., Kenora P9N 4J2  
Kirkland Lake - 10 Government Rd. E., Kirkland Lake P2N 1A8  
Red Lake - Box 324, Ontario Government Building, Red Lake P0V 2M0  
Sault Ste. Marie - 70 Foster Dr., Ste. 200, Sault Ste. Marie P6A 6V8  
Southern Ontario - P.O. Bag Service 43, Old Troy Rd., Tweed K0K 3J0  
Sudbury - Level B3, 933 Ramsey Lake Rd., Sudbury P3E 6B5  
Thunder Bay - Suite B002, 435 James St. S., Thunder Bay P7E 6S7  
Timmins - Ontario Government Complex, P.O. Bag 3060, Hwy. 101 East, South Porcupine P0N 1H0  
Toronto - MMIC, Macdonald Block, Room M2-17, 900 Bay St., Toronto M7A 1C3

This report has not received a technical edit. Discrepancies may occur for which the Ontario Ministry of Northern Development and Mines does not assume any liability. Source references are included in the report and users are urged to verify critical information. Recommendations and statements of opinions expressed are those of the author or authors and are not to be construed as statements of government policy.

If you wish to reproduce any of the text, tables or illustrations in this report, please write for permission to the Team Leader, Publication Services, Ministry of Northern Development and Mines, 933 Ramsey Lake Road, Level B4, Sudbury, Ontario P3E 6B5.

#### **Cette publication est disponible en anglais seulement.**

Parts of this report may be quoted if credit is given. It is recommended that reference be made in the following form:

**Berger, B.R. 2002. Geological synthesis of the highway 101 area, east of Matheson, Ontario; Ontario Geological Survey, Open File Report 6091, 124p.**



# Contents

---

Foreword .....	xv
Abstract .....	xvii
Introduction .....	1
History of Exploration .....	2
Previous Geological Work .....	3
Present Survey .....	3
Acknowledgments .....	5
General Geology .....	6
Introduction .....	6
Precambrian .....	6
Neoarchean .....	6
Kidd–Munro Assemblage .....	6
Ultramafic and Mafic Tholeiitic Metavolcanic Rocks .....	6
Ultramafic Metavolcanic Rocks .....	6
Mafic Metavolcanic Rocks .....	8
Variolitic Mafic Metavolcanic Rocks .....	9
Felsic Metavolcanic Rocks .....	10
Calc-alkalic Metavolcanic Rocks .....	10
Ghost Range Sill .....	12
Geochemistry .....	12
Ultramafic Metavolcanic Rocks .....	12
Mafic Metavolcanic Rocks .....	13
Variolitic Mafic Metavolcanic Rocks .....	16
Calc-alkalic Metavolcanic Rocks .....	17
Ghost Range Sill and Related Intrusions .....	18
Tisdale Assemblage .....	20
Ultramafic and Mafic Metavolcanic Rocks .....	21
Ultramafic Metavolcanic Rocks .....	21
Mafic Metavolcanic Rocks .....	21
Variolitic Mafic Metavolcanic Rocks .....	22
Calc-alkalic Metavolcanic Rocks .....	22
Geochemistry .....	23
Ultramafic and Mafic Metavolcanic Rocks .....	23
Kinojevis Assemblage .....	28
Mafic Metavolcanic Rocks .....	28
Variolitic Mafic Metavolcanic Rocks .....	29
Felsic Metavolcanic Rocks .....	30
Calc-alkalic Metavolcanic Rocks .....	31
Metasedimentary Rocks .....	31
Geochemistry .....	32
Mafic and Variolitic Metavolcanic Rocks .....	33
Felsic Metavolcanic Rocks .....	34
Calc-alkalic Metavolcanic Rocks .....	35





Porcupine Assemblage.....	36
Geochemistry .....	37
Timiskaming Assemblage.....	41
Metasedimentary Rocks .....	41
Alkalic Extrusive and Intrusive Rocks .....	44
Geochemistry .....	51
Metasedimentary Rocks.....	51
Intrusive and Extrusive Alkaline Rocks .....	51
Paleoproterozoic .....	56
Mafic Intrusions .....	56
Mesoproterozoic .....	56
Keweenawan Age.....	56
Mafic Intrusions.....	56
Phanerozoic.....	57
Mesozoic .....	57
Jurassic.....	57
Kimberlite Intrusions.....	57
Cenozoic.....	57
Quaternary .....	57
Pleistocene and Holocene.....	57
Structure and Metamorphism .....	58
Structure.....	58
Kidd–Munro Assemblage.....	58
Tisdale Assemblage.....	60
Kinojevis Assemblage.....	61
Porcupine Assemblage .....	61
Timiskaming Assemblage .....	62
Faults .....	63
Porcupine–Destor Deformation Zone .....	63
Arrow Fault.....	65
“Contact Fault” .....	65
Munro Fault .....	65
Ghostmount Fault .....	66
Cross Faults .....	66
Hislop Fault.....	66
Ross Fault.....	67
Garrison Fault.....	67
Folds.....	68
Metamorphism .....	68
Economic Geology .....	70
Gold .....	70
Nighthawk–Matheson Segment.....	70
Hislop–Michaud Segment .....	73
Ross Mine .....	74
St Andrew Goldfields Limited Hislop Mine (New Kelore Mine).....	74
Royal Oak Open Pit .....	76
Pangea Goldfields Incorporated Deposit .....	76



Pentland Firth Ventures Limited Ludgate Lake Deposit .....	77
Moneta Porcupine Mines Incorporated Property .....	78
Buffonta Mine and New Buffonta Gold Deposit Open Pit .....	80
Jonpol Explorations Limited Garrcon Deposit .....	81
Jonpol Explorations Limited Jonpol Deposit .....	81
Harker–Holloway Segment .....	81
Holloway Mine .....	82
Holt–McDermott Mine .....	84
Iris Deposit .....	85
Canamax Resources Incorporated “East Zone” Deposit .....	87
Base Metals .....	87
Platinum Group Elements .....	88
Recommendations For Mineral Exploration .....	89
References .....	91
Appendix 1: Geochemistry for the Kidd–Munro Assemblage in the Highway 101 Area .....	101
Appendix 2: Geochemistry for the Tisdale Assemblage in the Highway 101 Area .....	107
Appendix 3: Geochemistry for the Kinojevis Assemblage in the Highway 101 Area .....	110
Appendix 4: Geochemistry for Metasedimentary Rocks in the Highway 101 Area .....	114
Appendix 5: Geochemistry for Alkalic Intrusive and Extrusive Rocks in the Highway 101 Area .....	118
Metric Conversion Table .....	124

## FIGURES

1. General location map of the Highway 101 area .....	1
2. Distribution of southern Abitibi greenstone belt assemblages in Ontario .....	4
3. Jensen cation plot for the Kidd–Munro assemblage .....	13
4. a) Chondrite-normalized rare earth element (REE) patterns, and b) primitive-mantle normalized extended element patterns for Kidd–Munro assemblage komatiites .....	14
5. a) Chondrite-normalized REE patterns, and b) primitive-mantle normalized extended element patterns for Kidd–Munro assemblage mafic tholeiitic metavolcanic rocks .....	15
6. a) Chondrite-normalized REE patterns, and b) primitive-mantle normalized extended element patterns for Kidd–Munro assemblage variolitic rocks .....	16
7. a) Chondrite-normalized REE patterns, and b) primitive-mantle normalized extended element patterns for Kidd–Munro assemblage felsic metavolcanic rocks .....	18
8. a) Chondrite-normalized REE patterns, and b) primitive-mantle normalized extended element patterns for Kidd–Munro assemblage calc-alkalic metavolcanic rocks .....	19
9. Chondrite-normalized REE patterns and primitive-mantle normalized extended element patterns for Ghost Range and gabbroic intrusions in the Kidd–Munro assemblage .....	20
10. Jensen cation plot, Tisdale assemblage in the Highway 101 area .....	24
11. a) Chondrite-normalized REE patterns, and b) primitive-mantle normalized extended element patterns for Tisdale assemblage komatiitic rocks .....	25



12. a) Chondrite-normalized REE patterns, and b) primitive-mantle normalized extended element patterns for Tisdale assemblage tholeiitic mafic metavolcanic rocks .....	26
13. Chondrite-normalized REE patterns, and primitive-mantle normalized extended element patterns for Tisdale assemblage calc-alkalic and felsic metavolcanic rocks. ....	27
14. Jensen cation plot for the Kinojevis assemblage.....	32
15. Chondrite-normalized REE patterns and primitive-mantle normalized extended element patterns for Kinojevis assemblage mafic and variolitic metavolcanic rocks.....	33
16. a) Chondrite-normalized REE patterns, and b) primitive-mantle normalized extended element patterns for Kinojevis assemblage felsic metavolcanic rocks .....	34
17. a) Chondrite-normalized REE patterns, and b) primitive-mantle normalized extended element patterns for Kinojevis assemblage calc-alkalic metavolcanic rocks.....	35
18. Chondrite-normalized REE patterns and primitive-mantle normalized extended element patterns for clastic metasedimentary rocks.....	37
19. Alkalis versus SiO <sub>2</sub> discrimination diagrams for alkalic rocks .....	52
20. a) Chondrite-normalized REE patterns, and b) primitive-mantle normalized extended element patterns for selected alkalic plutonic rocks .....	53
21. Discrimination diagrams for alkalic metavolcanic rocks .....	54
22. a) Chondrite-normalized REE patterns, and b) primitive-mantle normalized extended element patterns for selected alkalic metavolcanic rocks .....	55
23. Inferred movement on segments in the Highway 101 area. ....	72
24. a) Chondrite-normalized REE patterns, and b) primitive-mantle normalized extended element patterns for gold-bearing syenite.....	75
25. Simplified cross-section looking west through the Lightning zone .....	83
26. Schematic cross-section of the Holt–McDermott deposit.....	84

## PHOTOS

1. Concentrically zoned core of variole surrounded by radial microlite growth in variolitic flow from Lot 10, Concession I, Munro Township. ....	9
2. Calc-alkalic, intermediate tuff breccia, part of the Kidd–Munro assemblage from northern Holloway Township .....	11
3. Massive and flow laminated variolitic flows from central Harker Township.....	29
4. Contact between flow banded rhyolite and massive, amygdaloidal rhyolite west of the Iris deposit .....	30
5. White albitite clast in Timiskaming assemblage conglomerate from diamond-drill core in Lot 6, Concession I, Guibord Township .....	42
6. Photomicrograph of Timiskaming assemblage sandstone showing detrital microcline, Highway 101 area. ....	43
7. Photomicrograph of octagonal cross-section of pseudo-leucite phenocryst from intermediate alkalic flow, Pangea deposit, Guibord Township. ....	45
8. Alkalic diatreme breccia with white potassium feldspar replacing leucite, mafic and ultramafic xenoliths from the Pangea property, Guibord Township. ....	77
9. Unconformity between iron formation and conglomerate at the southwest gold zone in Michaud Township. ....	79



## **TABLES**

1. Summary of southern Abitibi greenstone belt supracrustal assemblage names, ages, basal contacts, rock types and chemical affinities.....	5
2. Lithological units for the Highway 101 area.....	7
3. List of gold mines, past-producing mines, prospects and major occurrences in the Highway 101 area. ....	71
4. Gold, platinum and palladium for selected samples in the Highway 101 area. ....	86

## **GEOLOGICAL MAP**

Map 2676	Precambrian geology of the Highway 101 area, east of Matheson, Ontario.....	back pocket
----------	---	-------------





# Foreword

This reports presents a synthesis of 3 years of geological mapping in the Highway 101 area, east of Matheson. The project was initiated to improve the geological database, to provide a regional framework for mineralization, and, thereby, to provide an impetus for mineral exploration. The mapping was complemented by geological studies that resulted in a PhD, 2 MSc and 2 BSc theses from 3 Canadian universities. Some of the more important results from this study include: the delineation and characterization of 5 lithotectonic assemblages; the delineation and description of the major structures; the description of the major styles of gold mineralization and alteration; and the recognition, delineation and description of multiphase alkalic intrusions.

The Holt–McDermott and Holloway mines currently produce gold in the area. Several past-producing gold mines, including the Ross Mine, and many gold occurrences also occur. There is excellent potential for additional gold discoveries in the study area. As well, the potential for platinum group elements mineralization occurs in layered ultramafic to mafic intrusions, such as the Ghost Range sill, and the ultramafic to mafic phases of the alkalic intrusions. A number of Jurassic kimberlite intrusions along the Porcupine–Destor deformation zone are potential hosts for diamonds.



# Abstract

The Highway 101 area east of Matheson, commonly referred to as the Golden Highway, is bounded by latitudes 48°27' to 48°36' N and by longitudes 79°29' to 80°26' W. All of Harker, Holloway, Garrison, Michaud, Guibord and Hislop townships and parts of Marriott, Stoughton, Frecheville, Lamplugh, Rand, McCool, Munro, and Beatty townships were mapped during a three-year period from 1997 to 1999, inclusive. Traditional pace and compass traverses, compilation, examination of diamond-drill core and extensive use of geophysical data were used to complete the geological maps. The study also supported the completion of a PhD thesis at the Holloway and Holt–McDermott gold mines, a MSc thesis at the Holloway Mine, a MSc thesis on alkalic magmatism, and 2 BSc theses at the Holt–McDermott Mine.

The study area is underlain by Neoproterozoic supracrustal and intrusive rocks that are subdivided into 5 lithotectonic assemblages. The Kidd–Munro assemblage underlies the north part of the study area and is composed of a tholeiitic metavolcanic rock member and a calc-alkalic metavolcanic rock member. Ultramafic to mafic layered sills intruded the metavolcanic rocks. The Tisdale assemblage is composed of tholeiitic metavolcanic rocks and subordinate amounts of calc-alkalic metavolcanic rocks. The distribution of the assemblage is poorly constrained because the Porcupine–Destor deformation zone and related splay faults transect and assemblage in several places. The Kinojevis assemblage underlies the south part of the study area and is composed of predominantly mafic tholeiitic metavolcanic rocks that are intercalated with thin units of tholeiitic rhyolite and calc-alkalic metavolcanic rocks. The Porcupine assemblage underlies the northwest part of the study area and is composed of wacke, argillite and rare conglomerate that is intruded by small alkalic intrusions. The Timiskaming assemblage is composed of clastic and chemical metasedimentary rocks and rare alkalic metavolcanic rocks that are distributed within and near to the Porcupine–Destor deformation zone. Ultramafic to felsic alkalic intrusive rocks are also correlated with the Timiskaming assemblage and occur as dikes, small single-phase intrusions and large multi-phase intrusions throughout the area. The Neoproterozoic rocks are intruded by Paleoproterozoic quartz diabase dikes, Keweenaw-age olivine diabase dikes and Jurassic kimberlite dikes and diatremes.

The Porcupine–Destor deformation zone is a crustal-scale structure that transects the study area and is characterized by late south-side-up vertical movement. The fault zone and related northeast-striking splay faults, such as the Ghostmount fault and the McKenna fault, are the loci for gold mineralization. Northeast-striking faults with dominant vertical displacement transect the Porcupine–Destor deformation zone. Two of these faults, the Hislop fault and Garrison fault, are major structural features that act as boundaries to different metallogenic segments. Gold mineralization occurs in different structural settings, different styles and different types of alteration patterns in each segment.

Gold is extracted from the Holt–McDermott and Holloway mines in Holloway Township. Several past-producing gold mines are located in Hislop and Garrison townships. Many gold prospects and occurrences are located throughout the study area and there is excellent potential for future discoveries. There is potential for platinum group elements mineralization in the ultramafic to mafic layered intrusions and the ultramafic to mafic phases of the alkalic intrusions. Diamonds occur in some of the kimberlite intrusions.



# **Geological Synthesis of the Highway 101 Area, East of Matheson, Ontario**

**B.R. Berger<sup>1</sup>  
Ontario Geological Survey  
Open File Report 6091  
2002**

---

<sup>1</sup>Geoscientist, Precambrian Geoscience Section, Ontario Geological Survey  
Ministry of Northern Development and Mines, Sudbury, Ontario, Canada P3E 6B5



# Introduction

The Highway 101 area, east of Matheson, is commonly referred to as the Golden Highway because of the prolific gold deposits and occurrences throughout the area. It is bounded by latitudes 48°27' to 48°36'N and by longitudes 79°29' to 80°26' W and covers all of Harker, Holloway, Garrison, Michaud, Guibord and Hislop townships and parts of Marriott, Stoughton, Frecheville, Lamplugh, Rand, McCool, Munro, and Beatty townships (Figure 1). Paved highways 11, 101, 572 and 672 provide access from Timmins, Holtyre and Kirkland Lake. Numerous secondary roads and logging trails provide good access throughout the area except in the southern most parts of Michaud, Guibord and Marriott townships.

This report details the results of investigations during 3 summers, from 1997 to 1999, designed to update the geological database and to provide a better understanding of the rock types, structure and mineralization. Localized areas of abundant outcrop and large areas covered by extensive and thick overburden characterize this part of the Abitibi greenstone belt. The field work was designed to build on previous mapping by providing new data in the overburden-covered areas and to examine outcrop in critical places. This report makes use of data collected at the Holloway and Holt–McDermott gold mines as part of MSc and PhD theses carried out in partnership with the University of Ottawa, Battle Mountain Canada Incorporated and Barrick Gold Corporation. A second MSc thesis undertaken at the University of Ottawa studied alkaline magmatism in the area.

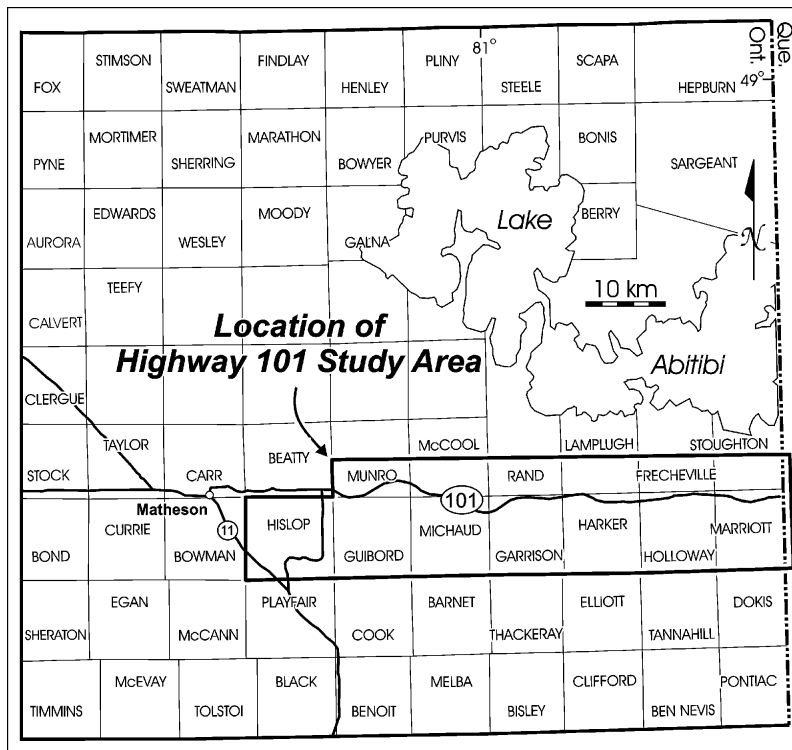


Figure 1. General location map of the Highway 101 area.

## HISTORY OF EXPLORATION

This section provides only a brief description of the long history of exploration and discovery throughout the Highway 101 area. Knight et al. (1919) reported that prospectors were active throughout the area in 1907–08 and that their activity resulted in discovery of the Croesus gold deposit in 1914. At about the same time, exploration resulted in discovery of gold at the Cochenour–Willans showing in southern Holloway Township. Subsequently, prospecting in the northern part of the township resulted in discovery of the Seager’s hill gold prospect in 1922. This discovery was developed in 1934–35 into the Teddy Bear Valley Mine, which had limited underground development (Satterly 1953b). Several other gold discoveries were made along the Mattawasaga River in Holloway and Harker townships in the 1930s; the most significant was the McDermott showing that was later developed into the Holt–McDermott Mine by Barrick Gold Corporation.

Several gold discoveries were made in Hislop, Garrison, Michaud and Guibord townships in the 1930s and 1940s. Gold was discovered in southeastern Hislop Township in 1933 and was developed into the Ross Mine, which produced greater than 1 million ounces gold and 1.6 million ounces silver before closing in 1990 (Bath 1990). Underground development and limited extraction were carried out at the Buffonta, Garrcon and Talisman prospects (Bath 1990; Satterly 1949b; Prest 1953). Extensive diamond drilling by Marchaud Mines Limited delineated a small deposit at Ludgate Lake. Gold was also discovered on the Miller claims southeast of Ludgate Lake. Several other occurrences were reported at the Brydges, Linton and Newfield properties in Garrison Township (Satterly 1949b) and the Caman and Gui–Por mines properties in Guibord Township (Prest 1953).

Increased gold prices in the 1980s spurred renewed exploration throughout the map area. Commercial gold production began at the Holt–McDermott Mine in 1988 (Bath 1990). Noranda Exploration Company Limited discovered the Lightning deposit in the same year. The Lightning deposit was developed into the Holloway Mine, which was opened officially in 1997 by Battle Mountain Canada Limited and Teddy Bear Valley Mines Limited, with reported reserves of 5.27 million tons at a grade of 6.69 grams gold per ton (*Canadian Mines Handbook, 1997–1998*). Falconbridge Gold Limited and, most recently, Pentland Firth Ventures Limited continued exploration at the Ludgate Lake deposit, in Michaud Township.

Moneta Porcupine Mines Incorporated, through various joint ventures, discovered and explored several gold prospects in southern and southeastern Michaud Township. The most important is the “Southwest” zone where a resource of 460 000 ounces gold is defined by diamond drill holes (Moneta Porcupine Mines Inc., Annual Report, 1997). Other significant gold discoveries in this area include the “Last Chance” zone and the “Twin Creek” zone.

Cominco Limited discovered gold mineralization on optioned ground in Guibord Township, referred to as the Fenn–Gibb property, in the 1970s. Subsequent exploration by Pangea Goldfields Incorporated outlined several low-grade deposits. St Andrew Goldfields Limited acquired an option on the property in 1998 with the intention of developing an open pit and underground operation on an indicated resource of 730 000 ounces of gold (St Andrew Goldfields Limited, Annual Report, 1997).

Perrex Resources Incorporated delineated gold and tungsten mineralization at the Iris deposit in south Harker Township through extensive surface and underground exploration in the 1980s. A resource of 160 000 ounces of gold at the Jonpol deposit, in central Garrison Township, had limited underground exploitation. Homestake Canada Incorporated encountered several gold occurrences along the Porcupine–Destor deformation zone (PDDZ) in southern Guibord Township. Several companies reported gold assays greater than 1 g/t gold from exploration programs throughout the Highway 101 area.



Canadian Johns–Manville Company Limited exploited asbestos in Munro Township from 1950 to 1964 (Bath 1990). This development triggered exploration throughout the map area and resulted in discovery of additional asbestos mineralization in Garrison and Harker townships.

Copper and zinc mineralization discovered in northern Munro Township in 1926 was explored by Potterdoal Mines Limited (Satterly 1952a). The Potter copper-zinc mineralization to the south was discovered in 1952 and was developed into the Potter Mine in 1967 (Bath 1990). Mining between 1967 and 1970 produced copper with minor gold and silver. Recent work by Millstream Mines Limited extended the mineralization to the west and down plunge (Millstream Mines Limited, News Release, April 16, 1998). Exploration for base metals in the rest of the map area is limited.

## **PREVIOUS GEOLOGICAL WORK**

The area was first investigated by Knight et al. (1919). More detailed geological maps were produced by Satterly (1947, 1949a, 1951a, 1951b, 1951c, 1953a), Satterly and Armstrong (1947), Prest (1951, 1955). Jensen (1978, 1982a–d, 1985a, 1985b) produced semi-detailed and compilation maps for parts of the area. Troop (1990a, 1990b) produced maps for Hislop, Guibord, Michaud and Garrison townships. Beatty and Munro townships were re-mapped by Johnstone (1991).

Ontario Geological Survey airborne electromagnetic and total intensity magnetic surveys cover the entire map area (OGS 1984a–n). Sonic drilling programs covering the Matheson area were carried out from 1984 to 1987 (Jensen and Trowell 1985; Jensen and Baker 1986; Johnstone and Steele 1989). Data Series maps and Geological Data Inventory Folios (GDIF) were produced for many of the townships in the area.

Precise U/Pb geochronology has been used to provide a general framework for the evolution of the Ontario portion of the Abitibi greenstone belt (Corfu et al. 1989; Corfu 1993; Ayer and Trowell 2001) (Figure 2; Table 1). Ayer, Trowell, Amelin and Corfu (1999) have revised the interpretation with new data and compilation. Additional geochronology is included in this report and integrated with regional work.

Geology maps are filed for assessment work credits by numerous individuals and companies over parts of the map area. These maps were consulted and verified, and relevant information is included on the synoptic map (Map 2676, back pocket). Numerous scientific investigations cover many parts of the area with most of these investigations in Beatty and Munro townships where komatiites are well exposed. Johnstone (1991) provides an excellent summary of research in these 2 townships. Some of the other studies that deal with specific parts of the map area and referred to in this report include Feng and Kerrich (1990), Fowler, Jensen and Peloquin (1987), McNeil and Kerrich (1986) and Robert (1997).

## **PRESENT SURVEY**

The Highway 101 area was mapped at 1:50 000 and 1:20 000 scales during the 1997, 1998 and 1999 field seasons. Previous detailed mapping accurately recorded the location and character of the major rock types. The author visited several outcrops only to verify previous mapping, collect geochemical samples and structural data. In all, 263 outcrops were visited by the author. Large portions of the Highway 101 area are covered with overburden and the present survey concentrated on collecting diamond- and sonic-drill core data and geophysical data from these areas. Diamond-drill hole data were examined and sampled from core stored at the Kirkland Lake Resident Geologist's Office Drill Core Library and from core provided by exploration companies active throughout the map area. Data from 414 diamond-drill logs and 43 sonic-drill holes were examined and compiled for this project. Airborne electromagnetic,

total field magnetic and vertical derivative maps were used to infer geological contacts. The applicability of using Radarsat data for geoscientific problems was tested in the east end of the map area (Madon et al. 1999).

B. Luinstra and J. Ropchan mapped the southern part of Holloway Township at 1:20 000 scale in August 1998. An additional 37 outcrop areas were examined and their results are reported on Map 2563 (Berger, Luinstra and Ropchan 2000).

This project was carried out in co-operation with PhD and MSc candidates from the University of Ottawa. Data from these theses are incorporated and synthesized in this report. B. Luinstra carried out detailed structural studies at the Holloway and Holt–McDermott mines as part of a PhD research project. Preliminary results were reported in OGS Open File Report 6045 (Luinstra and Benn 2001). J.C. Ropchan (2000) studied the geochemistry of the alteration system at the Holloway Mine as part of a MSc research project; and L. Pigeon examined various aspects of alkaline magmatism in Harker, Garrison, Michaud and Guibord townships.

The data, once collected, were stored digitally using CAD and Fieldlog software. The data were superimposed on the Ontario Base Maps, which were modified by the author for this part of the province.

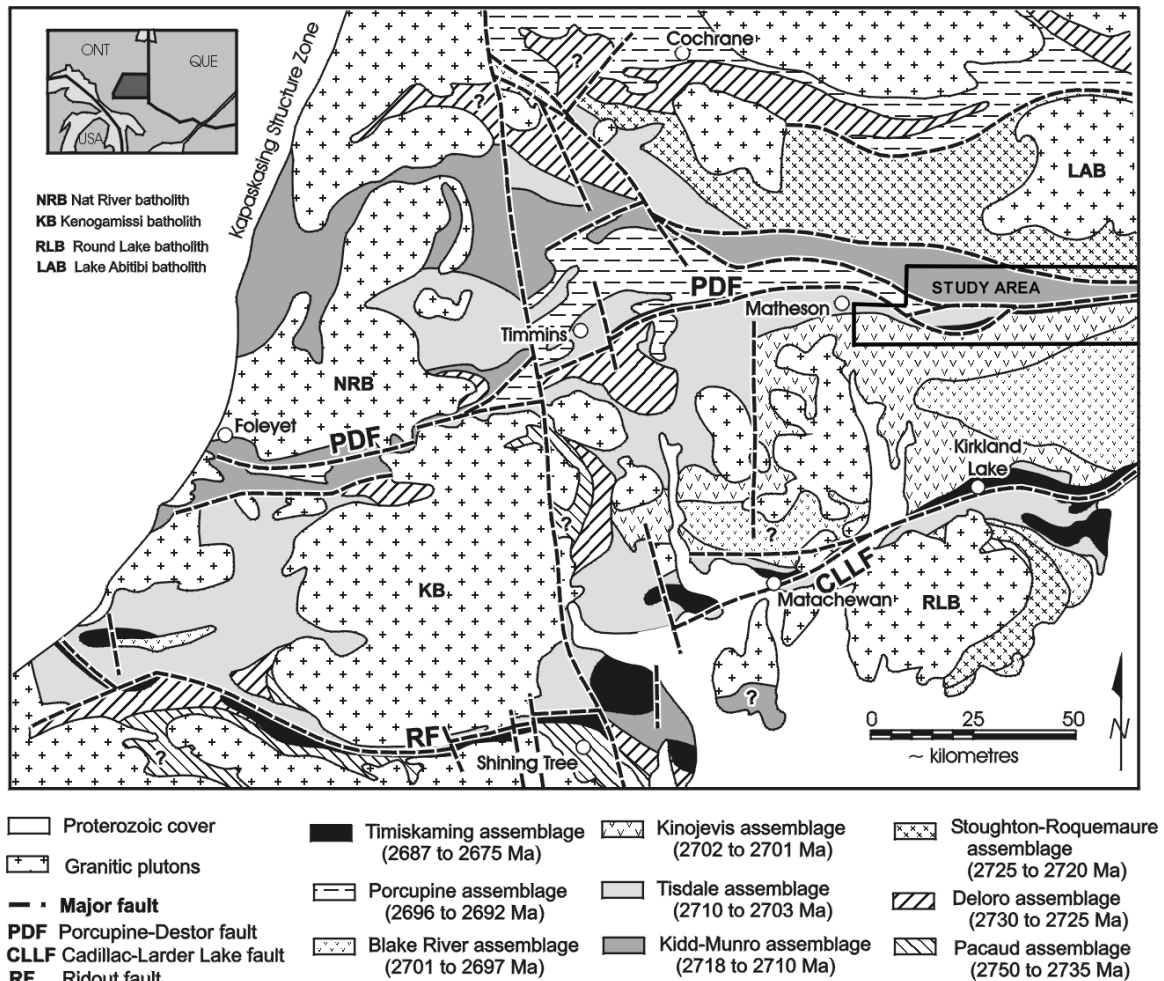


**Figure 2.** Distribution of southern Abitibi greenstone belt assemblages in Ontario (see Table 1 for details) (modified from Ayer and Trowell 2001). Inset box labelled “study area” represents the area shown in Figure 1.

**Table 1.** Summary of southern Abitibi greenstone belt supracrustal assemblage names, ages, basal contacts, rock types and chemical affinities (*from Ayer and Trowell 2001*).

<b>Assemblage Name (Age in Ma)</b>	<b>Includes all or parts of assemblages from Jackson and Fyon (1991)</b>	<b>Basal Contact Relationships</b>	<b>Dominant Rock Types</b>	<b>Volcanic Chemical Affinity</b>
Timiskaming (2687 to 2675)	Garrison, Hearst, Midlothian, Natal, Ridout, Timiskaming, Three Nations	Unconformable	Conglomerate, sandstone, mafic to intermediate volcanic	Alkalic to calc-alkalic
Porcupine (2696 to 2690)	Hoyle, Porcupine, Scapa, Whitney	Unconformable	Turbidite, minor conglomerate and iron formation	None observed
Blake River (2701 to 2697)	Blake River, Halcrow–Swayze, Krist, Skead, Watabeag	Conformable to disconformable	Mafic to felsic volcanic	Tholeiitic and calc-alkalic
Kinojevis (2702 to 2701)	Geike, Kinojevis (North and South), Watabeag	Conformable	Mafic and minor felsic volcanic	Tholeiitic
Tisdale (2710 to 2703)	Boston, Bowman, Cabot–Kevin, Duff–Rand, Eldorado, Kamiskotia, Garnet–Tooms, Geike, Halcrow–Swayze, Halliday, Horwood, Larder Lake, McElroy, Shining Tree, Tisdale, Watabeag	Conformable to disconformable	Ultramafic, mafic, intermediate to felsic volcanic and iron formation	Komatiitic, tholeiitic and calc-alkalic
Kidd–Munro (2719 to 2711)	Cabot–Kevin, Carscallen, Duff–Rand, Hong Kong, Kamiskotia, Kidd–Munro, Shining Tree	Conformable to disconformable	Ultramafic, mafic, intermediate and felsic volcanic and iron formation	Komatiitic, tholeiitic and calc-alkalic
Stoughton–Roquemaure (2723 to 2720)	Catherine–Pacaud, Kinojevis North, Stoughton–Roquemaure	Conformable to disconformable	Ultramafic, mafic, intermediate and felsic volcanic	Komatiitic, tholeiitic and calc-alkalic
Deloro (2730 to 2724)	Adair, Bartlett, Cabot–Kevin, Carscallen, Deloro, Eldorado, Hanrahan, Hong Kong, Marion, Stoughton–Roquemaure, Shining Tree	Disconformable	Mafic, intermediate and felsic volcanic and iron formation	Tholeiitic and calc-alkalic
Pacaud (2750 to 2735)	Catherine–Pacaud, Hong Kong, Peterlong, Marion, Shining Tree, Sinclair	Unknown—removed by batholith intrusions	Ultramafic, mafic and felsic volcanic	Komatiitic, tholeiitic and calc-alkalic

## ACKNOWLEDGMENTS

R. Jones, S. Natress and L. Pigeon provided capable assistance. B. Luinstra and J. Ropchan, in their capacities as senior assistants, provided valuable assistance and data to the maps and report. The author acknowledges the contributions made to this report from data obtained from BSc, MSc and PhD theses of the above named people. Discussions with Dr. A. Fowler, Dr. K. Benn, Dr. A. Lalonde and Dr. B. Luinstra from the University of Ottawa greatly aided in synthesis of this report.

A project of this type is heavily dependent upon the co-operation of property owners and exploration and/or mining companies. The following companies and individuals provided access to data from patented land or access to diamond drill core: H.E. Neal, A. Perron, Battle Mountain Gold Company, Franco–Nevada Mining Corporation Limited, Gwen Resources Limited, Jonpol Explorations Limited, Moneta Porcupine Mines Incorporated, Pangea Goldfields Incorporated, Tandem Resources Limited and Pentland Firth Ventures Limited. St Andrew Goldfields Limited, Glimmer Resources Incorporated, Exall Resources Limited and Barrick Gold Corporation provided access to their properties.

Unless otherwise noted, all data for geochemical analyses presented in this report were provided by the Geoscience Laboratories, Ontario Geoservices Centre, Sudbury, Ontario.

# General Geology

## INTRODUCTION

Neoproterozoic supracrustal rocks, which are intruded by Paleoproterozoic and Keweenawan-age diabase and Mesozoic kimberlite dikes and pipes, underlie the Highway 101 area. The supracrustal rocks are composed of ultramafic, mafic, intermediate and felsic metavolcanic rocks, related intrusive rocks, clastic and chemical metasedimentary rocks, and a suite of ultramafic to felsic alkalic plutonic and metavolcanic rocks. These rocks are divisible into 5 distinct packages based on morphology, petrography, geochemistry and geochronology. These packages or assemblages (cf. Thurston 1991) in the Highway 101 area are correlated with regional assemblages proposed by Jackson and Fyon (1991) and modified by Ayer, Trowell, Amelin and Corfu (1999) (*see* Figure 2; *see* Table 1). The 5 assemblages, from oldest to youngest, are the Kidd–Munro, Tisdale, Kinojevis, Porcupine and Timiskaming assemblages. The first 3 are predominantly composed of metavolcanic rocks; the latter 2 are predominantly composed of metasedimentary rocks, however, alkalic metavolcanic rocks and related intrusions occur within the Timiskaming assemblage. This report will describe only the main characteristics of each assemblage. Table 2 presents the major rock types for the map area.

## PRECAMBRIAN

### Neoproterozoic

#### KIDD–MUNRO ASSEMBLAGE

The Kidd–Munro assemblage underlies the northern part of the map area. Jackson and Fyon (1991) defined the assemblage as a package of ultramafic and mafic tholeiitic metavolcanic rocks with minor high-silica rhyolite that extended eastward from the Kidd Creek area to the point where it was terminated against the Porcupine–Destor fault in Harker Township. These rocks are 2717 to 2711 million years old (Corfu 1993; Bleeker and Parrish 1996). Ayer, Trowell, Amelin and Corfu (1999) included calc-alkalic metavolcanic rocks intercalated with clastic metasedimentary rocks, underlying the northeast part of the map area, with the Kidd–Munro assemblage based on precise U/Pb ages of 2716 to 2713 Ma (Berger and Amelin 1999). These 2 packages are described separately below.

Ultramafic and mafic layered sills were intruded and folded with the metavolcanic rocks. The Ghost Range sill, in the eastern part of the map area, is typical of these sills and is described below.

#### Ultramafic and Mafic Tholeiitic Metavolcanic Rocks

##### ULTRAMAFIC METAVOLCANIC ROCKS

Ultramafic metavolcanic rocks occur throughout the northwest part of the assemblage as narrow flows and as discrete mappable units up to 1.5 km wide. Komatiitic basalts and high-iron massive, pillowed and variolitic tholeiitic flows are commonly interlayered with the ultramafic flows and are rarely thick enough to form mappable units at 1:50 000 scale.

**Table 2.** Lithological units for the Highway 101 area.

---

**PHANEROZOIC**

**CENOZOIC**

**QUATERNARY**

**HOLOCENE**

Lake, stream, wetland deposits

**PLEISTOCENE**

Glacial, glaciofluvial and glaciolacustrine deposits, sand, gravel, till and clay

*UNCONFORMITY*

**MESOZOIC**

**JURASSIC**

Kimberlite dikes and diatremes

*INTRUSIVE CONTACT*

**PRECAMBRIAN**

**PROTEROZOIC**

Mafic Intrusive Rocks

Diabase dikes

*INTRUSIVE CONTACT*

**ARCHEAN**

**NEOARCHEAN**

Metamorphosed Alkalic Felsic and Intermediate Intrusive Rocks

Syenite, monzonite, quartz monzonite, granite, feldspar and quartz feldspar porphyry, intrusion breccia, pegmatitic syenite, schist, mylonite, albitite

*INTRUSIVE CONTACT*

Metamorphosed Alkalic Ultramafic and Mafic Intrusive Rocks

Hornblendite, pyroxenite, melasyenite, pegmatitic melasyenite, lamprophyre, gabbro and/or diorite

*INTRUSIVE CONTACT*

Metamorphosed Tholeiitic Ultramafic and Mafic Intrusive Rocks

Peridotite, pyroxenite, gabbro, gabbronorite, schist, diorite, pegmatitic gabbro

*INTRUSIVE CONTACT*

Mafic and Intermediate Alkalic Metavolcanic Rocks

Massive and porphyritic amphibole-biotite-foiid-bearing flows, flow breccia

Clastic and Chemical Metasedimentary Rocks: Timiskaming Assemblage

Wacke, sandstone, arkose, siltstone, argillite, polymictic conglomerate, schist, chert, laminated magnetite-hematite iron formation

*UNCONFORMITY*

Clastic and Chemical Metasedimentary Rocks: Turbidites

Wacke, siltstone, argillite, graphitic and pyritic mudstone, conglomerate, schist, chert

Felsic Metavolcanic Rocks

Flows, tuff, lapilli tuff, tuff breccia, schist

Intermediate Metavolcanic Rocks

Massive, flow-laminated and pillowed flows with flow top and pillow breccia, as well as amygdaloidal and variolitic varieties; tuff, lapilli tuff and tuff breccia, schist, breccia, feldspar porphyry

Mafic Metavolcanic Rocks

Massive and pillowed flows with pillow and flow top breccia, as well as variolitic and amygdaloidal and plagioclase-bearing varieties; tuff and lapilli tuff, schist, leucoxene-bearing units, graphite breccia, dikes, hornfelsic greenstone

Ultramafic and Mafic Metavolcanic Rocks: Komatiites

Massive, spinifex and polysuture textured flows, schist, basaltic komatiite

---

Talc-carbonate schist is most common. Tectonic strain is preferentially partitioned into the ultramafic rocks such that almost all drill data and most outcrops are schistose. The schist is typically friable, weathers recessively, and reliably defines the extent of shear zones. Iron carbonate and green mica are minerals signifying hydrothermal alteration and are most common in ultramafic flows along the contact between the Kidd–Munro and Porcupine assemblages and along portions of the Arrow fault (local name) (*see* “Structure” below).

A series of komatiitic flows, exposed along Highway 101 in northern Guibord Township, display well-preserved spinifex, cumulate and flow breccia textures. Each flow is generally less than 2 m thick and has a narrow or nonexistent cumulate base, a well-developed spinifex zone and a thin to thick flow breccia top. Primary mineralogy is mostly altered to chlorite, serpentine, talc, carbonate and iron oxides, but primary clinopyroxene is preserved locally. Basaltic komatiite and tholeiitic magnesium basalts, commonly with varioles, are spatially associated with these ultramafic flows. These limited data indicate that the ultramafic rocks are most likely distal facies flows in this area (Hill et al. 1990).

### **MAFIC METAVOLCANIC ROCKS**

Mafic tholeiitic flows are most abundant throughout the Kidd–Munro assemblage and consist of massive, pillowed, pillow-breccia, and variolitic varieties. Massive flows, which are most common, consist of green to black weathering, fine- to coarse-grained equigranular rocks. Epidote and chlorite veins, knots and clots are common in several places in southern Munro and McCool townships and less common in Michaud and Guibord townships. Massive flows are more common in this part of the Kidd–Munro assemblage than areas farther west, which suggests that the map area may be more proximal to a magma source (Berger 2000a; Easton and Johns 1986).

Pillowed mafic flows are common with well-defined pillow morphology displayed in several areas. Pillows vary between 30 to 150 cm long by 15 to 70 cm wide and form flows from a few metres to tens of metres thick. They are generally well formed, close packed with selvages less than 2 cm thick. Carbonate and chlorite amygdules are common, but not abundant. Quartz-filled lava levels (crescent-shaped voids marking lava retreat in the central parts of pillows), are rare and signify low and/or episodic rates of magma extrusion. Interpillow material is generally minor and may consist of hyaloclastite or less commonly chert and mudstone. Pillowed flows pass gradationally into massive flows in a few places, however, distinct contacts between flows are more common. More typically, pillowed flows grade into and are interlayered with hyaloclastite.

Hyaloclastite and pillow breccia occur as interpillow material, stratiform carapaces over massive and pillowed flows and as individual flow units interlayered with mafic flows. These rocks are typically dark green weathering, monolithic with subangular and rounded mafic fragments up to 8 cm in size. Individual units are generally less than 1 m thick and discontinuous along strike. In general, hyaloclastite and pillow breccia comprise only a minor portion of the Kidd–Munro assemblage in the map area.

Mafic graphite breccia is reported from one diamond-drill hole in northern Michaud Township. This rock type is characterized by angular fragments of mafic metavolcanic flows in a graphite ± chlorite ± carbonate-bearing matrix. The brecciation is interpreted to form by interaction of the hot magma with cold seawater and unconsolidated sediments that resulted in hydrofracturing of the flows. Such peperite textures are common in the Kidd–Munro assemblage north of Timmins; these textures have been described previously in greater detail (Berger 1999).

Mafic schist is a descriptive term used to describe green to black, foliated rock inferred to have developed by shearing of a mafic metavolcanic protolith. Unaltered schist is composed of chlorite and epidote with minor calcite and is commonly transitional into less foliated parent rock. It is most common

in faults and shear zones throughout the Kidd–Munro assemblage. Hydrothermally altered schist is composed of chlorite, iron carbonate, white mica, quartz and commonly contains up to 30% disseminated sulphide minerals (predominantly pyrite). This type of schist is most common near the contacts with the alkalic plutons in Michaud Township and along parts of the Arrow fault (local name) and Porcupine–Destor fault in Michaud and Garrison Townships.

### **Variolitic Mafic Metavolcanic Rocks**

Variolitic mafic flows are described separately because they have distinctive morphology which permits their use as marker units and because the flows host gold mineralization in scattered locations throughout the Kidd–Munro assemblage. This report adds to and expands on excellent descriptions and discussion of the varioles in Beatty and Munro townships provided by Johnstone (1991). The term “variole” is used in this report to describe a spherical mass of felsic material in a mafic groundmass and is consistent with the definition of Bates and Jackson (1980).

Variolites are most common along the southern contact of the Kidd–Munro assemblage where they form a distinct marker unit up to 50 m wide. Varioles in this unit occur as white to grey individual spheres up to 3 cm diameter, as dendritic chains, or as coalesced masses from a few centimetres to greater than 3 m long by 0.5 m wide. Some of the coalesced masses rarely form separate units approaching mappable proportions. One such unit, approximately 700 m long by 3 m wide, occurs at the contact between the Kidd–Munro and Hoyle assemblage in southern Munro Township. Similar felsic “pods” occur within the same variolitic unit, south of the Munro asbestos mine, and this same unit occurs along the contact between the Kidd–Munro and Hoyle assemblages in Beatty Township (R. Dahn, Battle Mountain Gold Limited, personal communication, August 1999).

Individual varioles typically have a grey to dark grey core with a white to light grey rim. In thin section, the varioles are characterized by tiny opaque microlites that define a concentrically zoned core.

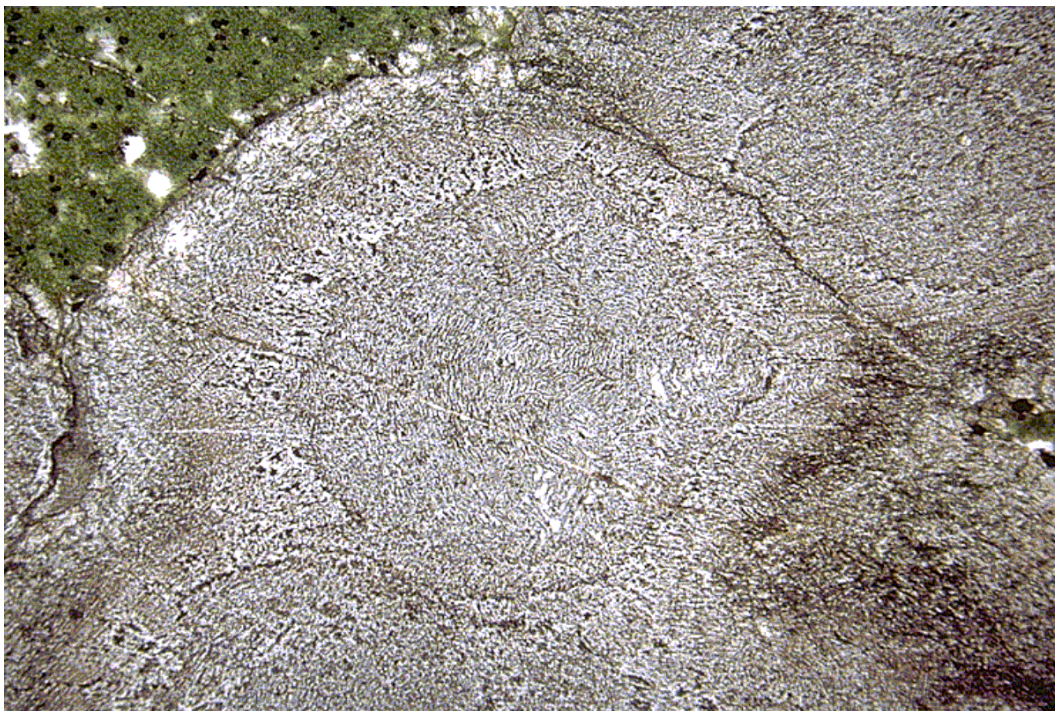


**Photo 1.** Concentrically zoned core of variole surrounded by radial microlite growth in variolitic flow from Lot 10, Concession I, Munro Township. Field of view is 10 mm, plane polarized light. Location: UTM Zone 17, NAD 27, 555595E 5376576N.

There is a marked boundary of opaque minerals across which the microlites become radially oriented (Photo 1). Very fine-grained quartz and albite occur in the variole mesostasis. Johnstone (1991) compared varioles with similar morphology to Blake River-type varioles described by Gélinas, Brooks and Trzcienski (1976). The origin of such rocks is controversial and may be either a result of immiscible liquids (Gélinas, Brooks and Trzcienski 1976) or by direct crystallization of varioles in response to undercooling of the host liquid (Fowler, Jensen and Peloquin 1987). Fowler et al. (2002) suggest that mixing of mafic and felsic magmas in a subvolcanic magma chamber may also give rise to the variole textures displayed in Munro Township.

## **Felsic Metavolcanic Rocks**

Felsic metavolcanic rocks composed of flows, minor hyaloclastite and tuff are uncommon in the map area. Johnstone (1991) mapped rhyolite flows and tuff north of the Croesus Mine in Munro Township. This unit extends into Beatty Township where U/Pb zircon geochronology indicates the unit is  $2714 \pm 2$  million years old (Corfu et al. 1989). Satterly (1947, 1948) reported that rhyolite occurred south of Perry Lake, however, outcrops examined by the author are spherulitic and locally flow-laminated felsic pods within the variolitic units described above. Felsic pods and segregations of the varioles along the contact of the Kidd–Munro and Hoyle assemblages were mapped as felsic flows by Johnstone (1991). One such unit labelled the “contact dike” by Johnstone (1991) occurs at the contact between the Kidd–Munro and Porcupine assemblages in Munro Township. This unit is approximately 3 to 25 m wide, extends for up to 700 m along strike and is composed of massive to weakly spherulitic, aphyric felsic material (Johnstone 1991). The physical characteristics of the felsic rocks in this part of the Kidd–Munro assemblage indicate that they are intimate parts of the variolitic flows which supports the contention that they formed by magma mixing (Fowler et al. 2002).

## **Calc-alkalic Metavolcanic Rocks**

Calc-alkalic metavolcanic rocks intercalated with clastic metasedimentary rocks underlie the northeast part of the map area. These rocks are up to 5.5 km thick and extend west of the area to Milligan and Warden townships. The calc-alkalic rocks are composed of basalt to dacite flows, pyroclastic and epiclastic tuff, lapilli tuff, tuff breccia and breccia. U/Pb zircon ages of  $2713 \pm 2$  Ma from feldspar porphyry in Rand Township (Corfu et al. 1989) and  $2716 \pm 1.5$  Ma from intermediate flows north of the Holloway Mine (Berger and Amelin 1999) indicate that these rocks belong to the Kidd–Munro assemblage (Ayer, Trowell, Amelin and Corfu 1999). An age of  $2714 \pm 2$  Ma was obtained from zircon from a dacite flow in southwest Milligan Township confirming its correlation with the Kidd–Munro assemblage (Barrie 1999a).

A conformable, stratigraphic contact with the tholeiitic and ultramafic members was observed in outcrop along the boundary between IR 70 and Garrison Township and in diamond-drill core northeast of the Holloway Mine. However, the calc-alkalic rocks are in shear contact with the Kinojevis assemblage along the Porcupine–Destor deformation zone in Marriott and Stoughton townships. A sheared contact with the Stoughton–Roquemaure assemblage is inferred along the north branch of the Porcupine–Destor fault.

Flows, in Lamplugh, Frecheville and northern Holloway townships, are composed of massive, flow-laminated and pillowed basalt, andesite and minor dacite. Massive and flow-laminated units are green to dark green weathering commonly with chlorite and epidote stringers and knots. Flow-laminated dacite, in northeast Harker Township, contains amphibole and plagioclase phenocrysts that provide reliable field



evidence for calc-alkalic geochemical affinity. Data from isolated outcrops and scattered drilling suggest that flows are thin discontinuous units no more than a few tens of metres thick. Pillowed flows, which are more common, are green to grey-green weathering and commonly contain chlorite- and calcite-filled vesicles. Pillows are well-formed, close-packed shapes with 1 to 8 cm thick rims. They vary in size from 80 to 150 cm long by 50 to 80 cm wide with some exceptionally large shapes up to 250 by 80 cm. The large size and thick rims serve to distinguish the calc-alkalic from the tholeiitic members of the Kidd–Munro assemblage. Geochemical analyses of these rocks confirm calc-alkalic geochemistry (*see* “Geochemistry”).

Pyroclastic and epiclastic deposits are voluminous and consist of tuff, lapilli tuff, tuff breccia and breccia. Breccia and tuff breccia deposits are heterolithic with diverse clast populations of ultramafic, mafic, intermediate and felsic metavolcanic rocks. The largest clast size is approximately 40 cm and these occur in southern Rand Township. Breccia units are clast supported and are generally poorly sorted, and poorly stratified with no grading. These units are less than 50 m thick and most are less than 10 m thick. Tuff and lapilli tuff units are interbedded with these units. Tuff breccia units are generally not graded and poorly stratified, but tend to be better sorted than breccia. Clasts are generally smaller (up to 30 cm), but are similar in composition to those in breccia units. Tuff breccia is generally matrix supported in green, grey to light grey tuff (Photo 2).

Tuff and lapilli tuff comprise much of the calc-alkalic portion of the Kidd–Munro assemblage in the map area. Predominantly, these rocks are intermediate in composition, although rare felsic tuff occurs in some diamond-drill holes in Stoughton and Frecheville townships. Lapilli tuff and lapillistone are commonly interlayered with tuff breccia and tuff. These heterolithic rocks are grey to light green weathering with diverse clasts of mafic, intermediate and felsic metavolcanic rocks. Many of the intermediate clasts contain amphibole phenocrysts and are similar to calc-alkalic rocks observed by the author in Clergue and Little townships to the west (Berger 2000a, 2000b).



**Photo 2.** Calc-alkalic, intermediate tuff breccia, part of the Kidd–Munro assemblage from northern Holloway Township (length of knife is 8 cm). Location: UTM Zone 17, NAD 27, 596477E 5376271N.

Tuff is light green, grey to brown where carbonatized and is well to poorly sorted, generally well bedded and rarely graded. Tuff that is intercalated with breccia and tuff breccia occurs as narrow and discontinuous beds. Tuff is generally more voluminous and intimately interbedded with metasedimentary rocks north of the Ghost Range sill. In the central parts of Stoughton, Frecheville and Lamplugh townships, tuff is interbedded with wacke, argillite and epiclastic tuff indicating that the calc-alkalic rocks are transgressive to metasedimentary units north of the map area.

## **Ghost Range Sill**

The Ghost Range sill is a layered intrusion, which underlies the northeast part of the map area, and is composed of peridotite, pyroxenite, gabbro, gabbro and quartz gabbro. Corfu (1993) indicated that the sill is 2713±7/-5 million years old, similar in age to the Kidd–Munro assemblage metavolcanic rocks. Jensen (1982c) and Jensen and Langford (1985) interpreted the rocks as flows, however, Satterly (1951a, 1951b, 1953a, 1953b), MacRae (1969) and the author believe the rocks are intrusive. Although peridotite occurs around the perimeter of the sill, the peridotite is exposed only along the south flank in Harker Township. The rock is black, medium grained, equigranular, strongly magnetic and weakly to moderately serpentinized. The unit is generally less than 200 m thick and was explored along the southern contact for asbestos in the 1950s and early 1960s. In thin section, rounded olivine crystals are altered to talc, serpentine and magnetite and comprise approximately 80 to 85% of the rock. Rare orthopyroxene was observed and secondary epidote and chlorite occurs in the groundmass. The contact between the peridotite and the underlying calc-alkalic rocks of the Kidd–Munro assemblage was observed in diamond-drill core northeast of the Holloway Mine. Here, the peridotite is weakly sheared and there is a narrow, but distinct, metamorphic thermal aureole developed in the metavolcanic rocks.

The peridotite is in gradational contact with pyroxenite, but this rock type is not present everywhere. More commonly, the peridotite is in abrupt contact with gabbro and gabbro that is characterized by a chalky grey to green weathered surface due to the presence of plagioclase. Olivine comprises less than 5% of the rock and, near the base of the unit, orthopyroxene and clinopyroxene occur. Olivine and orthopyroxene are absent and locally, toward the central portion of the sill, quartz is present. Quartz becomes more abundant near the most central portion of the intrusion and pegmatitic patches of quartz and plagioclase up to 15 cm in size occur at the abandoned fire tower at the top of the Ghost Range.

The Ghost Range sill is similar to other layered intrusions in the Kidd–Munro assemblage, most notably the Munro and Centre Hill intrusions in Munro and McCool townships (MacRae 1969). Asbestos-bearing peridotite intrusions in northern Garrison Township and gabbroic intrusions throughout the Kidd–Munro assemblage are compositionally similar to the Ghost Range sill.

## **Geochemistry**

Geochemical analyses for a variety of Kidd–Munro assemblage rocks are presented in Appendix 1. Figure 3 confirms that there are komatiitic, tholeiitic and calc-alkalic metavolcanic rocks in the assemblage.

### **ULTRAMAFIC METAVOLCANIC ROCKS**

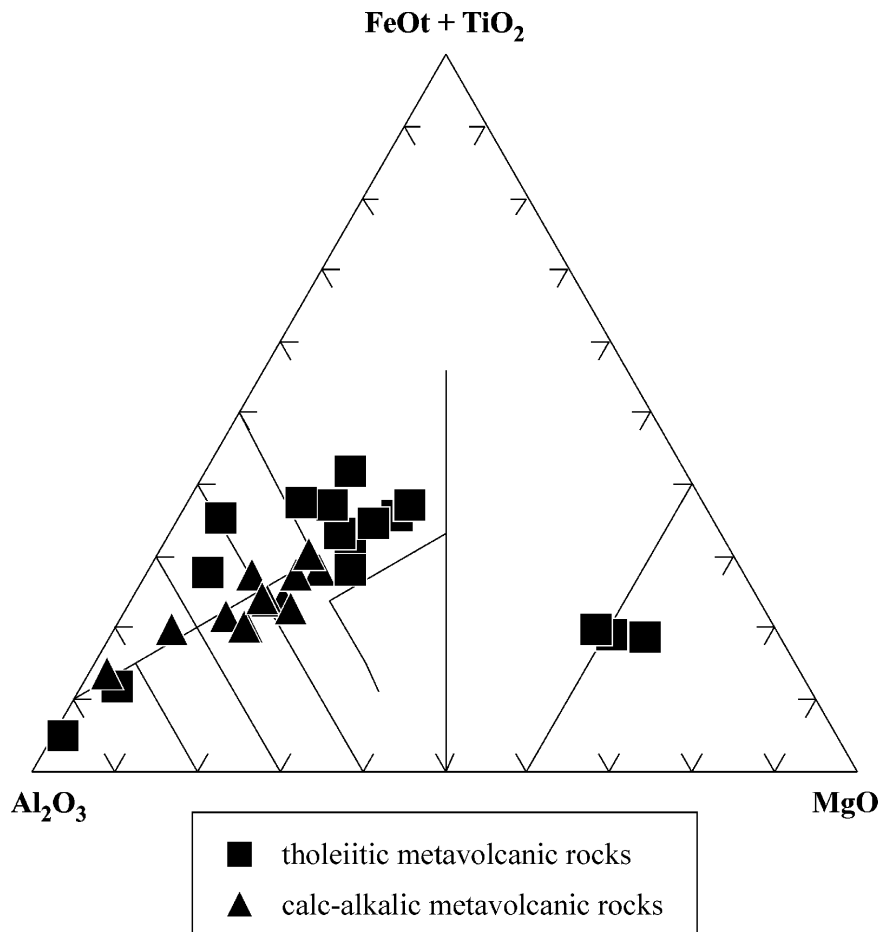
Three spinifex-textured komatiites were analyzed. These samples contain MgO contents between 18 and 27 weight %, which indicate that these rocks are basaltic and peridotitic komatiites (cf. Johnstone 1991; Barrie 1998). The basaltic komatiites have  $Al_2O_3/TiO_2$  between 15 to 20,  $CaO/Al_2O_3$  between 0.9 to 1.1. Chondrite-normalized rare earth element (REE) patterns for these rocks indicate light rare earth element

(LREE) depletion with relatively flat slopes and  $La/Yb_n$  equal to 0.25 to 0.77 (Figure 4). The data fall within the range for Kidd–Munro assemblage komatiites west of the map area (Berger 2000a) and correlate well with distal facies komatiitic rocks in Dundonald Township, which are also part of the Kidd–Munro assemblage (Barrie et al. 1999). LREE depletion is inferred to indicate magma derivation from a part of the mantle that underwent previous partial melting (Barrie 1999a). The Dundonald Township komatiites are not depleted in aluminum and are also inferred to be derived from significant partial melting of a depleted mantle with little or no influence of majorite garnet (Barrie 1998). All these data are compatible with komatiite derivation from mantle plumes (Barrie 1999a, 1999b; Xie, Kerrich and Fan 1993).

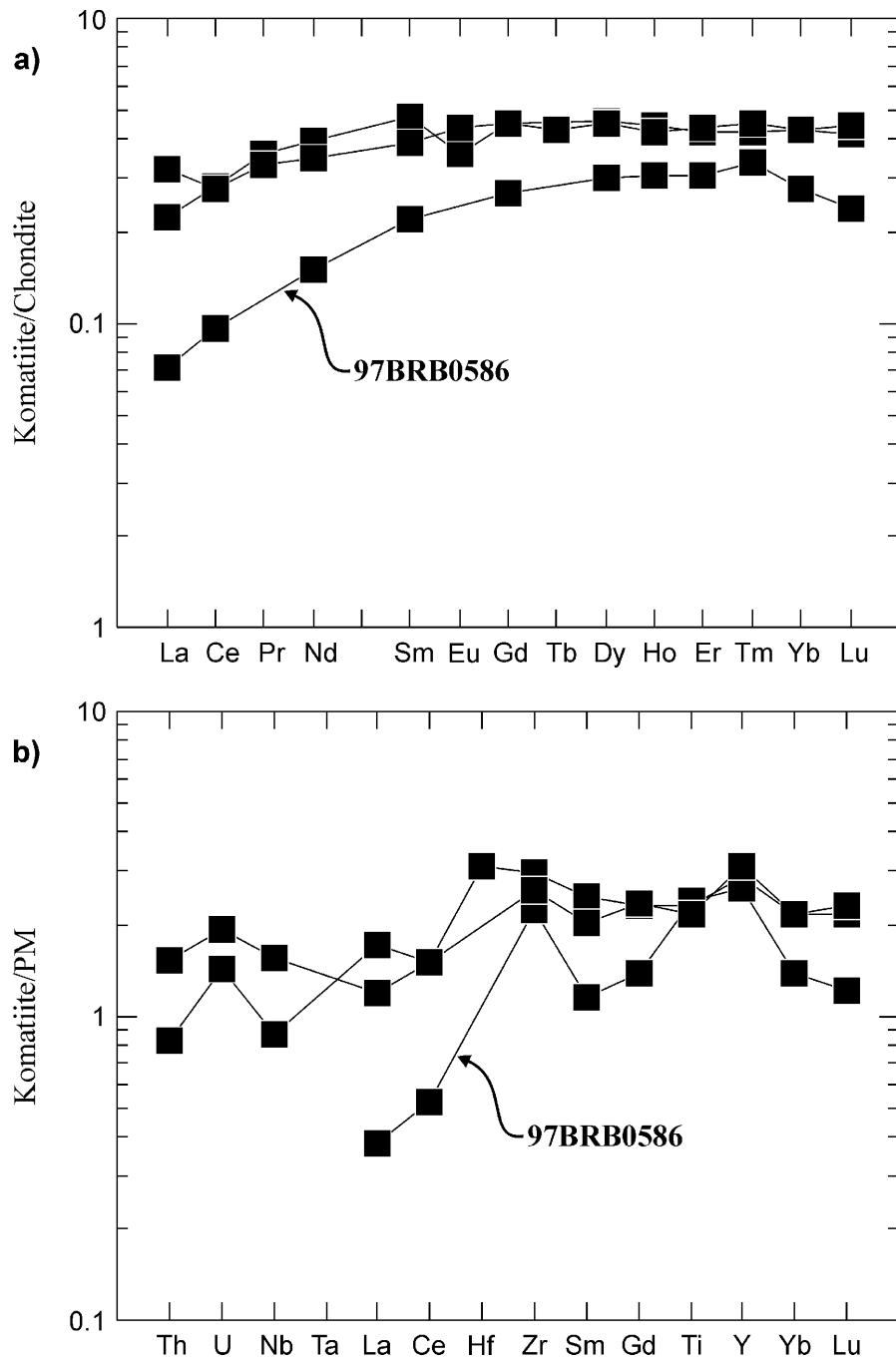
It should be noted that geochemical data from sample 97BRB0586 in Figure 4 plot within the field for komatiites with nickel deposits (not depicted) as defined by Barrie, Ludden and Green (1993).

### MAFIC METAVOLCANIC ROCKS

High-iron basalts are predominant (*see* Figure 3; *see* Appendix 1) with  $TiO_2$  content between 0.9 to 2.3 weight % and Mg numbers between 33 and 53. These values are slightly greater than values in the basalt up-section of the Kidd Creek base metal orebody in Kidd Township (Barrie, Hannington and Bleeker 1999), but are similar to mafic metavolcanic flows in other areas of the Kidd–Munro assemblage (Berger 1999, 2000a).

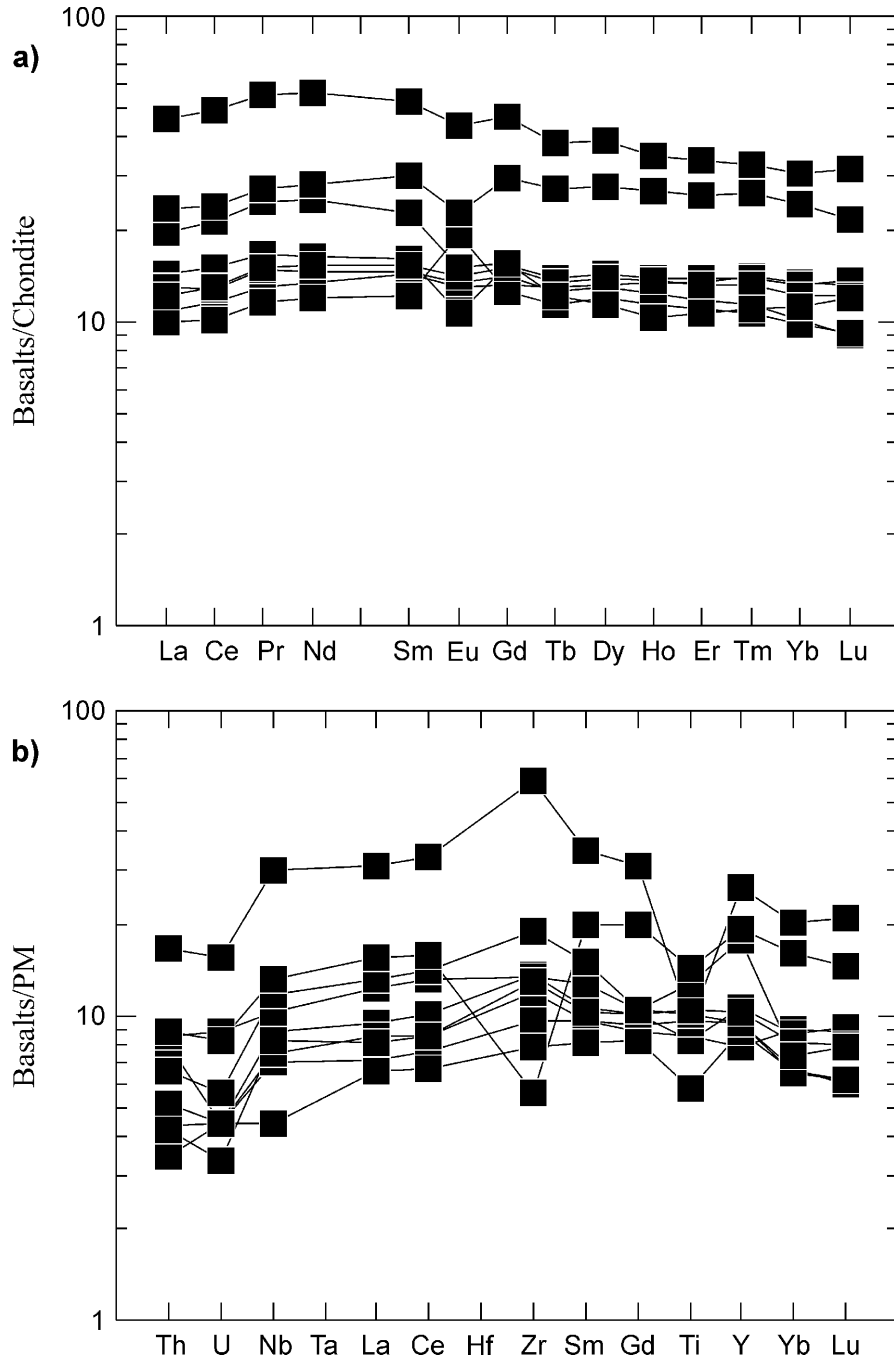


**Figure 3.** Jensen cation plot for the Kidd–Munro assemblage in the Highway 101 area (*after* Jensen 1976).



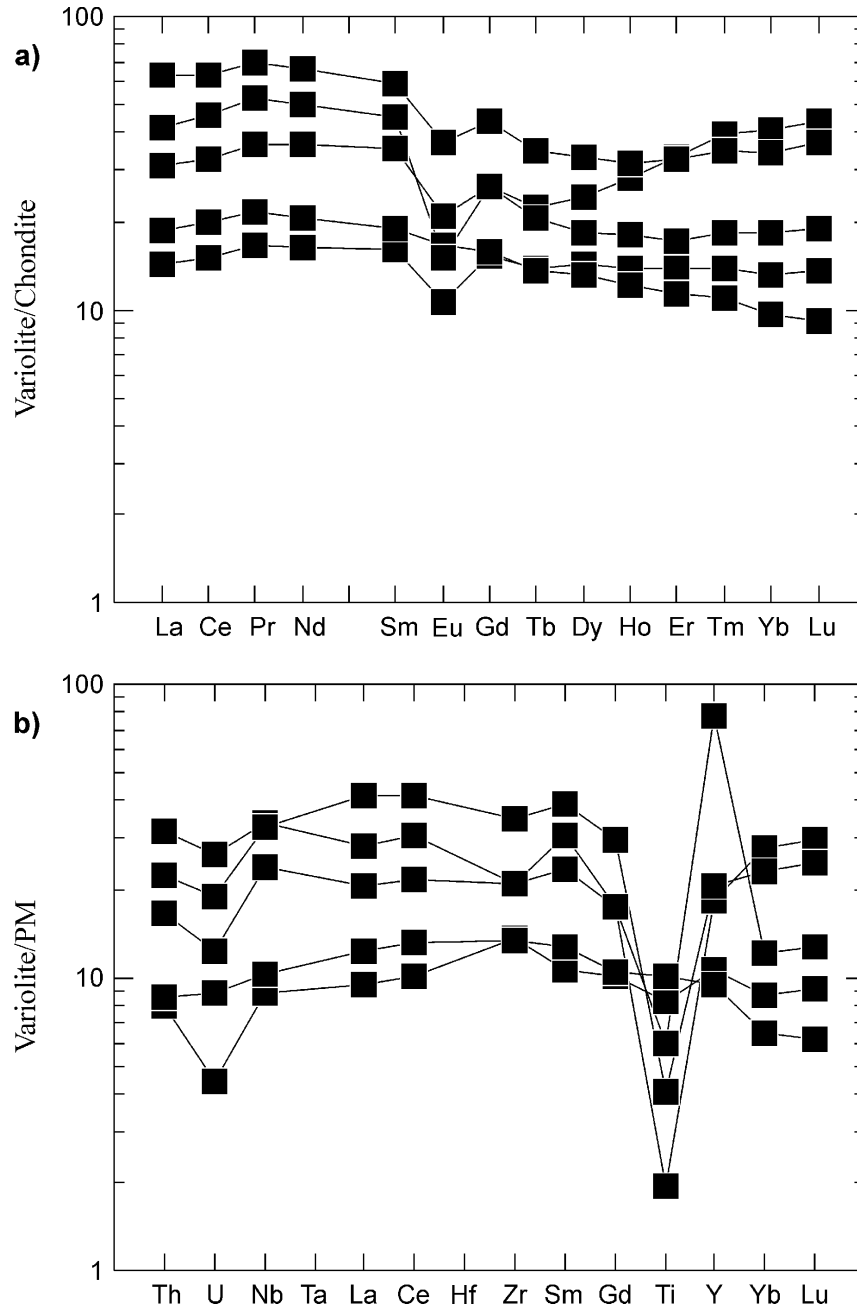
**Figure 4.** a) Chondrite-normalized rare earth element (REE) patterns, and b) primitive-mantle normalized extended element patterns for Kidd–Munro assemblage komatiites in the Highway 101 area.

Figure 5a shows a cluster of samples with essentially flat chondrite-normalized REE patterns. These patterns are similar to Kidd–Munro basalts west and north of the map area (Berger 2000a; Barrie 1999a, 1999b). These types of REE patterns are interpreted as transitional-type mid-ocean ridge basalts (MORB) (Pearce 1996). Barrie (1999a, 1999b) indicated that some basalts in Munro and Beatty townships displayed slightly elevated LREE patterns that approached calc-alkalic geochemical affinity. A minority of the samples in the study area also display LREE enrichment and may indicate a transition to the calc-



**Figure 5.** a) Chondrite-normalized REE patterns, and b) primitive-mantle normalized extended element patterns for Kidd–Munro assemblage mafic tholeiitic metavolcanic rocks in the Highway 101 area.

alkalic rocks discussed below. Figure 5b shows primitive-mantle normalized patterns with depleted uranium and thorium and slightly lowered titanium, similar to basalts in Munro and Beatty townships (Barrie 1999a, 1999b). However, Kidd–Munro assemblage basalts in the Monteith area, west of the map area, are distinctly enriched in titanium indicating that variation does occur in the assemblage along strike (Berger 2000a). Further, plagioclase phyric basalts that comprise a distinct subtype in the Monteith area are largely absent in the Highway 101 area. Therefore, the geochemistry by these various authors shows that the Kidd–Munro assemblage is composed of several different types of tholeiitic mafic flows. Future detailed mapping and sampling in well-exposed areas may reveal the presence of vertical and lateral chemostratigraphy in the assemblage.



**Figure 6.** a) Chondrite-normalized REE patterns, and b) primitive-mantle normalized extended element patterns for Kidd–Munro assemblage variolitic rocks in the Highway 101 area.

## VARIOLITIC MAFIC METAVOLCANIC ROCKS

Variolitic rocks and associated felsic segregations are identified in Appendix 1. Data from these rocks plot on Figure 3 as tholeiitic basalt, andesite, dacite and calc-alkalic rhyolite. Figure 6a shows that all variolitic rocks contain elevated REE with minor negative europium anomalies and all contain higher REE than associated Kidd–Munro assemblage mafic flows. Variolitic rocks all display depletion in titanium and various amounts of enrichment in yttrium and all are tholeiitic (Figure 6b). Fowler et al. (2002) suggested that the morphology of varioles in Munro Township were products of mixing mafic with felsic magma (*see* Photo 2). The geochemistry and field evidence presented here is not easily explained as resulting from supercooling and supports magma mixing. Variolitic rocks of the Kidd–Munro assemblage in the Monteith area display similar REE patterns and total abundance suggesting that similar processes formed these rocks as those in the map area (Berger 2000a).

Representative samples of the felsic segregations and the “contact dike” (see above) were submitted for geochemical analysis (*see* Appendix 1). These rocks plot as tholeiitic to calc-alkalic rhyolite (*see* Figure 3) and display essentially flat REE patterns with negative europium anomalies indicative of tholeiitic affinity (Figure 7a). The patterns mimic FIII-type high-silica rhyolite (Leshner et al. 1986), but contain lower total REE than a typical FIII-type rhyolite. The primitive-mantle normalized extended element patterns show strongly depleted titanium also in accordance with FIII-type geochemistry (Figure 7b). Zr/Y varies between 0.65 and 4.13 with yttrium values between 46 and 264 ppm Y, which indicates a wide variation in the felsic rocks that is not wholly compatible with FIII-type geochemistry (*see* Appendix 1). The association of volcanogenic massive sulphide mineralization with F-III rhyolite is well established in the Abitibi Subprovince and within the Kidd–Munro assemblage in particular (Barrie, Hannington and Bleeker 1999; Barrie, Ludden and Green 1993). The association of variolitic rocks with gold mineralization is discussed by Fowler et al. (2002) Ropchan (2000) and Jones (1992). That these 2 rock types are intimately associated and probably co-magmatic presents interesting topics for study of petrogenesis and sulphide mineralization. Although magma mixing is the process preferred by Fowler et al. (2002) to create this rock association, other possibilities, such as immiscible liquids, need to be investigated.

## CALC-ALKALIC METAVOLCANIC ROCKS

Calc-alkalic rocks in the eastern part of the map area are included in the Kidd–Munro assemblage based on U/Pb geochronology ( $2716 \pm 1.5$  Ma; Berger and Amelin 1999). Several representative samples were submitted for geochemical analysis and results are presented in Appendix 1. A calc-alkalic trend is indicated in Figure 3, although all rocks appear to contain elevated iron resulting in overlap into the tholeiitic field. All REE patterns are similar and show LREE enrichment with slight negative europium anomalies (Figure 8a). Figure 8b shows negative niobium and titanium anomalies consistent with derivation of magma by subduction-related processes. Calc-alkalic rocks in Milligan Township ( $2713 \pm 1.8$  Ma) appear to be correlative with the calc-alkalic rocks in the map area (Barrie 1998). Calc-alkalic rocks in northern Wilkie and Walker townships display similar geochemistry, but have not had ages determined and were previously correlated with the Duff–Couslon–Rand assemblage by Berger (2000a) and Jackson and Fyon (1991). Given the data presented in this report and by Barrie (1998), it is most likely that the calc-alkalic rocks in northern Wilkie and Walker townships belong to the Kidd–Munro assemblage. The extent of the calc-alkalic rocks indicates that evolution of the Kidd–Munro assemblage involved more than tholeiitic seafloor volcanism, but also involved a significant component of subduction and probable island-arc construction. Further, there is a distinct asymmetry to the assemblage, with tholeiitic rocks dominant in the west and south and the calc-alkalic rocks dominant in the east and north. Reconstruction of this area of the Abitibi Subprovince must account for the asymmetry and accommodate both tholeiitic and calc-alkalic magmas.

## GHOST RANGE SILL AND RELATED INTRUSIONS

A number of ultramafic and mafic intrusions occur within the Kidd–Munro assemblage. The largest of these is the Ghost Range layered intrusion and 3 representative samples were collected for geochemical analysis by the author (*see* Appendix 1). Figure 9 shows the chondrite-normalized REE and primitive-mantle normalized extended element patterns for the major phases of the intrusion. The peridotite and gabbro display flat to weakly LREE-enriched patterns, but the quartz gabbro phase is more strongly

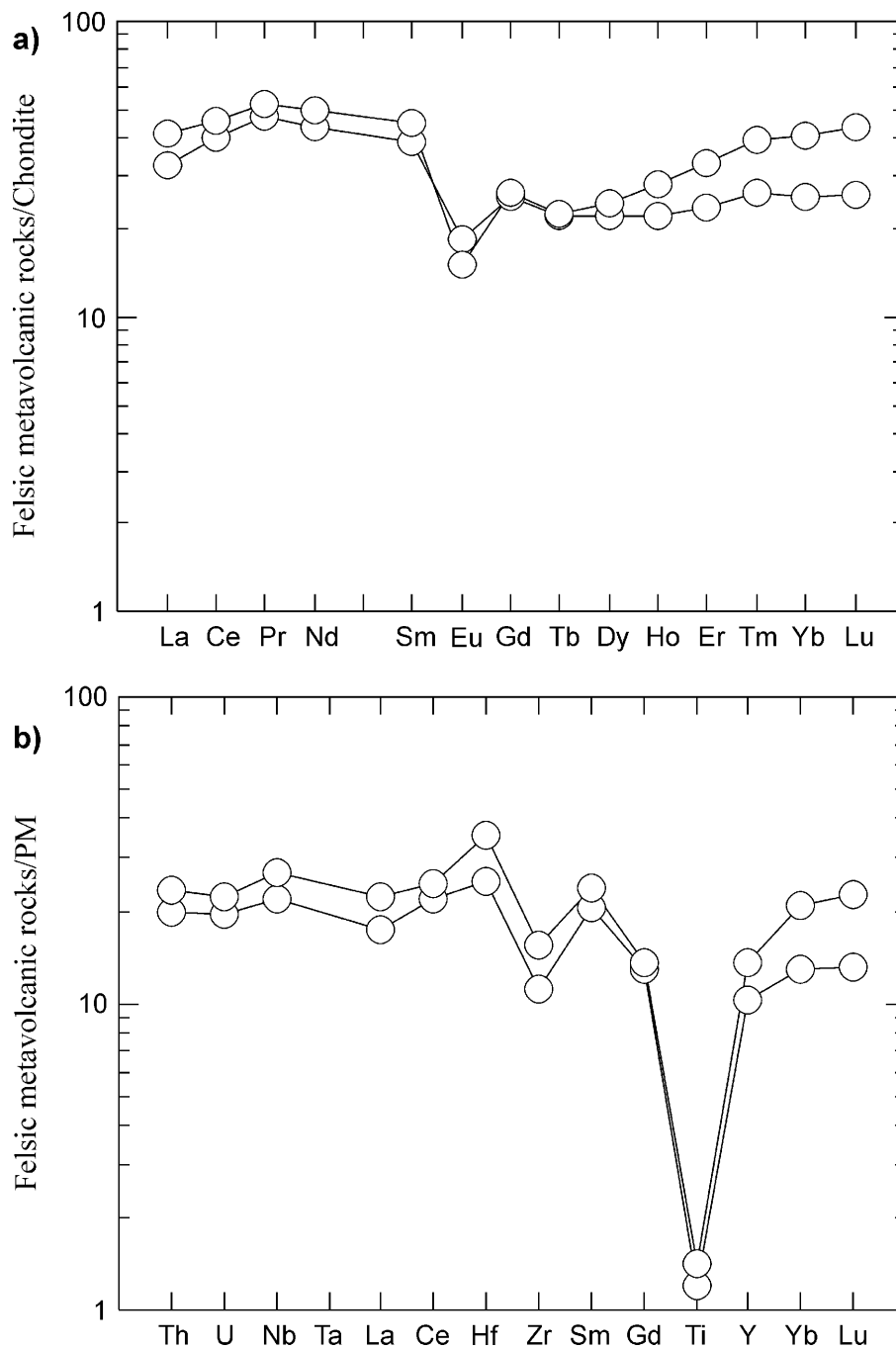


**Figure 7.** a) Chondrite-normalized REE patterns, and b) primitive-mantle normalized extended element patterns for Kidd–Munro assemblage felsic metavolcanic rocks in the Highway 101 area.



fractionated with La/Lu approximately equal to 5 (see Figure 9a). The primitive-mantle normalized extended element patterns reveal essentially flat tholeiitic patterns with slight heavy rare earth element (HREE) depletion for the quartz gabbro (see Figure 9b). Jensen and Langford (1985) inferred that 2 different magmas were responsible for the formation of the rocks of the Ghost Range sill. Although the geochemistry presented in this report could be interpreted to indicate 2 sources, the data could also represent fractionation from a single magma. Further detailed work is required.

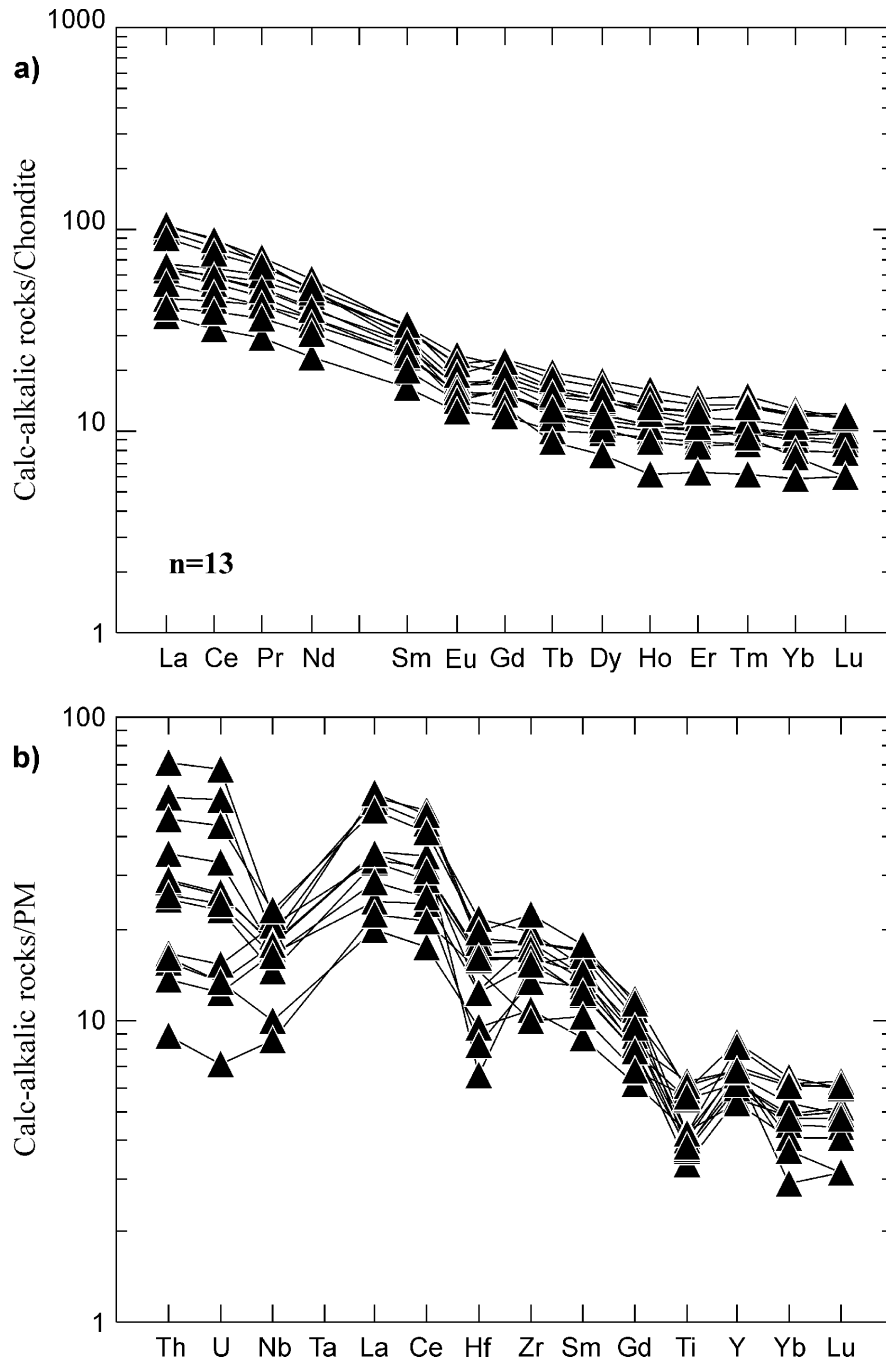


**Figure 8.** a) Chondrite-normalized REE patterns, and b) primitive-mantle normalized extended element patterns for Kidd–Munro assemblage calc-alkalic metavolcanic rocks in the Highway 101 area.

Quartz gabbro and/or diorite sills intruded the calc-alkalic rocks north of the OPP tower road in northeastern Harker Township. These intrusions are macroscopically similar to the quartz gabbro in the Ghost Range sill. However, geochemical characteristics of these rocks display weakly fractionated REE patterns with small positive europium anomalies and lower total REE than the quartz gabbro of the Ghost Range sill (Figure 9c). The primitive-mantle normalized extended element patterns show negative niobium and titanium anomalies indicating that the quartz gabbro magma was likely derived from subduction-related processes and are part of the calc-alkalic suite (Figure 9d). These gabbro intrusions are not related to the Ghost Range sill.

## TISDALE ASSEMBLAGE

The Tisdale assemblage underlies that part of Hislop Township that is north of the Arrow fault (local name) and south of the Porcupine–Destor deformation zone. Rocks south the Arrow fault and north of the Porcupine–Destor deformation zone, in Guibord and Michaud townships, are correlated with the Tisdale assemblage based on rock type morphology, geochemistry and structures. The Tisdale assemblage is predominantly tholeiitic mafic and komatiitic metavolcanic rocks with subordinate calc-alkalic intermediate and felsic flows, pyroclastic and epiclastic deposits. Jackson and Fyon (1991) referred to these rocks as the Bowman assemblage, however, Ayer, Trowell, Amelin and Corfu (1999) and Ayer, Trowell, Madon et al. (1999) included these rocks with the Tisdale assemblage based on U/Pb ages (ca. 2704 Ma) that are similar with those in the type area at Timmins. The Tisdale (or Bowman) assemblage is continuous west of the map area through Bowman, Taylor and Stock townships (Berger 2000a; Muir 1995) and continues into Sheraton Township where it was mapped by Vaillancourt (1999b).

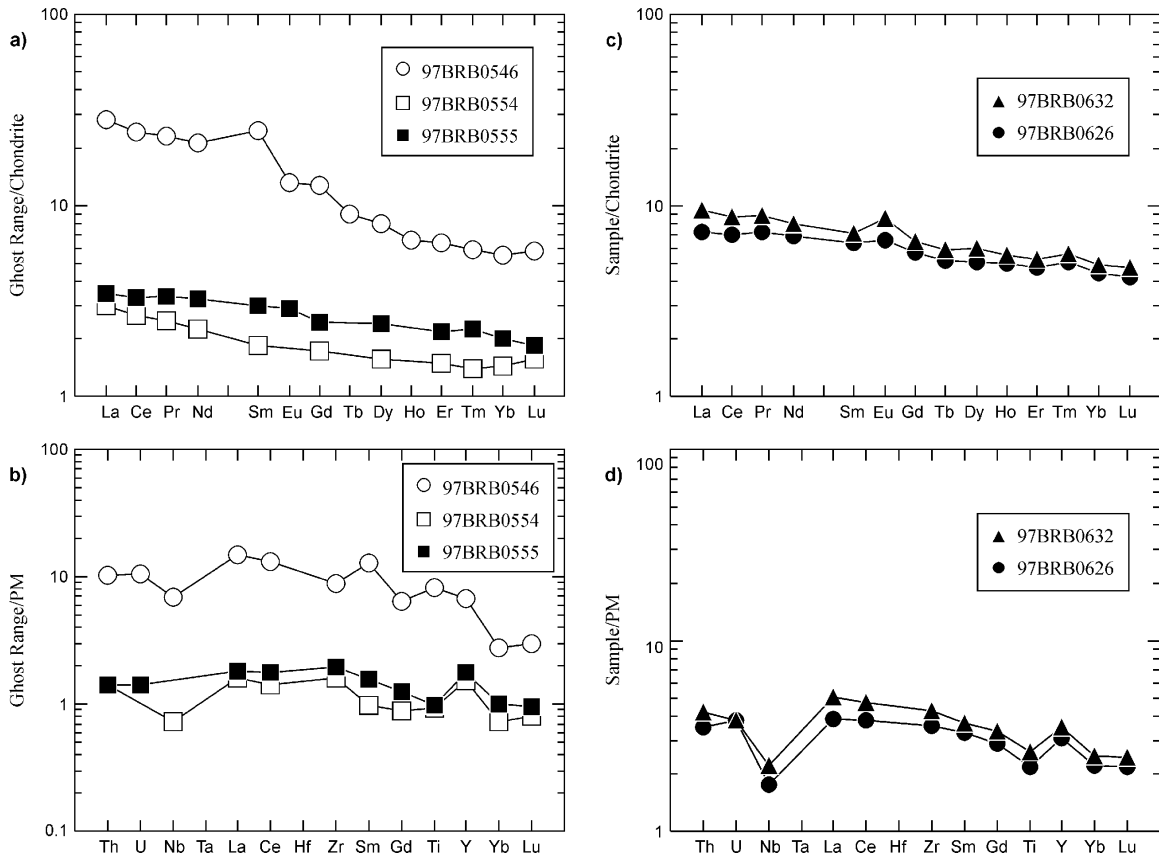


**Figure 9.** Chondrite-normalized REE patterns and primitive-mantle normalized extended element patterns for Ghost Range and gabbroic intrusions in the Kidd–Munro assemblage in the Highway 101 area.

## Ultramafic and Mafic Metavolcanic Rocks

### ULTRAMAFIC METAVOLCANIC ROCKS

Ultramafic metavolcanic rocks of the Tisdale assemblage are restricted to the Porcupine–Destor deformation zone (PDDZ) in Hislop Township. Talc-chlorite schist is most common and green mica, iron carbonate and quartz veins occur in hydrothermally altered zones. Altered schist is dark green to black to orange-brown. It is generally fissile, but is locally indurated where silica and albite are present. Relict spinifex-textured flows occur at the Royal Oak open pit, in Hislop Township, and are reported in diamond-drill logs near the Glimmer Mine.

Elsewhere, ultramafic metavolcanic rocks are poorly exposed and their distribution is derived from diamond-drill data and airborne geophysical magnetic surveys (OGS 1984i, 1984j, 1984k). The ultramafic flows are intercalated with mafic flows in Guibord, Michaud and Garrison townships and occur as continuous units that extend for a distance greater than 20 km along strike and are up to 1 km wide. Talc-chlorite schist is most common within and adjacent to shear zones and faults. Green mica, iron carbonate, albite and quartz mark hydrothermally altered zones that are extensive over large portions of the Porcupine–Destor deformation zone and related faults. Massive, spinifex-textured and brecciated flows are common in less deformed areas. Olivine spinifex was observed in diamond-drill core from southern Guibord Township and is reported in diamond-drill logs from nearby holes. Locally, flow breccia occurs at the tops of spinifex-textured flows, but the breccia is easily confused with schist and its extent may be underestimated by the author. Massive flows are rare, lamprophyric phases that contain abundant chlorite and phlogopite and were observed in only one place in Lot 10, Concession IV, Guibord Township.

### MAFIC METAVOLCANIC ROCKS

Mafic metavolcanic rocks comprise approximately 50% of the Tisdale assemblage and are composed predominantly of massive, pillowed and pillow breccia flows. Chlorite schist is common in faults and shear zones and iron carbonate, albite, sericite and quartz occur in hydrothermally altered zones. Variolitic flows, flow breccia and hyaloclastite are common and tuff is rare. Controversial breccia units at Guibord Hill, Guibord Township and at Froome Hill, Hislop Township are interpreted as fault scarp and synvolcanic flow breccia, respectively. The mafic metavolcanic rocks are geochemically divisible into tholeiite and calc-alkalic (*see* “Geochemistry”), but this difference is not visibly apparent.

Massive flows are exposed in several areas and are generally green, fine- to medium-grained, equigranular rocks with no distinguishing features. Flow thickness varies between a few metres to greater than 50 m with thicker flows more common in the western part of the assemblage.

Pillowed flows are common with pillows from 60 to 70 cm long by 30 to 40 cm wide and with rims up to 2 cm thick. Pillows are generally well formed and may be either close packed with little interpillow material or may have up to 15% interpillow chert and hyaloclastite. Flows are generally a few metres thick and are commonly capped by flow breccia and hyaloclastite. In a few places, flow breccia and hyaloclastite are up to 20 m thick and form mappable units at 1:20 000 scale. One such unit, on Froome Hill, in Hislop Township is characterized by poorly sorted, subangular to rounded, monolithic mafic fragments up to 20 cm in diameter that are poorly bedded and nongraded. Many of the fragments display chilled margins indicative of quenching, and hyaloclastite is common between the larger fragments. On the same outcrop, thin discontinuous ribbons of flow breccia occur between stacked massive flows indicating rapid magma extrusion that incorporated most of the flow breccia deposits. It is possible that the larger flow breccia units at Froome Hill represent fire fountain or spatter cone deposits.

Fragmental rocks interpreted as mafic intrusion breccia, younger than the Porcupine assemblage metasedimentary rocks, occur at Guibord Hill in Guibord Township (Prest 1953; Johnstone and Trowell 1985). These deposits are heterolithic with aphanitic and phaneritic mafic metavolcanic clasts, wacke, argillite, framboidal pyrite clasts and rare felsic porphyry clasts that are up to 30 cm in size, but average 2 to 8 cm.

The clasts are angular to rounded; some have reaction rims, some have chilled margins, few have very angular boundaries, most are subangular massive mafic metavolcanic clasts. The deposits are generally clast supported with a matrix composed of fine-grained mafic tuff or rarely highly indurated, very fine-grained hyaloclastite. The deposits are poorly sorted; clast gradation and bedding planes are absent. Pyrite is common throughout the deposits both as clasts and as disseminations in the matrix. The deposits in Guibord Township are similar to conglomerate at the base of the Porcupine assemblage turbidites that were observed by the author in Murphy Township (Berger 1999). The conglomerate in Murphy Township is interpreted as a fault scarp deposit with significant local derivation of clasts that unconformably overlies the older Tisdale assemblage. If this correlation is valid, then the Porcupine assemblage is regionally unconformable with the Tisdale and Kidd–Munro assemblages throughout the Abitibi Subprovince (Ayer, Trowell, Amelin and Corfu 1999; Bleeker and Parrish 1996).

Mafic schist occurs in faults and shear zones throughout the Tisdale assemblage and is characterized by light to dark green fissile rock that retain few, if any, primary features. Chlorite and secondary amphibole are common minerals in unaltered schist. Iron carbonate, white mica and quartz are common minerals in hydrothermally altered schist. At one location on the Pike River in Lot 1, Concession IV, Hislop Township, mafic schist weathers orange brown due to iron carbonate and is pale green on fresh surface due to the high amount of epidote and carbonate. Some diamond-drill logs have reported similar pale green rocks as felsic metavolcanic rocks, however, felsic metavolcanic rocks are not known to occur in this area.

### **Variolitic Mafic Metavolcanic Rocks**

Variolitic flows occur throughout the Tisdale assemblage, but are less abundant than in the Kidd–Munro assemblage. Variolitic flows are most common in lots 1 and 2, concessions III and IV, Hislop Township and west of the Garrison stock, in Garrison Township. In Hislop Township, individual varioles are white and less than 1 cm in diameter, commonly with dark green cores. Variolitic flows, which occur north of the New Kelore mine shaft and northeast of the St Andrew Goldfields Limited Hislop Mine, contain between 30 to 85% varioles that are commonly coalesced. Some outcrops that appear massive and green-grey weathering contain microscopic variole structures. Geochemistry (*see* “Geochemistry”) indicates that these rocks are related to high-iron tholeiites. Variolitic flows were also observed at the Royal Oak open pit in the north half of Lot 1, Concession IV, Hislop Township. The strong spatial association of variolitic flows with gold mineralization in the Abitibi Subprovince appears to be a function of the ratio of Fe to Mg (Fe/Mg) and brittle failure of the altered flows in response to stress (Fowler et al. 2002; Ropchan 2000; Jones 1992).

### **Calc-alkalic Metavolcanic Rocks**

Calc-alkalic metavolcanic rocks occur within the Tisdale assemblage, however, the mafic and intermediate varieties are macroscopically indistinguishable from the tholeiitic rocks. These rocks are generally massive, fine- to medium-grained, aphyric flows interlayered with tholeiitic units. In thin section, these rocks contain abundant plagioclase, which accounts for the calc-alkalic geochemistry.

A 500 m wide unit of calc-alkalic felsic metavolcanic rocks composed of feldspathic lapilli tuff, tuff breccia and rare autoclastic flows occur at the top of the Tisdale assemblage in Hislop Township. This unit extends west of the map area and is correlated with the felsic metavolcanic rocks that host base metal mineralization in Sheraton Township (Vaillancourt 1999b). The felsic unit is abruptly terminated at the Hislop fault in Lot 5, Concession IV, Hislop Township and was not observed east of this fault (*see* Map 2676, back pocket). Outcrops in Lot 5, Concession IV weather light brown to cream, are cream to light yellow on fresh surface, and are flecked with dark green to black chlorite fractures and specks. The rocks contain less than 1% disseminated pyrite that locally increases to 5%. Feldspar and rarely quartz-feldspar phytic clasts up to 15 cm in size occur in a tuffaceous matrix of similar composition. Sorting, clast gradation and bedding planes were not observed. These rocks appear to be primary pyroclastic deposits. Geochemistry of these rocks indicates calc-alkalic affinity (*see* “Geochemistry”).

Farther west in Lot 7, Concession IV, Hislop Township, epiclastic lapillistone, tuff and tuff breccia are exposed along the Pike River. Subangular to subrounded heterolithic mafic and felsic feldspar porphyritic metavolcanic clasts are matrix to clast supported in a chloritic and sericitic tuffaceous matrix. West of this area, the unit is interpreted from airborne geophysical data to extend into Bowman Township where it is exposed in Lot 7, Concession V (Leahy 1965). The intimate intermixing of mafic and intermediate calc-alkalic rocks with tholeiitic rocks suggests that there was a transition, rather than an abrupt change in magma geochemistry. Vaillancourt (1999a) indicated that calc-alkalic rocks occurred only at the top of the Tisdale assemblage in Sheraton Township, which indicates a lateral variation in the position and morphology of the mafic and intermediate calc-alkalic rocks. Further mapping in Bowman and Currie townships, immediately west of the map area, is recommended to provide a better understanding of the Tisdale assemblage in this area.

Felsic metavolcanic rocks occur only as clasts in the mafic fragmental deposits at Guibord Hill, east of the Hislop fault, which indicates that the fault is a fundamental structure across which stratigraphic correlation is tenuous.

## **Geochemistry**

Geochemical data for a number of rocks from the Tisdale assemblage are presented in Appendix 2. Figure 10 shows that most rocks are tholeiitic, but komatiitic and calc-alkalic rocks comprise a minor component of the assemblage. There is little to distinguish between the Tisdale and Kidd–Munro assemblages based on major oxide geochemistry as shown in Figure 10.

### **ULTRAMAFIC AND MAFIC METAVOLCANIC ROCKS**

Tisdale assemblage komatiitic rocks are not depleted in aluminum (*see* Appendix 2) and display LREE depletion similar to most komatiitic flows in the Kidd–Munro assemblage (Figure 11a; *see* Figure 4). Sproule et al. (2000) discussed the spatial and temporal variations of the komatiite geochemistry in the Abitibi greenstone belt and concluded that komatiitic rocks that are not depleted in aluminum are the most common and resulted from 30 to 50% partial melting of a garnet lherzolite or garnet harzburgite source at 2 to 8 gigapascals (GPa). This is similar to komatiites elsewhere in the world that host copper-nickel mineralization and implies that both the Tisdale and Kidd–Munro assemblages are prospective exploration targets for this type of mineralization (Sproule et al. 2000).

Sample 99-BRB-0849 (*see* Appendix 2) is intensely carbonatized and contains abundant green mica. It appears that the intense carbonatization resulted in trace element remobilization as indicated by the elevated LREE (*see* Figure 11a) and spiked nature of the incompatible trace elements (Figure 11b). This sample was collected from the vicinity of the abandoned New Kelore mine shaft in Hislop Township and

indicates the limited ability of geochemistry to distinguish the protolith of extremely altered rocks. Readers are referred to Sproule et al. (2000) for further discussion and references to element mobilization caused by alteration of komatiitic rocks.

Mafic metavolcanic rocks are divisible into tholeiitic and calc-alkalic varieties (*see* Appendix 2; *see* Figure 10). Tholeiitic rocks are most abundant and display REE and trace element patterns consistent with normal mid-ocean ridge basalt (N-MORB) (Figure 12). Sample 98-BRB-0743 (*see* Appendix 2) displays HREE enrichment and is similar to low-titanium basalt recognized in the Kidd–Munro assemblage by Barrie (1999b). Low-titanium basalts are generally associated with boninite lavas in the Cenozoic and are inferred to originate from partial melting of mantle that underwent a previous melt extraction (Barrie 1998). The absence of LREE enrichment, coupled with elevated uranium, thorium, cesium, barium and rubidium (*see* Appendix 2; Figure 12b), indicates hydrated basalt was the main melt component in the source region and that few sedimentary rocks were present (Barrie 1998). Barrie (1998) maintained that low-titanium basalt was unique to the Kidd–Munro assemblage, however, data in this report and data presented previously (Berger 1999) demonstrate that low-titanium basalt is present in the Tisdale assemblage. Similar processes, invoked by Barrie (1998) to account for rocks of the Kidd–Munro assemblage, are also applicable to the Tisdale assemblage.

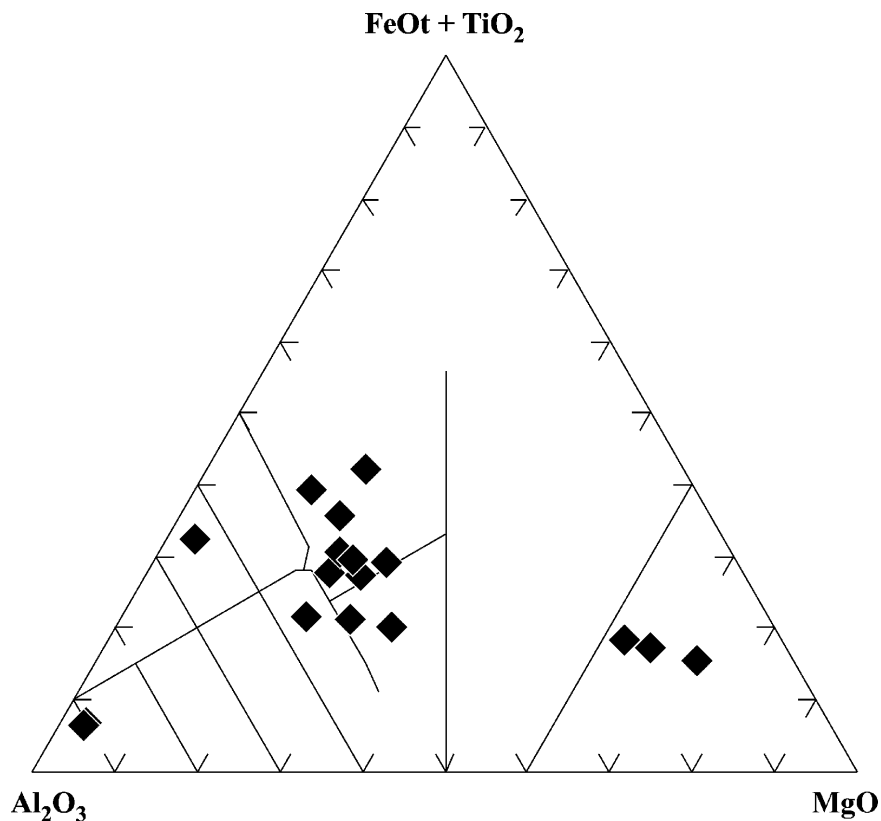
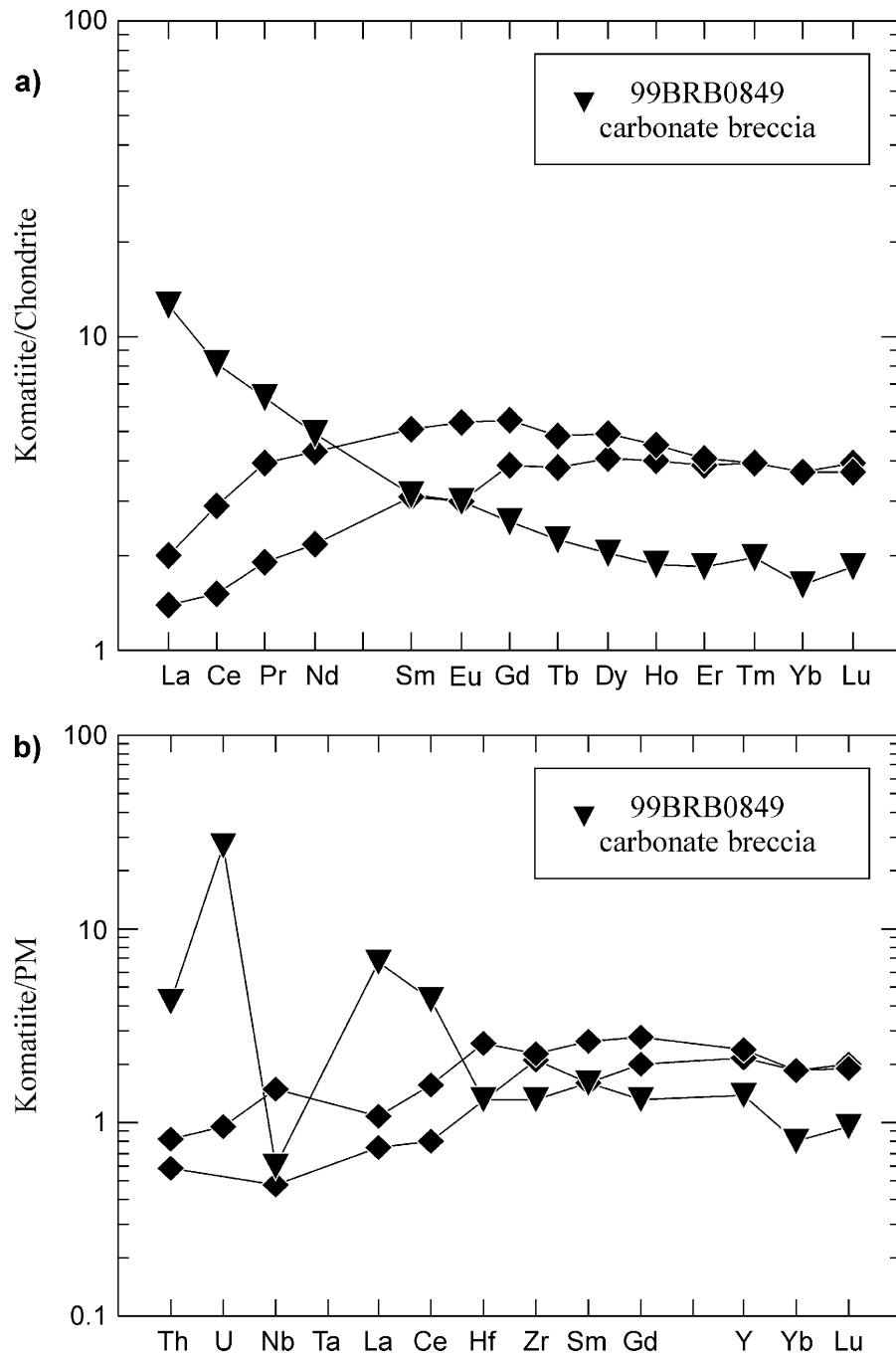
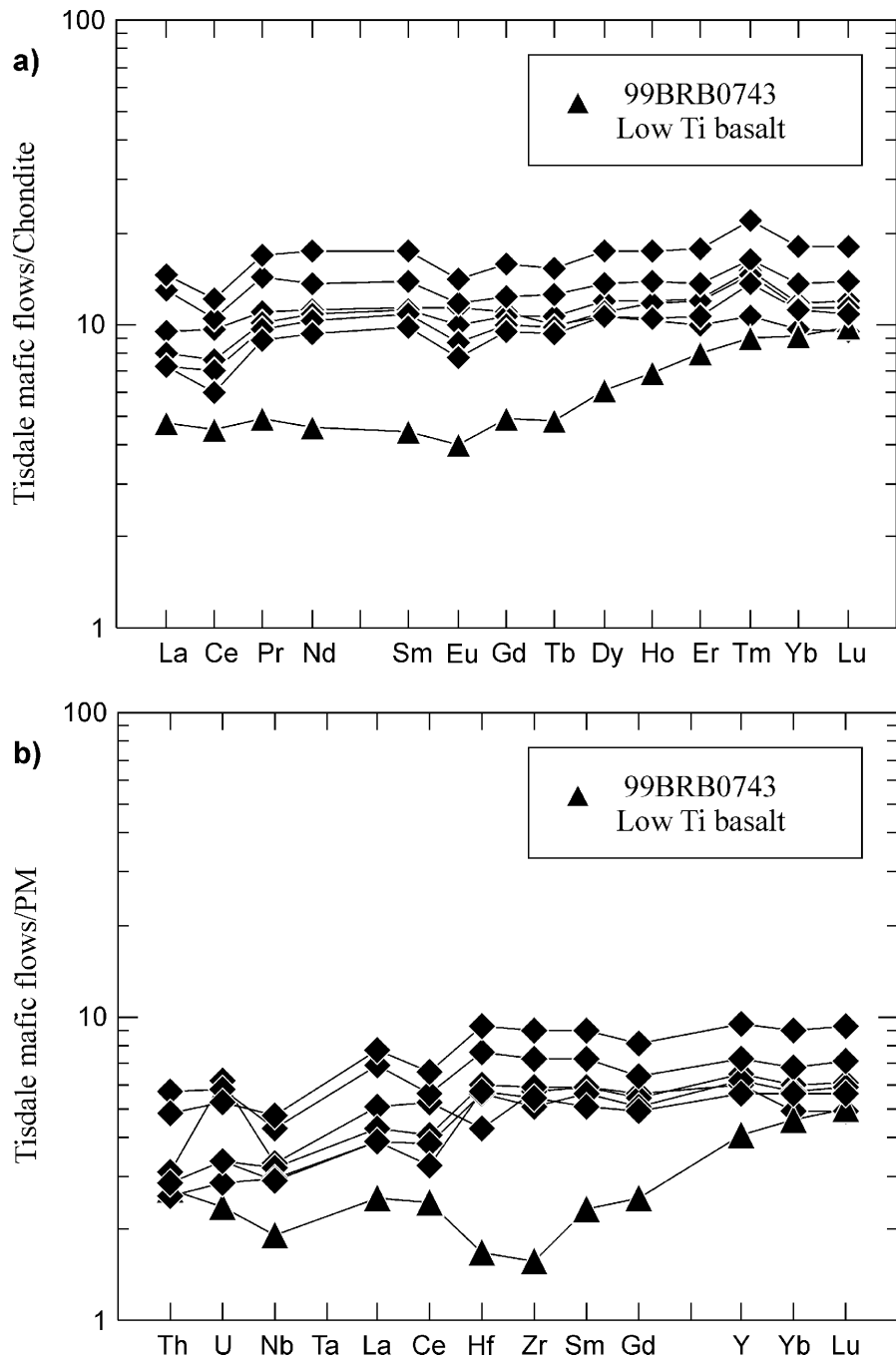


Figure 10. Jensen cation plot, Tisdale assemblage in the Highway 101 area.



**Figure 11.** a) Chondrite-normalized REE patterns, and b) primitive-mantle normalized extended element patterns for Tisdale assemblage komatiitic rocks in the Highway 101 area.



**Figure 12.** a) Chondrite-normalized REE patterns, and b) primitive-mantle normalized extended element patterns for Tisdale assemblage tholeiitic mafic metavolcanic rocks in the Highway 101 area.



Geochemical data for mafic and intermediate calc-alkalic rocks are presented in Appendix 2 and Figure 13. Mafic calc-alkalic rocks are macroscopically indistinguishable from the tholeiitic rocks in the Tisdale assemblage, however, in thin section, they contain more plagioclase than their tholeiitic counterparts. Figure 10 indicates that these rocks plot as high-magnesium tholeiite to calc-alkalic basalt, but the REE patterns show a fractionated pattern consistent with calc-alkalic rocks (*see* Figure 13a). The primitive-mantle normalized extended element patterns show pronounced negative niobium and tantalum anomalies, which are distinctly different than the tholeiitic rocks and consistent with magma derived by partial melting in a subduction zone (Figure 13b).

Felsic calc-alkalic metavolcanic rocks display fractionated REE and primitive-mantle normalized extended element patterns typical of adakite (Figures 13c and 13d; Barrie 1998). These patterns are similar to FI-type rhyolites that are believed to originate and fractionate at lower crustal levels and then ascend rapidly to surface without upper crustal level fractionation (Leshner et al. 1986; Barrie 1998). The geochemistry is similar to felsic calc-alkalic rocks in Sheraton Township that host base-metal mineralization and the Watabeag Lake area (Vaillancourt 1999c).

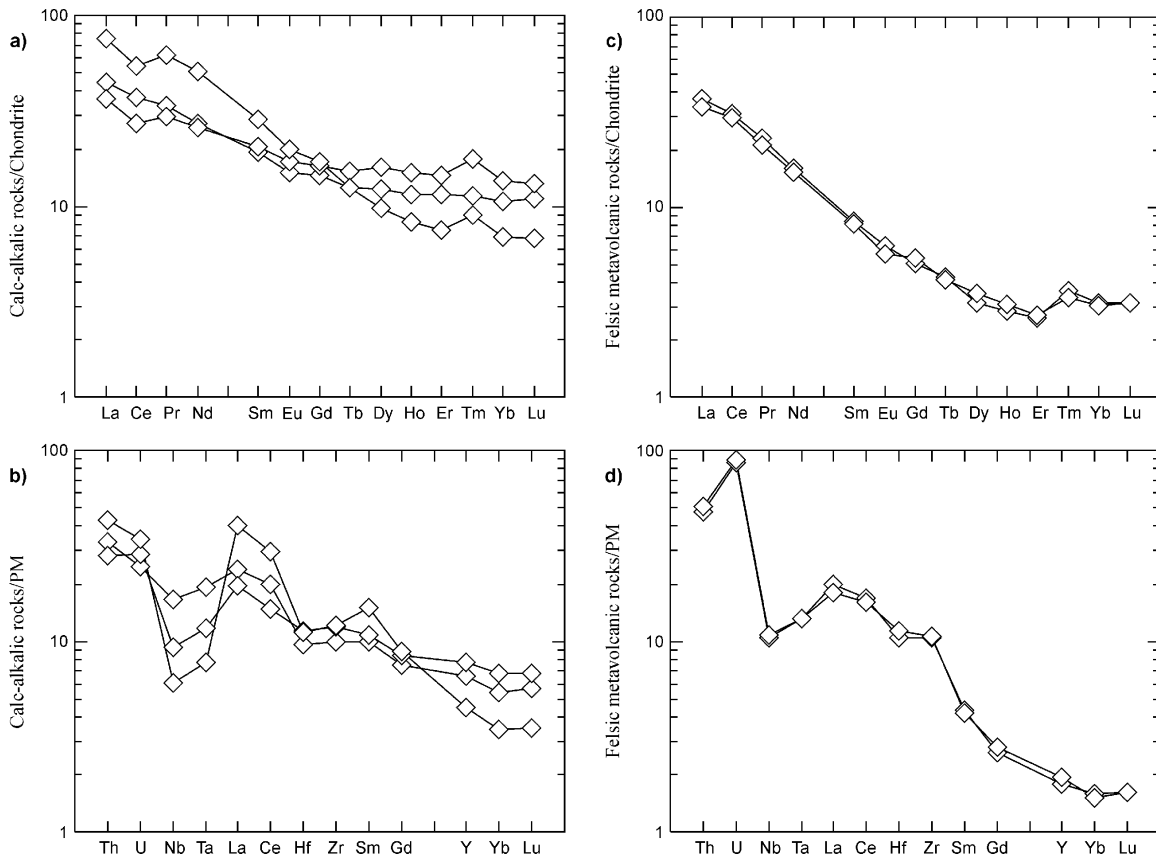


**Figure 13.** Chondrite-normalized REE patterns, and primitive-mantle normalized extended element patterns for Tisdale assemblage calc-alkalic and felsic metavolcanic rocks in the Highway 101 area.

## KINOJEVIS ASSEMBLAGE

The Kinojevis assemblage underlies the south part of the map area and includes all mafic, intermediate and felsic metavolcanic rocks south of the Porcupine–Destor deformation zone and south of the Arrow fault (local name) in Hislop Township. Wacke and argillite interbedded with the metavolcanic rocks are also included in the assemblage. Ultramafic metavolcanic rocks are unknown in the Kinojevis assemblage, unlike the Kidd–Munro and Tisdale assemblages. A U/Pb zircon age of  $2701 \pm 1$  Ma was obtained from a rhyolite flow in south Harker Township and is similar to previous ages obtained in the same area (Corfu 1993; Berger and Amelin 1999). Ayer, Trowell, Amelin and Corfu (1999) inferred that the Kinojevis assemblage is conformable on top of the Tisdale assemblage primarily due to the short time interval recorded between the 2 assemblages. The Kinojevis assemblage is dominantly tholeiitic with minor calc-alkalic intermediate metavolcanic rocks in the west part of the assemblage.

### Mafic Metavolcanic Rocks

Mafic metavolcanic rocks comprise greater than 90% of the Kinojevis assemblage and are composed of massive, pillowed, flow brecciated and variolitic flows. Massive flows are green to dark green weathering and are commonly fine to medium grained. Rare coarse-grained flows are local. These rocks are most commonly aphyric, although plagioclase phenocrysts up to 1 cm in size occur in some flows in Harker and Marriott townships. Flows are commonly 10 to 20 m thick with some flows greater than 100 m thick. Individual flows can be traced on airborne geophysics magnetic maps for a distance of several kilometres in strike length (OGS 1984l, 1984m, 1984n). A linear pattern of alternating airborne magnetic highs and lows is characteristic of the Kinojevis assemblage and was interpreted to result from alternation of high iron and magnesium tholeiitic flows (Jensen and Langford 1985). The present mapping indicates that metasedimentary rocks interlayered with high iron flows accounts for some of the linear airborne magnetic lows.

Pillowed flows are almost as common as massive flows. Pillows are typically between 50 to 100 cm long by 50 to 80 cm wide, well to poorly formed, close packed with selvages between 2 and 3 cm thick. The pillowed flows provide reliable indicators of stratigraphic “tops” throughout the assemblage. Amygdaloidal and variolitic pillows are common, however, variolitic rocks are more abundant in the east part of the map area. Some pillowed flows contain up to 15% interpillow material composed of hyaloclastite and less commonly chert. Pillowed flows commonly overlie massive flows and may be intercalated with pillow breccia.

In many areas, massive and pillowed flows pass vertically into pillowed and flow breccia units. A well-exposed area of several outcrops in central Holloway Township shows massive flows conformably overlain by pillow and flow breccia. Rounded to angular mafic clasts up to 30 cm in size, many with chilled rims, are embedded in a hyaloclastite matrix. The breccia unit is up to 15 m thick and serves as a local marker unit as it continues along strike for a distance of 1 km. In other locations, flow breccia forms discontinuous units between flows and also occurs as interpillow material or hyaloclastite. Flow and pillow breccia is much more common in the Kinojevis assemblage than in the Tisdale and Kidd–Munro assemblages.

Mafic schist at the Buffonta Mine in Garrison Township is localized in a northwest-striking shear zone that hosts the gold deposit. In the vicinity of the open pit, dark green to black amphibole- and chlorite-bearing schist is hydrothermally altered to iron carbonate, epidote and garnet with or without pyrite. The presence of garnet indicates a higher metamorphic grade in this part of the map area. The author infers that the Buffonta Mine is in the contact thermal aureole of the Garrison stock, which is less than 1 km east of the mine.

The continuity of units along strike, combined with the restricted volcanic facies of mafic flows and subordinate flow breccia and hyaloclastite, indicates that volcanism was most likely derived from submarine rifts or shield volcanoes in a basal plain environment. Jensen and Langford (1985) reached a similar conclusion for derivation of the Kinojevis assemblage. The Kinojevis assemblage is approximately 7.5 km thick in the map area, which suggests that the mafic metavolcanic rocks were rapidly extruded and preserved over 2 to 3 million years (Ayer, Trowell, Amelin and Corfu 1999; Ayer, Trowell, Madon et al. 1999).

### VARIOLITIC MAFIC METAVOLCANIC ROCKS

Variolitic flows similar to those described in the Tisdale and Kidd–Munro assemblages occur throughout the Kinojevis assemblages, but are more abundant in the east part of the map area. Massive and pillowed flows occur with individual varioles varying between 1 to 15 mm in diameter and vary in abundance between 10 and 95% of the rock. Most flows are less than 10 m thick, although some flows are up to 30 m thick as exposed in diamond-drill core. An extensive area of variolitic flows and hyaloclastite is exposed on a stripped outcrop in east-central Harker Township. Massive variolitic flows commonly display flow banding (Photo 3) and are light grey weathering and pale green on fresh surface. Varioles are 2 to 7 mm in diameter and locally comprise up to 80% of the rock. The flows are capped by hyaloclastite units with delicate primary structures preserved and local imbrication.

Variolitic flows were also observed in southwest Holloway Township near the Cochenour–Willans gold occurrence. Centimetre-sized varioles that comprise approximately 30% of the rock are coalesced along strike and up-section to approximately 95% of the rock. The felsic component of the flow is rhyolitic in composition and enriched in yttrium, zirconium and REE (*see* “Geochemistry”) similar to FIII-type rhyolites (Leshner et al. 1986). Variolitic flows also occur at the Iris deposit in south Harker Township where millimetre-sized varioles cluster around the rims of pillows southwest of the prospect.

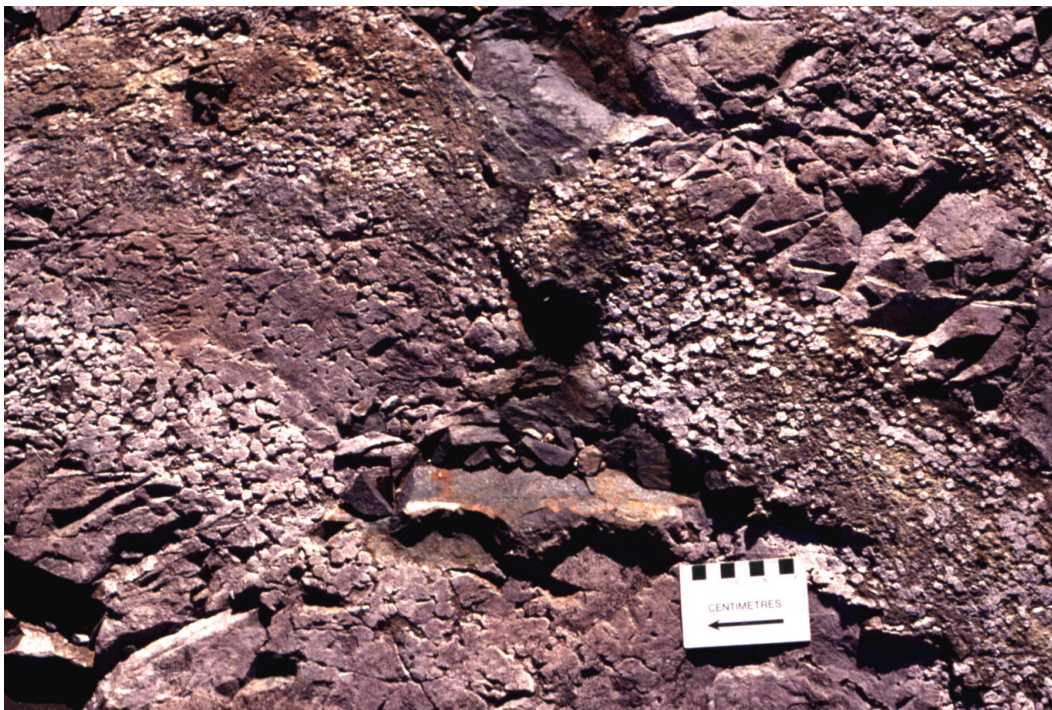


**Photo 3.** Massive and flow laminated variolitic flows from central Harker Township. Location: UTM Zone 17, NAD 27, 590927E 5370689N.

Felsic flows in this area are characterized by millimetre-sized spherules that physically resemble, and have similar geochemistry to, the coalesced varioles at the Cochenour–Willans gold occurrence. There is a strong spatial correlation with variolitic and felsic flows in this part of the map area and the author infers that many of the felsic flows are coalesced varioles.

Variolitic flows in Garrison Township contain 10 to 30% white centimetre-sized varioles in a green to grey-green basaltic groundmass. The massive and pillowed flows are best exposed at the New Buffonta gold deposit open pit, but also occur at the original Buffonta Mine approximately 750 m to the northwest. Individual varioles are most common, however, coalesced varioles are present locally. Variolitic flows are also reported in nearby diamond-drill holes and outcrop.

## Felsic Metavolcanic Rocks

Felsic metavolcanic rocks comprise less than 2% of the Kinojevis assemblage and occur as narrow units (30 to 50 m thick) that are continuous for up to 7 km along strike. Felsic flows are well exposed west of the Iris deposit adit, in south Harker Township, where primary flow laminations, autoclastic breccia, gas cavities and spherules are preserved (Photo 4). The felsic rocks weather chalky white and have an aphanitic to glassy black fresh surface. Quartz-filled gas cavities and millimetre-sized amygdules are abundant, which suggests that the original magma was highly gaseous. The lower stratigraphic contact is irregular and conforms to the underlying mafic flow breccia. There appears to have been some local mechanical mixing of material as angular felsic fragments up to 2 cm in size occur within the mafic flow. The upper stratigraphic contact is abrupt and well defined with the overlying massive mafic flows. This type of contact would not be expected if the felsic rocks were silicified basalts, which has been suggested by some explorationists. In thin section, these rocks are composed of essential and secondary quartz, plagioclase and rare opaque minerals. White mica, epidote and chlorite occur in the groundmass.



**Photo 4.** Contact between flow banded rhyolite (left of hammer) and massive, amygdaloidal rhyolite west of the Iris deposit (length of hammer is 39 cm). Location: UTM Zone 17, NAD 27, 590264E 5367678N.

Rare garnet and biotite occur in amygdules near the contact with the Iris syenite stock. Feldspar and quartz display fan extinction in some parts of the massive flows, which is indicative of rapid cooling similar to cooling features observed in high-silica rhyolites in the Abitibi Subprovince (Berger 2000a). A sample collected from the outcrop west of the Iris deposit returned a U/Pb zircon age of  $2701 \pm 1.2$  Ma (Berger and Amelin 1999).

Unit continuity of such felsic and presumably viscous magmas is controversial. In general, rhyolitic magmas form domes and flows that have limited areal extent (Easton and Johns 1986; Gibson, Morton and Hudak, 1999). Felsic flows in the Kinojevis assemblage may be related to fissure-type eruptions, however, the close spatial association with variolitic flows indicates that a process involving coalescence of varioles, similar to that observed near the Cochenour–Willans gold occurrence, is responsible. The great volume of amygdules and gas cavities in the flows at the Iris deposit suggest that the felsic magma was gas rich and had a lower viscosity than typical felsic magma. This lower viscosity resulted in enhanced flow mobility and may account for the extensive lateral distribution of the flows.

## **Calc-alkalic Metavolcanic Rocks**

Calc-alkalic metavolcanic rocks occur as narrow, discontinuous units in Holloway, Michaud and Hislop townships. These rocks weather beige to light green in contrast to the dark green to black weathering tholeiitic rocks of the Kinojevis assemblage. The units in Holloway and Hislop townships are andesitic pyroclastic deposits and flows that contain plagioclase and amphibole phenocrysts up to 7 mm in size. The pyroclastic deposits are well-bedded crystal tuff with preserved primary grain gradation and commonly amygdaloidal clasts. The Hislop Township unit is up to 250 m wide by 6 km long and is restricted to east of the Hislop fault. Prest (1957) described the unit as crystal ash tuff with rare chert fragments. Beds vary between a few centimetres to greater than 2 m thick and the author observed rare grain gradation. Intermediate flows are restricted to south Holloway Township where pillow breccia and hyaloclastite are chaotically mixed with variolitic flows. These rocks occur high in the stratigraphy of the Kinojevis assemblage and indicate that the contact with the overlying calc-alkalic Blake River assemblage is possibly transitional.

Felsic lapilli tuff and tuff breccia occur in one diamond-drill hole in southeast Michaud Township. Feldspar porphyry, quartz-feldspar porphyry and massive pyrite clasts (locally to 5%) are clast supported in a tuffaceous matrix composed of quartz, feldspar and rare argillite. The rock is interlayered with wacke and argillite, but was not observed elsewhere in the Kinojevis assemblage. The felsic unit appears to be isolated and the author is uncertain of its stratigraphic or environmental significance.

## **Metasedimentary Rocks**

Metasedimentary rocks composed of wacke, argillite and graphitic argillite are interlayered with mafic metavolcanic flows near the base of the Kinojevis assemblage. Metasedimentary units vary between tens of centimetres to greater than 500 m thick and are continuous along strike for up to 18 km (south Harker and Garrison townships). Massive to poorly bedded wacke is the most common rock type and contains beds that vary in thickness from a few centimetres to approximately 60 cm. Grain gradation is locally developed and provides reliable stratigraphic “top” determinations. Load casts, isolated lithic clasts and unequivocal Bouma sequences are rare. Most beds are fine to very fine grained and are composed of subangular to subrounded quartz, plagioclase, minor chert and lithic clasts. The wacke is matrix rich and composed of chlorite, white mica and biotite. The occurrence of biotite and rarely secondary amphibole indicates that the rocks underwent metamorphism at middle greenschist facies (Winkler 1979) especially in the vicinity of the Garrison stock and syenite stock in west Harker Township.

Argillite is pale green to dark grey, very fine grained and well indurated. Graphitic argillite is black and is well indurated to fissile depending upon the graphite content. Argillite beds are commonly laminated to 5 cm thick and rarely form units thicker than 30 cm. Disseminated and framboidal pyrite comprises from a trace amount to 5% of the rock. The graphite and pyrite account for airborne electromagnetic anomalies (OGS 1984k, 1984l, 1984m), which has been verified by diamond-drill holes sunk by various mineral exploration companies.

## Geochemistry

Geochemical analyses for 25 samples of the Kinojevis assemblage, from the Highway 101 area, are presented in Appendix 3. Whole rock geochemical analyses demonstrate the absence of ultramafic metavolcanic rocks and the dominance of mafic tholeiitic rocks in the assemblage as shown on Figure 14. Calc-alkalic rocks of the Blake River assemblage are intercalated near the top of the Kinojevis assemblage in Hislop and Michaud townships and are represented on Figure 14.

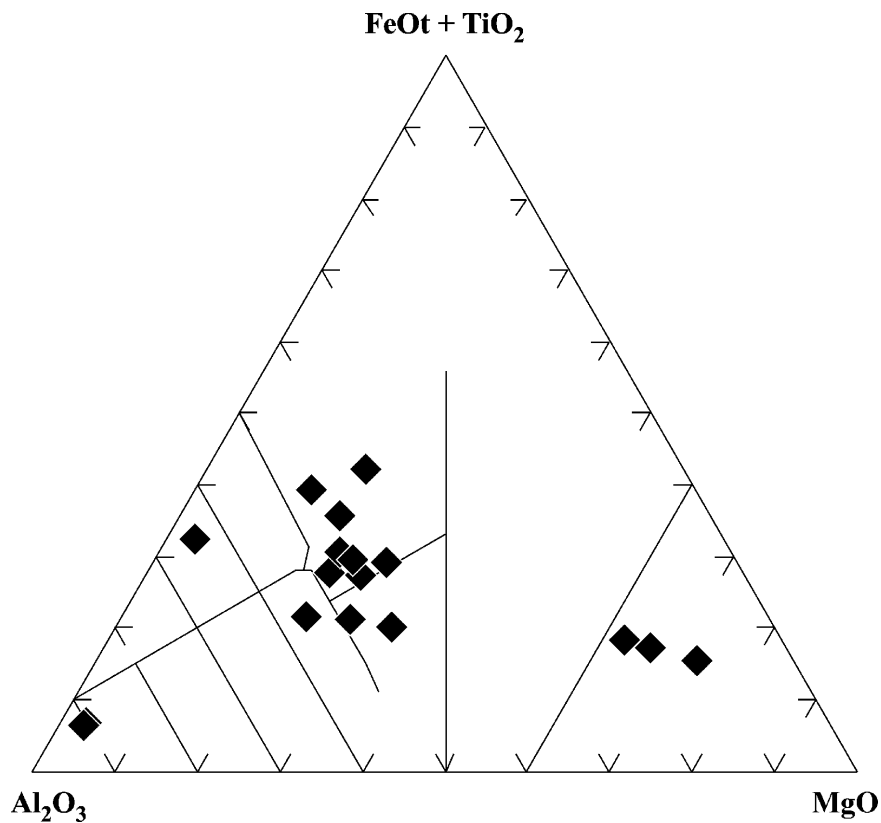
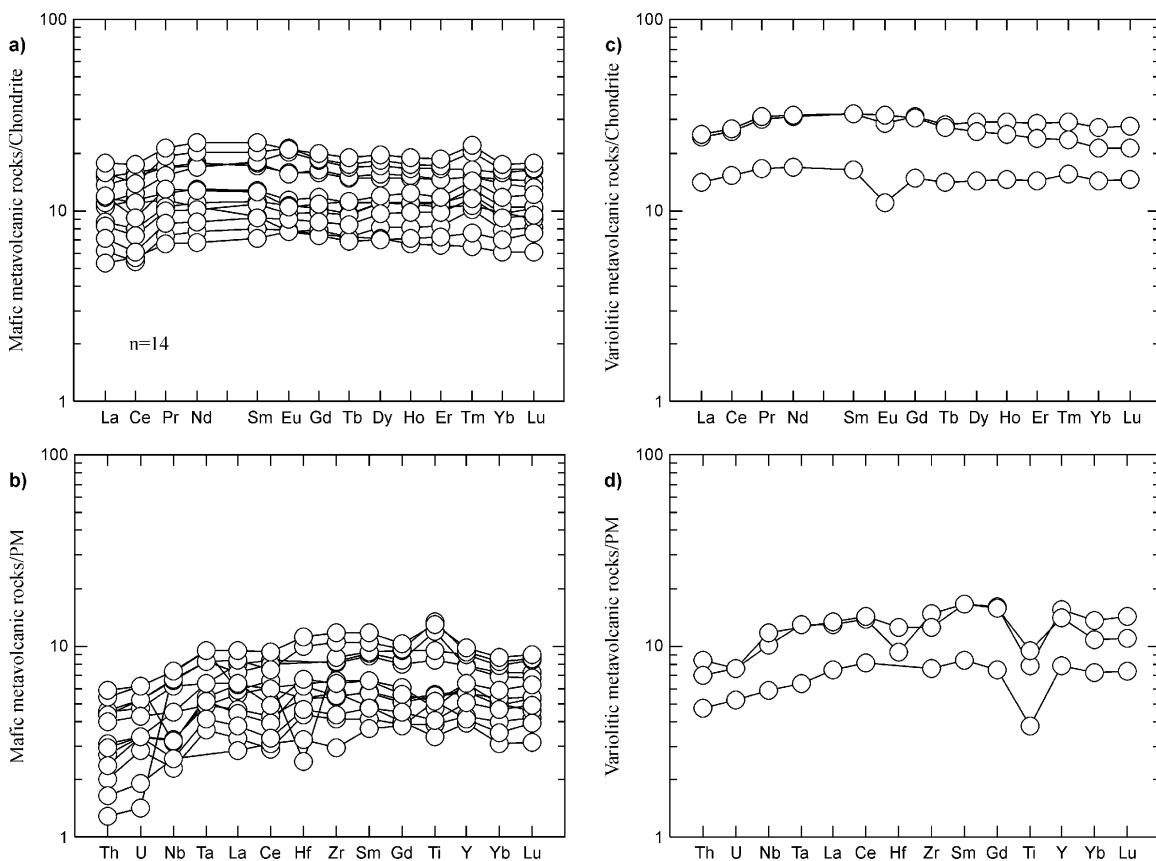


Figure 14. Jensen cation plot for the Kinojevis assemblage in the Highway 101 area.

## MAFIC AND VARIOLITIC METAVOLCANIC ROCKS

Mafic metavolcanic flows are characterized by flat chondrite-normalized REE patterns typical of tholeiitic basalt (Figure 15a; *see* Henderson 1984). All analyses are similar and mimic the monotonous field characteristics of the flows of this assemblage. Primitive-mantle normalized extended element patterns show that all flows are similar to N-MORB and there is little lateral variation along strike (Figure 15b). Jensen and Langford (1985) indicated that the basalts became more iron rich up-section, but the author did not confirm this. Kinojevis assemblage mafic flows are geochemically similar to those of the Tisdale assemblage, but contain lower total REE than mafic flows in the Kidd–Munro assemblage (*see* Figures 5 and 12).

Variolitic flows are common throughout the Kinojevis assemblage and geochemical analyses are presented in Appendix 3. Variolitic flows display flat chondrite-normalized REE patterns with or without europium depletion and contain more total REE than non-variolitic flows (Figure 15c). Primitive mantle normalized extended element patterns are similar to N-MORB and display less titanium depletion and generally lower total REE than variolitic rocks of the Kidd–Munro assemblage (Figure 15d; *see* Figure 6). Therefore, although variolites from the Kinojevis assemblage are morphologically similar to variolitic rocks in the Kidd–Munro assemblage, there are distinct geochemical differences between them. These differences may be used to distinguish members of the different assemblages.



**Figure 15.** Chondrite-normalized REE patterns and primitive-mantle normalized extended element patterns for Kinojevis assemblage mafic and variolitic metavolcanic rocks in the Highway 101 area.

## FELSIC METAVOLCANIC ROCKS

Felsic metavolcanic rocks are rare in the Kinojevis assemblage and only 2 samples were analyzed (*see* Appendix 3). The felsic flows are tholeiitic with minor negative europium and strong negative titanium anomalies (Figure 16). The rocks are similar to felsic metavolcanic rocks in the Kidd–Munro assemblage and also occur in close spatial association with variolitic flows (*see* Figure 7). It should be noted the elevated cerium in sample 97-BRB-0568 is attributed, by the author, to laboratory error.

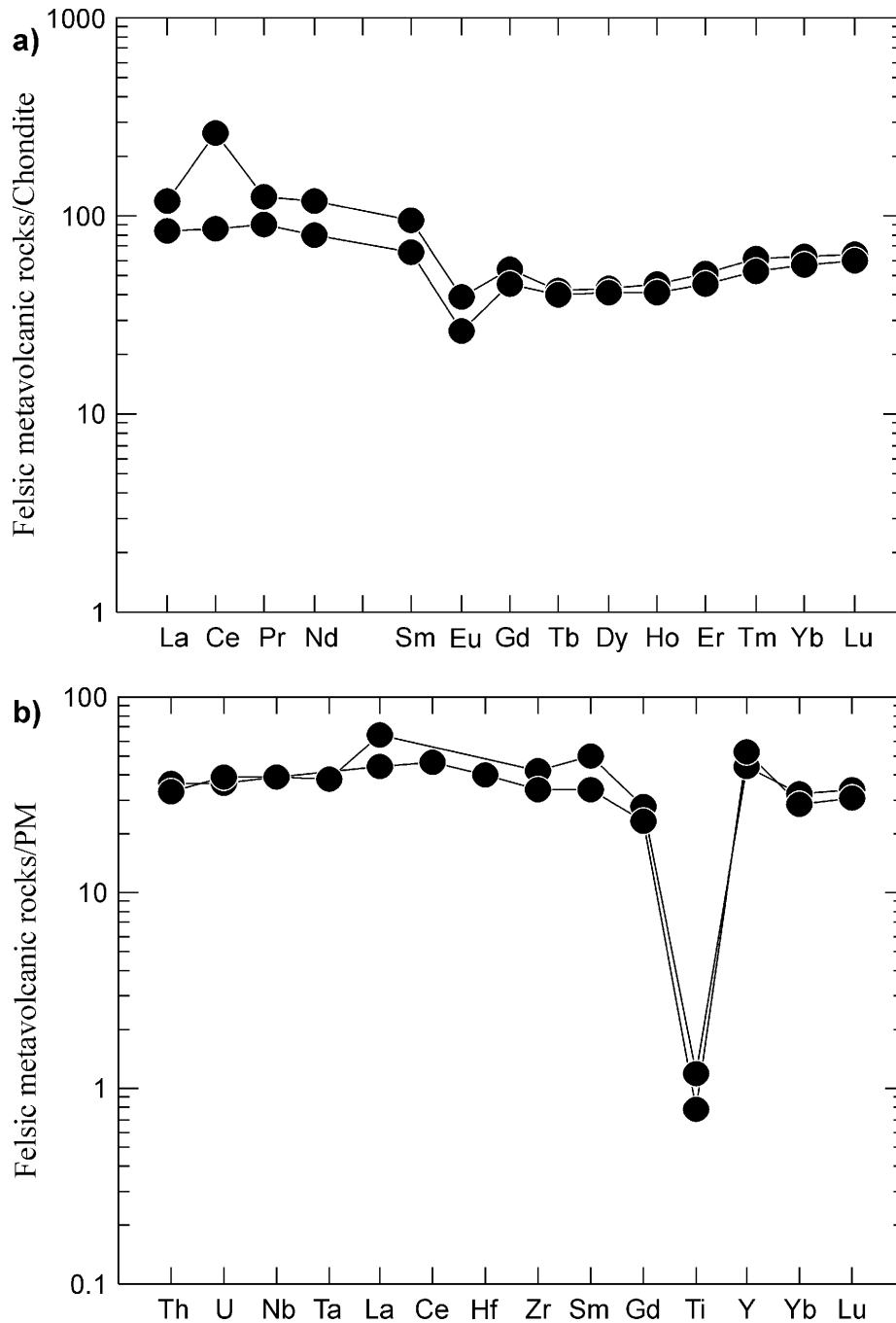


**Figure 16.** a) Chondrite-normalized REE patterns, and b) primitive-mantle normalized extended element patterns for Kinojevis assemblage felsic metavolcanic rocks in the Highway 101 area.



## CALC-ALKALIC METAVOLCANIC ROCKS

Calc-alkalic metavolcanic rocks occur near the top of the Kinojevis assemblage and are believed by the author to be intercalated units of the Blake River assemblage. These rocks are distinctly plagioclase and amphibole phyric and whole rock geochemistry (*see* Figure 14) indicates that these rocks are calc-alkalic basalt, andesite and dacite. Figure 17 shows that these rocks have fractionated chondrite-normalized REE patterns with distinct negative niobium and tantalum anomalies generally attributed to subduction-related processes (Henderson 1984). Kinojevis assemblage calc-alkalic rocks are similar to those in the Tisdale assemblage, however, calc-alkalic rocks in the Kidd–Munro assemblage generally display negative titanium anomalies, which serve to geochemically distinguish between the other 2 assemblages (*see* Figures 13 and 8).

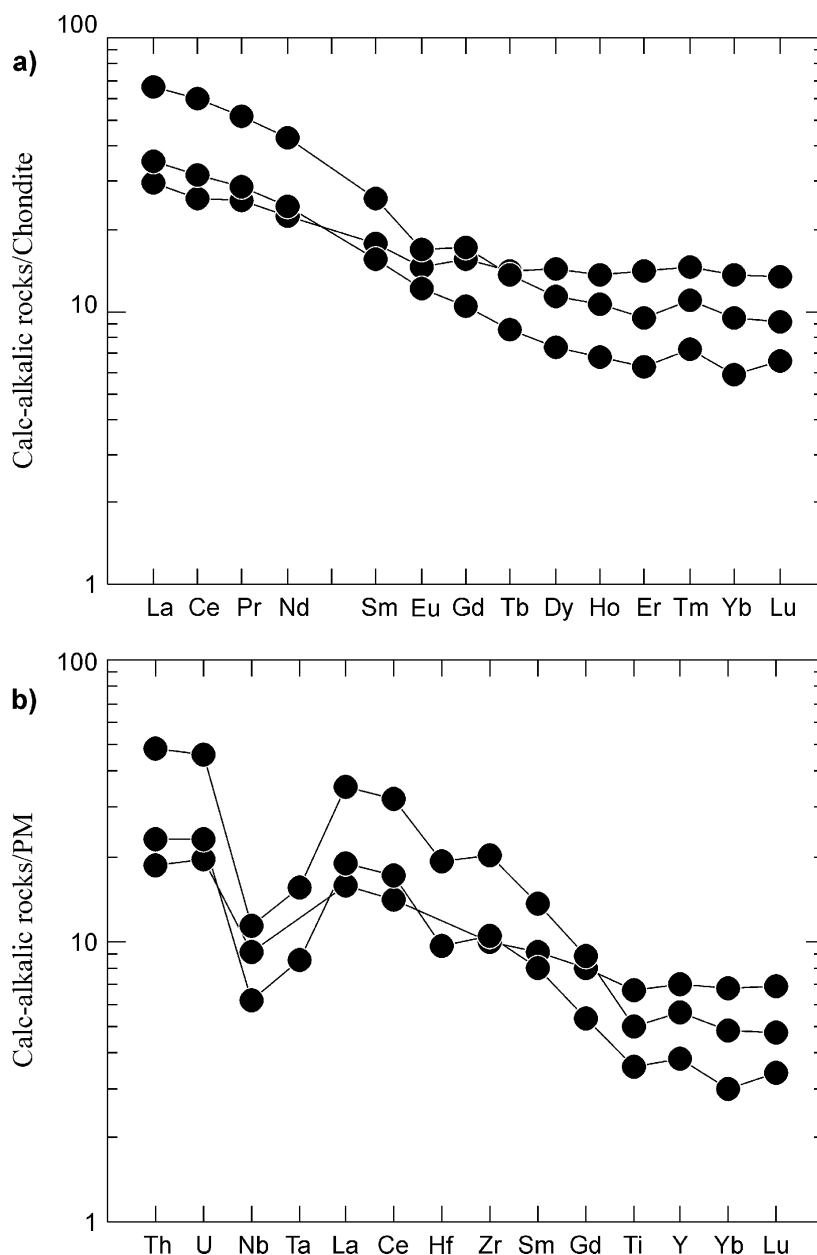


**Figure 17.** a) Chondrite-normalized REE patterns, and b) primitive-mantle normalized extended element patterns for Kinojevis assemblage calc-alkalic metavolcanic rocks in the Highway 101 area.

## PORCUPINE ASSEMBLAGE

The Porcupine assemblage underlies the northwest part of the map area and extends east to Guibord Township where the assemblage is terminated at a northeast-striking fault. The Porcupine assemblage is composed of wacke, siltstone, argillite and rare pebble conglomerate. Gabbro, quartz-feldspar porphyry, syenite stocks and lamprophyre dikes intruded the metasedimentary rocks. Rare felsic metavolcanic tuff is interbedded with the metasedimentary rocks in Beatty Township, north of the map area. Ayer, Trowell, Amelin and Corfu (1999) indicated that the Porcupine assemblage is widespread in the Abitibi Subprovince and, generally, the youngest detrital zircons are approximately 2695 million years old.

Fine- to very fine-grained wacke and siltstone are the most abundant metasedimentary rock types and commonly weather light brown to light grey with a grey to dark grey fresh surface. Graded beds 2 to 25 cm thick are common; however, massive wacke beds up to 70 cm thick were observed north of Highway 101 in Munro Township. Other common bed forms include “rip-up” argillite and, rarely, chert clasts as well as load casts. In thin section, plagioclase and quartz are most abundant; lithic fragments generally comprise less than 5% of the framework grains. Wacke is texturally immature with angular to subrounded grains that are clast to matrix supported in a white mica-, chlorite- and rarely epidote-bearing matrix. The absence of biotite indicates that metamorphism at low greenschist facies affected these rocks (Winkler 1979).

Light green to black argillite beds, a few millimetres to 5 cm thick, commonly overlie wacke beds and locally form units up to 3 m thick near the contact with the Kidd–Munro and Tisdale assemblages. Argillite beds that cap wacke are commonly laminated or massive and, as such, form the “D” and “E” subdivisions of the Bouma sequence (Walker 1992). Recognition of the Bouma sequence indicates that turbidity currents deposited these sediments in a subaqueous environment below wave base. Argillite is composed of very fine-grained quartz, feldspar, white mica and chlorite. Graphite, and less commonly disseminated pyrite, are opaque minerals that comprise up to 65% of the rock near Guibord Hill and most likely account for airborne electromagnetic conductors in this area (OGS 1984i).

Pebble conglomerate occurs near the Talisman gold mine in northern Guibord Township. The outcrop area is heavily overgrown, but the author’s observations largely support previous data collected by Bath (1990). The conglomerate is confined to a narrow interval approximately 1.5 to 2 m wide and is composed of 1 to 7 mm subangular to subrounded fragments, which are composed of chert, argillite, siltstone, felsic metavolcanic and quartz-feldspar porphyry clasts. Carbonate and sericite alteration, combined with quartz veining and rusty weathering pyrite, mask surface relationships with other rock types. Greater than 25% of the pebbles were derived from felsic metavolcanic and quartz-feldspar porphyry sources. Some of the felsic clasts are amphibole phyric and a calc-alkalic geochemical affinity is inferred. Quartz occurs as clasts; as phenocrysts within fragments; and in the matrix as detrital grains and as secondary crystals introduced by the alteration events. The silicification, combined with the carbonate and sericite alteration, mask many of the primary textures. The rock is texturally immature indicating that transportation and reworking of the fragments was not extensive.

The Porcupine assemblage has a higher ratio of argillite to wacke than similar rocks west of the map area (Berger 2000a, 2000b, 1999, 1998, 1994). From west to east in the assemblage, there is a progressive increase in the proportion of argillite and decrease in the average grain size of wacke. Turbidite beds are thicker in the west and massive sandstone units are common. The author infers west to east transport of detritus. Conglomerate units occur throughout, but are more common in the west part of the assemblage. Clast populations reflect local point source deposition into the basin, however, the wacke and siltstone units contain much more quartz and plagioclase than would be expected from erosion of a

predominantly mafic metavolcanic provenance. Geochemistry (*see* “Geochemistry”) indicates that most of the detritus in the wacke and argillite is extra-basinal, which supports the conclusion reached by Born (1995) that the major provenance for the Porcupine assemblage was a continent exposed much farther west of the map area.

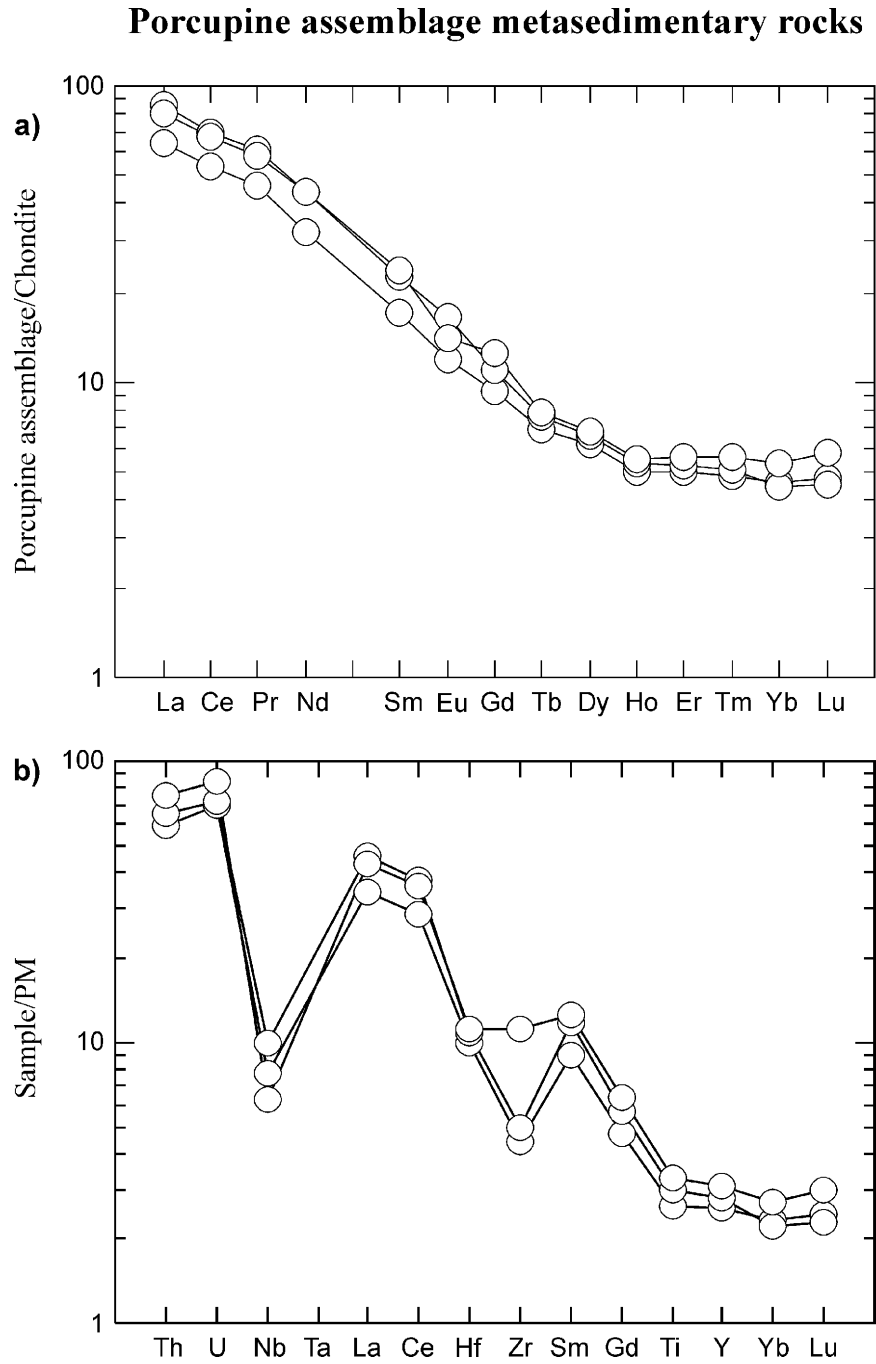


**Figure 18.** Chondrite-normalized REE patterns and primitive-mantle normalized extended element patterns for clastic metasedimentary rocks in the Highway 101 area.

## Geochemistry

Appendix 4 presents data for all metasedimentary rocks from the study area. Figure 18 and Appendix 4 show that there is virtually no difference in whole rock or trace element geochemistry among metasedimentary rocks of the major assemblages. The fractionated chondrite-normalized REE patterns,

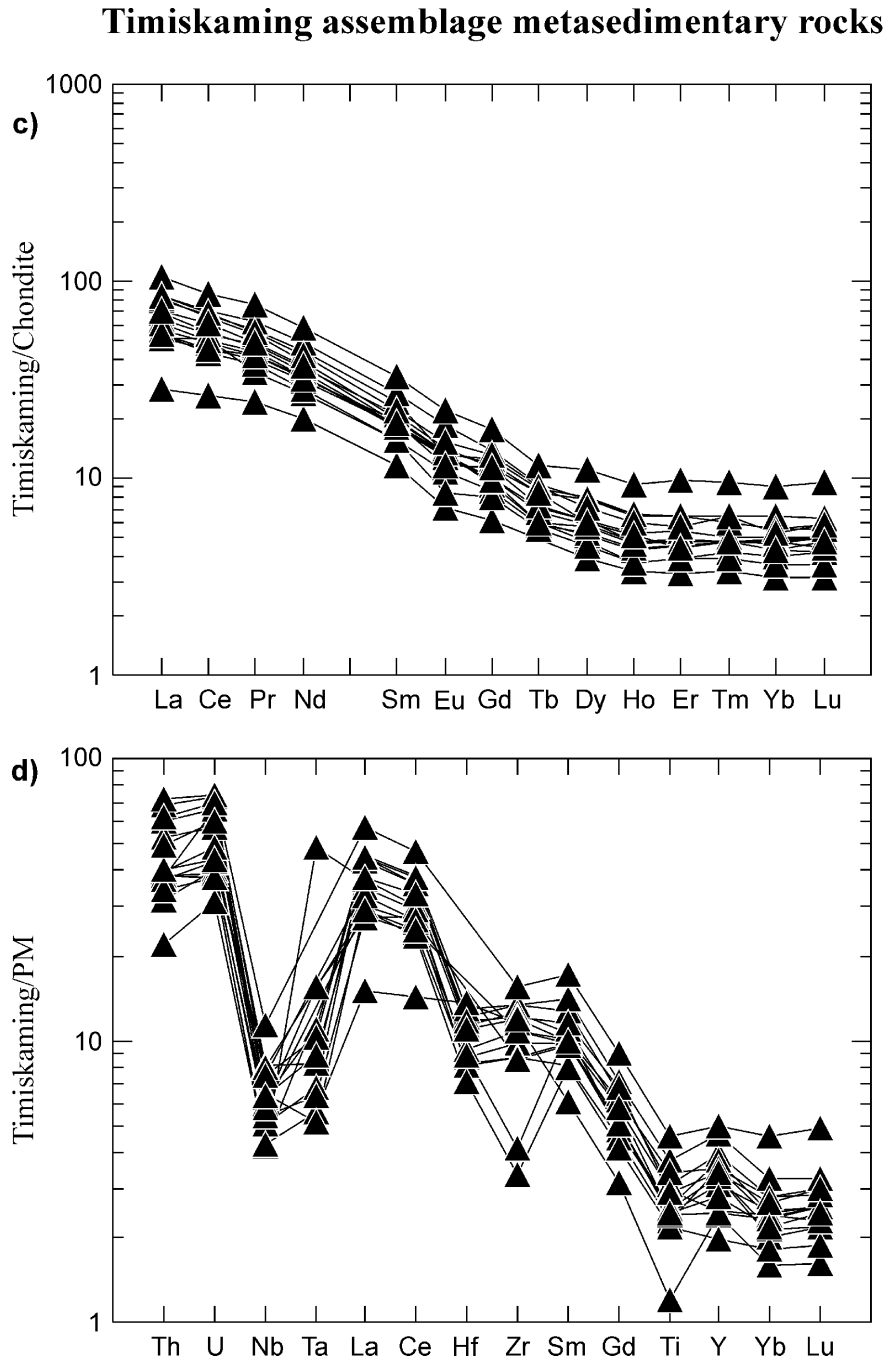


Figure 18. Continued

combined with the negative niobium and tantalum anomalies in the Porcupine assemblage, indicate that the major source of detritus must have been from calc-alkalic rocks. The high proportion of quartz and plagioclase detritus suggests a granitic source as postulated by Born (1995). Clastic metasedimentary rocks near the base of the Kinojevis assemblage display less pronounced negative niobium anomalies than in the other assemblages, which may indicate a greater contribution of detritus from the interlayered mafic metavolcanic flows (see Figures 18e and 18f).

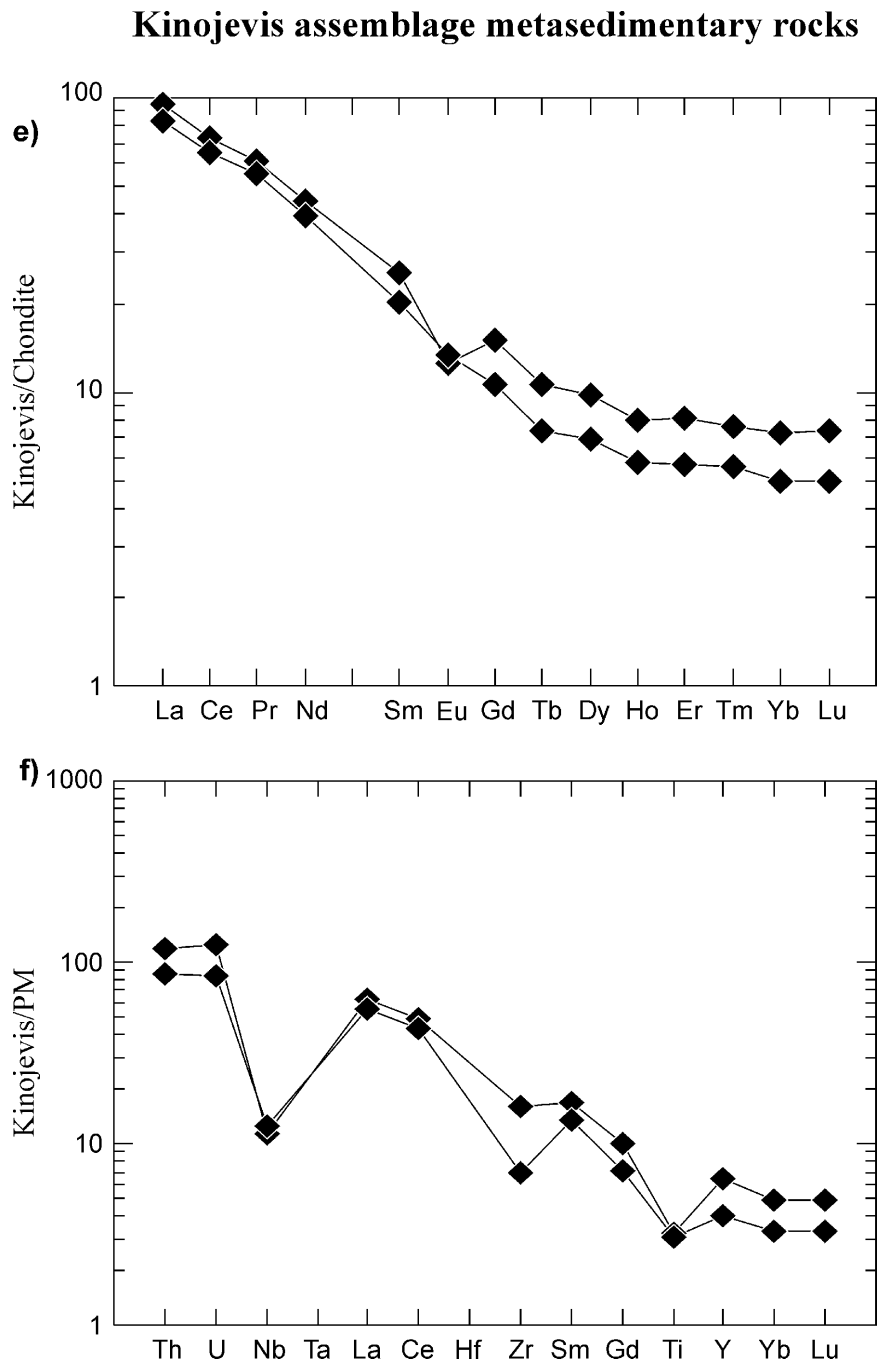


Figure 18. Continued

97BRB0847 - Ross Mine

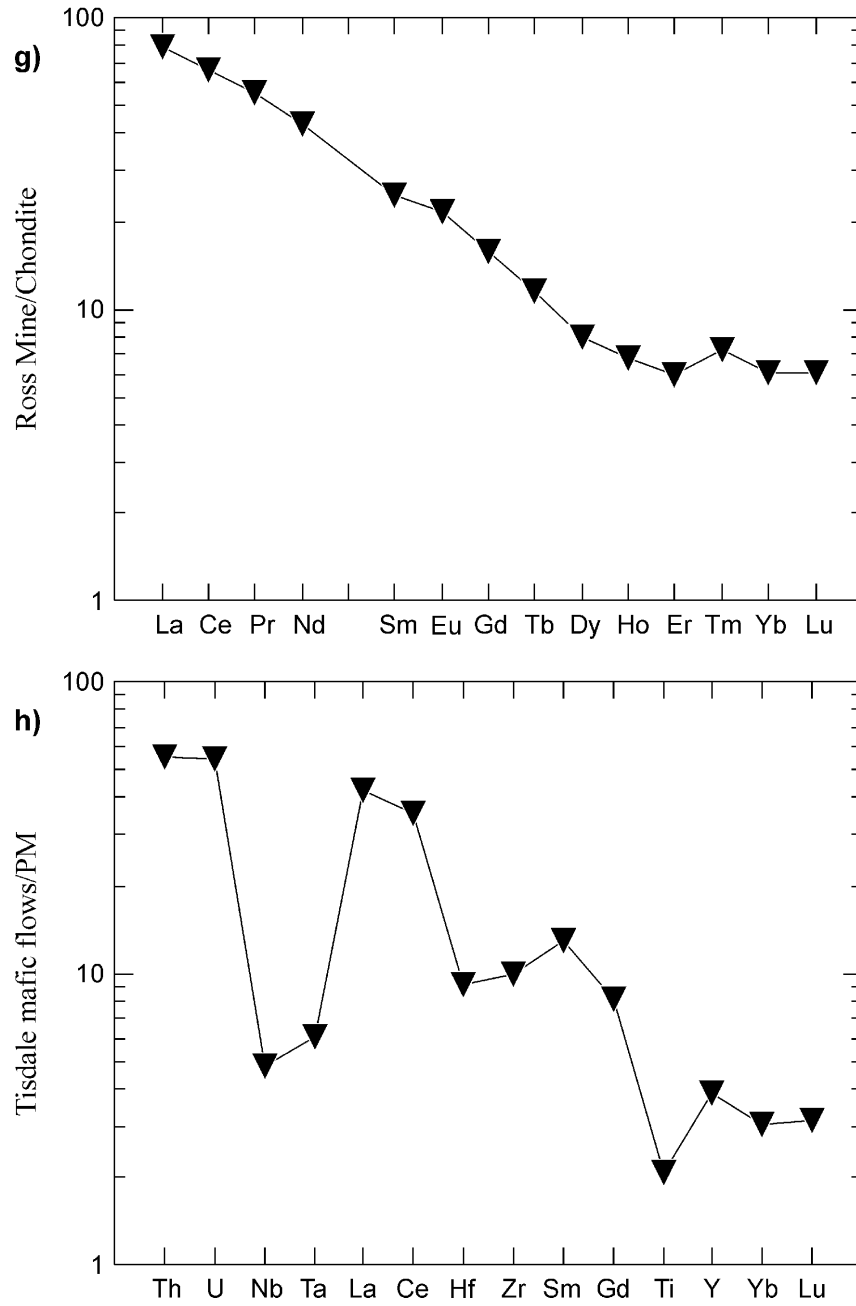


Figure 18. Continued

## TIMISKAMING ASSEMBLAGE

The Timiskaming assemblage is separated into 2 subdivisions in this report: 1) clastic and chemical metasedimentary rocks spatially associated with the Porcupine–Destor deformation zone and related faults; and 2) alkalic intrusive and extrusive rocks that are broadly coeval with the metasedimentary rocks. The Timiskaming assemblage spans approximately 15 million years in the study area. The youngest detrital zircon, separated from sandstone interbedded with conglomerate, at the Holloway Mine, returned an age of  $2684 \pm 1.3$  Ma (Ayer, Trowell, Amelin and Corfu 1999; Ayer, Trowell, Madon et al. 1999). Zircon ages of  $2678 \pm 2$  Ma and  $2671 \pm 1.5$  Ma, from the Garrison stock and from an alkalic intermineral dike at the Holloway Mine, respectively, provide representative ages for the alkaline intrusions in the study area (Corfu 1993; Luinstra and Benn 2001). The youngest detrital zircons in Timiskaming metasedimentary rocks in the Timmins and Kirkland Lake areas are 2679 million years old, whereas, zircons from Timiskaming alkalic intrusions are between  $2685 \pm 3$  and  $2673 + 6 / - 2$  million years old (Corfu 1993).

### Metasedimentary Rocks

Timiskaming assemblage clastic metasedimentary rocks, composed of conglomerate, wacke-sandstone, siltstone, argillite and schist, are closely associated with the Porcupine–Destor deformation zone from the Quebec border to Hislop Township. Metasedimentary and alkalic metavolcanic rocks that are correlated with the Timiskaming assemblage underlie the southeast part of Hislop Township, south of the Porcupine–Destor deformation zone, and display a close spatial relationship with the Hislop and Ross faults. Banded magnetite-hematite iron formation is complexly interbedded and structurally interleaved with clastic metasedimentary rocks.

Polymictic conglomerate occurs in several places in the study area. At the Holloway Mine, this rock type is characterized by rounded to subangular ultramafic, mafic and felsic metavolcanic clasts; jasper, chert and iron formation clasts; and alkalic metavolcanic and alkalic intrusive rock clasts up to 25 cm in size. This conglomerate is clast to matrix supported and generally forms units 1 to 5 m thick, however, units up to 40 m thick are present in the vicinity of the Holloway Mine. Clast gradation is absent in the thicker conglomerate units and rare in thinner units. Massive and less commonly graded sandstone is interbedded with the conglomerate and forms beds that are from a few centimetres to greater than a metre thick. The jasper and alkalic rock clasts are definitive field indicators that the conglomerate deposits are part of the Timiskaming assemblage. A local disconformity between metasedimentary and mafic metavolcanic rocks was observed in core from a diamond-drill hole situated south of the Holloway Mine head frame. This evidence further strengthens the affinity to the Timiskaming assemblage. The conglomerate units resemble Timiskaming conglomerate in the Kirkland Lake area, which are interpreted as alluvial–fluvial deposits (Hyde 1978; Mueller, Donaldson and Doucet 1994). A sample of sandstone, interbedded with the conglomerate, was submitted for geochronology and a maximum age for sedimentation of  $2684 \pm 1$  Ma was obtained (Ayer, Trowell, Madon et al. 1999). Other zircon populations at 2695 Ma and 2724 Ma were present in the sample: these ages correspond to the Blake River and Hunter Mine assemblages, respectively, which are most common in Quebec. The Hunter Mine assemblage is capped by iron formation and is the likely source for jasper clasts in the conglomerate.

Conglomerate outcrop northwest of the Holloway Mine, along the boundary with Harker Township, is foliated and crenulated, but shows many of the same features as conglomerate observed in diamond-drill core. This “north conglomerate” (local mine terminology) contains subangular to subrounded green mica clasts, quartz-feldspar porphyry, and mafic metavolcanic clasts, in a coarse sand matrix. The limited extent of the outcrop does not permit detailed assessment of the deposits, however, this conglomerate appears to reflect very local source derivation of the clasts that have undergone little reworking.

Narrow conglomerate units were observed in diamond-drill core from south Guibord Township. These rocks contain rounded to subrounded ultramafic, variolitic, argillite and jasper fragments up to 8 cm in size. Rare white albitite fragments were observed in the core of one diamond-drill hole and indicate Timiskaming alkalic rocks were uplifted and eroded in an active tectonic environment (Photo 5). Albitite is a field name applied to alkalic intrusive rocks that contain greater than 80% albite crystals. Albitite has also intruded the Timiskaming metasedimentary rocks to the east in Harker Township and to the west in Matheson and Cody townships (Berger 1994). The alkalic rocks are inferred to be synchronous with sedimentation. Wacke and hematitic argillite are interbedded with the conglomerate. Moderate to strong foliation obscures many of the contact relationships with surrounding rocks, however, these deposits appear to be more reworked than conglomerate at the Holloway Mine.

Conglomerate occurs adjacent to the east side of the Hislop fault in south Hislop Township. This conglomerate unit contains large boulders, up to 50 cm in size, composed mainly of mafic scoria, syenite, feldspar porphyry and diorite with lesser quantities of vein quartz, sulphide clasts, jasper and felsic metavolcanic rocks. The clasts are unsorted, ungraded and intercalated with hematized alkalic flows and flow breccia. The conglomerate deposits are clast supported in a sandy matrix that contains abundant chlorite. The spatial restriction adjacent to the Hislop fault; the organization of the deposits; and the association with alkalic flows indicates that the conglomerate is likely a fault scarp deposit developed in rifted shallow water to subaerial tectonic environments.

Conglomerate occurs in southeast Michaud Township at the “Southwest” zone owned by Moneta Porcupine Mines Inc. This unit is exposed in several diamond-drill holes and contains jasper, mafic metavolcanic, argillite and rare syenite clasts, up to 6 cm in size, in a coarse sand matrix. Fine- to medium-grained sandstone, commonly with pinpoint jasper chips, overlies the conglomerate. Rare grain gradation and load casts provide reliable stratigraphic indicators. The conglomerate unconformably overlies banded magnetite-hematite iron formation. In core from one diamond-drill hole, bedding in the iron formation is approximately 65° to bedding in the conglomerate and clasts of iron formation were observed in the conglomerate and overlying sandstone. More typical is the disconformable contact observed between the iron formation and conglomerate in other diamond-drill holes in the same area. These data indicate that the iron formation is older than the Timiskaming assemblage conglomerate in this area. However, sandstone interbedded with iron formation, stratigraphically below the conglomerate, also

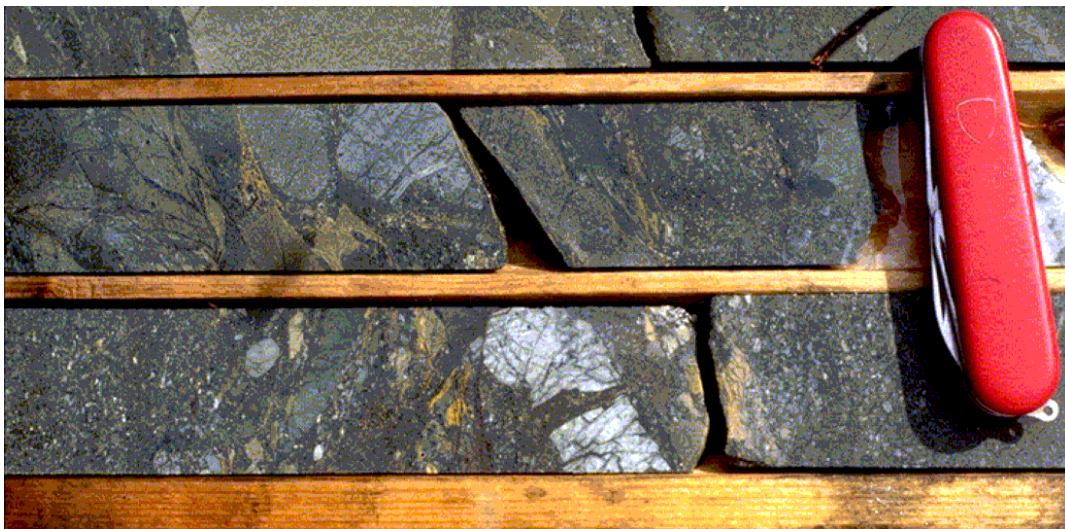


**Photo 5.** White albitite clast in Timiskaming assemblage conglomerate from diamond-drill core in Lot 6, Concession I, Guibord Township (length of knife is 8.5 cm). Location: UTM Zone 17, NAD 27, 559210E 5367999N.



contains jasper clasts and detrital microcline, which suggests the iron formation occurs within the Timiskaming assemblage. The unconformity may represent a local stratigraphic break rather than separation between the Porcupine and Timiskaming assemblages. The unconformity is significant, nevertheless, as gold mineralization is spatially associated with this contact. Recent geochronology from iron formation-bearing metasedimentary rocks east of Kirkland Lake gave an age of  $2674 \pm 4$  Ma, which is correlative with the Timiskaming assemblage (J.A. Ayer, OGS, unpublished data, 2001). The iron formation in the Highway 101 area occurs both with rock types and in a tectonic setting similar to the Kirkland Lake area. By analogy, the iron formation in the map area is inferred to be part of the Timiskaming assemblage.

Sandstone and wacke are the most common rock types in the Timiskaming assemblage. Extensive outcrop of fine- to coarse-grained, light brown weathering sandstone in Garrison Township is massive, poorly bedded and weakly to strongly foliated. Beds a few centimetres thick, rare grain gradation and argillite clasts were observed locally. Thin, discontinuous argillite beds and rare magnetite-hematite iron formation are interbedded with the sandstone. Subdivisions of the Bouma sequence were not observed, therefore, these deposits could not be definitely termed turbidites. In thin section, the sandstone is characterized by angular to subrounded quartz and feldspar grains with up to 25% lithic fragments. The lithic fragments are composed of chert, jasper, metavolcanic fragments, and felsic plutonic fragments containing microcline and myrmekitic quartz. Detrital microcline and perthite are common, but never abundant, and their presence serves to distinguish these rocks from Porcupine assemblage wacke (Photo 6). Matrix minerals are composed predominantly of chlorite with lesser amounts of white mica and carbonate.

The sandstone and wacke units extend east of Garrison Township to the Holloway Mine area, where they are known mostly from diamond-drill hole data. Drill core from widely spaced diamond-drill holes

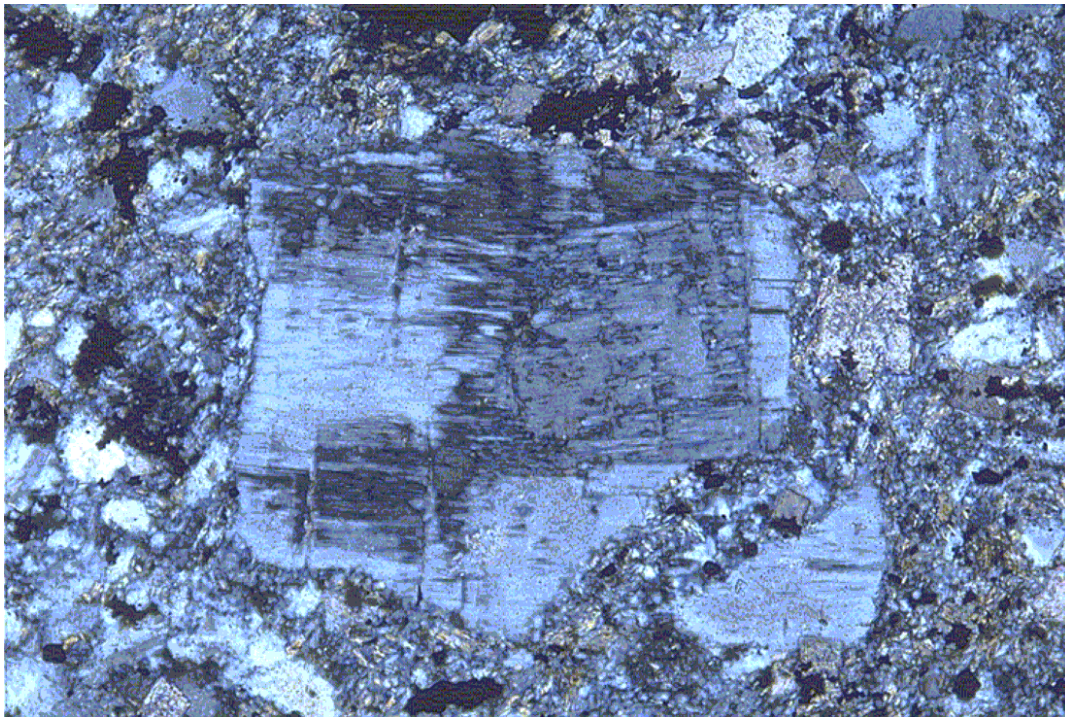


**Photo 6.** Photomicrograph of Timiskaming assemblage sandstone showing detrital microcline, Highway 101 area. Field of view is 5 mm, crossed nicols. Location: UTM Zone 17, NAD 27, 591310E 5374351N.

indicate that the sandstone and wacke are fine to coarse grained and composed of angular to subrounded quartz and feldspar grains with minor amounts of lithic fragments, principally composed of jasper and mafic metavolcanic rocks. Laminated iron formation (LIF) is local and argillite is widespread, but not voluminous. The jasper chips and detrital microcline grains identify these rocks as part of the Timiskaming assemblage.

Sandstone and siltstone underlie parts of lots 3, 4 and 5, concessions IV and V, Hislop Township. These metasedimentary rocks are fine to very fine grained, laminated to thinly bedded and massive. Light grey to green argillite is interbedded with the siltstone and locally comprises greater than 50% of the unit. These units are massive and display no grain gradation or load casts. They are strongly fractured and commonly featureless in outcrop and diamond-drill core. Quartz and plagioclase are the major detrital grains; rare argillite clasts are less than 5 mm in size and detrital microcline grains occur locally. White mica, carbonate, biotite and minor chlorite are the main matrix minerals. Apatite and zircon are common accessory minerals.

Rocks described by explorationists as felsic tuff and agglomerate in diamond-drill logs in southeast Hislop and southwest Michaud townships are inferred by the author to be pebbly sandstone, siltstone and argillite. This inference is based on petrographic and geochemical examination of samples collected from the open cut at the Ross Mine and nearby diamond-drill core. In some thin sections, the rocks are strongly altered to sericite and carbonate, however, relict detrital quartz and plagioclase grains are still visible. In other thin sections, relict trachytic textures are preserved indicating that the rocks may be intermediate alkalic metavolcanic flows.

Magnetite-hematite iron formation is closely associated with clastic metasedimentary rocks correlated with the Timiskaming assemblage. In southeast Michaud Township, laminated and thinly bedded iron formation forms units up to 1 m thick separated by narrow wacke and argillite beds up to 15 cm thick. An angular unconformity between iron formation and jasper-bearing conglomerate at the “Southwest” zone indicates that the iron formation is older than the conglomerate. However, laminated magnetite-hematite iron formation in Garrison and Harker townships form narrow discontinuous units up to 2 m thick and a few tens to hundreds of metres in strike length. Observed iron formation contacts are conformable with microcline-bearing sandstone in at least three places indicating that, in this part of the study area, the iron formation is interbedded with the sandstone. Magnetite-bearing iron formation is not present in the Porcupine assemblage and has not been observed elsewhere west of the study area to Timmins (Berger 2000a, 2000b, 1999, 1998, 1994). Magnetite iron formation is interbedded with fine-grained wacke east of Kirkland Lake. Recent geochronology indicates that these deposits are less than 2670 million years old, which indicates that Timiskaming iron formation is present. Therefore, the author infers that all iron formation in the map area is part of the Timiskaming assemblage.

The implications are that Timiskaming sedimentation involved early alluvial–fluvial coarse clastic sedimentation followed by finer grained basin-fill clastic and chemical sedimentation. Coarser grained units that eroded underlying strata periodically punctuated the finer grained portions of the sequence and resulted in iron formation fragments throughout the upper part of the Timiskaming assemblage. Uplift in response to active tectonism is inferred to control this style of sedimentation and is similar to conclusions reached for other Timiskaming-age basins in the Abitibi and Wabigoon subprovinces (Mueller and Corcoran 1998).

## **Alkalic Extrusive and Intrusive Rocks**

Alkalic extrusive rocks are very rare in the study area. Intermediate flows and flow breccia are interlayered with Timiskaming assemblage metasedimentary rocks in Lot 2, Concession I, Hislop

Township. These rocks weather earthy red to light grey and are deep red on fresh surface due to extensive hematization. Monolithic fragments, up to 3 cm in size, appear to be the same composition as the fine-grained groundmass. The flows are up to 200 m thick and are exposed for less than 300 m along strike. In thin section, most of the primary textures are masked by very fine-grained disseminated hematite, however, fragments and rare trachyte texture is locally preserved. Feldspar phenocrysts (up to 2 mm) are most common, mafic phenocrysts are altered to calcite and chlorite, and apatite phenocrysts occur throughout the rock. Geochemistry indicates that these rocks are shoshonitic trachyandesites.

Very fine-grained alkalic flows are exposed at the Garrcon deposit in Garrison Township. These strongly silicified flows are interlayered with sandstone and siltstone, but locally preserve flow laminations. The rocks weather light pink to white, are strongly fractured and are commonly brecciated with quartz flooding and specular hematite on fractures. The alkalic flows at the Garrcon deposit have limited areal extent and it is possible these flows are part of a dome complex derived from the Garrison stock, which has very similar geochemistry.

Mafic and intermediate alkalic flows are preserved as xenoliths and discontinuous units exposed in diamond-drill core from the Pangea property in Guibord Township. The mafic flows are fine grained, dark green to black and commonly contain biotite and/or amphibole phenocrysts. Intermediate alkalic flows are light grey, red and green and are characterized by potassium feldspar and pseudoleucite phenocrysts. Pseudoleucite is recognized by its distinctive octagonal crystal habit even though the original mineral has been altered to potassium feldspar and muscovite (Photo 7). Collison (1993) identified pseudoleucite in the alkalic flows near Kirkland Lake and more detail about the petrogenesis of this mineral is provided in his work.

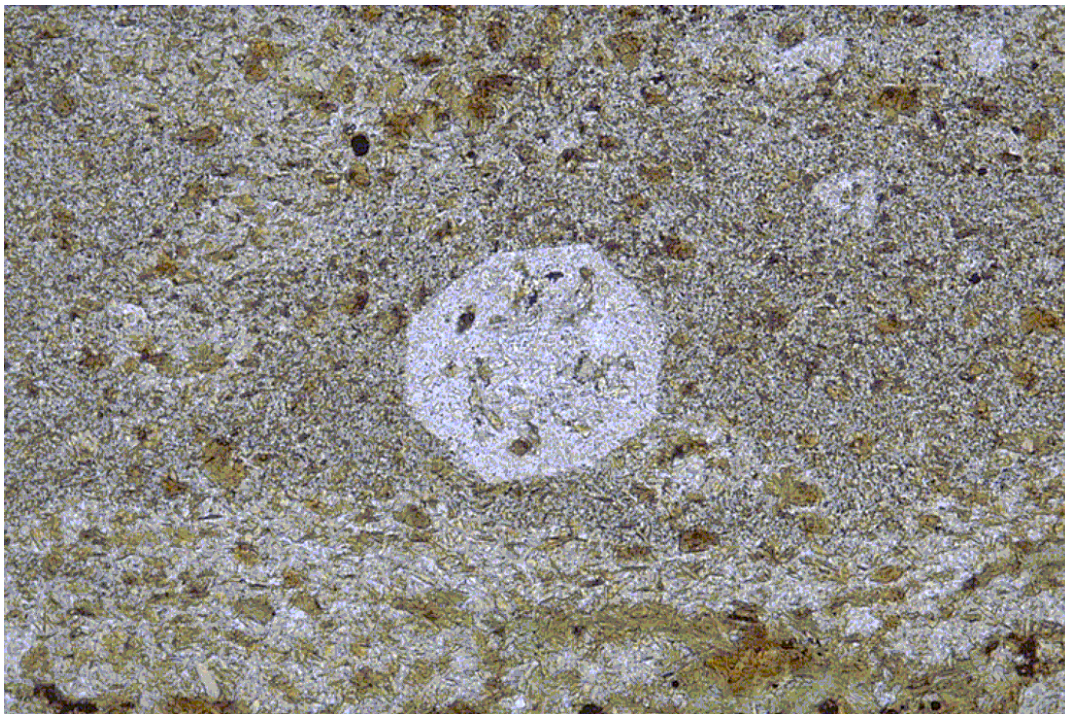


**Photo 7.** Photomicrograph of octagonal cross-section of pseudo-leucite phenocryst from intermediate alkalic flow, Pangea deposit, Guibord Township. Field of view is 2.5 mm, plane polarized light. Location: UTM Zone 17, NAD 27, 560206E 5374096N.

The alkalic flows are associated with intrusive alkalic rocks and breccia of similar composition. The breccia is characterized by different clasts: 15 to 25% mafic and ultramafic clasts, some of which contain amphibole phenocrysts; minor porphyritic syenite and intermediate alkalic flow clasts; rare greenstone clasts; and very rare feldspathoid-bearing clasts. Many of the fragments have reaction rims or have diffuse contacts indicative of reaction with fluids passing through the matrix. The matrix is composed of fine- to very fine-grained material similar in composition to the intermediate clasts. In many places, white to light grey “spots” occur that vary in size between 1 and 10 mm in size. In places, the “spots” are subhedral and appear as pseudomorphs of primary magmatic crystals. In some places, the “spots” occur in fragments and, in other places, the “spots” are anhedral and appear to be amygdules. In thin section, the “spots” are composed of aggregates of white mica and orthoclase feldspar suggesting that secondary potassic alteration affected the rock. In the core of one diamond-drill hole, white to light octahedral phenocrysts up to 5 cm in size are present and interpreted to be pseudoleucite (*see* Photo 7). The breccia unit has transitional contacts with the surrounding rock types and is interpreted to form an arcuate unit based on limited diamond-drill hole data (assessment files, Resident Geologist’s Office, Kirkland Lake). The breccia is interpreted as a diatreme related to phreatic and/or phreatomagmatic processes associated with alkaline magmatism in this part of the study area.

Recognition of the alkalic rocks strengthens the comparison between the study area and Kirkland Lake where alkalic metavolcanic rocks are well documented (Collison 1993; Hattori, Hart and Shimizu 1996). Such rocks are formed by subduction accompanied by mantle metasomatism and are analogous to alkaline rocks in the Roman Province of Italy (Collison 1993; Hattori, Hart and Shimizu 1996) (in the literature, the Roman Province is also called the Roman Comagmatic Province).

Alkaline intrusive rocks are common throughout the study area and vary in composition from lamprophyre, “pyroxenite and/or hornblendite”, monzonite, syenite and alkalic granite. These rocks may occur as isolated dikes, small dike swarms, and single-phase or multiphase intrusions up to 25 km<sup>2</sup> in extent. Lamprophyre occurs as isolated dikes and part of intrusions and is divided into 2 groups based on composition and relative age relationships. Amphibole- and biotite- and/or phlogopite-bearing lamprophyre occurs as relatively early phases of alkalic intrusions and is most commonly spatially restricted to the periphery of larger intrusions. At the Iris deposit in Harker Township, lamprophyre is black weathering, dark green to black on fresh surface and is medium to coarse grained. Black mica crystals, up to 7 mm in size, serve to distinguish this rock from other mafic phases that intruded the lamprophyre. Compositionally similar, but finer grained, lamprophyre is associated with an alkalic intrusion in northwest Harker Township. This rock, exposed only in diamond-drill core, occurs as xenoliths in syenite and as dikes in the host rocks near the northern contact of the intrusion. In thin section, the lamprophyre is composed of bladed biotite, anhedral, green pleochroic amphibole and minor epidote with plagioclase and lesser carbonate. Lamprophyre also occurs marginal to the mafic alkaline intrusion on the Pangea property in Guibord Township. Here, very fine-grained, dark green lamprophyre contains amphibole and green biotite with few opaque minerals and carbonate. It is possible that, in this location, the lamprophyre represents a chilled phased of the larger intrusion.

Narrow (up to 2 m wide), discontinuous lamprophyre dikes occur most commonly near the Porcupine–Destor deformation zone, but are also found throughout the study area. These dikes are inferred to be younger than the lamprophyre described above based on crosscutting relationships with all rock types except the Paleoproterozoic dikes, Keweenaw-age diabase and the Jurassic kimberlite intrusions. Most dikes at surface are orange brown and recessively weathered due to extensive carbonatization and less common hematization. These rocks are composed of mainly biotite and/or phlogopite phenocrysts (up to 2 cm in size in some dikes) with amphibole, carbonate, feldspar and chlorite confined to the groundmass.

Ultramafic and mafic alkaline intrusive rocks are composed of “pyroxenite/hornblendite”, alkali feldspar gabbro and melasyenite. “Pyroxenite/hornblendite” is a field name applied to dark green, medium- to coarse-grained rocks that contain clinopyroxene and amphibole phenocrysts commonly up to 2 cm in size. This rock occurs around the periphery of larger intrusions, as separate intrusions, as xenoliths in more felsic alkaline rocks, and as dikes within the supracrustal assemblages. Euhedral to subhedral clinopyroxene and amphibole phenocrysts occur in a groundmass composed of biotite and/or phlogopite, amphibole, pyroxene, titanite, apatite and albite. The presence of clinopyroxene, titanite and apatite serves to distinguish this rock from lamprophyre.

Hornblendite occurs at the Iris deposit as dikes in the Kinojevis assemblage and as a border phase to the syenite intrusion. South of the Iris stock, younger syenite dikes cut hornblendite dikes with pegmatitic feldspar pods and amphibole phenocrysts up to 2 cm in size. Hornblendite occurs along the east border of the main intrusion where it contains pyroxene and up to 15% biotite. Hornblendite is massive to weakly foliated, but magmatic layering was observed in a few places. The hornblendite is the oldest phase of the intrusion and contains abundant hydrous minerals. The author infers that the hydrous phases of the intrusion provided a pathway through the surrounding metavolcanic rocks for the later anhydrous felsic phases.

“Pyroxenite/hornblendite” comprises a major phase of the Emens Lake intrusion in Michaud Township. The rock is only exposed in diamond-drill core, from under and north of Emens Lake, so the areal extent of the intrusion is unknown. The equigranular rock is dark green, medium grained with abundant clinopyroxene, biotite and amphibole. Epidote, titanite, apatite and albite with rare microcline comprise most of the accessory minerals. The “pyroxenite/hornblendite” rarely contains ultramafic xenoliths, up to 3 cm in size, that are characterized by reaction rims composed of amphibole and bright red mica, tentatively identified as tetraferri-phlogopite (A.E. Lalonde, University of Ottawa, personal communication, 1999). The presence of such a mineral indicates the strongly alkaline nature of the parent magmas. The “pyroxenite/hornblendite” is gradational to melasyenite and gabbro, however, these rock types alternate to such an extent that units could not be separated at the present map scale.

Hornblendite, very similar to that at the Iris deposit, occurs in diamond-drill core at the Pangea deposit in Guibord Township. The dark green to black rock is medium to coarse grained, equigranular and intruded by melasyenite and syenite dikes. Andradite garnet is a common accessory mineral and, locally, titanite comprises up to 5% of the rock. Poikilitic amphibole crystals enclose pyroxene, titanite and, less commonly, epidote grains. The hornblendite at the Pangea deposit displays greater textural variation than at other localities, with pegmatitic, aplitic and equigranular textures developed and visible over a few metres of diamond-drill core. This is interpreted to indicate rapid fluctuations in volatile content and confining pressure during emplacement. Numerous mafic metavolcanic xenoliths and lamprophyre dikes characterize the contact between the hornblendite and the Kidd–Munro assemblage, indicating that the alkalic intrusion aggressively invaded the host rocks. This feature is interpreted as additional evidence supporting abundant volatiles in the magma.

Hornblendite occurs approximately 400 m east of Highway 672 in central Harker Township. The single outcrop is composed of black, medium-grained rock with greater than 85% amphibole and accessory albite, epidote, chlorite and magnetite. An airborne magnetic high corresponds to the location of the hornblendite (OGS 1984). Other high magnetic geophysical anomalies, farther west, are inferred by the author to be hornblendite as well (OGS 1984). This represents a significant change to previous mapping.

Mafic alkalic rocks are composed of gabbro, diorite and melasyenite. These rocks occur principally in the larger intrusions at Emens Lake and at the Pangea deposit. Narrow, discontinuous dikes occur sporadically in the east part of the study area, but are not common. Alkalic gabbro and diorite are dark green to light green and are generally medium grained and equigranular. Amphibole and clinopyroxene

commonly comprise more than 50% of the rock with biotite, albite, titanite, apatite and, less commonly, microcline as accessory minerals. At the Pangea deposit, titanite can compose up to 15% of gabbro and diorite, where it is in close spatial proximity to hornblendite. In thin section, euhedral and subhedral pyroxene, amphibole and biotite crystals with anhedral interstitial albite display hypidiomorphic granular to ophitic textures. Commonly, pyroxene is zoned concentrically, especially at the Pangea deposit, which is interpreted to result from rapid cooling and possible near surface retention of the magma.

The distribution of gabbro and/or diorite at the Emens Lake intrusion is poorly understood due to the limited amount of data. Nevertheless, gabbro and/or diorite is inferred to comprise a significant portion of the intrusion based on the airborne magnetic patterns (OGS 1984j) and data from diamond-drill holes. Subhedral and anhedral green pleochroic biotite comprises up to 20% of the rock and occurs as discrete crystals or as inclusions within pyroxene. Green pleochroic amphibole also occurs as inclusions within pyroxene or as individual crystals commonly with secondary epidote and biotite developed along twin planes. Gabbro and/or diorite is gradational with hornblendite and with melasyenite.

Melasyenite is a field term applied to an alkalic rock that contains 50 to 75% feldspar phenocrysts in a groundmass containing pyroxene, amphibole and biotite with accessory apatite, titanite and rare zircon. The melasyenite is common throughout the map area, but is most abundant in the Emens Lake intrusion. Melasyenite is commonly porphyritic with large euhedral feldspar crystals up to 6 cm in size. The feldspar is white to pink depending the amount of hematization in the rock. Oscillatory zonation is locally developed in the larger crystals. In thin section, the porphyritic feldspar is dominantly antiperthite and perthite is rarely developed. The groundmass is composed of albite, microcline, amphibole and biotite. Pyroxene, titanite, apatite and epidote are common, but not abundant, accessory minerals. The porphyritic texture and common occurrence of microcline serves to distinguish this rock from gabbro and/or diorite.

Intermediate and felsic alkalic rocks are composed of monzonite, granodiorite, granite and syenite. Feldspar and quartz-feldspar porphyritic dikes, spatially associated with alkalic intrusions, are located in or near the Porcupine–Destor deformation zone and are included in this suite of rocks for convenience. These rocks occur as dikes, minor phases of large plutons or comprise the major phase of smaller plutons. They are widespread throughout the study area and, although they are most abundant near the Porcupine–Destor deformation zone, they may occur at some distance from the fault zone as, for example, at the Iris deposit. Monzonite to quartz monzonite is the main phase at the Canadian Arrow deposit and a satellite intrusion approximately 1 km to the east in southwest Hislop Township. In both intrusions, monzonite is medium grained, equigranular and is light pink to pink weathering. Feldspars display strong concentric zonation and are mostly plagioclase of albite or albite to oligoclase composition, and rare microcline. Quartz is interstitial to feldspar and rarely exceeds 10% of the groundmass. Mafic minerals comprise less than 15% of the rock and are principally green to blue-green pleochroic amphibole with lesser quantities of titanite, epidote and magnetite. Accessory apatite and secondary muscovite occur in most samples of monzonite.

Monzonite comprises a minor phase of the Garrison stock in Garrison Township. Monzonite dikes at the New Buffonta gold deposit open pit are medium grained, equigranular and grey to red weathering. Euhedral amphibole comprises up to 30% of the rock and, in thin section, is partly altered to magnesium-rich chlorite. Anhedral plagioclase, quartz and rare perthite comprise most of the rest of the rock, however, sericite, carbonate and rare hematite are present as alteration products. The monzonite dikes are similar in composition to monzonite in the main part of the pluton.

Granodiorite is the main phase of the Garrison stock and is pink weathering, equigranular, and medium to coarse grained. The granodiorite is very homogenous throughout the intrusion and is generally massive, although a weak east-striking spaced cleavage is locally present. Mafic greenstone

xenoliths comprise less than 1% of the rock near the west contact of the stock and xenoliths of indeterminate composition are reported in some diamond-drill holes near the northwest contact. Albite, microcline and perthite with up to 20% quartz make up approximately 85% of the groundmass. The feldspars are not zoned and are only weakly altered. Green to blue-green pleochroic amphibole is the main mafic mineral with minor titanite and magnetite. Chlorite, epidote and rare hematite occur around the rims and along twin planes of the some of the amphibole. Feng and Kerrich (1990) estimated that the Garrison stock was emplaced under approximately 1.3 kilobars pressure based on hornblende geobarometry. The lack of feldspar zonation implies that the pluton crystallized quickly at a relatively shallow depth.

Granite occurs in several places in the central part of the map area. Granite dikes occur around the periphery of the Garrison stock and are characterized by a medium-grained equigranular texture. These dikes contain less amphibole and more quartz than the monzonite dikes in the same area. Granite occurs in the central part of an alkalic intrusion northwest of Ludgate Lake in Michaud Township. Here, the rock is white weathering, medium-grained and equigranular and is cut by many small discontinuous quartz veins and pods. The granite has hypidiomorphic granular texture with greater than 90% quartz, albite, and microcline in the groundmass. Many of the larger feldspar phenocrysts display concentric zonation; some display perthitic texture; and a few crystals display myrmekitic texture. Amphibole is the main mafic mineral with minor epidote, titanite and trace magnetite. The rock appears to be transitional to syenite farther east and south.

Feldspar porphyritic and equigranular granite comprise the main phase of an elongate pluton situated in southeast Guibord Township. Samples from diamond-drill core are pink to red, medium-grained porphyritic and equigranular. The porphyritic rocks contain square and lath-shaped perthite phenocrysts, up to 2 cm in size, in a groundmass composed of quartz, plagioclase, microcline and amphibole with accessory apatite, titanite, magnetite and secondary epidote and muscovite. Groundmass plagioclase displays pronounced concentric zoning and the large perthite crystals commonly enclose the zoned plagioclase. Porphyritic samples from the south part of the pluton contain very complex phenocryst relationships. Perthite crystals with enclosed albite also display secondary albite rims. Zoned porphyritic albite crystals locally enclose microcline and rarely display secondary microcline rims. Green pleochroic biotite is the main mafic mineral in this part of the pluton. These textures are interpreted to indicate complex crystal growth accompanied by rapid cooling during ascent of the magma to the upper crust. Equigranular granite occurs near the southwest margin of the pluton near the trace of the Porcupine–Destor deformation zone. Here, the rock is composed of 85 to 90% albite, microcline and quartz with biotite and minor secondary carbonate, chlorite, hematite and magnetite. Cataclastic textures are common around the edges of crystals and locally define a preferred orientation in the groundmass. Hydrothermal alteration expressed as secondary sericite, hematite and chlorite accompanied by pyrite is present in this part of the intrusion.

Syenite is common throughout the map area and occurs in several intrusions. Albite syenite comprises the felsic phase of the Iris stock and an intrusion approximately 4 km to the northwest in Harker Township. This red to white weathering rock is composed of coarse-grained, equigranular albite that makes up to 95% of the rock. The euhedral crystals are randomly aligned, close packed and commonly display pronounced concentric zonation. There are very few mafic minerals in the rock and those that are present are altered to chlorite and tend to cluster in the feldspar interstices. The syenite intrusion in northwest Harker Township is characterized by an airborne magnetic low anomaly indicative of magnetite depletion in this rock. In thin section, the albite syenite contains large (up to 3 cm) euhedral feldspar crystals that display albite twinning, common antiperthite and less common perthite exsolution. Albite overgrowth on several of the large phenocrysts indicates that a late magmatic or metasomatic sodic event affected the syenite. Secondary muscovite occurs in veins and around the edges of larger crystals in the northwest intrusion indicating potassium remobilization during deformation and metamorphism.

Syenite composed principally of albite occurs as a dike approximately 2000 m long by 30 m wide at the St Andrew Goldfields Limited's Hislop property in Hislop Township. The rock is mauve to pink weathering and composed of very coarse-grained feldspar with minor mafic minerals. The dike is transected and sinistrally offset by several northeast-striking faults, which created extensive fracturing and gouging of the rock. In thin section, secondary muscovite fills the cracks and fractures in albite and antiperthite crystals. Crushed zones contain angular crystal fragments of albite, microcline and secondary quartz. The rock is a primary target for gold exploration in this part of the study area.

Potassium feldspar syenite is exposed in diamond-drill core and stripped outcrop near the Ludgate Lake deposit and the "Noel zone" in Michaud Township. The syenite is pink to white weathering, medium grained and commonly displays zoned feldspar crystals. The rock is equigranular to weakly porphyritic and varies from massive to mylonitic in texture. Pegmatitic and aplitic phases occur throughout the south part of the intrusion near Ludgate Lake. Fine-grained amphibole is the main mafic mineral in the syenite; however, magnetite and tourmaline are common mafic minerals in the pegmatitic phases. In thin section, microcline occurs as individual crystals, as cores in albite rimmed feldspar, and as exsolution in perthite crystals. Albite occurs as individual crystals in the groundmass, as rims around perthite crystals, and as exsolution with microcline in perthite. These relationships indicate complex crystal growth during magma emplacement and subsequent metasomatic activity. Green to blue-green anhedral amphibole identified as magnesioriebeckite is the major mafic mineral and commonly occurs interstitial to the feldspar (Pigeon, Lalonde and Berger 2001). Rare green biotite occurs locally. Titanite and apatite are accessory minerals. Secondary quartz occurs in veins and is recrystallized in the groundmass as well.

Cataclastic textures are well developed in a mylonite at the "Noel zone" near Ludgate Lake. Equigranular syenite with minor recrystallization and crushing around the edges of feldspar grains becomes increasingly finer grained and recrystallized as the mylonite zone is approached. The margins of the zone are intensely red due to hematization, but the interior is white and very fine grained and sugary in texture. In thin section, the crystals are crushed and recrystallized commonly with a preferred orientation to the new grains. Such textures were most likely formed by ductile deformation during metamorphism (Hobbs, Means and Williams 1976).

Feldspar and quartz-feldspar porphyritic dikes occur throughout the study area, but are most common near the larger alkalic intrusions and the Porcupine–Destor deformation zone. A distinctive type of deep red weathering dike occurs in Hislop and Guibord townships north and northeast of the Ross Mine. White albite and, less commonly, quartz phenocrysts, up to 5 mm in size, are randomly aligned in a trachytic-textured groundmass composed mostly of quartz and albite. Extensive carbonate, sericite and hematite alteration occurs in veins and fractures throughout the rock and has destroyed original mafic minerals. Quartz-feldspar porphyry is reported in diamond-drill holes in northeast Hislop Township. The rocks are part of a small intrusion that extends east into Guibord Township where similar rocks were identified as syenite in diamond-drill core (assessment files, Resident Geologist's Office, Kirkland Lake). The author does not doubt that a felsic alkalic intrusion underlies this area, however, its composition is uncertain.

Albitite is a field name applied to alkalic intrusive rocks that contain greater than 80% albite crystals. White to red albitite dikes occur throughout the study area and are associated with gold mineralization at the Holt–McDermott and Holloway mines. The albitite is holocrystalline and commonly displays well-defined contacts with the host rocks suggesting that the albitite is intrusive and not just the result of intense metasomatism. Albitite dikes at the "south zone" deposit of the Holt–McDermott Mine are grey to red. Contacts are obscured by intense pervasive hematization, albitization and carbonatization. Several white to pink albitite dikes and small intrusions occur within the Porcupine–Destor deformation zone in southern Michaud Township. White, medium-grained albitite, with euhedral pyrite cubes up to



7 mm in size, occurs in diamond-drill core from the “Last Chance” zone, a gold occurrence on property owned by Moneta Porcupine Mines Limited. The albitite forms the core of the intrusion and passes abruptly to pink, altered syenite toward the contacts with the ultramafic schist host. The syenite is fine to medium grained, contains more quartz and microcline than the albitite, and contains sericite, carbonate and fine-grained pyrite veins and disseminations. The significance of this transition with respect to gold mineralization is discussed more fully below (*see* “Economic Geology”).

White albitite dikes intruded ultramafic and mafic schist at the Glimmer Mine in northern Hislop Township. Although the dikes are relatively narrow and discontinuous, they contain high-grade gold mineralization where stringer and disseminated pyrite is present (M. Hoxha, Exall Resources Limited, personal communication, 1999). The dikes also contain fluorapatite, which is very similar to albitite at the Taylor gold deposit approximately 20 km to the west (Berger 2000a).

## **Geochemistry**

### **METASEDIMENTARY ROCKS**

Geochemical data for several clastic metasedimentary rocks are presented in Appendix 4. Figures 18c and 18d indicate that the Timiskaming assemblage metasedimentary rocks are geochemically similar to other metasedimentary rocks. The negative tantalum and niobium anomalies (*see* Figure 18d) indicate that calc-alkalic to alkalic source areas supplied most of the detritus to the basin. Detrital zircons in Timiskaming assemblage wacke, collected from diamond-drill core, at the Holloway Mine, returned 3 major zircon populations with ages clustered at 2724, 2695 and 2684 Ma (Ayer, Trowell, Madon, et al. 1999). The older ages correspond to the Hunter Mine group and Blake River assemblage, both of which contain significant proportions of calc-alkalic metavolcanic rocks in Quebec (Jensen and Langford 1985). The youngest age corresponds to alkalic plutons in the map area and in Quebec. The tholeiitic components of the various assemblages are subordinate sources of detritus. Born (1995) indicated that a continental source supplied much of the sediment for the Timiskaming assemblage in the Timmins area; however, there appears to be a local metavolcanic and plutonic source for the Timiskaming assemblage in the map area.

### **INTRUSIVE AND EXTRUSIVE ALKALINE ROCKS**

Geochemical data for a number of alkalic intrusive and extrusive rocks are presented in Appendix 5. Data and some of the interpretations presented here are derived from Pigeon (2002) and readers are referred to this source for more complete discussions of the alkalic rocks in the Highway 101 area. This section will demonstrate the alkalic geochemistry of the rocks, compare the rocks to the Kirkland Lake area where alkalic magmatism is better studied, and provide some inferences into tectonic settings. There is a wide variation in alkalic rock composition from calc-alkalic to ultrapotassic (Figure 19a). Many of the rocks are strongly sodic and some, referred to as albitite in the field, contain up to 11 weight % Na<sub>2</sub>O (Figure 19b). Although alkalis are susceptible to remobilization, petrography indicates that most of the analyzed rocks are unaltered. Chondrite-normalized REE and primitive-mantle normalized extended element patterns of representative samples show 1) that the mafic plutonic rocks generally contain more total REE than felsic phases, and 2) that the felsic rocks generally display strongly fractionated patterns with flat heavy rare earth elements (HREE) (Figure 20). All samples display negative niobium and tantalum anomalies indicative of subduction-related processes (*see* Figure 20). Pigeon, Lalonde and Berger (2000) indicated that the Emens and Pangea intrusions and mafic phases of the Iris stock are nepheline normative and suggested that the high titanite content in the mafic plutonic rocks might account for their higher total REE content.

Alkalic metavolcanic rocks previously identified as mugearite, hawaiiite and benmorite occur within the Porcupine–Destor deformation zone in Holloway and Harker townships (Jensen and Langford 1985). This study confirms their presence, provides better separation of units, and identifies trachyte and trachyandesite in Garrison, Guibord and Hislop townships (*see* Figure 19). Alkalic metavolcanic rocks occur along the Larder–Cadillac deformation zone in the Kirkland Lake area and have been extensively studied (Rowins, Lalonde and Cameron 1991; Collison 1993). Collison (1993) concluded that the

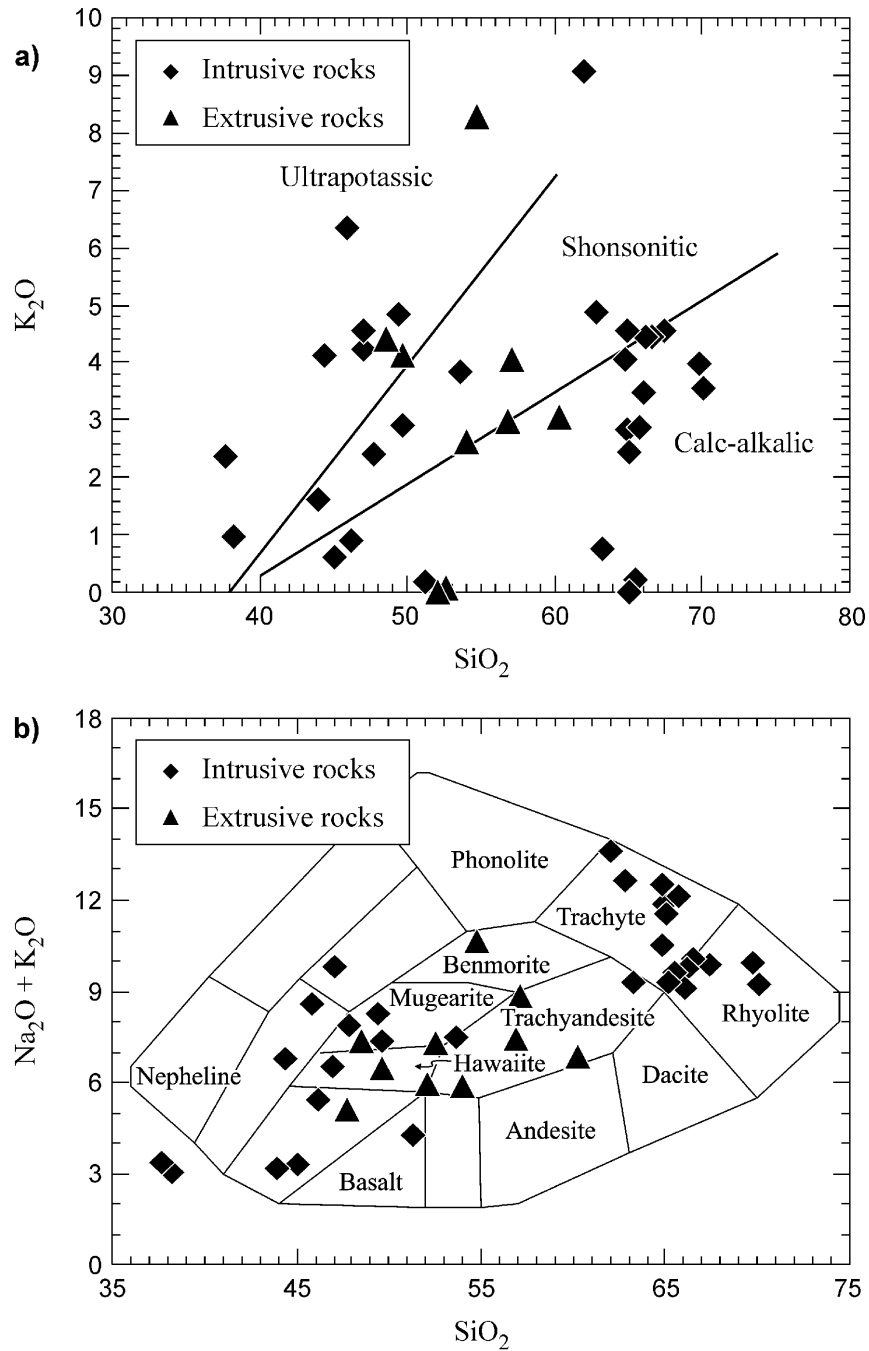


**Figure 19.** Alkalis versus  $\text{SiO}_2$  discrimination diagrams for alkalic rocks in the Highway 101 area (*modified after* Wheller et al. 1987; Peccerillo and Taylor 1976).

Kirkland Lake alkalic magmatism resulted from the final stages of subduction over stable continental crust underlain by a deep-seated Benioff zone (a term from plate tectonic theory that refers to a zone of seismic activity along the leading edge of a continental plate). Postmagmatic alteration precluded direct comparison to modern environments, nevertheless, several discrimination diagrams were used to infer tectonic setting (Collison 1993). Figure 21 summarizes data for the study area and shows that the alkalic metavolcanic rocks are similar to the Roman Province and that most rocks fall within continental to

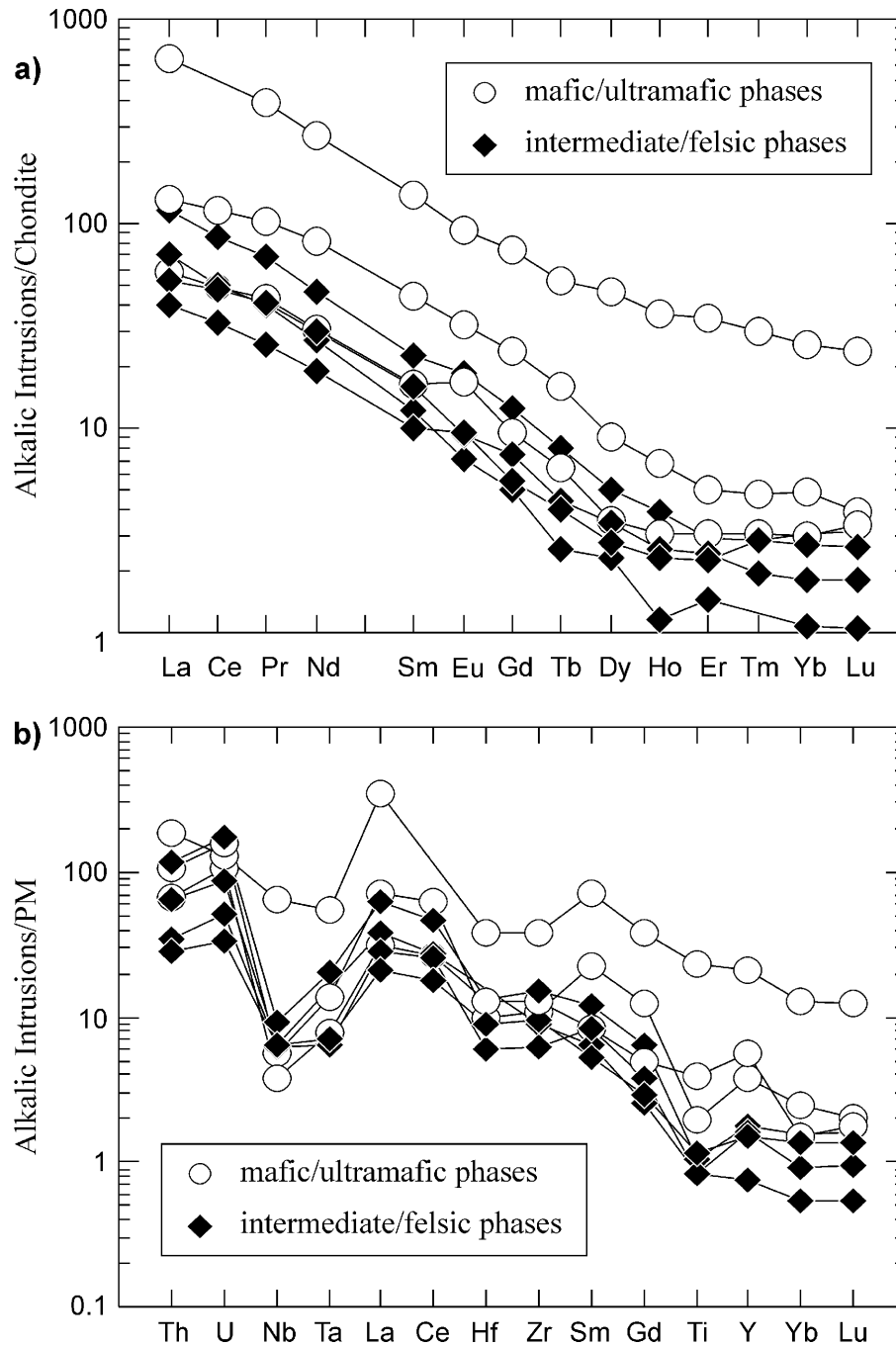


**Figure 20.** a) Chondrite-normalized REE patterns, and b) primitive-mantle normalized extended element patterns for selected alkalic plutonic rocks in the Highway 101 area.

postcollisional arc settings (Müller and Groves 2000). Trace element and REE data for selected metavolcanic rocks are similar to the Roman Province and to the Kirkland Lake area (Figure 22; Müller and Groves 2000). There is wider variation in the data than observed at Kirkland Lake, which suggests that magmatism was longer lived and spanned more than one tectonic setting. Similar trends are observed in other modern environments (Wheller et al. 1987; Peccerillo and Taylor 1976). Hattori and Percival (1999) concluded that, based on geochemistry and isotopes, alkalic rocks at Kirkland Lake and in other parts of the Superior Province originated from a depleted mantle source.

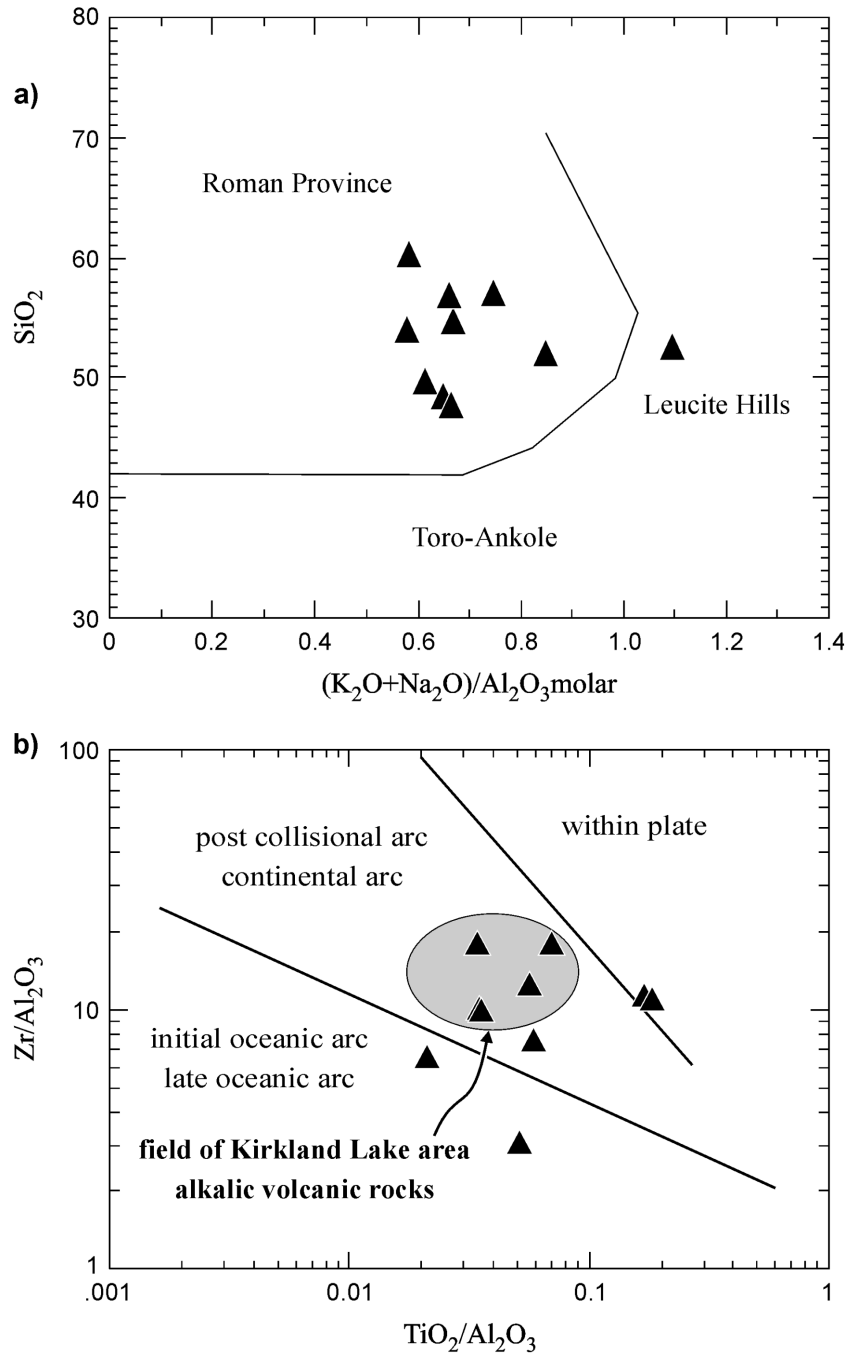


**Figure 21.** Discrimination diagrams for alkalic metavolcanic rocks in the Highway 101 area (after Müller and Groves 2000).

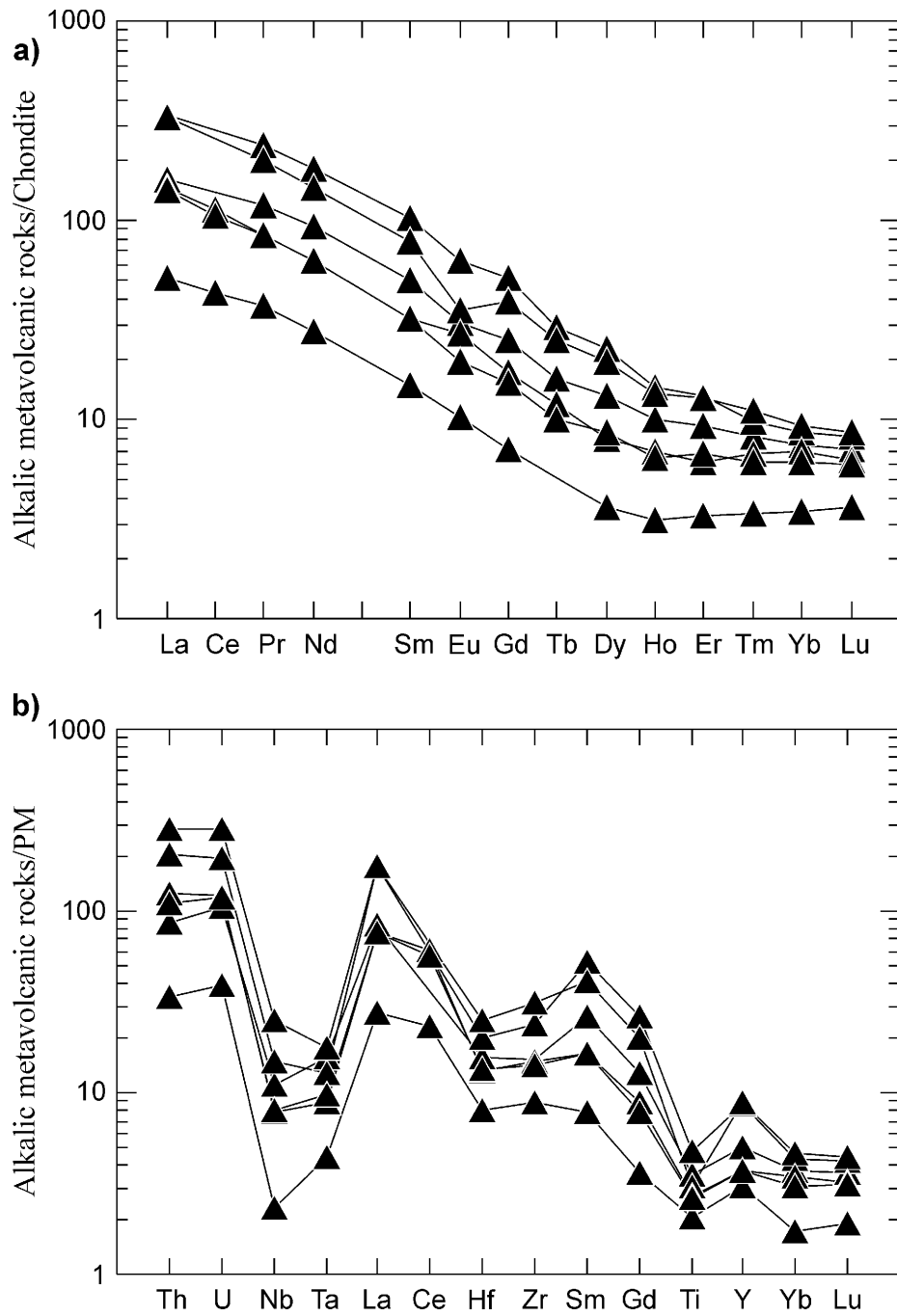


**Figure 22.** a) Chondrite-normalized REE patterns, and b) primitive-mantle normalized extended element patterns for selected alkalic metavolcanic rocks in the Highway 101 area.

## PALEOPROTEROZOIC

### Mafic Intrusions

Paleoproterozoic mafic intrusions are composed of diabase and quartz diabase dikes. North-striking dikes are correlated with the Matachewan dike swarm (Osmani 1991), and Prest (1953) recognized 2 phases. The older phase of the Matachewan dike swarm is aphyric and generally weathers dark green, black or orange brown. The rock is fine to medium grained and, in many places, is difficult to distinguish from hornfelsic basalt flows, or finer grained gabbro related to sills in the Kidd–Munro assemblage. Although the diabase is generally magnetic, it is only through petrographic or geochemical analysis that aphyric diabase can be ascertained absolutely. In thin section, diabase is characterized by subophitic-textured clinopyroxene and plagioclase ( $An_{35-52}$ ) with minor quartz, magnetite and/or ilmenite, and secondary white mica and chlorite. In most places, the primary mineralogy displays incipient alteration resulting in plagioclase having indeterminate anorthite contents by optical determinations. This suggests that the rocks were affected by weak Proterozoic or younger metamorphism.

The younger phase of the Matachewan dike swarm contains prominent white or light green plagioclase phenocrysts that comprise 1 to 50% of the rock and are from 5 to 50 mm in size. These dikes are more abundant in the west part of the study area and locally attain widths up to 50 m. The dikes contain the same mineralogy as the aphyric dikes, although graphic-textured quartz tends to be more abundant. White mica and chlorite alteration of the primary mineralogy suggests that the dikes were affected by Proterozoic or younger low-grade metamorphism.

## MESOPROTEROZOIC

### Keweenawan Age

#### MAFIC INTRUSIONS

Keweenawan-age olivine diabase is reported to occur in Garrison Township (Satterly 1949b). East-northeast-striking dikes occur in the southeast part of the township and along the Porcupine–Destor deformation zone north of the Garrison stock. A single sample was collected by the author from diamond-drill core northeast of the Garrison stock. This rock is dark green, medium grained and equigranular. In thin section, the rock is characterized by brown pleochroic clinopyroxene, plagioclase ( $An_{40-55}$ ), rare biotite, small granular olivine and magnetite. The mineralogy is similar to olivine diabase in Carr Township west of the study area and indicates that Keweenawan-age dikes are widespread.

# PHANEROZOIC

## Mesozoic

### JURASSIC

#### Kimberlite Intrusions

Satterly (1948) first noted the occurrence of kimberlite in the study area. Since then, several kimberlite dikes and intrusions were discovered as a result of gold exploration programs. Sage (1996) documented the major kimberlite occurrences in the study area and provided mineral geochemistry for some of the intrusions. All kimberlite intrusions are situated between the Arrow fault (local name) and the Porcupine–Destor deformation zone with the greatest number occurring near alkaline intrusions. Kimberlite dikes occur in Harker, Garrison, Michaud and Guibord townships. A kimberlite dike in southern Guibord Township contains ruby, microdiamond and “G-10” garnets indicative of favourable geochemistry for diamond-bearing kimberlite (Sage 2000). Kimberlite intrusions are reported in the open pit at the New Buffonta gold deposit open pit in Garrison Township, the Buzz pipes in south Guibord Township, and within the alkalic intrusion in southeast Guibord Township (Sage 1996). A U/Pb age of  $164.6 \pm 3$  Ma was obtained on perovskite from the Tandem Resources Limited kimberlite in Lot 7, Concession II, Guibord Township (Sage 2000). This is the oldest kimberlite known in the area and indicates that kimberlite intrusion spans 40 million years in the Lake Timiskaming structural zone (Sage 2000).

Sage (1996, 2000) indicated that hypabassal and diatreme facies kimberlite is most prevalent in the Lake Timiskaming structural zone and most dikes and pipes are deeply weathered and friable. The Tandem Resources Limited dike is exceptional for the pristine state of mineral preservation and excellent samples were collected for mineral geochemistry (Sage 2000). All kimberlite can be recognized by their dark grey, grey or black weathered surface. Almost all kimberlites in the area contain abundant xenoliths and xenocrysts. Xenoliths commonly consist of Paleozoic limestone, rarely with preserved coral and other fossils; greenstone; rare mantle derived fragments; and gneiss. Mineralogy is quite varied and intrusions may contain one or more of olivine, garnet, phlogopite, chrome diopside, chromite, pyroxene and ilmenite. Diamond and ruby are only known to occur in the Tandem kimberlite; other occurrences are underexplored (Sage 1996, 2000).

## Cenozoic

### QUATERNARY

#### Pleistocene and Holocene

The surficial Quaternary geology is summarized by Vagners (1985), Vagners and Courtney (1985), Baker (2000), and Baker, Seaman and Steele (1980). Aerially extensive deposits of glaciolacustrine clay and organic deposits cover much of the area. The large Munro esker, glaciofluvial outwash and reworked eolian sand dunes occur in the central part of Michaud Township (Baker 2000).

The paleotopography is quite varied and overburden thickness varies from none to greater than 90 m. Three till horizons are recognized, with the oldest till preserved only in the deepest topographic basins (McClenaghan 1991). The Matheson till is the youngest till in the area. It is aerially extensive, varies from 1 to greater than 30 m thick and is characterized by grey silt and sand with 5 to 15% clasts composed mostly of mafic metavolcanic rocks from proximal sources (McClenaghan 1991). South to southeast ice flow directions are indicated by glacial striations oriented between 150 and 190° in the map area. In Hislop Township, striae oriented 190° consistently transect striae oriented between 150° and 160°. The 2 older tills vary from 1 to 20 m thick, are dark grey to greenish and contain an average of 13% carbonate (McClenaghan 1991).

Proximal and distal varved clay, from 1 to 15 m thick, of the Barlow–Ojibway Formation overlies the Matheson till in the west part of the study area. Sand, gravel and loess of the Munro esker and its reworked members cover large parts of Michaud Township and barcan dunes up to 10 m high are a common physiographic feature (Satterly 1948).

Holocene deposits consist of swamp, lake, river and wetland deposits. Rivers such as the Ghost River in Harker Township have incised banks up to 10 m high, however, many small creeks are narrow with little or no erosion of the overburden. Extensive swamp and minor peatland occurs throughout the area.

## Structure and Metamorphism

This chapter will describe the structural features and contact relationships within and between the various assemblages. It will also describe the general features of the major and minor faults, fault zones and related structures and will try to relate these elements to mineralization in the study area. The lack of outcrop hampers a detailed analysis of all the structural features, nevertheless, geophysical data and underground investigations at the Holloway and Holt–McDermott mines by B. Luinstra (Luinstra and Benn 2001) greatly enhance this section.

### STRUCTURE

#### Kidd–Munro Assemblage

Primary volcanological features are well preserved and reversals in facings indicate that the Kidd–Munro assemblage is folded about easterly to southeasterly trending axes. In many outcrops, a layer-parallel first-generation cleavage or foliation is developed with a trend between 060 to 100° and is inferred to be axial planar to the folds. Locally, this foliation developed into a strong schistosity along the Pipestone shear zone south of Perry Lake and in the area of the Pangea deposit. It is possible that development of these faults resulted from reactivation during a later deformation event, but more detailed analysis is required. In many places, the first foliation is transected by a second northeast-striking foliation or, less commonly, a crenulation cleavage that is parallel to a set of ductile–brittle faults. In some locations, north-striking spaced fractures and joints are parallel to the Matachewan diabase dikes and correspond to brittle faults, such as the fault that transects the Garrison stock. Similar structural elements occur in the Monteith area (Berger 2000a), which indicates that this style of deformation is regional.

The Kidd–Munro assemblage is complex and composed of an intercalated, bimodal, tholeiitic and komatiitic metavolcanic suite of rocks that are separated from intercalated calc-alkalic metavolcanic and metasedimentary rock suite. The bimodal tholeiitic and komatiitic suite underlies the northwest portion



of the study area and extends west to the Kidd Creek Mine north of Timmins. The calc-alkalic suite underlies the northeast portion of the study area and is also exposed in the Swayze greenstone belt, west of Timmins (Ayer, Trowell, Madon et al. 1999). The contact between the 2 suites is conformable in the study area. In north Garrison Township, calc-alkalic lapilli tuff conformably overlies and is intercalated with massive, tholeiitic basalt. The contact between calc-alkalic metavolcanic rocks and tholeiitic plus komatiitic metavolcanic rocks is conformable as observed in core from a diamond-drill hole northeast of the Holloway Mine. This indicates that the 2 suites were not structurally juxtaposed and that different, contemporaneous magma sources contributed to the construction of the assemblage.

The contact between the Kidd–Munro and Porcupine assemblages is exposed in Lot 10, Concession I, Munro Township. Variolitic flows with segregated felsic pods are in abrupt contact with folded wacke and argillite. Foliation is similar in the metasedimentary and metavolcanic rocks, however, it is more intensely developed in the former. Metasedimentary and ultramafic metavolcanic schist occur farther along strike, to the southeast, and have been referred to as the “contact fault” (Johnstone 1991). It appears that the intensity of the foliation at the contact is a function of rock competency. The contact between the Kidd–Munro and Porcupine assemblages is structural and stratigraphic facings are unreliable. Prest (1953) and Johnstone (1991) inferred that the metasedimentary rocks of the Porcupine assemblage are older than the metavolcanic rocks of the Kidd–Munro assemblage, however, the structural nature of the contact and recent high-precision U/Pb zircon ages demonstrate that the Porcupine assemblage is younger than the Kidd–Munro assemblage (Ayer, Trowell, Amelin and Corfu 1999; *see* Table 1).

The Kidd–Munro assemblage displays complex contact relationships with the Timiskaming assemblage. Mafic and felsic alkalic rocks intruded the Kidd–Munro assemblage from the vicinity of the Pangea deposit to central Michaud Township. Metavolcanic rocks of the Kidd–Munro assemblage are intruded by lamprophyre and syenite dikes and display hornfels textures from contact metamorphism. They also display local development of intense foliation parallel to the contact. East from Michaud Township, the Kidd–Munro assemblage is in fault contact with the Timiskaming assemblage metasedimentary rocks. Ultramafic and mafic metavolcanic schist, in a discrete zone up to 100 m wide, marks the contact with Timiskaming metasedimentary rocks in north Garrison Township. From this point east to Marriott Township, Kidd–Munro and Timiskaming assemblage rocks are isoclinally folded, sheared and structurally interleaved within the Porcupine–Destor deformation zone that is up to 1250 m wide. However, south of the Holloway Mine, mafic metavolcanic flows are unconformably overlain by Timiskaming assemblage conglomerate indicating that original stratigraphy is locally preserved in weakly deformed lozenges in the deformation zone. Metasedimentary rocks are reduced to thin slivers of schist, due to intense shearing, where the Porcupine–Destor deformation zone narrows to 250 m wide from Marriott Township to the Quebec border.

Barrie (1999b) concluded that the earliest folding of the Kidd–Munro assemblage resulted in east-trending folds without associated penetrative fabrics. The oldest penetrative fabrics were developed after 2705 Ma, which is the age of the folded Warden layered sill in Munro Township (Barrie 1999b). Subsequent deformation was related to granitoid intrusion and trans-tensional tectonics related to development of large-scale crustal structures, such as the Porcupine–Destor and Pipestone faults. The author’s observations in the study area are consistent with Barrie’s (1999b) interpretation, however, the presence of northeast-striking faults are inadequately explained. The northeast structures are commonly brittle and display left lateral and vertical movement that transects other fabrics. This suggests that the structures are possibly Proterozoic or younger (Brisbin 1997). However, many of these structures are also ductile, a feature that suggests they are Neoproterozoic and related to late-stage deformation associated with the Porcupine–Destor deformation zone. The author infers that brittle gouge and deformation formed by reactivation of the faults during the Proterozoic and Paleozoic.

## Tisdale Assemblage

Structural features in the Tisdale assemblage were inferred mostly from airborne geophysical data and from the few outcrops that are visible. The assemblage is structurally complex because 1) the Porcupine–Destor deformation zone (PDDZ) bounds and transects the assemblage; 2) folding and numerous cross faults create stratigraphic and correlation complexities; and 3) numerous alkalic intrusions are present that further hamper correlation.

The PDDZ is the dominant structural feature of the Tisdale assemblage. The fault zone strikes east along the contact with the Porcupine assemblage in north Hislop Township and curves to the southeast in east Hislop and west Guibord townships. The PDDZ crosses the Tisdale assemblage through Guibord Township, then strikes east in south Michaud Township along the contact with the Timiskaming and Kinojevis assemblages. Numerous splay faults merge with the PDDZ and several satellite faults, such as the east-striking Ludgate Lake fault (local name), cut the Tisdale assemblage. Penetrative foliation associated with the PDDZ varies between 95 to 140° with steep to moderate dips to the southwest or near vertical.

Northeast-striking faults, fractures and penetrative foliation planes transect the foliation associated with the PDDZ. The east-striking Arrow fault (local name) and associated foliation also transects the PDDZ, however, it is uncertain if this structure transects the northeast-striking structures. There are several reversals in stratigraphic facings, east of the Hislop fault, which indicate that the rocks are folded about southeast-trending axes. The assemblage is homoclinal and southward younging, west of the Hislop fault.

Schistose ultramafic and mafic metavolcanic rocks are structurally interleaved with graphitic argillite and wacke within the PDDZ and mark the contact between the Tisdale and Porcupine assemblages in north Hislop Township. Stratigraphy is obscured by the deformation and the contact is structural. In central Hislop to Guibord townships, the contact between the Tisdale and Porcupine assemblages is north of the PDDZ and is well preserved in diamond-drill core and outcrop. At Guibord Hill, mafic metavolcanic rocks of the Tisdale assemblage are unconformably overlain by mafic breccia, conglomerate, graphitic argillite and wacke of the Porcupine assemblage. The rocks are weakly deformed and shearing is not evident in this area. Grain gradation in the wacke indicates that stratigraphy youngs to the north, which supports observations by Prest (1953). A stratigraphic contact between the Tisdale and Porcupine assemblages also occurs in Hoyle and Murphy townships, north of Timmins, and indicates that the unconformity is regional (Berger 1999, 1998).

The contact between the Tisdale and Kinojevis assemblages is poorly understood. West of the Hislop fault, the contact is interpreted to occur at the contact between calc-alkalic pyroclastic rocks and tholeiitic mafic rocks. Felsic and intermediate tuff breccia and tuff in Lot 5, Concession IV, Hislop Township extend west of the study area into Sheraton Township, where the tuff breccia is correlated with the upper Tisdale or Bowman assemblage (Vaillancourt 1999b). The Kinojevis assemblage appears to be in stratigraphic contact with the Tisdale assemblage with minimal structural complications (Vaillancourt 1999b). The felsic and intermediate pyroclastic rocks of the Tisdale assemblage are not found east of the Hislop fault. Troop (1985) suggested that the felsic rocks were displaced to the south in the vicinity of the Ross Mine, however, based on their geochemistry, the author believes these “felsic” rocks to be Timiskaming assemblage metasedimentary rocks. Therefore, the contact between the Tisdale and Kinojevis assemblages is unknown in this area. The author has interpreted the contact to be south of the Arrow fault (local name) and north of the Ross Mine.

The contact between the Tisdale assemblage and metasedimentary rocks of the Timiskaming assemblage is fault bounded along the PDDZ as observed in the core from several diamond-drill holes in south Guibord Township. Ultramafic and mafic metavolcanic schist is in direct contact with less deformed clastic metasedimentary rocks of the Timiskaming assemblage. Diabase dikes and rarely kimberlite are intruded along this contact. The distribution of Timiskaming assemblage metasedimentary rocks is poorly known in west Garrison Township, consequently, contact relationships and assemblage correlation is poorly constrained. The author believes that the Tisdale assemblage terminates in this vicinity, however, further data are required to confirm this inference. Timiskaming-age alkalic intrusions created narrow strain and contact metamorphic aureoles in Tisdale assemblage rocks in Guibord, Michaud and Garrison townships. Hornfels-textured basalt occurs adjacent to the south contact with the Ludgate Lake intrusion and adjacent to smaller intrusions to the west. These intrusions appear to have deflected pre-existing fold axes, caused minor intense foliation along some of the contacts, and brecciated locally the surrounding greenstone.

## **Kinojevis Assemblage**

The Kinojevis assemblage underlies the south part of the study area and is locally well exposed. In all places, the assemblage is a south-facing homocline with steep south-dipping to vertical strata. A layer-parallel to slightly discordant spaced cleavage occurs in many places and is commonly cut by a second-generation north-northwest-striking spaced cleavage. This pattern is distorted around the margins of alkalic intrusions, such as the Garrison stock, and the syenite in west Harker Township, where pillow facings suggest warping of stratigraphy into broadly open folds about northwest-trending axes. Locally, within a couple of hundred metres of the intrusion–greenstone contacts, the northwest-striking structures become ductile in the greenstone, but remain as a spaced cleavage or fractures in the intrusions.

The contact between metasedimentary rocks of the Kinojevis and Timiskaming assemblages is complex and generally fault-bounded along the Porcupine–Destor deformation zone. Diamond-drill core, from holes that penetrated the contact in south Guibord Township, display weak foliation, strong chloritization and local brecciation of the Kinojevis assemblage before passing into foliated and folded Timiskaming assemblage conglomerate and wacke. Diamond-drill core data near Holloway Lake, in the east part of the study area, indicate that jasper-bearing Timiskaming assemblage wacke is structurally interleaved with mafic metavolcanic rocks of the Kinojevis assemblage. East of Holloway Lake, weakly foliated and brecciated members of the Kinojevis assemblage are in contact with strongly sheared and hydrothermally altered ultramafic rocks (correlated with the Kidd–Munro assemblage) and sheared Timiskaming assemblage metasedimentary rocks. Most of the strain is accommodated in the metasedimentary or ultramafic rocks.

## **Porcupine Assemblage**

The Porcupine assemblage consists of turbiditic metasedimentary rocks that are best exposed in north Guibord and south Munro townships. Bedding is west-northwest-striking and overturned with east-northeast-younging directions. Facing reversals are reported in diamond-drill data and are consistent with data to the west that indicate the assemblage is folded about east- to southeast-trending axes (Berger 2000a, 1999, 1994). In most outcrops, a first-generation spaced cleavage to penetrative foliation is subparallel to bedding or rotated 10 to 15° counterclockwise to bedding. This foliation is axial planar to mesoscopic, northwest-closing folds at or near the contact between the Porcupine and Kidd–Munro assemblages. In many places, a second-generation foliation to spaced cleavage is oriented between 40 and 65°. In rare instances, for example, at the Talisman gold mine in Lot 7, Concession VI, Guibord

Township, a dominant east-striking foliation is accompanied by carbonate, green mica and sericite alteration.

The contact between the Porcupine and Kidd–Munro assemblages is structural as described above. Tightly folded Porcupine assemblage wacke and argillite are confined to a narrow zone, up to 50 m wide, adjacent to the Kidd–Munro assemblage. At outcrop scale, structures are approximately parallel in the Kidd–Munro and Porcupine assemblages, however, at map scale, volcanic units are truncated by the contact. At the regional scale, this contact is always marked by a fault or deformation zone, such as the Pipestone fault to the west (Berger 2000a), the “contact fault” northwest of the study area (Johnstone 1991), or several small faults and shear zones west of Frederick House Lake (Berger 2000b, 1999).

The contact between the Porcupine and Tisdale assemblages is partly stratigraphic and structural in the study area. From Guibord Hill west to Hislop Township, the contact is marked by a local basal conglomerate and graphitic argillite in stratigraphic contact with basalt. Through Hislop Township, the contact is coincident with the Porcupine–Destor deformation zone and is marked by ultramafic and mafic metavolcanic schist in contact with graphitic schist and sheared wacke. This type of contact persists west of the study area to the vicinity of the Aquarius gold mine in Macklem Township, where the Porcupine–Destor deformation zone no longer coincides with the contact (Berger 2000a; Muir 1995). In Hoyle and Murphy townships, north of Timmins, the Porcupine assemblage unconformably overlies the Tisdale assemblage, but the contact is also sheared in many locations (Berger 1999, 1998). These observations demonstrate that the Tisdale assemblage is the regional substrate to the Porcupine assemblage and that the 2 assemblages are autochthonous.

## Timiskaming Assemblage

The Timiskaming assemblage is composed of 2 members: 1) a metasedimentary and alkalic metavolcanic rock member, and 2) an alkalic intrusive rock member. Structures in these members were developed after 2685 Ma, the maximum age of sedimentation in the assemblage (Ayer, Trowell, Amelin and Corfu 1999). The metasedimentary and alkalic metavolcanic rocks are largely confined to the Porcupine–Destor deformation zone (PDDZ) in the east part of the study area and show a close spatial relationship with north-northwest-striking faults and deformation zones in Hislop and southwest Guibord townships. Timiskaming assemblage rocks in the PDDZ are variously deformed. Metasedimentary schist occurs throughout the assemblage, however, moderately and weakly foliated rocks are common. Locally, there is excellent preservation of depositional features such as cross-bedding, grain gradation and weakly strained clasts in conglomerate. In most outcrops, a layer-parallel foliation is evident. A moderately northeast-plunging crenulation cleavage with “Z” asymmetry is developed in the metasedimentary and adjacent metavolcanic rocks in the Holloway Mine area. Reversals in stratigraphic facings indicate that tight to isoclinal folding about east-striking axes affected the metasedimentary rocks in this part of the PDDZ. In most places, this deformation was so intense that transposition of rock units occurred along fold axes and limbs. The resultant map pattern is wedge-shaped rock units throughout the PDDZ. This deformation is referred to as  $D_1$  in the Holloway Mine by Luinstra and Benn (2001). The entire package of supracrustal rocks throughout the region, from Timmins to the Quebec border, were tilted to near vertical and folded prior to development of the PDDZ in the study area.

Well-preserved lozenges (*see* Colvine et al. 1988, p.16) of less deformed rocks occur in several places within the PDDZ. In one such area, south of the Holloway Mine, Timiskaming assemblage conglomerate unconformably overlies and contains clasts of Kidd–Munro assemblage mafic metavolcanic flows. Timiskaming assemblage conglomerate unconformably overlies and contains clasts of magnetite-jasper iron formation in southeast Michaud Township. Iron formation clasts throughout the Timiskaming assemblage metasedimentary sequence indicate that the iron formation was exposed to erosion prior to

and during deposition of the Timiskaming assemblage rocks. Timiskaming assemblage conglomerate and intermediate alkalic flows unconformably overlie and are in fault contact with Kinojevis assemblage mafic metavolcanic rocks in Hislop Township east of the Hislop fault. These unconformities are significant because they indicate that tectonism occurred prior to and during deposition of the Timiskaming assemblage metasedimentary rocks. Mueller et al. (1996) indicated that there was a tectonic influence on sedimentation in the Timiskaming basin at Duparquet, Quebec, which is consistent with observations in the study area.

Data are very sparse in southwest Guibord and central Hislop townships and interpretation is further hampered by intense hydrothermal alteration in the Ross Mine area. However, the map pattern and limited outcrop suggest that the Timiskaming assemblage metasedimentary rocks are folded and fault bounded in this part of the study area. Additional work east and west of the Ross Mine is required to define rock types, geochemical affinities, contact and structural relationships.

Alkalic intrusive rocks comprise the second member of the Timiskaming assemblage. Most intrusions occur within or near the PDDZ, however, isolated intrusions (e.g., the Iris stock in Harker Township) occur up to 7.5 km south of the fault zone. Alkalic intrusions are rare or absent north of the Arrow fault (local name) and the PDDZ. Several of the intrusions correspond with northwest-striking airborne geophysical magnetic lineaments and many of the intrusions are elongated along a northwest-striking axis. Geochemistry indicates that these magmas were derived from deep-seated magmas, which suggests that the present distribution of intrusions reflects proximity to original crustal-scale structural conduits that are south dipping in the study area. These observations also suggest that some of the northwest-striking faults were probably active in the Archean and also penetrate the deep crust.

An early east-striking spaced cleavage is transected by north-northwest to north-northeast-striking fractures, quartz veins and rare mylonite zones. Contacts between intrusions and supracrustal rocks are generally abrupt, but numerous dikes may occur around the peripheries of the intrusions. The north and parts of the south contact of the Ludgate Lake intrusion (Michaud Township) are sheared and characterized locally by intrusion breccia. The north contact of the Pangea intrusion with mafic metavolcanic rocks of the Kidd–Munro assemblage is abrupt, although numerous lamprophyre dikes extend into the supracrustal rocks. The contact between the Pangea intrusion and the Porcupine assemblage is fault bounded. Contact metamorphism around the intrusions hardened and formed hornfels textures in the host supracrustal rocks. Secondary amphibole and epidote are the most common metamorphic minerals in the contact aureoles, however, garnet occurs around the periphery of the Garrison stock, and chlorite porphyroblasts, minor biotite and garnet occur in felsic metavolcanic rocks around the periphery of the Iris stock. These minerals indicate that high heat flow accompanied the intrusion of these stocks. This is very anomalous for the Iris stock, as the exposed portion of the intrusion appears to be too small to generate high heat. This indicates that the Iris stock must be much larger at depth than is exposed at surface, which is supported by the large airborne geophysical magnetic high in this area (OGS 1984).

## **Faults**

### **PORCUPINE–DESTOR DEFORMATION ZONE**

The Porcupine–Destor deformation zone (PDDZ) extends across the study area, and is traced west to the Kapuskasing Structural Zone (Ayer, Trowell, Amelin and Corfu 1999) and east through Quebec to the area of the Grenville Front (Mueller et al. 1996) for a total distance of greater than 600 km. The PDDZ strikes southeast in Hislop Township and becomes more east striking in south Guibord and Michaud

townships. The zone strikes northeast in Garrison Township and then strikes east through Harker, Holloway and Marriott townships. The deformation zone is complex with different structural styles restricted to specific segments. Each segment is bounded, to a first-order approximation by prominent north-northwest-striking faults that transect the PDDZ. For example, distinct differences in structural style occur across the Hislop and Garrison faults.

West of the Hislop fault, the PDDZ is southeast- to east-striking and moderately (45 to 65°) south dipping. The PDDZ marks the contact between the Porcupine and Tisdale assemblages and is characterized by mafic and ultramafic schist in zones from 250 to 800 m wide; numerous foliation parallel and crosscutting brittle faults; and albitite, lamprophyre and quartz-feldspar porphyritic sills and dikes that intruded the zone. Basalt and some clastic metasedimentary rocks occur as relatively undeformed wedges within the deformation zone and provide competent hosts for gold mineralization. Kinematics are poorly understood along this portion of the PDDZ, however, reverse vertical movement (south-over-north) is interpreted at the Glimmer Mine (M. Hoxha, Exall Resources Limited, personal communication, 1999) and south-over-north thrusting is interpreted on the fault zone in the Monteith area (Berger 2000a).

The main trace of the PDDZ is arcuate through Hislop, Guibord, Michaud and Garrison townships, between the Hislop and Garrison faults. The deformation zone transects the Tisdale assemblage and corresponds with the contact with the Kinojevis assemblage in south Guibord and Michaud townships. Timiskaming assemblage clastic and chemical metasedimentary rocks occur within the deformation zone that varies between 100 and 1500 m wide. Talc-chlorite schist occurs along the north margin of the deformation zone in the Tisdale assemblage and is indicative of ductile strain. The southern limit of the deformation zone is marked by brittle–ductile faulting accompanied by diabase dike intrusions and abrupt contacts between the Kinojevis and Timiskaming assemblages. The deformation zone is near vertical and kinematics are poorly constrained. North-northeast and north-northwest brittle and brittle–ductile faults transect and offset the PDDZ. Several poorly exposed shear zones occur parallel to and splay off of the main PDDZ to the north. The map pattern suggests that high strain and clockwise rotation affected the entire area between the PDDZ and Arrow fault (local name).

East of the Garrison fault, the PDDZ becomes increasingly focussed from a zone greater than 1000 m wide to approximately 200 m wide at the Quebec border (*see* Map 2676, back pocket). The deformation zone strikes east, dips steeply to the south (70 to 80°) and is characterized by ductile shear zones that separate less deformed lozenges of metavolcanic and metasedimentary rocks. Brittle faults coincide with many of the ductile zones and north-northwest-striking brittle faults transect the PDDZ. Several splay faults, the most significant being the Ghostmount fault, occur south of the main trace of the PDDZ and generally strike at 060 to 070°. These faults are mainly brittle in nature with significant amounts of infilling fault gouge. Both the main PDDZ and the splay faults display south-over-north reverse movement that includes late folding about subhorizontal axes (Luinstra and Benn 2001).

Jensen and Langford (1985) referred to rocks within the PDDZ, in this portion of the study area, as the “Porcupine–Destor complex”, however, recent geochronological analyses and detailed logging of diamond-drill core permit greater definition and separation of the various rock types. Ultramafic and mafic metavolcanic rocks of the Kidd–Munro assemblage are tectonically interleaved with clastic metasedimentary rocks of the Timiskaming assemblage. Albitite, lamprophyre and strongly altered intermediate alkalic dikes were intruded and deformed in the PDDZ. These rocks are isoclinally folded and display transposition along east-trending axes and limbs in the vicinity of the Holloway Mine. A moderately northeast-plunging crenulation cleavage is locally developed and late brittle–ductile north-northwest-striking faults transect the entire package of rocks. These structural elements have resulted in the present map pattern of wedge-shaped rock units that apparently “pinch-out” along strike and have hampered stratigraphic correlation and mineral exploration.

## ARROW FAULT

The Arrow fault is a local name applied to a shear zone striking 085° that extends from northeast Michaud Township to west of the study area. The fault is defined by a prominent linear disruption in airborne magnetic patterns (OGS 1984h, 1984i, 1984j) and corresponds to sheared rock on the ground. Addition of this fault to Map 2676 (*see* back pocket) is a major revision to previous government maps that did not indicate the presence of the fault. A secondary splay fault striking approximately 080° diverges from the Arrow fault in west Michaud Township and is expressed as a more subtle disruption of airborne magnetic patterns (OGS 1984h, 1984i, 1984j). This secondary splay fault has no surface expression, but is inferred to exist from the offset of rock units, mainly in Guibord Township.

The Arrow fault is described in diamond-drill logs from an area 300 m south of Wayne Lake, Guibord Township, as a zone, up to 70 m thick, of intensely sheared and altered fine-grained syenite and/or ultramafic schist. The fault is interpreted to transect syenite and ultramafic rocks south of Guibord Hill in the vicinity of the Caman gold occurrence (Prest 1953) and to transect strongly sericitized and carbonatized basalt near the Pike River bridge in Hislop Township. The Arrow fault appears to transect the PDDZ, but its relationship to the regional structures is poorly understood due to lack of exposure and study.

## “CONTACT FAULT”

Satterly (1952a) named the structure that separates the Kidd–Munro and Porcupine assemblages in Munro Township the “contact fault”. This is a brittle–ductile structure that strikes approximately 300° and dips near vertical. It is traced from the west boundary of the study area southeast to the vicinity of the Pangea deposit, where it is apparently truncated by an east-striking fault. The “contact fault” varies from a very narrow brittle structure, a few centimetres wide, that separates weakly deformed mafic metavolcanic and metasedimentary rocks, to a zone, up to 60 m wide, that separates altered and folded metasedimentary and ultramafic metavolcanic rocks from weakly deformed mafic metavolcanic rocks. A foliation, that is axial planar to mesoscopic west-closing folds and parallel to the contact between the Kidd–Munro and Porcupine assemblages, is developed in this wider deformation zone. Outside of the deformation zone, this same foliation is generally layer parallel in the metasedimentary rocks, but is rotated slightly counterclockwise to the long axis of pillows and flow contacts in the metavolcanic rocks. Ultramafic schist, intensely carbonatized metasedimentary rocks and fault breccia crop out in southeast Munro Township and form a narrow unit that widens to the southeast in northwest Guibord Township.

The map pattern (*see* Map 2676, back pocket) indicates that rock units in the Kidd–Munro assemblage are truncated against the contact fault, whereas units in the Porcupine assemblage are rotated parallel to the fault (Johnstone 1991). The contact between the Porcupine and Kidd–Munro assemblages is structural and this precludes simple stratigraphic correlation across the contact fault. Therefore, stratigraphic indicators used by Satterly (1952a, 1952b) and Johnstone (1991) to interpret that the Kidd–Munro assemblage was younger than the Porcupine “sediments” are misleading. Recent U/Pb geochronology indicates that the Porcupine assemblage is younger than the Kidd–Munro assemblage (Corfu 1993; Bleeker and Parish 1996; Ayer, Trowell, Amelin and Corfu 1999; *see* Table 1).

## MUNRO FAULT

The Munro fault is a brittle–ductile structure that extends from Hewitt Lake in northeast Michaud Township to Carr Township northwest of the map area. The author believes that the Munro fault

connects with the regional Pipestone shear zone that extends from Carr Township to Frederick House Lake (30 km in length), however, the exact position and nature of the connection is speculative (Satterly 1952a, 1952b; Johnstone 1991). The Munro fault strikes approximately 290° in the study area and is described as a broad zone (up 900 m wide) composed of carbonatized ultramafic schist (Johnstone 1991). The location of the fault is interpreted from diamond-drill data in north Guibord and Michaud townships, as there are no outcrops in this area. The fault is characterized by talc-chlorite schist with various amounts of carbonate, green mica and sulphide mineralization. The author interprets the fault to merge with the Arrow fault in the vicinity of Hewitt Lake based on airborne geophysical data (OGS 1984j) and limited data from diamond-drill holes.

Johnstone (1991) indicated that movement on the fault was mainly vertical based on the minimal disruption of fold axes across the fault and subvertical slickensides on individual fault planes. There is little evidence in the study area to determine sense of movement, however, like other major deformation zones in this area, movement appears to be predominantly vertical.

## **GHOSTMOUNT FAULT**

The Ghostmount fault and related McKenna fault are splay faults of the PDDZ that strike approximately 70° and dip steeply south. The faults originate at the junction with the PDDZ in Holloway Township and strike west-southwest from that point (*see* Map 2676, back pocket). These are predominantly brittle faults that are gouge filled and vary from a few centimetres to a few metres wide. The McKenna fault hosts the Holt–McDermott Mine and the Ghostmount fault acts as the south-bounding fault to the “south zone” ore deposit at the Holt–McDermott Mine (Luinstra and Benn 1999). Both faults are characterized by south-side-up reverse movement and developed late in the tectonic history of the area (Luinstra and Benn 1999). Gold mineralization is spatially associated, along strike to the west-southwest, with the Ghostmount fault indicating that this is an important subsidiary structure to the PDDZ.

## **CROSS FAULTS**

Numerous faults transect the PDDZ orthogonal to its strike. The faults are typically steeply dipping, strike between 345 and 15°, and are brittle–ductile in character. Displacement is vertical on these cross faults, most commonly with east-side-down displacement, in every place where the author has observed them. The majority of these faults have limited strike length extending from a few hundred metres to a few kilometres. Some of the faults are regional in extent and are described in more detail separately (*see* “Hislop Fault”, “Ross Fault” and “Garrison Fault”). Many of the faults occur as linear disruptions of the airborne magnetic patterns, which facilitates interpretation of their linear extent (*see* Map 2676, back pocket). Diabase dikes of the Matachewan dike swarm occupy some of these faults, which the author interprets as passive emplacement along pre-existing structures as the dikes are only rarely deformed. The majority of the dikes are characterized by brittle calcite-annealed fault gouge or are fractured with calcite–quartz veins. Some of the faults, such as those near the Ludgate Lake deposit, the Buffonta Mine and the St Andrew Goldfields Limited Hislop Mine, are ductile with well-developed penetrative foliation, fissile schist and mylonite. This suggests that these faults originated as a late phase in the development of the Porcupine–Destor deformation zone.

### **Hislop Fault**

The Hislop fault strikes approximately 345° and extends from south of the study area through east-central Hislop Township and north into Carr Township. The Hislop fault corresponds with a pronounced



lineament across which there is a 40° clockwise rotation of the airborne magnetic pattern (OGS 1984h), which corresponds with a change in the strike of stratigraphy. The fault is described from diamond-drill data as a brittle–ductile structure that contains schist, fault gouge and extensive fracturing. Feldspar porphyry and syenite dikes are reported to intrude along the fault. Drost (1987) suggested that the Hislop fault represented a “mega-kink” structure that reflected a phase of development along the PDDZ, based on airborne geophysical magnetic patterns. However, the fault appears to have a fundamental control on geology and gold mineralization beyond that associated with kink-folding in the study area. West of the fault, the stratigraphy is an east-striking, south-facing homoclinal sequence. Structural fabrics are commonly nonpenetrative fracture cleavage. Gold mineralization is largely confined to the vicinity of alkalic plutons, such as the Canadian Arrow deposit. East of the Hislop fault, stratigraphy is folded about southeast-trending axes in the Tisdale assemblage and is a homoclinal south-facing sequence in the Kinojevis assemblage. Ductile structures associated with folding are overprinted by brittle–ductile faults. Hydrothermal alteration and associated gold mineralization occur in a variety of structural and geological settings. Timiskaming assemblage metasedimentary and alkalic metavolcanic rocks are most common adjacent to the east side of the Hislop fault. These data indicate that the Hislop fault most likely controlled deposition of the Timiskaming assemblage metasedimentary rocks, that it is characterized by east-side-down vertical movement, and that it separates different structural blocks in the study area. As explained below, the Hislop fault is 1 of 5 regional bounding cross faults that separate different segments along the PDDZ from Timmins to Quebec. The structural style and setting of gold mineralization in each segment is different and knowledge of these differences can be used to tailor exploration programs specific to each segment (Berger 2001).

## **Ross Fault**

Jensen (1985a) identified a northwest-striking lineament immediately east of the Ross Mine as the Ross fault. The author has modified the extent and strike of the fault based on detailed airborne geophysical data (OGS 1984h). The fault is located near or on the inferred axis of an anticline that closes in the vicinity of the Ross Mine. The fault is a brittle–ductile structure characterized by schist in the vicinity of the mine and by extensive fracturing and veining to the southeast in Cook Township (K. Germundson, Consultant, personal communication, 2000). The author believes that the Ross fault is one of the important structural features responsible for localization of gold mineralization at the Ross Mine.

## **Garrison Fault**

The Garrison fault (local name) is a north-striking structure that bisects the Garrison stock and is responsible for the pronounced physiographic feature referred to as the “The Canyon” (*see* Satterly 1949a, 1949b). This fault extends north from south Garrison Township into Rand Township and is coincident with a lineament that disrupts and offsets airborne magnetic patterns (OGS 1984k). The Garrison fault acts as a boundary between two segments along the PDDZ. West of the Garrison fault, the PDDZ is characterized by a broad zone of sheared and fractured rocks that separate more competent rock units (lithons). Large multiphase alkalic intrusions occur within and near the PDDZ. Several splay and ancillary faults originate in this block, including the Arrow and Munro faults. Gold mineralization occurs in diverse structural settings, but always has a strong spatial association with alkalic rocks. East of the Garrison fault, the PDDZ progressively narrows from a zone greater than 1 km wide to 250 m wide toward the Quebec border. Alkalic intrusions also decrease in size and abundance toward the east. Gold mineralization remains spatially associated with alkalic intrusive rocks or related hydrothermal alteration (Robert 1997), but a strong spatial association with the PDDZ and related splay faults is also observed. The Holloway and Holt–McDermott mines occur east of the Garrison fault.

## Folds

All assemblages are folded, however, the fold geometry is manifested differently in different parts of the study area. Map-scale folding is most evident in the Kidd–Munro assemblage. Tight folds about west-northwest- to west-trending axes are evident from reversals in stratigraphic facing indicators. The facing reversals correspond with airborne magnetic patterns that display east- and west-fold closures (OGS 1984a–n). The Ghost Range mafic to ultramafic layered sill and surrounding rocks are good examples of this style of folding. Reversals in pillowed flows and graded tuff indicate that the sill occupies a syncline. Airborne magnetic patterns (OGS 1984e, 1984f, 1984l, 1984m) show east and west closures along the fold axis of the sill indicating that the sill is folded with the metavolcanic rocks. Airborne magnetic patterns in McCool and Munro townships (OGS 1984b, 1984c) mimic the tight fold of the Ghost Range sill and indicate that this style of folding is characteristic of the Kidd–Munro assemblage.

Luinstra and Benn (2001) discovered that isoclinal folding occurred within the PDDZ in the Holloway Mine area. These folds are commonly intrafolial and rootless about east-trending, steeply east-plunging axes, which indicate transposition of stratigraphy (Luinstra and Benn 2001). Ayer, Trowell, Madon et al. (1999) and Berger and Amelin (1999) attributed those folds in the PDDZ and in the Kidd–Munro assemblage to the same deformation event. Folds in the PDDZ were the products of continued compression, which resulted in transposition.

The Kinojevis assemblage is homoclinal and southward younging in the study area, but regionally situated on the north limb of the Blake River synclinorium (Jensen and Langford 1985). The synclinorium is folded about an east-trending axis and is similar to other described folds except it is more open. It appears likely that folding in the Kinojevis and Kidd–Munro assemblages is related to the regional development of the PDDZ, which occurred either during or after deposition of the Timiskaming assemblage metasedimentary rocks.

Folding in the Tisdale assemblage is ambiguous due to modification of structural patterns by the alkalic intrusions. Reversals in pillow facings indicate folding about southeast-trending axes, however, folds appear to be arcuate in Michaud Township and are offset by the Arrow fault and related splay faults of the PDDZ. The author believes that the large plutons acted as resistant buttresses during folding of the supracrustal rocks and refracted the fold axes, as none of the plutons are entirely undeformed.

## METAMORPHISM

All rocks in the study are metamorphosed to some extent. Most of the rocks contain metamorphic mineral assemblages indicative of regional greenschist-facies metamorphism (Winkler 1979). Primary plagioclase, amphibole and, less commonly, pyroxene are largely replaced by metamorphic chlorite and epidote in mafic metavolcanic rocks. Epidote and quartz knots and stringers are locally abundant in pillow selvages and occur as amygdules. Leucoxene commonly replaces magneto-ilmenite and secondary quartz occurs in narrow stringers in many places. Secondary amphibole occurs only adjacent to the alkalic plutons and is considered part of a contact metamorphic aureole. Low-grade metamorphism is not apparently preserved in the mafic metavolcanic rocks, since zeolite minerals were not identified in the field or in thin section.

Greenschist-facies metamorphic minerals in pelitic metasedimentary rocks are characteristically iron-rich chlorite and, less commonly, white mica. Primary detrital grains are well preserved in all metasedimentary rocks that have not undergone extensive hydrothermal alteration. In most places, biotite is absent indicating that metamorphism at low greenschist facies affected much of the area. Biotite does

occur in metasedimentary rocks adjacent to some of the alkalic plutons, which is interpreted to result as a product of contact metamorphism.

Intermediate and felsic metavolcanic rocks of the Kidd–Munro assemblage underlie the northeast part of the study area. Chlorite, epidote and white mica are the most common metamorphic minerals that replace original plagioclase and amphibole phenocrysts and occur in the groundmass and matrix of flows and pyroclastic deposits. Brown pleochroic biotite occurs locally in feldspar- and amphibole-phyric dacite in Rand Township. Secondary pale green to brown-green pleochroic amphibole occurs in trace quantities in several places east of Rand Township. These observations indicate that this part of the study area underwent regional metamorphism at a slightly higher grade than areas to the south and west.

The numerous alkalic intrusions imparted contact metamorphic halos on the surrounding supracrustal rocks. Mafic metavolcanic rocks, which underwent contact metamorphism, are typically hornfels textured, fine to medium grained and equigranular. Amphibole is the most common metamorphic mineral and, in many places, it is blue-green pleochroic, indicating high sodium content. This evidence suggests that alkaline metasomatism affected the host supracrustal rocks (Pigeon, Lalonde and Berger 2000). Secondary epidote is also common and occurs as disseminations and veins localized in shear zones and fractures around the periphery of the intrusion. Green pleochroic biotite is rare in mafic metavolcanic rocks and indicates potassium metasomatism affected these rocks. Garnet occurs in shear zones around the periphery of the Garrison stock indicating anomalous heat and/or pressure in this area (Winkler 1979).

Clastic metasedimentary rocks, located within contact-metamorphic aureoles, contain abundant brown biotite and pale green pleochroic amphibole. Wacke units south of the Garrison stock and south of the syenite intrusion in northwest Harker Township are strongly affected by metamorphism. The wacke unit in Harker Township contains narrow stringers of leucosome, which is indicative of the onset of partial melting. Wacke and argillite, correlated with the Timiskaming assemblage in north-central Hislop Township, contain abundant biotite suggesting that alkalic magmatism postdates sedimentation in this part of the area.

Contact-metamorphic aureoles are heterogeneously developed around the plutons. For example, the metamorphic effects of the Garrison stock extend for a distance of greater than 1 km from the contact in clastic metasedimentary rocks, but are confined to within 500 m of the contact in the mafic metavolcanic rocks. The contact-metamorphic aureole is less than 100 m in all rock types around the intrusion at the Pangea deposit. The contact-metamorphic aureole around the Iris stock is anomalous, in that the stock is exposed over an approximately 200 m radius and is composed mostly of coarse-grained syenite with lesser hornblende, lamprophyre and melasyenite. However, chlorite, epidote and rare garnet porphyroblasts are developed in felsic metavolcanic rocks for up to 150 m from the contact. The metamorphic aureole is anomalously large compared to the largely felsic composition of the intrusion and its size (*see* Winkler 1979). It is likely that the Iris stock is up to 7 times larger than the exposed portion, a conclusion that is supported by the airborne magnetic data (OGS 1984).

# Economic Geology

This section provides an overview of the styles of mineralization and associated alteration rather than describe individual properties in detail. Luinstra and Benn (2001) and Ropchan (2000) provide detail for the Holloway Mine. Luinstra and Benn (1999) and Workman (1986) discuss salient aspects of the Holt–McDermott Mine. Troop (1985, 1986) provided the most recent descriptions of the Ross Mine area. Descriptions of other showings and deposits are in reports filed for assessment work credits at the Kirkland Lake Resident Geologist’s Office or were compiled from private company files by the author.

## GOLD

Satterly (1951c) summarized the discovery of the Croesus deposit, the first significant gold discovery in the study area. Exploration sparked by this discovery continues to the present and gold remains the most important economic commodity in the study area. Table 3 lists producing mines, past producing mines and the most significant prospects and deposits in the area. The list does not include the numerous gold showings greater than 1 g/t gold that are reported. Different mineralization styles and structural settings occur throughout the study area and there appears to be systematic variation along the Porcupine–Destor deformation zone (PDDZ) (Berger 2001). The Hislop and Garrison faults serve as approximate boundaries that divide the PDDZ into segments; each segment is characterized by a dominant style of mineralization. Figure 23 is a simplified cartoon of the interaction of faults, folds and stratigraphy along the PDDZ and of the different styles of gold mineralization most common in each segment. Although greatly simplified, the figure illustrates the essential features that are common in each segment.

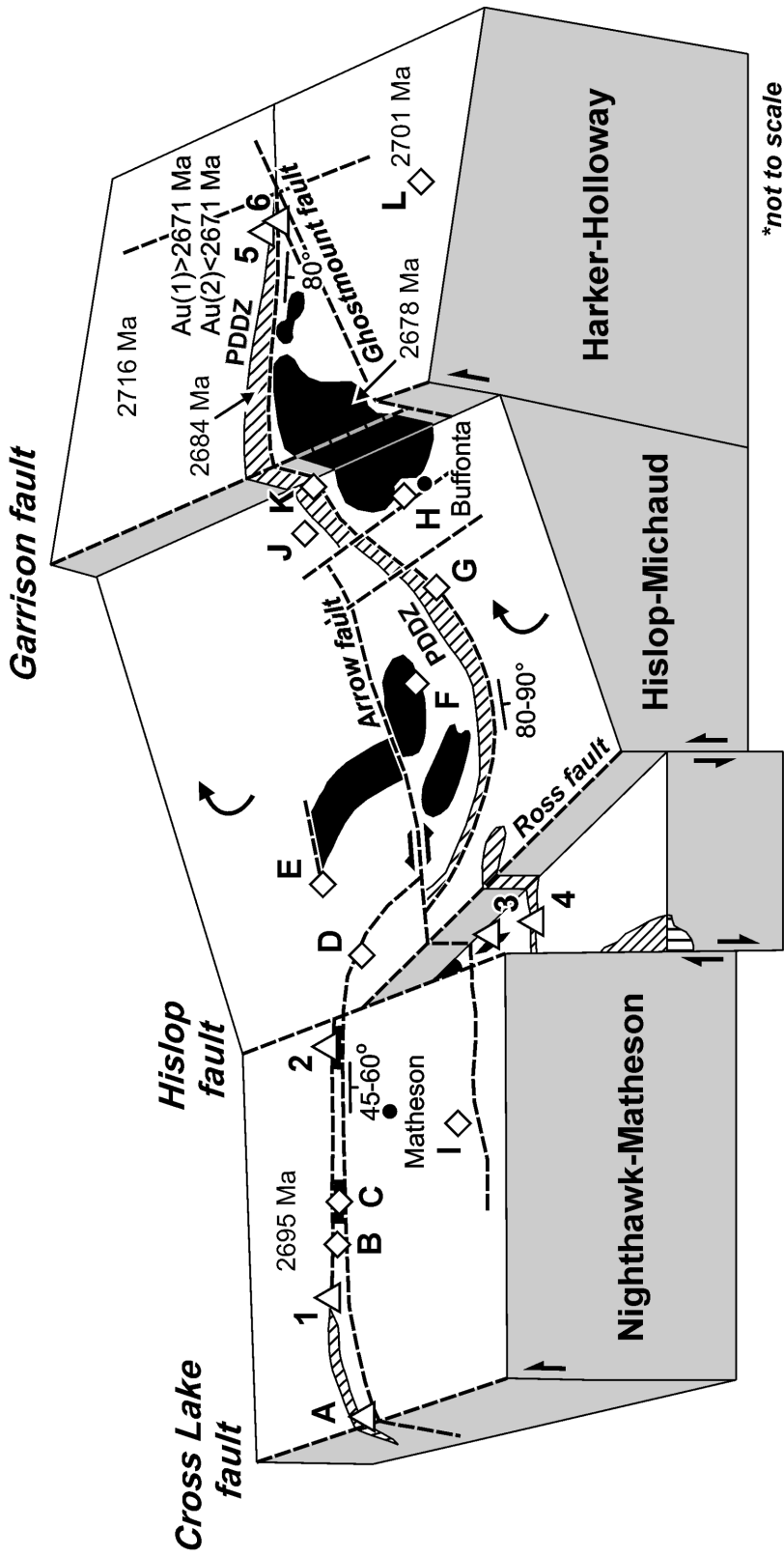
### Nighthawk–Matheson Segment

The Nighthawk–Matheson segment (*see* Figure 23) is west of the Hislop fault and extends to the vicinity of the Aquarius gold mine in Macklem Township (37 km west). The Glimmer Mine in Hislop Township is representative of most gold mineralization in the segment. The deposit is hosted by sheared ultramafic and mafic schist within the PDDZ. Mineralized zones strike and dip parallel to the local structure and geology. Free-milling gold occurs in quartz stockwork and breccia veins and with pyrite in altered wall rock and albitite sills and dikes (Hoxha 1999). Other trace minerals include chalcopyrite and rare gersdorffite [(Ni, Fe, Co)AsS], which is similar to mineralogy at the Shoot Zone in Taylor Township (Hamilton et al. 1995; *see* Figure 23). Ankerite and green chromium mica are the most common hydrothermal alteration minerals and generally increase in abundance toward the ore zones. Albitization is characteristic of the most proximal alteration to ore and significant apatite occurs with albitite sills at the Glimmer Mine, the Taylor gold deposit and the Aquarius gold mine (King and Kerrich 1987). Silicification as quartz veins and stockworks is dominant and pervasive silicification is rare. The PDDZ is up to 800 m wide in this area and is characterized by brittle–ductile deformation with schist and ductile shear zones dominant. The PDDZ dips between 45 to 60° to the south, which is much more shallow dipping than elsewhere between Timmins and the Quebec border (Brisbin 1997; Berger 2001). Hoxha (1999) and Siragusa (1993) indicated that south-over-north reverse movement is characteristic of the PDDZ in this segment and the low dips suggest that late thrusting may have occurred along the structure.

**Table 3.** List of gold mines, past-producing mines, prospects and major occurrences in the Highway 101 area.

	<b>Township</b>	<b>Comments</b>
<b>Producing Mines (as of January 2000)</b>		
Holloway Mine	Holloway	Producer: gold
Holt–McDermott Mine	Holloway	Producer: gold
<b>Past Producers and Developed Prospects</b>		
Glimmer Mine	Hislop	Past producer: gold
St Andrew Goldfields Limited Hislop Mine	Hislop	Open pit: started mining August 1999, closed December 2000
Iris deposit	Harker	Surface stripping, adit, minimal production
Golden Harker deposit	Harker	305 m shaft with 2134 m lateral work; closed 1929; no production figures
Teddy Bear Valley Mine	Holloway	91 m shaft and 338 m lateral work; no production figures; near the present site of the Holloway Mine
Jonpol Explorations Limited Jonpol deposit	Garrison	Adit and underground working to develop a gold deposit in Garrison Township: 997 500 tons at 0.235 opt (1988); limited mining until 1998
Buffonta Mine	Garrison	Open pit: reserves 85 000 tons at 0.295 opt (1944)
New Buffonta deposit	Garrison	Open pit: southeast of Buffonta; drill indicated reserves 600 000 tons at 0.17 opt (1989)
Garrcon deposit	Garrison	78 m shaft and 315 m lateral work in 1935; 350 900 tons at 0.19 opt (1988)
Talisman Mine	Guibord	33 m shaft and 396 m lateral work in 1934; reserves of gold not reported
Ross Mine	Hislop	Past producer: 1.037 million ounces gold, 1.639 million ounces silver, 2537 tons copper
Royal Oak open pit	Hislop	Open pit: mined 100 000 tons at 0.1 opt until mid 1990s
Gibson deposit	Hislop	Exploration decline; surface and underground drilling to define 19 230 tons at 0.59 opt
Canadian Arrow Mine	Hislop	Open-pit past producer: 17 045 ounces gold at 0.06 opt to end of 1982
Vimy Mine	Hislop	23 m shaft to extract 1073 kg bulk of bulk sample; no production; estimated 20 000 tons at 0.21 opt (1971)
New Kelore Mine	Hislop	Open pit: 145 m shaft and lateral workings to explore gold mineralization that is currently mined by St Andrew Goldfields Limited
<b>Undeveloped Prospects and Occurrences</b>		
Ludgate Lake deposit	Michaud	Resource of 462 800 ounces gold at 5.91 g/t gold
Pangea deposit	Guibord	1.95 million tonnes at 5.13 g/t gold in top 250 m
“Southwest” zone	Michaud	Resource of 460 000 ounces gold (2.4 million tonnes at 6.1 g/t gold)
“Last Chance” zone	Michaud	Best assay: 9.46 g/t gold over 7.1 m
Tousignaut zone	Harker	Bath (1990) reported a “small shallow deposit grading 0.20 ounces of gold per ton”
Windjammer property	Garrison	4.9 g/t gold over 12 m, along strike NE of “Twin Creek” zone
H.E. Neal prospect	Guibord	Several gold assays covering an aerielly extensive part of the PDDZ
Cochenour–Willans showing	Holloway	Original gold discovery in Holloway Township led to subsequent discoveries in the area
Black Top zone	Holloway	Gold mineralization southeast of Holloway Mine along Highway 101
Pumphouse zone	Holloway	Gold mineralization under Holloway Lake
Gunnex deposit	Hislop	102 000 tons of material at 0.17 ounce per ton gold (Bath 1990)
Camán property	Guibord	Gold mineralization in association with altered ultramafic metavolcanic schist and intrusive alkalic rocks
Linton–Brydges properties	Garrison	Gold mineralization associated with Timiskaming-type or Timiskaming assemblage metasedimentary rocks and ultramafic metavolcanic rocks
“Twin Creek” zone	Michaud	Gold mineralization in association with altered ultramafic and mafic metavolcanic schist in the PDDZ
Stoughton zone	Marriott	Gold mineralization in the PDDZ

Abbreviations: opt, ounce per ton; PDDZ, Porcupine–Destor deformation zone.



- |   |                               |                                  |
|---|-------------------------------|----------------------------------|
| <b>GEOLOGY</b>                                | <b>MINES</b>                  | <b>GOLD DEPOSITS</b>             |
| Timiskaming assemblage metasedimentary rocks  | 1 Stock Mine                  | <b>A</b> Aquarius mine           |
| Alkalic intrusions                            | <b>2</b> Glimmer Mine         | <b>B</b> Shoot zone              |
| <b>PDDZ</b> Porcupine-Destor deformation zone | <b>3</b> St Andrew Goldfields | <b>C</b> Taylor deposit          |
|   | Hislop Mine                   | <b>D</b> Royal Oak open pit      |
|   | <b>4</b> Ross Mine            | <b>E</b> Pangea deposit          |
|   | <b>5</b> Holloway Mine        | <b>F</b> Ludgate Lake deposit    |
|   | <b>6</b> Holt-McDermott Mine  | <b>G</b> "Southwest" zone        |
|   |                               | <b>H</b> Buffonta & New Buffonta |
|   |                               | <b>I</b> Canadian Arrow mine     |
|   |                               | <b>J</b> Jonpol deposit          |
|   |                               | <b>K</b> Garroon deposit         |
|   |                               | <b>L</b> Iris deposit            |

Figure 23. Inferred movement on segments in the Highway 101 area.

The Canadian Arrow deposit represents a style of gold mineralization that occurs south of the PDDZ and west of the Hislop fault. Prest (1957), Cherry (1983), and McNeil and Kerrich (1986) summarize the geology and salient features of gold mineralization at the deposit. Northeast-striking auriferous quartz veins with red alteration halos are confined to a trondhjemitic stock approximately 1 km in diameter. Bath (1990) indicated that 17 045 ounces of gold were recovered by open pit mining from 279 593 tons of ore (average grade of 0.06 ounce per ton gold) between 1934 and 1982 when mining operations ceased. Stable isotope (oxygen, carbon, and sulphur) and fluid inclusion studies indicate that gold precipitated from highly oxidized, low salinity hydrothermal fluids at approximately 320°C (McNeil and Kerrich 1986). Abundant miarolitic cavities and veins containing quartz and calcite crystals indicate that crystallization occurred in relatively low confining pressures. The nearby Watabeag batholith crystallized at a pressure between 0.7 and 1.2 kilobars suggesting depths of emplacement between 2 and 4 km (Feng and Kerrich 1990). The Silidor deposit in Quebec shares some similarities to the Canadian Arrow deposit and indicates that highly oxidized gold-bearing hydrothermal systems operated elsewhere in the Abitibi Subprovince (Carrier et al. 2000).

## Hislop–Michaud Segment

The Hislop–Michaud segment is between the Hislop and Garrison faults (27 km, *see* Figure 23). A number of gold deposits occur within this segment: the St Andrew Goldfields Limited’s Hislop Mine, the Ross Mine, Pangea Goldfields Incorporated’s Pangea deposit, Pentland Firth Ventures Limited’s Ludgate Lake deposit, the “Southwest” zone at the Moneta Porcupine Mines Incorporated property, the Buffonta Mine and New Buffonta gold deposit open pit, and Jonpol Explorations Limited’s Garcon and Jonpol deposits. Geology in the Hislop–Michaud segment is more complex and less well understood than other parts of the study area. Stratigraphic correlation is complicated by the intrusion of several multiphase alkalic plutons ranging in composition from hornblendite to granite. The location of the PDDZ (interpreted to follow the arcuate contact between Timiskaming assemblage metasedimentary rocks and ultramafic to mafic metavolcanic rocks tentatively correlated with the Tisdale–Bowman assemblage) is ambiguous as several east-northeast-striking, subvertical ductile shear zones and faults converge and transect the PDDZ. In the east part of the segment, the PDDZ bifurcates into the main branch and the Pipestone shear zone, another major gold-bearing crustal structure. Several north-, northeast- and northwest-striking brittle and ductile faults further complicate stratigraphic correlation in this segment. Some of these faults host economically significant gold mineralization, which is a feature more common in the Hislop–Michaud segment than elsewhere along the PDDZ.

Gold deposits are hosted in a variety of rock types, but are all structurally controlled and spatially associated with alkalic rocks. Deposits, such as the Ross Mine and the “Southwest” zone, are hosted in Timiskaming assemblage metasedimentary rocks associated with lamprophyre and albitite dikes and possibly alkalic extrusive rocks. Deposits, such as the Buffonta Mine, the New Buffonta open pit, the St Andrew Goldfields Limited Hislop Mine and the Royal Oak open pit, are hosted in mafic and ultramafic metavolcanic rocks adjacent to alkalic intrusions or lamprophyre dikes (*see* Figure 23). The Ludgate Lake and Pangea deposits are hosted in alkalic intrusive and mafic metavolcanic rocks. Gold occurs most commonly in disseminated sulphide minerals (mainly pyrite), however, quartz-carbonate stockworks and veinlets are also important hosts of gold mineralization. Free gold is uncommon and most is associated with pyrite and, less commonly, chalcopyrite, sphalerite and galena. Hydrothermal alteration products vary in proportion with the different host rock types. For example, iron carbonate is abundant at deposits hosted by ultramafic and metasedimentary rocks, such as at the Ross Mine, the St Andrew Goldfields Limited Hislop Mine and the Royal Oak open pit. However, carbonate is minor or absent at deposits hosted by syenite or mafic metavolcanic rocks, such as at the Ludgate Lake and Buffonta deposits. Hematite, albite and sericite are common to all deposits. Apatite, fluorite, and andradite garnet occur at

the Pangea deposit; molybdenite is reported around the periphery of the Garrison stock; and arsenopyrite is common at the Jonpol deposit. The following is a brief description of geological features at the more important deposits in the Hislop–Michaud segment.

## **ROSS MINE**

The Ross Mine is a past producer of greater than 1 million ounces gold and 1.6 million ounces of silver (Bath 1990). The mine is located in a down-dropped block between the Hislop and Ross faults in south-central Hislop Township (*see* Figure 23). The host rocks are strongly altered and were interpreted as felsic metavolcanic breccia (Prest 1957), felsic pyroclastic rocks and volcanically derived metasedimentary rocks (Ploeger 1978), or as altered mafic metavolcanic rocks (Troop 1986). All authors agree that the only unaltered rocks in the mine are well-bedded wacke and argillite that have fault-bounded or gradational contacts with the altered rocks. Rare earth element geochemistry from rock samples, collected by the author from diamond-drill core and from the open-cut north of the shaft, display fractionated patterns more similar to Timiskaming assemblage metasedimentary and metavolcanic rocks than to other rock types in the immediate area (*see* Figures 18c and 18d). The author infers that Timiskaming assemblage rocks host the deposit.

Several studies indicate that the Ross Mine is unique to the Abitibi greenstone belt. Gold, silver and copper were extracted from quartz–calcite stockworks, breccia pipes and veins in brittle faults surrounded by alteration zones that contain sericite, hematite, anhydrite, gypsum, albite, sphalerite, galena and telluride minerals (Ploeger 1978; Prest 1957). The ore zones are steeply west-plunging pipe-like zones or north-striking veins localized in brittle structures that overprint ductile shear zones (Ploeger 1978; Troop 1986). The ore contained a silver–gold ratio (1.6:1) unlike other gold deposits along the PDDZ (typically Ag:Au = 1:10; *see* Colvine et al. 1988). This led LaRocque (1952) to speculate that mineralization at the Ross Mine could be temporally related to Proterozoic silver–cobalt mineralization at Cobalt, Ontario. Ploeger (1978) and Troop (1986) indicated that strongly oxidized fluids produced the alteration mineralogy and inferred that alkalic magmas were associated with the mineralization. Stable isotope geochemistry at the Ross Mine is similar to other gold deposits along the PDDZ (Wood et al. 1986; Hattori and Cameron 1986). Lead isotopes indicate that different sources may account for variations in alteration and ore mineralogy among deposits although the fluid source may be common (Hattori 1993). The Ross Mine shares many similarities to epithermal gold–silver deposits and may represent shallow crustal level preservation of an alkalic hydrothermal system (Panteleyev 1988). Troop (1986) recommended that future exploration should concentrate north of the mine. The author notes that exploration was restricted to within 300 m of the head frame and there has been little exploration west of the mine (K. Jensen, Consulting Geologist, personal communication, June 1999). Given the number of small gold deposits outlined near the Hislop fault (e.g., Gunnex, Gibson and Creek zones), exploration west of the mine within the Timiskaming assemblage rocks is recommended.

## **ST ANDREW GOLDFIELDS LIMITED HISLOP MINE (NEW KELORE MINE)**

The St Andrew Goldfields Limited Hislop Mine, an open pit in Hislop Township, was started in August 1999 near the site of the former New Kelore Mine (Kelwren Gold Mines Limited) headframe and closed in December 2000. The pit was sunk to exploit a gold reserve of 325 000 tonnes at 3.4 g/t Au (St Andrew Goldfields Limited, <http://www.standrewgold.com>, information from web site accessed September 6, 2000).

The pit geology consists of a central, coarse-grained mauve to red, east-striking syenite dike separating variolitic basaltic rocks to the north from ultramafic and mafic metavolcanic rocks to the south. Pegmatitic lamprophyre and hornblendite occurs sporadically along the south contact of the syenite and



was mistakenly included with the metavolcanic rocks by previous workers. Gold is hosted in pyritic mafic and ultramafic metavolcanic rocks along the south side of the syenite and is rarely present in the intrusion. Localized, but intense, carbonatization, sericitization and hematization accompany the mineralization. The syenite dike is petrographically and chemically similar to the Iris syenite stock, in Harker Township, which hosts gold mineralization. The dike also displays similar geochemistry to another albite dike associated with gold mineralization in northwest Harker Township. Figure 24 shows the distinctive chondrite-normalized rare earth element patterns for these 3 rock types. The author

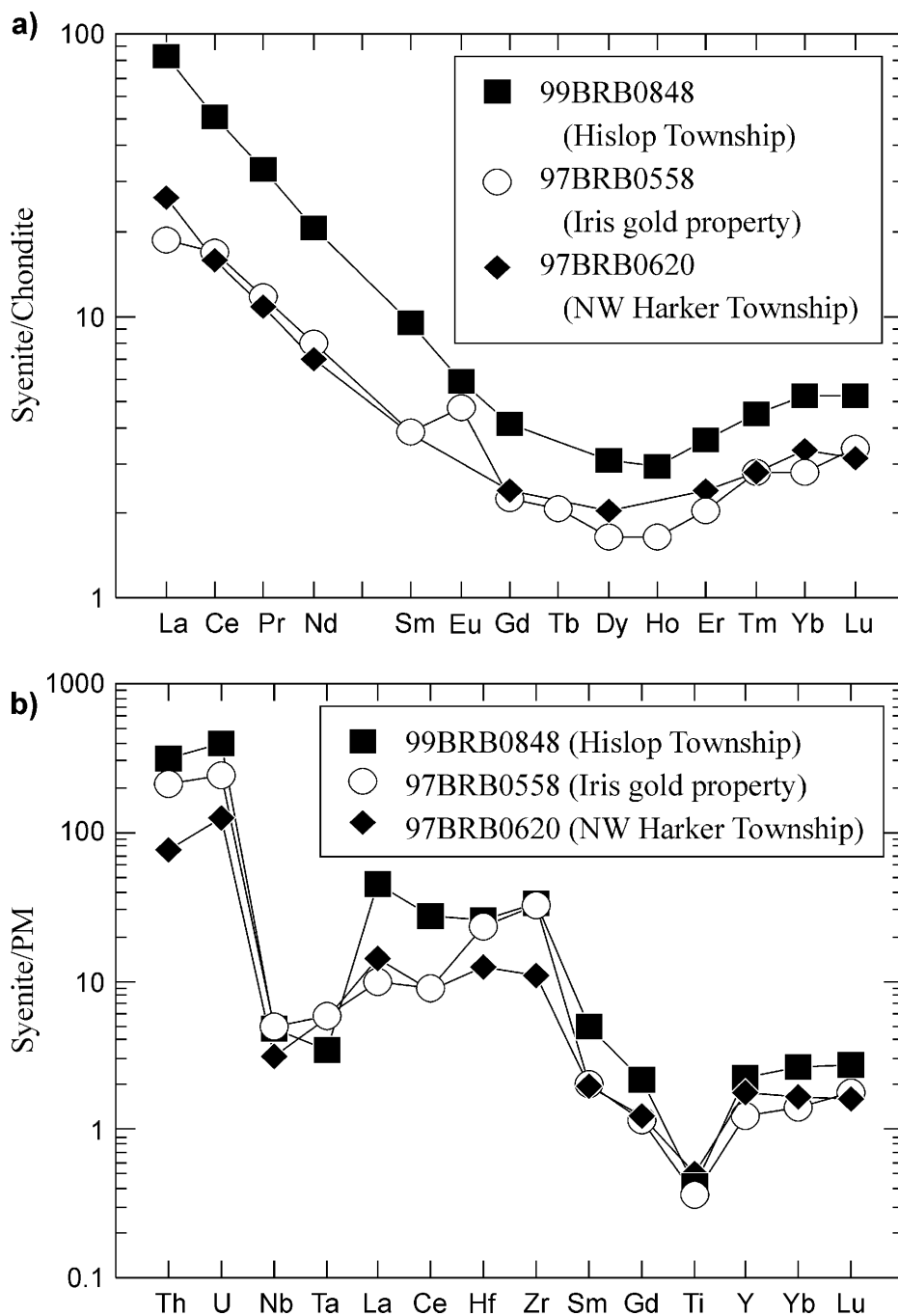


**Figure 24.** a) Chondrite-normalized REE patterns, and b) primitive-mantle normalized extended element patterns for gold-bearing syenite in the Highway 101 area.

suggests that the REE patterns are probably the result of alteration associated with gold mineralization as all rocks contain very high sodium. The affinity of gold with alkalic metasomatism is noted elsewhere in the Abitibi Subprovince (King and Kerrich 1987; McNeil and Kerrich 1986; Watson and Kerrich 1983).

The open pit is situated between the Arrow fault and a southwest-striking splay fault. Rocks display a penetrative southeast-striking, south-dipping penetrative foliation that is overprinted by northeast-striking brittle–ductile faults and associated foliation. Apparent left lateral displacement along the northeast-striking faults offset all rock units in the area of the pit. Southeast-striking ore zones are also offset by the faults, however, there are ore zones aligned parallel to the northeast faults suggesting that gold mineralization occurred both before and after development of the faults. It appears the combination of alkalic magmatism accompanied by clockwise rotation between the Arrow and splay faults accounts for the geometry and localization of gold in this area.

## **ROYAL OAK OPEN PIT**

The Royal Oak open pit is located in Lot 1, Concession IV, Hislop Township approximately 1400 m northeast of the St Andrew Goldfields Hislop Mine (*see* Figure 23). One hundred thousand tons grading 0.1 ounce per ton gold was extracted from the pit and processed in Timmins by Royal Oak Mines Limited in the early 1990s (P. Harvey, Royal Oak Mines Limited, personal communication, 1997). No further work was carried out on the property.

Mafic and ultramafic metavolcanic rocks and their derived schist and lamprophyre dikes are exposed in the pit, which is located within the PDDZ. Nearby outcrops along Highway 572 expose variolitic and nonvariolitic pillowed flows, lamprophyre dikes, and rare quartz porphyry dikes. The PDDZ strikes approximately 120° with moderate to steep south dips in this part of the study area. Mineral and stretching lineations on foliation planes plunge steeply southeast indicating dominant vertical movement. Rocks in the pit are strongly foliated to schistose and display intense carbonatization, sericitization (green mica), pervasive and vein silicification and abundant disseminated pyrite (locally up to 30% of the rock). Visible gold is contained in discontinuous quartz stringers, striking approximately 25° and dipping 75° east, that are located along both contacts between a narrow (30 m) basalt flow and ultramafic metavolcanic rocks. These veins are tensional features and emphasize the importance of searching for mineralization orthogonal to the main trend of the PDDZ.

## **PANGEA GOLDFIELDS INCORPORATED DEPOSIT**

The Pangea deposit, also known as the Fenn–Gibb property, is located immediately south of Highway 101 in lots 6 and 7, Concession VI, Guibord Township and is owned by Pangea Goldfields Incorporated (*see* Figure 23). Probable ore reserves of the main zone in the top 250 m are calculated at 1.95 million tonnes grading 5.13 g/t gold (Pangea Goldfields Incorporated, press release, August 31, 2000). Additional mineralized zones without reported reserves occur on the property. In July 2000, Pangea Goldfields Incorporated was acquired by Barrick Gold Corporation.

The Pangea deposit encompasses rocks from 3 assemblages. Mafic metavolcanic rocks of the Kidd–Munro assemblage underlie the north part of the property. Massive, pillowed and variolitic basalts crop out and can be seen in diamond-drill core from holes collared near Highway 101. Hydrothermally altered variolitic basalts are the principal hosts of the main zone mineralization. These basalts were affected by pervasive and vein silicification, carbonatization, albitization, pervasive but weak hematization, and vein sericitization. Syenite and lamprophyre dikes intruded the basalts and are locally mineralized. Pyrite is the main sulphide mineral and occurs as disseminations and in veins, locally up to 50%, over narrow

intervals (average 5 to 10%). Wacke and argillite of the Porcupine assemblage underlie the south and west parts of the property. These rocks are weakly hematized, sericitized and carbonatized. The rocks host sporadic gold mineralization of generally low tenor. The Porcupine assemblage metasedimentary rocks are in fault contact with the Kidd–Munro assemblage along the “contact fault” (Satterly 1952a) and are in fault contact with alkalic intrusive rocks that are correlated with the Timiskaming assemblage.

The alkalic intrusive rocks are composed of hornblendite, melasyenite, diorite, lamprophyre and syenite. The various rock types form an elongated east-striking intrusion that is varitextured, pegmatitic and aplitic in the west and becomes more equigranular, homogenous and mafic (diorite to gabbro) to the east. The presence of andradite garnet, abundant titanite and magmatic epidote indicate that the rocks crystallized under highly oxidized conditions (Pigeon 2002; Pigeon, Lalonde and Berger 1999). The intrusion progressively widens eastward from approximately 150 to greater than 1000 m and becomes more felsic to the south. Syenite and lamprophyre dikes extend up to 800 m west of the intrusion, but are most abundant near the west contact of the intrusion with the Kidd–Munro assemblage (in the vicinity of the main zone). The alkalic rocks display an intrusive contact with the Kidd–Munro assemblage. Greenstone xenoliths occur in the intrusion near the contact. There is a narrow contact-metamorphic aureole developed along the north side of the intrusion. The intrusion is in shear contact with the Porcupine assemblage. This east-striking shear zone extends west of the Pangea deposit to the Talisman Mine. Pangea Goldfields Incorporated discovered 3 gold-bearing zones within this shear zone. The intrusive rocks on the Pangea property possibly represent a cupola of the larger multiphase alkalic intrusion centred on Wayne Lake (*see* Map 2676, back pocket).

A diatreme breccia was encountered in diamond-drill core in the southeast part of the property. This breccia is associated with anomalous gold mineralization and represents another exploration target on the Pangea property (Photo 8). Rocks in this area are ultrapotassic; pseudoleucite bearing and associated with fluorite. Fluorine-bearing, ultrapotassic alkalic rocks are potential hosts for tin and tungsten mineralization (Müller and Groves 2000).

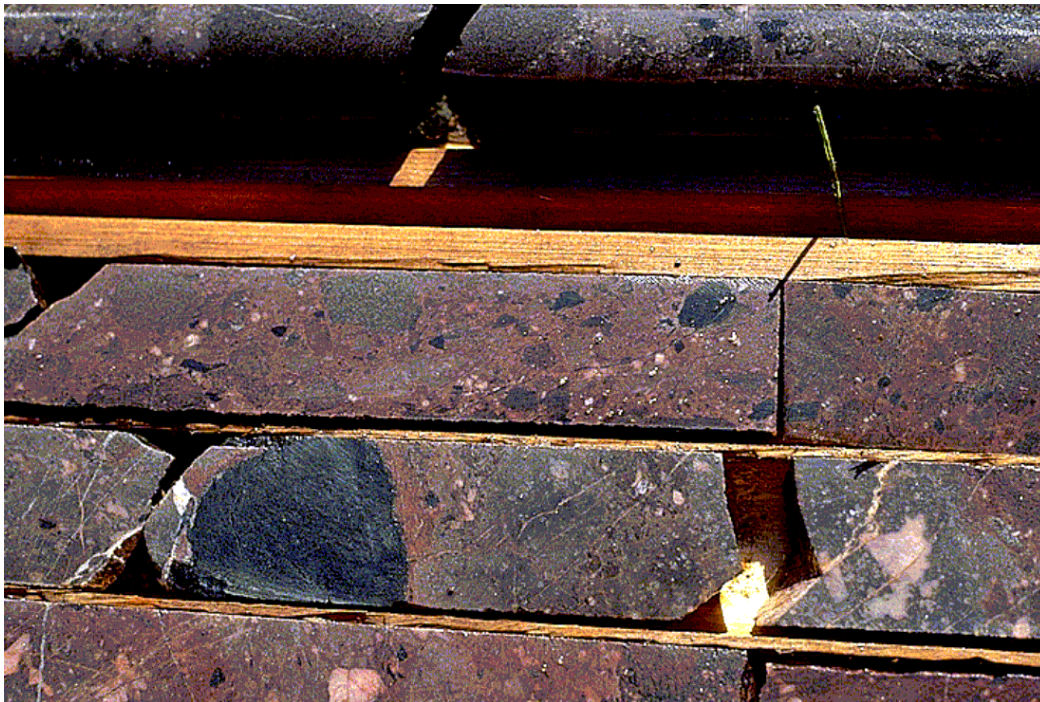


**Photo 8.** Alkalic diatreme breccia with white potassium feldspar replacing leucite, mafic and ultramafic xenoliths from the Pangea property, Guibord Township. Drill core diameter is 3.5 cm. Location: UTM Zone 17, NAD 27, 560341E 5374580N.

## PENTLAND FIRTH VENTURES LIMITED LUDGATE LAKE DEPOSIT

The Ludgate Lake deposit in south-central Michaud Township hosts a resource of 462 800 tonnes at 5.91 g/t gold (Pentland Firth Ventures Limited, web site: <http://www.pfo.com>, see web page: <http://www.pfo.com/projects/golden.htm> (web page accessed July 9, 2002)). The deposit is contained within an east-striking shear zone where it intersects syenitic phases of an alkalic intrusion along the north shore of Ludgate Lake (Bath 1990). Recent exploration by Pentland Firth Ventures Limited discovered additional mineralization to the south, referred to as the “Noel Zone”, but a resource has not been published (Pentland Firth Ventures Limited, see web page: <http://www.pfo.com/projects/golden.htm> (web page accessed July 9, 2002)). Gold occurs in disseminated and vein pyrite and is also free milling, but is not correlative with quartz veins (Bath 1990). The host syenite displays hematization, silicification, sericitization and little carbonatization.

A stripped outcrop, northwest of the deposit, exposes several geological features relevant to the mineralization. The outcrop exposes pegmatitic, aplitic and equigranular phases of the syenite suggesting that the intrusion is multiphase. Blue-green amphibole, identified as magnesioriebeckite (Pigeon, Lalonde and Berger 2001), is the main mafic silicate mineral in the syenite. Magnetite and tourmaline are characteristic of the pegmatitic phase. An auriferous mylonite zone, up to 3 m wide, transects the syenite at 190°, dip 65°, and also transects a foliation striking 317°, dip 58° (note: all orientations use right-hand rule). The mylonite is marked by red hematized borders, referred to as “jasper” by explorationists, which grades into a bleached white interior marked by narrow quartz ribbons and pyrite stringers. Thin sections collected from samples across the mylonite display progressive grain size reduction, cataclasis, and ductile deformation, which is characteristic of mylonite as described by Hobbs, Means and Williams (1976). A weak spaced cleavage striking 92°, dip 85°, offsets the mylonite zone in a sinistral sense, indicating that some deformation occurred after development of the mylonite. Free-milling gold occurs in the pyrite stringers and within pyrite grains. The pyrite stringers are folded within the mylonite indicating that mineralization was most likely synkinematic with development of the mylonite. Another key feature of this style of mineralization is the relative paucity of carbonatization. It indicates that widespread carbonate alteration is not necessary for gold mineralization to occur in the Hislop–Michaud segment.

## MONETA PORCUPINE MINES INCORPORATED PROPERTY

Moneta Porcupine Mines Incorporated owns the mining rights to a substantial part of central and southeast Michaud Township. Several potentially economic gold occurrences are known in this area. The most important is the “Southwest” zone where a resource of 460 000 ounces of gold (2.4 million tons at 6.1 grams gold per ton) is outlined over a true width of 6.4 m (Moneta Porcupine Mines Incorporated, Annual Report, 1997; web site: <http://www.monetaporcupine.com>; text of Annual Report available at web page: <http://www.monetaporcupine.com/annuals/pages97.pdf> (web pages accessed July 9, 2002)).

The “Southwest” zone occurs within the PDDZ, which is up to 1250 m wide in this area, and appears to be controlled by a combination of structure and stratigraphy. This mineralization appears to be unique in the study area because gold-bearing quartz stringers and veins occur at a depositional unconformity between magnetite-hematite iron formation, and Timiskaming assemblage conglomerate (Photo 9) host the gold. The author examined this unconformity in the core from several diamond-drill holes and observed that bedding in the iron formation has an angular discordance from 5 to 70° with the conglomerate. Hydrothermal alteration characterized by pervasive and vein sericitization, silicification, hematization and carbonatization is well developed in the conglomerate, but does not penetrate a short distance into the iron formation. Further, the unconformity appears to be fold repeated on the south limb of a synform, however, mineralization does not appear to occur along the southern contact (Moneta

Porcupine Mines Incorporated, Internal Report, 1998). The iron formation and conglomerate are inferred to be Timiskaming assemblage based on field relationships and recent geochronology in the Kirkland Lake area by J.A. Ayer (2670 Ma: J.A. Ayer, OGS, unpublished data, 2001). Hydrothermal fluids were probably channelled by the original porosity of the conglomerate and the iron formation served as a chemical trap that aided gold deposition.

The “Landing”, “Miller” and “Twin Creek” zones consist of gold mineralization hosted within sheared mafic and ultramafic metavolcanic rocks, lamprophyre and syenite dikes intruded along a brittle-ductile shear zone near the north margin of the PDDZ (*see* Map 2676, back pocket). The mineralization occurs within quartz breccia and stockwork zones with 2 to 5% disseminated pyrite and rare visible gold. The breccia and stockwork are accompanied by strong silicification, albitization, carbonatization and sericitization (green mica) within a larger carbonate envelope (Moneta Porcupine Mines Incorporated, 1996, report filed for assessment work credits, Kirkland Lake Resident Geologist’s Office, file KL-3914). This style of mineralization is erratic and difficult to trace along strike and down dip.

The “Last Chance” zone occurs approximately 2.5 km along strike and to the southwest of the “Twin Creek” zone (*see* Map 2676, back pocket). Mineralization at the “Last Chance” zone is hosted in a multiphase alkalic dike that intruded ultramafic metavolcanic schist near the north boundary of the PDDZ. The alkalic dike has an inner white albitite core characterized by large pyrite cubes, up to 7 mm in size, and essential albite and apatite with minor vein sericite and carbonate. This rock contains 9.38 weight % Na<sub>2</sub>O, 0.23 weight % K<sub>2</sub>O and anomalous gold (sample 98BRB0668, *see* Appendix 5; Moneta Porcupine Mines Incorporated, Internal Report, 1998). This albitite phase of the intrusion is similar to other white albitite intrusions observed at the Glimmer Mine, Taylor gold deposit, and the Aquarius gold mine west of the map area (Berger 2000a, 1994). The large pyrite cubes are inferred to be part of the primary crystallization of the albitite as they are not corroded and are interstitial to silicate minerals.

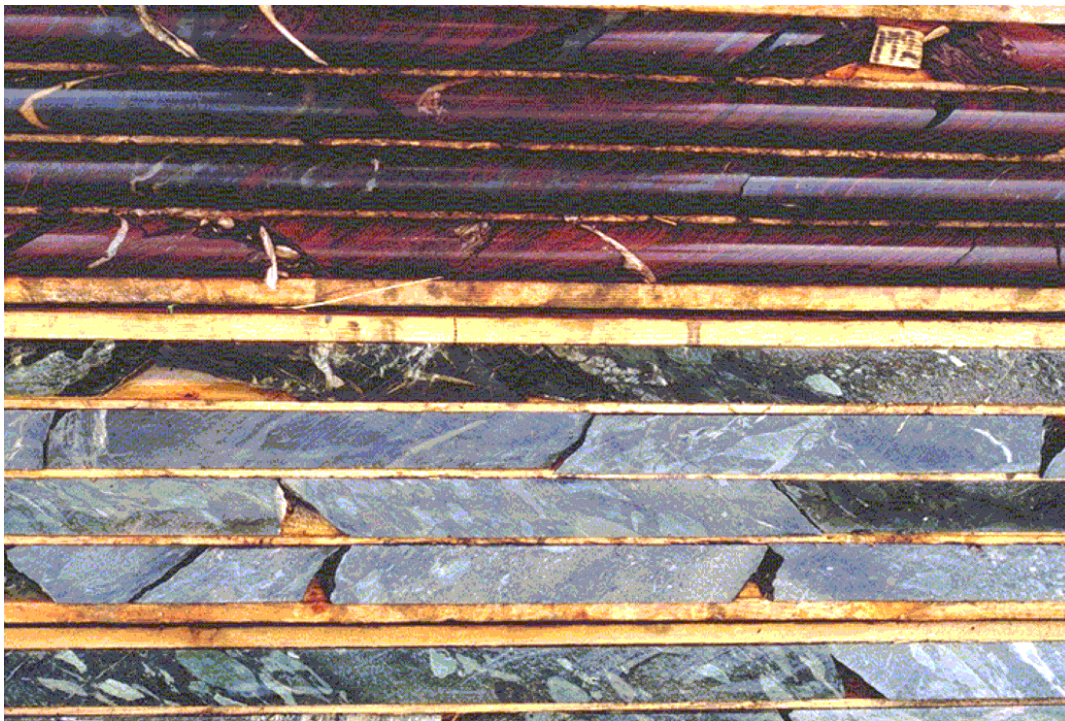


**Photo 9.** Unconformity between iron formation and conglomerate at the southwest gold zone in Michaud Township. Diamond-drill core is 3.5 cm in diameter. Diamond-drill hole M87-58, UTM Zone 17, NAD 27, 571638E, 5369756N.

The white albitite core passes gradationally into an outer rim of red-brown to brick red syenite composed of albite, microcline and minor quartz. Pyrite occurs as veins and hematite rimmed clots up to 3 mm in size. Secondary sericite, hematite, vein quartz and carbonate are common throughout the rock. The syenite is more foliated than the inner albitite and contains 5.32 weight % Na<sub>2</sub>O, 4.44 weight % K<sub>2</sub>O and potentially economic gold where quartz- and pyrite-filled fractures exceed more than 20% of the rock (sample 98BRB0667, *see* Appendix 5; Moneta Porcupine Mines Incorporated, Internal Report, 1998). Gold appears to be associated with the pyrite and quartz veins especially where pyrite occurs with quartz in stringers. The clotted pyrite, rimmed by hematite, indicates that oxidized fluids corroded the original cubic pyrite. This process may have liberated any gold in the pyrite and remobilized it into the quartz and pyrite veins. The “Last Chance” zone is a good example of the type of gold paragenesis envisaged by McNeil and Kerrich (1986) and Wyman and Kerrich (1988) for gold mineralization in other parts of the Abitibi greenstone belt. The potential for additional discoveries of this style of mineralization is good along the PDDZ and the south margin of the Ludgate Lake intrusion.

## **BUFFONTA MINE AND NEW BUFFONTA GOLD DEPOSIT OPEN PIT**

The Buffonta Mine and New Buffonta gold deposit open pit are located along the west contact of the Garrison stock in Garrison Township (*see* Figure 23). Both deposits are hosted in mafic, variolitic pillowed metavolcanic rocks of the Tisdale–Bowman assemblage and occur within shear zones situated within the contact-metamorphic aureole of the Garrison stock. Bath (1990) indicated that approximately 9200 ounces of gold were recovered from greater than 72 000 tons milled between 1937 and 1981 by various operators.

Strongly foliated to sheared (140°/62°) variolitic pillowed basalts display strong flattening and vertical plunges on stretching lineations in the foliation planes at the Buffonta Mine. Garnet and epidote occur as knots and boudins along the foliation planes and around pillow rims suggesting that the deformation and contact metamorphism were broadly synchronous. Gold mineralization is associated with quartz veins localized along the foliation planes and accompanied by carbonate and pyrite alteration halos. Cherry (1983) indicated that several vein orientations were present and all were mineralized, but the author did not observe this feature. The localization of mineralization in southeast-oriented structures is significant because it indicates that gold mineralization occurs orthogonal to the main trend of the PDDZ in the Hislop–Michaud segment.

The New Buffonta gold deposit open pit is located approximately 500 m southeast of the Buffonta Mine and is also referred to as the “No. 5 zone” (Bath 1990; Satterly 1949b). This deposit is closer to the contact of the Garrison stock (less than 200 m) and is characterized by foliated (125°/78°), massive, variolitic basalt and rare intermediate lapilli tuff intruded by monzonite and granite dikes along the foliation. Spaced cleavages oriented at 215°/74° displace the dikes and earlier foliation in a dextral sense indicative of local counterclockwise rotation of the rocks. Garnet and epidote associated with the contact-metamorphic aureole of the Garrison stock occurs along the main foliation planes and flow contacts of the variolitic basalts. Gold is associated with quartz-carbonate-pyrite veins and breccia developed along the contacts of a lamprophyre or kimberlite dike that intruded along the foliation (Bath 1990). There is a kimberlite dike exposed in the pit and Sage (1996) describes the dike in detail. The relationship of the kimberlite to gold mineralization is fortuitous, as the dike is Jurassic and the gold mineralization is Archean. The juxtaposition of the dike with gold indicates that the kimberlite exploited crustal-scale structures like the PDDZ and its related fault splays.

## **JONPOL EXPLORATIONS LIMITED GARRCON DEPOSIT**

The Garrcon deposit (*see* Figure 232), in Garrison Township, was developed by Consolidated Mining and Smelting Company of Canada Limited from 1935 to 1937 (Satterly 1949b). More recent work by Jonpol Explorations Limited defined a resource of 350 900 tons at 0.191 ounce per ton gold on the property (Bath 1990).

The main point of interest at the Garrcon deposit is exposed on the large stripped outcrop coincident with one of the mineralized zones. Here, intermediate to felsic alkalic flows, previously mapped as clastic metasedimentary rocks (Satterly 1949a), are so strongly altered and quartz veined that identification is difficult. However, the rocks are petrographically distinct from the nearby metasedimentary rocks in that the flows contain interlocking quartz and microcline and the metasedimentary rocks contain discrete detrital grains. The flows are also geochemically similar to the granitic dikes of the Garrison stock, whereas the metasedimentary rocks display less pronounced titanium, niobium and tantalum depletion (*see* Figures 18, 20 and 22). The recognition of alkalic flows in this area further strengthens comparison of the study area to the Kirkland Lake gold camp and provides strong field evidence that the metasedimentary rocks are part of the Timiskaming assemblage.

## **JONPOL EXPLORATIONS LIMITED JONPOL DEPOSIT**

The Jonpol deposit occurs approximately 750 m south of Highway 101 and 450 m west of Garrison Creek in Garrison Township (*see* Figure 23). An indicated resource, from diamond-drill hole data, of 513 000 tons at 0.28 ounce per ton gold is reported and a bulk sample of 55 000 tons at 0.243 ounce per ton gold was mined in early 1997 (*Canadian Mines Handbook, 1996–1997; Canadian Mines Handbook, 1997–1998*). The deposit is hosted in mafic and ultramafic metavolcanic rocks of the Kidd–Munro assemblage, north of the inferred trace of the PDDZ. The deposit is characterized by arsenopyrite and pyrite accompanied by various amounts of silicification, carbonatization and sericitization. There is little description of the deposit and the author infers that the mineralization is similar to other metavolcanic-hosted deposits east and west of the study area.

## **Harker–Holloway Segment**

The Harker–Holloway segment extends from the Garrison fault to the Quebec border (29 km in length, *see* Figure 23). The author notes that north-striking faults are identified by Couture (1991) in Quebec and may serve as bounding structures in this area. The Holloway and the Holt–McDermott mines exploit the 2 major gold deposits in the area and several other gold deposits and occurrences are known in the segment. Stratigraphy is relatively well understood. The Kidd–Munro assemblage occurs north of the Porcupine–Destor deformation zone (PDDZ) and as tectonic slivers within the PDDZ. The Kinojevis assemblage only occurs south of the PDDZ. Timiskaming assemblage clastic metasedimentary rocks are confined to the PDDZ. Several, multiphase, Timiskaming assemblage alkalic intrusions occur within and south of the PDDZ.

The PDDZ is an east-striking structure that narrows toward the east from greater than 1000 m to less than 300 m wide at the Quebec border. The structure is composed of a number of discrete brittle–ductile shear zones that separate wedges of relatively undeformed rocks. Several splay faults oriented at approximately 70° merge with, and possibly transect, the PDDZ. The Ghostmount and McKenna faults are the most important as gold mineralization is associated with these splay faults. Luinstra and Benn (2001, 1999) indicated that south-side-up reverse displacement was dominant along the main part of the PDDZ and the Ghostmount fault in the vicinity of the Holloway and Holt–McDermott mines. These

authors also demonstrated that complex isoclinal folding involving metasedimentary rocks of the Kidd–Munro and Timiskaming assemblages preceded the main shearing along the PDDZ. The majority of gold deposits occur within the PDDZ or along splay faults to the south. Gold mineralization at the Iris and Golden Harker deposits is associated with alkalic intrusive rocks well south of the PDDZ.

Gold mineralization in the PDDZ occurs with disseminated and vein pyrite in quartz-carbonate stockworks within tholeiitic metavolcanic rocks. Focussed and commonly intense albitization, silicification and sericitization is proximal to ore and occurs within a larger halo of iron-carbonate and hematite alteration. Chalcopyrite, arsenopyrite and rare scheelite are accessory minerals in the ore zones. Syenite dikes are associated with the highest gold grades at the Holt–McDermott Mine, however, barren alkalic intermineral dikes cut the Lightning zone at the Holloway Mine. Robert (1997) classified these deposits as syenite-associated disseminated sulphide deposits. Mineralization at the Iris and Golden Harker deposits is associated with alkalic intrusive rocks. Gold occurs with disseminated pyrite and quartz veins in the intrusions and surrounding metavolcanic rocks. Hematite and albite are common alteration minerals in the intrusive rocks, whereas hematite, epidote, chlorite and sericite are common in the metavolcanic rocks. Scheelite and rare molybdenite are reported as accessory minerals. The rest of this section will deal with specific features at the major deposits and will relate them to the regional setting.

## **HOLLOWAY MINE**

The Holloway Mine, situated in Holloway Township just north of Highway 101, was opened in 1997 to extract gold from the Lightning zone on reserves of 5.2 million tons at 7.9 g/t gold (Luinstra and Benn 2001). Geology at the Holloway Mine is summarized by Luinstra and Benn (2001) and Ropchan (2000). Readers are referred to these sources for detailed information. The Lightning zone is hosted by altered tholeiitic metavolcanic rocks that contain varioles and hyaloclastite and are correlated with the Kidd–Munro assemblage. Sheared ultramafic metavolcanic schist forms the immediate structural footwall and Timiskaming assemblage metasedimentary rocks comprise the structural hanging wall of the deposit (Luinstra and Benn 2001). The ore zone is composed predominantly of albite, carbonate and pyrite with minor sericite and occurs within a broader sericite-iron carbonate halo. A barren intermineral lamprophyre dike, from which an age of  $2671 \pm 1.7$  Ma has been obtained from zircons, cuts the ore zone and provides a maximum age for the alteration and main mineralizing event (Luinstra and Benn 2001; Kirkham 1971).

There are several interesting aspects to the mineralization at the Holloway Mine. The Lightning zone was a “blind” discovery located about 400 m below surface that was found after years of dedicated exploration. This emphasizes the necessity to explore at depth, as well as along the strike of, in an area of economic potential.

Berger (2001, 2000c) recognized that different styles of gold mineralization occurred within discrete segments along the PDDZ. Gold mineralization within the Harker–Holloway segment occurs within the PDDZ or on splay faults to the south. The Lightning zone occurs entirely within the PDDZ and future exploration is recommended within the deformation zone from the Garrison fault to the Quebec border (*see* Figure 23). The occurrence of metavolcanic rocks within the PDDZ appear to be the favoured targets for gold mineralization. Ropchan (2000) indicated that a tholeiitic metavolcanic rock with a high Fe/Mg ratio was a favoured host and emphasized that rock competency within the deformation zone was also a factor that favoured mineralization (i.e., brittle versus ductile deformation). Additionally, the author believes that an area of economic potential occurs where the PDDZ is greater than 250 m wide, thus permitting the preservation of folds and lozenges of relatively undeformed rocks. The area west of the Holloway Mine is also an area of economic potential. The area north of the syenite intrusion in west



Harker Township may contain unrecognized metavolcanic units within the Timiskaming assemblage metasedimentary rocks and requires more exploration in the author's opinion.

Luinstra and Benn (2001) constrained the timing of mineralization at the Holloway Mine and characterized the structural history (Figure 25). The PDDZ displays predominant reverse movement with an undetermined amount of vertical displacement. Lithological contacts, the Lightning zone and foliation developed during the reverse movement are folded by a second foliation that dips shallowly to the north (Luinstra and Benn 2001). This foliation may have resulted from continued compression during reverse movement or by a separate deformation event. In either case, both of these structural elements are observed all along the PDDZ from the Quebec border to west of Timmins (Berger 2001; Diné and Benn 2000; Vaillancourt 2000).

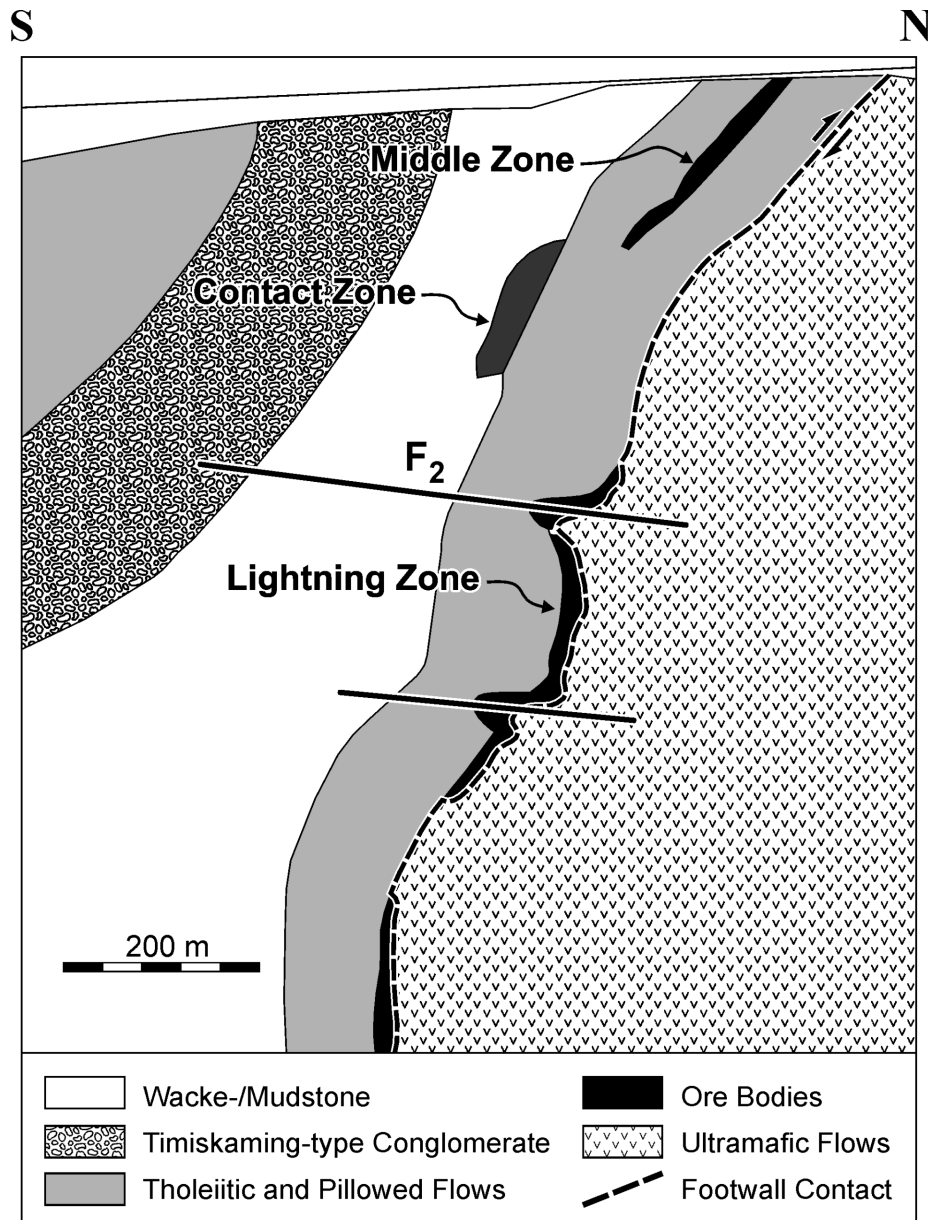


**Figure 25.** Simplified cross-section looking west through the Lightning zone in the Highway 101 area (*modified after* Luinstra and Benn 2001).

Gold-bearing quartz veins, hosted within the second foliation, transect the Lightning zone and occur at or near lithological contacts elsewhere in the Holloway Mine and within the PDDZ (Luinstra and Benn 2001). The pyrite associated with these quartz veins contains more arsenic than pyrite within the Lightning zone, which led Luinstra and Benn (2001) to conclude there were 2 distinct episodes of gold mineralization at the Holloway Mine. Gold mineralization in the Lightning zone is older than  $2671 \pm 1.7$  million years old (Luinstra and Benn 2001). Morasse et al. (1995) documented gold mineralization in Quebec before 2686 million years ago. Data from this study area support a widespread “early” gold mineralizing event in the Abitibi Subprovince. Robert (1997) proposed a geological model to account for the close spatial association of gold deposits, such as the Lightning zone, with alkalic intrusive rocks. In the author’s opinion, the evidence at the Holloway Mine is not compelling if considered in isolation to the surrounding area. However, Robert’s model (1997) is strongly supported when data from the Lightning zone are combined with data from the Holt–McDermott Mine and the Iris deposit.

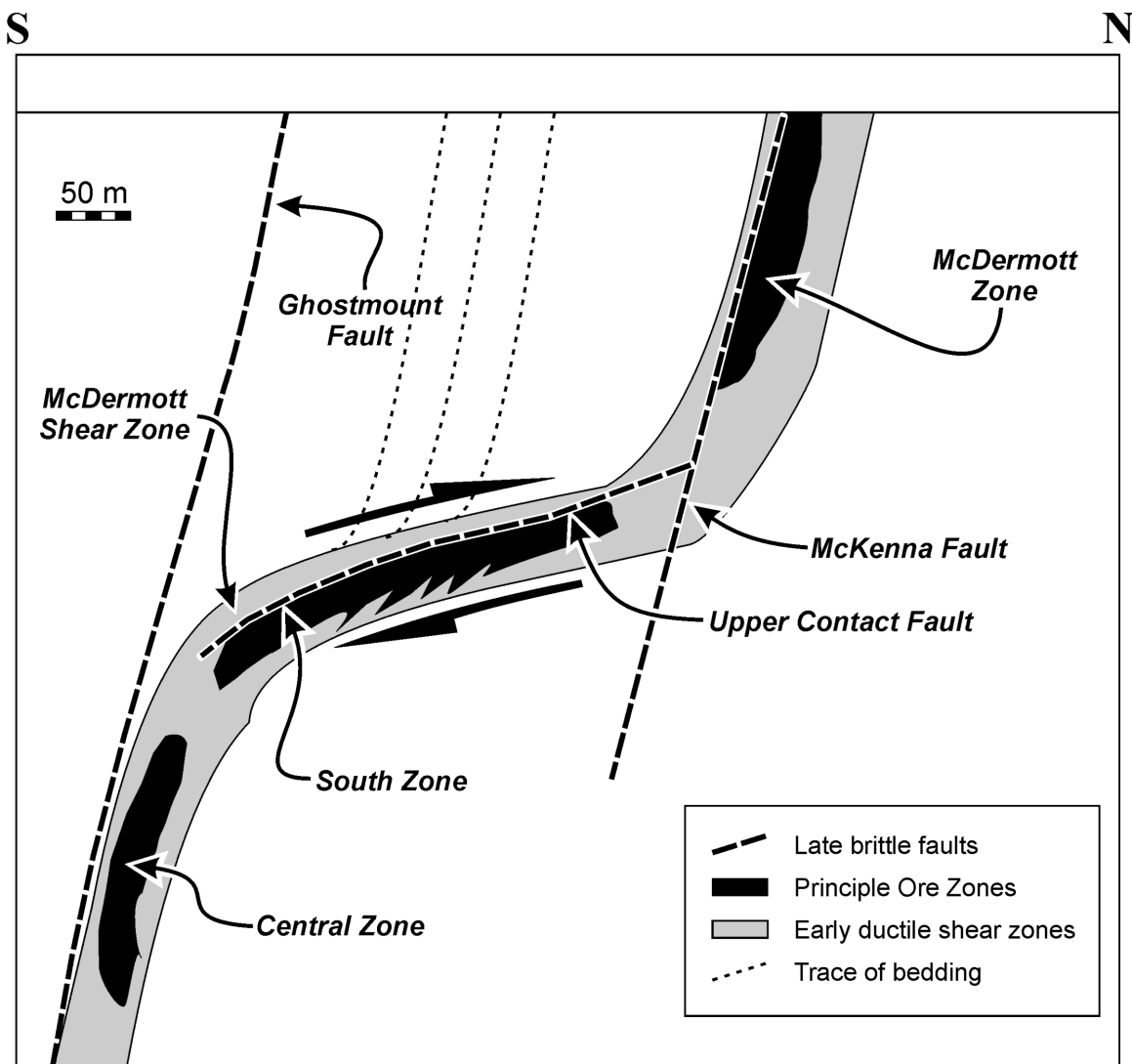


**Figure 26.** Schematic cross-section of the Holt–McDermott deposit in the Highway 101 area (*modified after* Luinstra and Benn 2001).

## HOLT–McDERMOTT MINE

The Holt–McDermott Mine is approximately 1 km south of the Holloway Mine and exploits gold from several ore bodies (*see* Figure 23). The geology is described by Luinstra and Benn (2001), Robert (1997) and Workman (1986). The ore deposits are hosted entirely within the Kinojevis assemblage and there is a pronounced structural control on the gold mineralization as a result of the Ghostmount and McKenna faults. The shallow dip of the “South zone” is a consequence of the reverse movement along the Ghostmount and McKenna faults, which resulted in the geometry of a vertically oriented sigmoidal tension gash (Figure 26; Luinstra and Benn 2001). The Tousignaut zone, approximately 3 km southwest of the Holt–McDermott Mine, is also shallow dipping and may represent another “flat-lying” deposit with similar geometry to the “South zone”. If this assumption is true, there is additional potential for other gold deposits along strike and at depth. Berger (2001) indicated that south-side-up movement was common all along the PDDZ from Timmins to the Quebec border. Such shallow-dipping ore shoots commonly referred to as “flat veins” by explorationists occur elsewhere along the PDDZ and indicate that the model proposed by Luinstra and Benn (2001) for the Holt–McDermott Mine is widely applicable.

Robert (1997) indicated that the Holt–McDermott Mine was a member of disseminated gold deposits spatially associated with syenite intrusions. Sodium-rich alkalic dikes in the “South zone” are the focus of intense silicification accompanied by sericite, hematite, pyrite and gold mineralization (Jones 2000). The dikes appear to be restricted to the “South zone” in the mine, but work by Ropchan, Nattress and Fowler (1999) shows that felsic dikes and associated auriferous alteration occur in the down-dip extension of the “Central zone” along the Ghostmount fault (*see* Figure 26). These data support the model proposed by Robert (1997) and suggest that the dikes and development of the faults are broadly synchronous.

## IRIS DEPOSIT

The Iris deposit, located in southern Harker Township, has an estimated resource of approximately 1 000 000 tons at 0.08 ounce per ton gold (Bath 1990). Gold is hosted in a coarse-grained, pyritic syenite intrusion that is cut by north-striking quartz veins, which also contain gold and scheelite. An exploration ramp, 10 by 10 by 500 feet in length, provides underground access to the deposit. Extensive surface stripping makes the Iris deposit an ideal area for detailed studies of syenite-associated gold mineralization. Pigeon, Lalonde and Berger (1999, 2000, 2001) provide summary descriptions and data for the Iris deposit and more detailed discussion is provided by Pigeon (2002).

The Iris stock is a multiphased intrusion with 1) “hornblendite and/or clinopyroxenite” around the east and south periphery; 2) medium-grained syenite and/or monzonite mostly along the south part of the intrusion; and 3) coarse-grained syenite along the north and west flanks (Pigeon, Lalonde and Berger 1999). The coarse-grained syenite is composed of centimetre-size perthite and anti-perthite crystals that comprise between 80 and 90% of the rock. Strongly chloritized mafic phenocrysts and trace amounts to 3% pyrite comprise the remainder of this phase. Only the coarse-grained syenite contains appreciable gold. Geochemistry of this phase (*see* Figure 24; *see* Appendix 5) indicates that the syenite is highly sodic and probably a result of late sodium-rich volatiles in the magma (Pigeon, Lalonde and Berger 2001). The Iris deposit is 7 km south of the PDDZ and is not associated with any major structure features. Kerrich and Cassidy (1994), Müller and Groves (2000), and Rowins, Lalonde and Cameron (1991) comment on the spatial and temporal association of gold mineralization with alkalic magmatism. Robert (1997) developed a geological model for syenite-associated disseminated gold deposits based, in part, on examples from the study area. The Iris deposit fits very well with the geological model developed by Robert (1997). The distinctive REE patterns displayed by the Iris syenite stock and related gold-bearing sodium-rich rocks may be significant (*see* Figure 24). Explorationists are recommended to look for similar patterns in alkalic rocks elsewhere in the Abitibi Subprovince (*see* Figure 24).

**Table 4.** Gold, platinum and palladium for selected samples in the Highway 101 area.

Sample	Rock Type	Township	Easting (m)	Northing (m)	Au (ppb)	Pt (ppb)	Pd (ppb)
*							
LMP99-068	Hornblendite	Harker	590489	5367381	ND	68.00	67.00
LMP99-103	Syenite	Harker	590461	5367414	198.00	ND	ND
LMP99-104	Syenite	Harker	590443	5367454	14.00	ND	ND
LMP99-105	Syenite	Harker	590443	5367421	31.00	ND	ND
LMP99-106	Syenite	Harker	590378	5367379	595.00	ND	ND
LMP99-114	Syenite	Harker	590331	5367341	810.00	ND	ND
LMP99-126	Hornblendite	Harker	590488	5367365	ND	44.00	17.00
LMP99-128	Hornblendite	Harker	590348	5367332	ND	18.00	17.00
LMP99-129	Hornblendite	Harker	590349	5367319	ND	11.00	8.00
LMP99-151	Hornblendite	Harker	589602	5367044	ND	ND	ND
!							
98BRB0655	Granodiorite	Garrison	577577	5369800	143.76	343.54	337.68
98BRB0660	Lamprophyre	Michaud	566690	5368523	84.42	247.68	249.09
98BRB0667	Altered albitite	Michaud	567915	5369329	15.44	23.04	20.74
98BRB0668	Unaltered albitite	Michaud	567915	5369329	124.70	12.61	11.51
98BRB0673	Melasyenite	Michaud	570101	5371093	13.94	10.61	11.16
98BRB0675	Hornblendite	Michaud	569608	5371245	19.52	17.95	20.04
98BRB0678	Melasyenite	Michaud	569097	5372033	17.72	15.34	15.51
98BRB0684	Hornblendite	Harker	588044	537082	4.92	12.23	17.43
98BRB0697	Alkali granite	Guibord	559617	5370796	3.36	10.97	12.08
HISLOP	Alkalic flow	Hislop	552061	5366397	3.18	11.82	12.56
98BRB0748	Hornblendite	Guibord	558578	5374938	3.70	7.66	7.26
98BRB0749	Lamprophyre	Guibord	558578	5374938	6.24	13.93	12.88
98BRB0758	Alkalic mafic flow	Guibord	560341	5374580	4.89	9.42	10.63
98BRB0760	Monzonite	Guibord	560206	5374096	5.50	11.38	12.96
98BRB0763	Leucite-bearing flow breccia	Guibord	560206	5374096	11.42	40.21	33.78
98BRB0777	Syenite	Michaud	566920	5370435	1.53	9.13	7.29
98BRB0779	Altered syenite	Michaud	566920	5370435	12.80	5.58	6.02
98BRB0782	Alkalic flow breccia	Guibord	560341	5374580	10.70	20.60	21.16
#							
01-RAS-131A	Peridotite	Harker	585471	5376312	ND	2.44	3.69
01-RAS-132A	Pyroxenite	Harker	585480	5376360	0.91	2.20	1.38
01-RAS-133A	Olivine pyroxenite	Harker	585482	5376370	ND	2.43	2.82
01-RAS-134A	Mesogabbro	Harker	585559	5376399	ND	5.62	7.33
01-RAS-135A	Leucogabbro	Harker	585615	5376398	ND	94.71	74.94
01-RAS-136A	Varitextured mesogabbro	Harker	586815	5376614	ND	ND	ND
01-RAS-137A	Leucogabbro	Harker	586815	5376616	1.76	1.50	ND
01-RAS-138A	Mesogabbro	Lamplugh	588086	5376690	ND	ND	ND
01-RAS-139A	Pegmatoidal gabbro	Lamplugh	588053	5376998	ND	ND	ND
01-RAS-140A	Gabbro	Lamplugh	587886	5377753	ND	ND	ND

Notes:

\* Data from Pigeon (2002), Iris property; detection limits Au = 5 ppb, Pt = 8 ppb, Pd = 8 ppb; UTM co-ordinates in NAD27, Zone 17.

! Data from Berger (this report); detection limits Au = 0.9 ppb, Pt = 0.9 ppb, Pd = 0.9 ppb; UTM co-ordinates in NAD27, Zone 17.

# Data from Hulbert and Vaillancourt (2002); detection limits Au = 0.9 ppb, Pt = 0.5 ppb, Pd = 0.9 ppb; UTM co-ordinates in NAD83, Zone 17.

The large positive airborne magnetic anomaly situated over the Iris stock (OGS 1984) is interpreted by the author to indicate that there is a subsurface extension of the intrusion. Subsurface syenite dikes are reported at the Golden Harker deposit, approximately 1000 m north of the Iris deposit, suggesting that an alkalic intrusion occurs in this area. Additionally, previous mapping included the mafic and ultramafic portions of the intrusion with the greenstone, which suggests that additional detailed mapping may locate additional exposures of the hornblendite and melagabbro. These rock types are economically important as Müller and Groves (2000) have indicated that platinum group elements (PGE) and gold can be enriched in mafic alkalic and shoshonitic intrusive rocks. Data from the Iris stock suggest that there is potential economic PGE mineralization in the hornblendite (Pigeon 2002; Table 4). The entire south part of Harker Township should be mapped in detail and any mafic alkalic rocks should be sampled and analyzed for possible PGE mineralization. Additional deep drilling around the Iris syenite stock may also indicate encouraging gold mineralization.

## **CANAMAX RESOURCES INCORPORATED “EAST ZONE” DEPOSIT**

The “East zone” deposit is located in Holloway Township approximately 4 km east of the Holloway Mine and north of Highway 101 (*see* Map 2676, back pocket). Reserves of 576 400 tons at 0.216 ounce gold per ton in 2 separate zones were reported by Canamax Resources Incorporated at the end of 1987 (*Canadian Mines Handbook, 1987–1988*). Approximately 42 700 tons of ore mined via an exploration drift yielded 5391 ounces of gold (approximately 0.13 ounce per ton gold). A further 72 000 tons of proven and probable material averaging 0.17 ounce per ton gold remained in place to the end of 1988 (Bath 1990). The mineralization is hosted near the contact between schistose mafic and ultramafic metavolcanic rocks of the Kidd–Munro assemblage and is characterized by quartz-carbonate-albite veins with gold, pyrite and arsenopyrite. Wall-rock alteration includes quartz, carbonate, chlorite, sericite, green mica and hematite (Bath 1990).

The “East zone” deposit, although small, is important because it provided the impetus to explore the PDDZ beyond the area of the Holt–McDermott and Holloway mines. It is also a near-surface example of the style of gold mineralization typical in the Harker–Holloway segment. The deposit emphasizes that mafic metavolcanic rocks within the PDDZ are the preferred host rocks for mineralization in this part of the study area. There are several other mineralized zones, such as the Pumphouse zone, the Black Top zone and the Teddy Bear Valley Mine, that are similar to the “East zone” deposit. Other zones may occur at depth or along strike in the area.

## **BASE METALS**

The Ross Mine produced approximately 2500 tons of copper (average grade 0.108% Cu) as a byproduct (Bath 1990). Chalcopyrite, bornite and copper-rich tennantite occurred in flat-lying tension veins in sections of the ore bodies. Galena, sphalerite, niccolite and rarely molybdenite were also reported from various veins (H. Lovell, Mineral Deposit Inventory Records, Resident Geologist’s Office, Kirkland Lake).

Copper mineralization is reported from a single diamond-drill hole at the “Noel zone” near Ludgate Lake in Michaud Township, but grade and width are unknown (G. Yule, Pentland Firth Ventures Limited, personal communication, 1998). Molybdenum values up to 4300 ppm are reported from diamond-drill holes in the Garrison stock and nearby ultramafic schist in Garrison Township by Cream Silver Mines Limited (1987, report filed for assessment work credits, AFRI#32D12SW0150). This occurrence is largely unexplored and suggests that there is potential for shear zone-hosted and porphyry-style mineralization in this part of the study area.

Copper, zinc and cobalt mineralization occurs at the Potter Mine in Munro Township north of the study area. This style of mineralization is hosted by hydrothermally altered komatiitic flows and hyaloclastite deposits intruded by synvolcanic sills (Gibson 1998). Exploration work continues on this deposit, however, preliminary synthesis suggests that the mineralization may be distal to a larger hydrothermal system and larger deposit (Gibson 1998). Komatiitic units extend southeast and along strike into McCool Township. Similar rock types are reported in north Michaud Township in the vicinity of Perry Lake (*see* Map 2676, back pocket). The author observed disseminated sulphide mineralization in cherty interflow metasedimentary rocks near the contact of the McCool sill just north of the map area. This area is recommended for further exploration.

Nickel assays, up to 2.71% Ni over narrow widths, are reported to occur in an ultramafic intrusion that underlies parts of lots 7 and 8, Concession VI, Hislop Township (various company reports filed for assessment work credits, Kirkland Lake Resident Geologist's Office). The exploration work was carried out for asbestos in the 1950s, and there is no indication that follow-up exploration was done or that analyses for platinum group element mineralization were performed. There is very little known about this intrusion as it is unexposed. Further exploration is recommended.

Tholeiitic or high-silica rhyolite is a favoured host for volcanogenic massive sulphide mineralization (Leshner et al. 1986; Barrie, Ludden and Green 1993). These rhyolites occur in the map area and have distinctive REE patterns that are similar to those shown in Figures 15c and 16a. There has been limited exploration along any of these units and it is recommended that any airborne electromagnetic anomaly associated with these units be tested. In rocks in the map area, Fowler et al. 2002) recognized a distinctive variole morphology, which is interpreted to be formed by magma mingling. Rock units with these varioles occur in Munro and Michaud townships and their geochemistry indicates that the felsic component is similar to high-silica rhyolite. The potential for base metals and gold to occur in these rock types remains untested and the author notes that disseminated sulphide mineralization occurs in rhyolites in Lot 11, Concession I, Munro Township.

## **PLATINUM GROUP ELEMENTS**

Platinum and palladium analyses were carried out on a number of samples in the study area (*see* Table 4). The mafic and ultramafic portions of the Iris stock display elevated platinum and palladium at levels consistent with primary magma PGE-enrichment (Müller and Groves 2000). Exploration for areas with increased sulphides in these phases may prove worthwhile for economic concentrations of platinum group elements. Several other alkalic intrusions contain ultramafic and mafic phases in Michaud and Guibord townships. These intrusions should be investigated for their platinum group element content.

The Ghost Range sill was sampled for platinum group elements as part of a regional project supported by Operation Treasure Hunt (Vaillancourt et al. 2001). Samples of leucogabbro, collected from the southwest part of the intrusion, returned elevated levels of platinum and palladium, which indicate that there is potential for PGE mineralization in the intrusion (*see* Table 4, samples with RAS prefix). There is little exploration reported in the Ghost Range sill, except for asbestos in the 1950s. The north and east portions of the intrusion are covered by overburden and there is virtually no exploration reported in these areas. Airborne electromagnetic anomalies occur in several areas around the periphery of the intrusion and most have not been explored (OGS 1984e, 1984f, 1984l, 1984m). Several ultramafic and mafic intrusions west of the Ghost Range sill in Garrison and McCool townships may also contain platinum group elements. Exploration of these intrusions is recommended.

## Recommendations For Mineral Exploration

Nearly continuous exploration over the last 90 years has resulted in numerous discoveries in the Highway 101 area. Two currently producing gold mines, several past producers and numerous occurrences and showings indicate that the area has a very good potential for gold exploration. However, in recent years, the rate of discovery has decreased and the cost of exploration has increased. Specific recommendations are included for each property or area above, however, some of the following general recommendations may be useful.

There are variations in geological setting and styles of gold mineralization along the Porcupine–Destor deformation zone (PDDZ) that appear to occur in blocks bounded by north-northwest-striking faults. Each block is interpreted by the author to expose different levels of the crust by various amounts of vertical, lateral and rotational movement of the north-northwest-striking faults. Gold mineralization is interpreted within the frame work of a crustal continuum depositional model, first proposed by Colvine et al. (1988) and improved by Groves et al. (1992).

Gold deposits, such as the Holt–McDermott and Holloway mines, that are east of the Garrison fault, occur within or south of the PDDZ. These deposits are classified by Robert (1997) as syenite-associated disseminated sulphide ores that are characterized by albite, hematite, sericite, silica and carbonate alteration. Exploration for such deposits would be best accomplished by deep penetrating electromagnetic methods along the PDDZ near alkalic intrusions or along the southwest-striking Ghostmount fault. Also, the north portion of the syenite intrusion in west Harker Township would be a good gold exploration target. The geometry of the ore zones at the Holt–McDermott Mine (*see* Figure 26) indicate that reverse vertical movement on the faults resulted in subhorizontal ore zones. Explorationists should be aware that such deposits may be present in this part of the study area.

Gold deposits, west of the Garrison fault and east of the Hislop fault, occur within the PDDZ, along subsidiary faults and along north-northwest-striking. Alkalic intrusive rocks are almost always spatially associated with the deposits and alteration characterized by hematite, silica, sericite and albite is most common. Carbonate alteration may be abundant, as at the Royal Oak open pit, or almost totally absent, as at the “Noel zone” near the Ludgate Lake deposit. The abundance of carbonate appears to depend upon the composition of the host rock with ultramafic and mafic metavolcanic rocks more strongly carbonatized than alkalic intrusive rocks. Most of Michaud and Guibord townships have the potential for successful gold exploration, however, emphasis should be devoted to locating areas where north-northwest-striking faults penetrate alkalic intrusions. The PDDZ is arcuate in this part of the study area and most gold is located on the northeast-striking portion of the deformation zone. The area between the “Southwest” zone and the Garrison fault is considered to be another area of economic potential by the author. Lithological contacts and rocks that respond to deformation in a brittle manner, such as iron formation and mafic metavolcanic rocks, are preferred host rocks.

The Ross Mine is a past producer of a million ounces of gold and 1.6 million ounces of silver. The deposit appears to occur within a down-faulted block between the Hislop and Ross faults and is characterized by anhydrite, barite, gypsum and sericite alteration indicative of extreme oxidization (Hattori and Cameron 1986; Ploeger 1978). The ore zones are described as steeply west-plunging pipes that are interpreted by the author to have developed in a brittle epizonal structural regime. There has been limited exploration outside of the Ross Mine west to the Hislop fault and future work in this area is recommended.

West of the Hislop fault, gold is confined to the PDDZ or occurs within and around the periphery of alkalic intrusions, such as at the Canadian Arrow deposit. The Glimmer Mine is typical of gold mineralization within the PDDZ, west of the Hislop fault, and is similar to the other gold deposits west of the study area. High-grade gold is confined to discontinuous quartz veins, pyritic albitite dikes and as free gold on chloritic fractures. Carbonate, sericite (commonly as green mica), quartz and albite are common alteration minerals that are tightly focussed around the ore zones. Ore zones are also commonly hosted in ultramafic and mafic metavolcanic schist. Exploration for these types of deposits is difficult, however, induced polarization geophysical surveys, supplemented with ground magnetometer geophysical surveys, may prove useful anywhere along the PDDZ.

Base metal exploration throughout the Highway 101 area is subordinate to gold and is concentrated in the few felsic metavolcanic units in the area. The Potter Mine, in Munro Township, is just north of the study area and is hosted in chloritized mafic hyaloclastite (Gibson 1998). There has been limited exploration for base metals in this type of host rock and the author notes that hyaloclastite, chert and disseminated sulphides occur along strike, to the southeast, in McCool Township. There are several untested airborne electromagnetic anomalies in this vicinity (OGS 1984c) and exploration is recommended.

Finally, it is important to emphasize that the discovery of new resources in the Highway 101 area must rely on thorough compilation of all existing geoscience data, not only at the property scale, but within a sizeable area of influence, in order to maximize exploration possibilities. Use of modern GIS (geographic information system) software and databases can only aid in this process.

“Good luck and happy hunting to all concerned.”



## References

- Ayer, J.A. and Trowell, N.F. 2001. The Abitibi greenstone belt: a program update; *in* Summary of Field Work and Other Activities 2001, Ontario Geological Survey, Open File Report 6070, p.4-1 to 4-10.
- Ayer, J.A., Trowell, N.F., Amelin, Y. and Corfu, F. 1999. Geological compilation of the Abitibi greenstone belt, Ontario: toward a revised stratigraphy based on compilation and new geochronology results; *in* Summary of Field Work and Other Activities 1998, Ontario Geological Survey, Miscellaneous Paper 169, p.14-24.
- Ayer, J.A., Trowell, N.F., Madon, Z., Kamo, S., Kwok, Y.Y. and Amelin, Y. 1999. Compilation of the Abitibi greenstone belt in the Timmins–Kirkland Lake area: revisions to stratigraphy and new geochronological results; *in* Summary of Field Work and Other Activities 1999, Ontario Geological Survey, Open File Report 6000, p.4-1 to 4-14.
- Baker, C.L. 2000. Quaternary geology of the Magusi River area; Ontario Geological Survey, Map 2648, scale 1:50 000.
- Baker, C.L., Seaman, A.A. and Steele, K.G. 1980. Quaternary geology of the Ramore area, districts of Cochrane and Timiskaming; Ontario Geological Survey, Preliminary Map P.2381, scale 1:50 000.
- Barrie, C.T. 1998. Kidd–Munro extension project, final report, Year 2; unpublished internal report, Joint Industry, Ontario Government and Government of Canada partnership project, 82p.
- 1999a. The Kidd–Munro extension project: geology of the Munro north area; *in* Summary of Field Work and Other Activities 1999, Ontario Geological Survey, Open File Report 6000, p.9-1 to 9-10.
- 1999b. The Kidd–Munro extension project: geology of the Mann Township area, *in* Summary of Field Work and Other Activities 1999, Ontario Geological Survey, Open File Report 6000, p.8-1 to 8-14.
- Barrie, C.T., Corfu, F., Davis, P., Coutts, A.C. and MacEachern, D. 1999. Geochemistry of the Dundonald komatiite-basalt suite and genesis of Dundead Ni deposit, Abitibi Subprovince, Canada; *Economic Geology*, v.94, p.845-866.
- Barrie, C.T., Hannington, M.D. and Bleeker, W. 1999. The giant Kidd Creek volcanic-associated massive sulfide deposit, Abitibi Subprovince, Canada; *in* Volcanic-associated massive sulfide deposits; processes and examples in modern and ancient settings, Society of Economic Geologists, *Reviews in Economic Geology*, v.8, p.247-269.
- Barrie, C.T., Ludden, J.N. and Green, T.H. 1993. Geochemistry of volcanic rocks associated with Cu-Zn and Ni-Cu deposits in the Abitibi Subprovince; *Economic Geology*, v.88, p.1341-1358.
- Bates, R.L. and Jackson, J.A. 1980. *Glossary of geology*, 3rd ed.; American Geological Institute, Alexandria, Virginia, 749p.
- Bath, A.C. 1990. Mineral occurrences, deposits and mines of the Black River–Matheson area; Ontario Geological Survey, Open File Report 5735, 1883p.
- Berger, B.R. 1994. Geology of Matheson and Evelyn townships, District of Cochrane; Ontario Geological Survey, Open File Report 5900, 109p.
- 1998. Precambrian geology, Hoyle and Gowan townships; Ontario Geological Survey, Report 299, 49p.

- 1999. Geology of Murphy and Wark townships, District of Cochrane; Ontario Geological Survey, Open File Report 5994, 64p.
- 2000a. Geology of the Monteith area; Ontario Geological Survey, Open File Report 6024, 77p.
- 2000b. Geology of Tully and Little townships, District of Cochrane; Ontario Geological Survey, Open File Report 6025, 73p.
- 2000c. Variation in styles of gold mineralization along the Porcupine–Destor fault zone in Ontario, Canada: an exploration guide; *in* Geology and ore deposits 2000: the great basin and beyond, Program with Abstracts, Geological Society of Nevada Symposium 2000, p.36.
- 2001. Variation in styles of gold mineralization along the Porcupine–Destor deformation zone in Ontario: an exploration guide, *in* Summary of Field Work and Other Activities 2001, Ontario Geological Survey, Open File Report 6070, p.9-1 to 9-13.
- Berger, B. and Amelin, Y. 1999. Geological investigations along Highway 101: Guibord, Michaud and Garrison townships, *in* Summary of Field Work and Other Activities 1998, Ontario Geological Survey, Miscellaneous Paper 169, p.25-32.
- Berger, B.R., Luinstra, B. and Ropchan, J. 2000. Precambrian geology of the Ghost Range area; Ontario Geological Survey, Map 2563, scale 1:50 000.
- Bleeker, W. and Parrish, R.R. 1996. Stratigraphy and U–Pb zircon geochronology of Kidd Creek: implications for the formation of giant volcanogenic massive sulphide deposits and the tectonic history of the Abitibi greenstone belt; *Canadian Journal of Earth Sciences*, v.33, p.1213-1231.
- Born, P. 1995. A sedimentary basin analysis of the Abitibi greenstone belt in the Timmins area, northern Ontario, Canada; unpublished PhD thesis, Carleton University, Ottawa, Ontario, 489p.
- Brisbin, D.I. 1997. Geological setting of gold deposits in the Porcupine gold camp, Timmins, Ontario; unpublished PhD thesis, Queen's University, Kingston, Ontario, 523p.
- Carrier, A., Jébrak, M., Angelier, J. and Holyland, P. 2000. The Silidor deposit, Rouyn–Noranda District, Abitibi belt: geology, structural evolution, and paleostress modeling of an Au quartz vein-type deposit in an Archean trondhjemite; *Economic Geology*, v.95, p.1049-1065.
- Cherry, M.E. 1983. The association of gold and felsic intrusions – examples from the Abitibi belt; *in* The geology of gold in Ontario; Ontario Geological Survey, Miscellaneous Paper 110, p.48-55.
- Collison, M.S. 1993. Mineralogy, petrology and geochemistry of Upper Timiskaming flow rocks near Kirkland Lake, Ontario; unpublished MSc thesis, University of Western Ontario, London, Ontario, 291p.
- Colvine, A.C., Fyon, J.A., Heather, K.B., Marmont, S., Smith, P.M. and Troop, D.G. 1988. Archean lode gold deposits in Ontario; Ontario Geological Survey, Miscellaneous Paper 139, 136p.
- Corfu, F. 1993. The evolution of the southern Abitibi greenstone belt in light of precise U-Pb geochronology; *Economic Geology*, v.88, p.1323-1340.
- Corfu, F., Krogh, T.E., Kwok, Y.Y. and Jensen L.S. 1989. U–Pb zircon geochronology in the southwestern Abitibi greenstone belt, Superior Province; *Canadian Journal of Earth Sciences*, v.26, p.1747-1763.
- Couture, J-F. 1991. Carte géologique des gîtes métallifères des districts de Rouyn–Noranda et de Val-d’Or; Ministère de l’Énergie et des ressources du Québec, carte DV90-11, échelle de 1:250 000.

- Dinel, E. and Benn, K. 2000. Structural investigations of the Echo Bay and International Falcon properties in Ogden Township; *in* Summary of Field Work and Other Activities 2000, Ontario Geological Survey, Open File Report 6032, p.12-1 to 12-5.
- Drost, A.P. 1987. Geological analysis of gradient aeromagnetics with implications for gold exploration in the Black River–Matheson area, Cochrane District, northeastern Ontario; unpublished report, Department of Geological Sciences, Queen’s University, Kingston, Ontario, 25p.
- Easton, R.M. and Johns, G.W. 1986. Volcanology and mineral exploration: the application of physical volcanology and facies studies; *in* Volcanology and mineral deposits, Ontario Geological Survey, Miscellaneous Paper 129, p.2-40.
- Feng, R. and Kerrich, R. 1990. Geobarometry, differential block movements, and crustal structure of the southwestern Abitibi greenstone belt, Canada; *Geology*, v.18, p.870-873.
- Fowler, A.D., Berger, B., Shore, M., Jones, M.I. and Ropchan, J. 2002. Supercooled rocks: development and significance of varioles, spherulites, dendrites and spinifex of Archean volcanic rocks, Abitibi greenstone belt, Canada; *Precambrian Research*, v.115, p.311-328.
- Fowler, A.D., Jensen, L.S. and Peloquin, S.A. 1987. Varioles in Archean basalts: products of spherulitic crystallization; *The Canadian Mineralogist*, v.25, p.275-289.
- Gélinas, L., Brooks, C. and Trzcienski, W.E., Jr. 1976. Archean variolites – quenched immiscible liquids; *Canadian Journal of Earth Sciences*, v.13, p.210-230.
- Gibson, H.L. 1998. A petrographic and geochemical study of the Potter Mine and interpretation on its volcanic environment, Munro Township, Ontario; for Millstream Mines Limited, <http://www.millstreammines.com/PotGeoGib.html>, [web page accessed July 3, 2002]
- Gibson, H.L., Morton, R.L. and Hudak, G.J. 1999. Submarine volcanic processes, deposits and environments favorable for the location of volcanic-associated massive sulfide deposits; *in* Volcanic-associated massive sulfide deposits: processes and examples in modern and ancient settings, Society of Economic Geologists, *Reviews in Economic Geology*, v.8, p.13-51.
- Groves, D.I., Barley, M.E., Barnicoat, A.C., Cassidy, K.F., Fare, R.J., Hagemann, S.G., Ho, S.E., Hronsky, J.M.A., Mikucki, E.J., Mueller, A.G., McNaughton, N.J., Perring, C.S., Ridley, J.R. and Vearncombe, J.R. 1992. Sub-greenschist- to granulite-hosted Archean lode-gold deposits of the Yilgarn Craton: a depositional continuum from deep-sourced hydrothermal fluids in crustal-scale plumbing systems; The University of Western Australia, Geology Department (Key Centre) and University Extension, Publication 22, p.325-337.
- Hamilton, S.M., Bajc, A.F., Farrow, C.E.G. and McClenaghan, M.B. 1995. Multi-media geochemical sampling in areas of thick overburden: a case study; *in* Summary of Field Work and Other Activities 1995; Ontario Geological Survey, Miscellaneous Paper 164, p.258-262.
- Hattori, K. 1993. Diverse metal sources of Archean gold deposits: evidence from in situ lead-isotope analysis of individual grains of galena and altaite in the Ross and Kirkland Lake deposits, Abitibi greenstone belt, Canada; *Contributions to Mineralogy and Petrology*, v.113, p.185-195.
- Hattori, K. and Cameron, E.M. 1986. Archean magmatic sulphate; *Nature*, v.319, p.45-47.
- Hattori, K., Hart, S.R. and Shimizu, N. 1996. Melt and source mantle compositions in the Late Archean: a study of strontium and neodymium isotope and trace elements in clinopyroxenes from shoshonitic alkaline rocks; *Geochimica et Cosmochimica Acta*, v.60, p.4551-4562.

- Hattori, K. and Percival, J. 1999. Archean carbonate- and nepheline-bearing alkaline igneous complexes of the western Quetico metasedimentary belt, Superior Province, Canada; *in* 1999 Western Superior Transect, Fifth Annual Workshop, Lithoprobe Report #70, Lithoprobe Secretariat, University of British Columbia, Vancouver, British Columbia, p.76-79.
- Henderson, P. ed. 1984. *Developments in geochemistry 2: rare earth element geochemistry*; Elsevier, Amsterdam, 510p.
- Hill, R.E.T., Barnes, S.J., Gole, M.J. and Dowling, S.E. 1990. *Physical volcanology of komatiites*; Geological Society of Australia, Excursion Guide Book No. 1, 100p.
- Hobbs, B.E., Means, W.D. and Williams, P.F. 1976. *An outline of structural geology*; John Wiley and Sons, Inc., Toronto, 571p.
- Hoxha, M. 1999. A preliminary model for emplacement of gold bearing structures at the Glimmer Mine gold deposit: guidelines for exploration and mining; unpublished extended abstract, Northeastern Ontario Mines and Minerals Symposium 1999, Ontario Prospector's Association, Timmins, Ontario, 3p.
- Hulbert, L. and Vaillancourt, C. 2002. Magmatic Ni-Cu  $\pm$  PGE occurrences and mafic-ultramafic bodies in Ontario; Ontario Geological Survey, Miscellaneous Release—Data 100.
- Hyde, R.S. 1978. Sedimentology, volcanology, stratigraphy and tectonic setting of the Archean Timiskaming Group, Abitibi greenstone belt, northeastern Ontario, Canada; unpublished PhD thesis, McMaster University, Hamilton, Ontario, 422p.
- Jackson, S.L. and Fyon, J.A. 1991. The western Abitibi Subprovince of Ontario; *in* *Geology of Ontario*, Ontario Geological Survey, Special Volume 4, Part 1, p.405-484.
- Jensen, L.S. 1976. A new cation plot for classifying subalkalic volcanic rocks; Ontario Division of Mines, Miscellaneous Paper 66, 22p.
- 1978. *Geology of Stoughton and Marriott townships, District of Cochrane, Ontario*; Ontario Geological Survey, Report 173, 72p.
- 1982a. *Precambrian geology of the Ghost Range area, Lightning River area, Cochrane District, Ontario*; Ontario Geological Survey, Preliminary Map P.2431, scale 1:15 840.
- 1982b. *Precambrian geology of the Lightning Mountain area, Lightning River area, Cochrane District, Ontario*; Ontario Geological Survey, Preliminary Map P.2432, scale 1:15 840.
- 1982c. *Precambrian geology of the Lightning River area, Cochrane District, Ontario*; Ontario Geological Survey, Preliminary Map P.2433, scale 1:63 360.
- 1982d. *Precambrian geology of the Magusi River area, Cochrane and Timiskaming districts, Ontario*; Ontario Geological Survey, Preliminary Map P.2434, scale 1:63 360.
- 1985a. *Precambrian geology of the Ramore area, northwestern part, District of Cochrane, Ontario*; Ontario Geological Survey, Preliminary Map P.2860, scale 1:15 840.
- 1985b. *Precambrian geology of the Ramore area, northeastern part, District of Cochrane, Ontario*; Ontario Geological Survey, Preliminary Map P.2861, scale 1:15 840.,
- Jensen, L.S. and Baker, C.L. 1986. Preliminary results of bedrock samples from the sonic drilling program (1985) in the Lake Abitibi–Matheson area, Cochrane District; Ontario Geological Survey, Preliminary Map P.2986, scale 1:100 000.

- Jensen, L.S. and Langford, F.F. 1985. Geology and petrogenesis of the Archean Abitibi belt in the Kirkland Lake area, Ontario; Ontario Geological Survey, Miscellaneous Paper 123, 130p.
- Jensen, L.S. and Trowell, N.F. 1985. Preliminary results of bedrock samples from the sonic drilling program, Matheson area, Cochrane District, Ontario; Ontario Geological Survey, Preliminary Map P.2848, scale 1:100 000.
- Johnstone, R.M. 1991. The geology of the northwestern Black River–Matheson area, District of Cochrane; Ontario Geological Survey, Open File Report 5785, 288p.
- Johnstone, R.M. and Steele, K.G. 1989. Bedrock samples from the sonic drilling program (1987) in the Matheson area, District of Cochrane, Ontario; Ontario Geological Survey, Preliminary Map P.3114, scale 1:100 000..
- Johnstone, R.M. and Trowell, N.F. 1985. Precambrian geology of the Black River–Matheson (BRIM) area, District of Cochrane; *in* Summary of Field Work and Other Activities 1985, Ontario Geological Survey, Miscellaneous Paper 126, p.291-296.
- Jones, L.R. 2000. Geochemical alteration phases associated with gold mineralization at Holt–McDermott Mine, Holloway Township, Ontario; unpublished BSc thesis, Saint Mary’s University, Halifax, Nova Scotia, 442p.
- Jones, M.I. 1992. Variolitic basalts: relations to Archean epigenetic gold deposits in the Abitibi greenstone belt; unpublished MSc thesis, Ottawa–Carleton Geoscience Centre, University of Ottawa, Ottawa, Ontario, 300p.
- Kerrich, R. and Cassidy, K.F. 1994. Temporal relationships of lode gold mineralization to accretion, magmatism and deformation – Archean to present: a review; *Ore Geology Reviews*, v.9, p.263-310.
- King, R.W. and Kerrich, R. 1987. Fluorapatite fenitization and gold enrichment in sheeted trondhjemites within the Destor–Porcupine fault zone, Taylor Township, Ontario; *Canadian Journal of Earth Sciences*, v.24, p.479-502.
- Kirkham, R.V. 1971. Intermineral intrusions and their bearing on the origin of porphyry copper and molybdenum deposits; *Economic Geology*, v.66, p.1244-1249.
- Knight, C.W., Burrows, A.G., Hopkins, P.E. and Parsons, A.L. 1919. Abitibi–Night Hawk gold area, Ontario; Ontario Bureau of Mines, Annual Report, 1919, v.28, pt 2, p.1-70.
- LaRocque, J.A. 1952. A study of the mineralogy of “13” and “14” veins and their influence on the gold-silver ratio at the Ross Mine, Ramore area, Ontario; unpublished MSc thesis, University of Toronto, Toronto, Ontario, 84p.
- Leahy, E.J. 1965. Currie and Bowman townships, District of Cochrane, Ontario Department of Mines, Map 2071, scale 1:31 680.
- Leshner, C.M., Goodwin, A.M., Campbell, I.H. and Gorton, M.P. 1986. Trace-element geochemistry of ore-associated and barren, felsic metavolcanic rocks in the Superior Province, Canada; *Canadian Journal of Earth Sciences*, v.23, p.222-237.
- Luinstra, B. and Benn, K. 1999. Structural geology of the Holloway Township gold camp, Abitibi greenstone belt, northeastern Ontario; *in* Summary of Field Work and Other Activities 1999, Ontario Geological Survey, Open File Report 6000, p.10-1 to 10-4.
- 2001. Structural geology of the Holloway Mine, Abitibi greenstone belt, Ontario; Ontario Geological Survey, Open File Report 6045, 36p.
- MacRae, N.D. 1969. Ultramafic intrusions of the Abitibi area, Ontario; *Canadian Journal of Earth Sciences*, v.6, p.281-303.

- Madon, Z., Trowell, N.F., Berger, B.R. and Ayer, J.A. 1999. Geological investigation and data integration of “typical” Canadian Shield terrain using airborne and satellite imagery including RADARSAT radar: Lightning River area, Abitibi greenstone belt, Ontario; *Canadian Journal of Remote Sensing*, v.25, p.229-244.
- McClenaghan, B.M. 1991. Geochemistry of tills from the Black River–Matheson (BRIM) sonic overburden drilling program and implications for exploration; Ontario Geological Survey, Open File Report 5800, 263p.
- McNeil, A.M. and Kerrich, R. 1986. Archean lamprophyre dykes and gold mineralization, Matheson, Ontario: the conjunction of LILE-enriched mafic magmas, deep crustal structures and Au concentration; *Canadian Journal of Earth Sciences*, v.23, p.324-343.
- Morasse, S., Wasteneys, H.A., Cormier, M. and Helmstaedt, H. 1995. A pre-2686 Ma intrusion-related gold deposit at the Kiena mine, Val d’Or, Quebec, southern Abitibi Subprovince; *Economic Geology*, v.90, p.1310-1321.
- Müller, D. and Groves, D.I. 2000. Potassic igneous rocks and associated gold-copper mineralization, 3rd ed.; Springer, Berlin, 252p.
- Mueller, W.U. and Corcoran, P.L. 1998. Late-orogenic basins in the Archaean Superior Province, Canada: characteristics and inferences; *Sedimentary Geology*, v.120, p.177-203.
- Mueller, W.U., Daigneault, R., Mortensen, J.K. and Chown, E.H. 1996. Archean terrane docking: upper crust collision tectonics, Abitibi greenstone belt, Quebec, Canada; *Tectonophysics*, v.65, p.127-150.
- Mueller, W., Donaldson, J.A. and Doucet, P. 1994. Volcanic and tectono-plutonic influences on sedimentation in the Archaean Kirkland Basin, Abitibi greenstone belt, Canada; *Precambrian Research*, v.68, p.201-230.
- Muir, T.L. 1995. Geology of Stock Township, District of Cochrane, Ontario Geological Survey, Preliminary Map P.3347, scale 1:20 000.
- Ontario Geological Survey 1984a. Airborne electromagnetic and total intensity survey, Matheson–Black River area, Beatty Township, District of Cochrane; Ontario Geological Survey, Map 80 585, scale 1:20 000.
- 1984b. Airborne electromagnetic and total intensity survey, Matheson–Black River area, Munro Township, District of Cochrane; Ontario Geological Survey, Map 80 586, scale 1:20 000.
- 1984c. Airborne electromagnetic and total intensity survey, Matheson–Black River area, McCool Township, District of Cochrane; Ontario Geological Survey, Map 80 587, scale 1:20 000.
- 1984d. Airborne electromagnetic and total intensity survey, Matheson–Black River area, Rand Township, District of Cochrane; Ontario Geological Survey, Map 80 588, scale 1:20 000.
- 1984e. Airborne electromagnetic and total intensity survey, Matheson–Black River area, Lamplugh Township, District of Cochrane; Ontario Geological Survey, Map 80 589, scale 1:20 000.
- 1984f. Airborne electromagnetic and total intensity survey, Matheson–Black River area, Frecheville Township, District of Cochrane; Ontario Geological Survey, Map 80 590, scale 1:20 000.
- 1984g. Airborne electromagnetic and total intensity survey, Matheson–Black River area, Stoughton Township, District of Cochrane; Ontario Geological Survey, Map 80 591, scale 1:20 000.
- 1984h. Airborne electromagnetic and total intensity survey, Matheson–Black River area, Hislop Township, District of Cochrane; Ontario Geological Survey, Map 80 595, scale 1:20 000.
- 1984i. Airborne electromagnetic and total intensity survey, Matheson–Black River area, Guibord Township, District of Cochrane; Ontario Geological Survey, Map 80 596, scale 1:20 000.

- 1984j. Airborne electromagnetic and total intensity survey, Matheson–Black River area, Michaud Township, District of Cochrane; Ontario Geological Survey, Map 80 597, scale 1:20 000.
- 1984k. Airborne electromagnetic and total intensity survey, Matheson–Black River area, Garrison Township, District of Cochrane; Ontario Geological Survey, Map 80 598, scale 1:20 000.
- 1984l. Airborne electromagnetic and total intensity survey, Matheson–Black River area, Harker Township, District of Cochrane; Ontario Geological Survey, Map 80 599, scale 1:20 000.
- 1984m. Airborne electromagnetic and total intensity survey, Matheson–Black River area, Holloway Township, District of Cochrane; Ontario Geological Survey, Map 80 600, scale 1:20 000.
- 1984n. Airborne electromagnetic and total intensity survey, Matheson–Black River area, Marriott Township, District of Cochrane; Ontario Geological Survey, Map 80 601, scale 1:20 000.
- Osmani, I.A. 1991. Proterozoic mafic dike swarms in the Superior Province of Ontario; *in* Geology of Ontario, Ontario Geological Survey, Special Volume 4, Part 1, p.661-681.
- Panteleyev, A. 1988. A Canadian Cordilleran model for epithermal gold-silver deposits, *in* Ore Deposit Models, Geological Association of Canada, Geoscience Canada Reprint Series 3, p.31-43.
- Pearce, J. 1996. A user's guide to basalt discrimination diagrams; *in* Trace element geochemistry of volcanic rocks: applications for massive sulphide exploration; Geological Association of Canada, Short Course Notes Volume 12, p.79-113.
- Peccerillo, A. and Taylor, S.R. 1976. Geochemistry of Eocene calc-alkalic volcanic rocks from the Kastamonu area, northern Turkey; *Contributions to Mineralogy and Petrology*, v.58, p.63-81.
- Pigeon, L. 2002. Petrogenesis of syenitic magmatism associated with gold mineralization along the Destor–Porcupine fault zone near Matheson, Ontario; unpublished MSc thesis, Ottawa–Carleton Geoscience Centre, University of Ottawa, Ottawa, Ontario, 21p.
- Pigeon, L., Lalonde, A.E. and Berger, B.R. 1999. Petrogenesis of syenitic magmatism associated with gold mineralization along the Destor–Porcupine fault zone near Matheson, Ontario; *in* Summary of Field Work and Other Activities 1999, Ontario Geological Survey, Open File Report 6000, p.12-1 to 12-4.
- 2000. Petrogenesis of syenitic magmatism associated with gold mineralization along the Destor–Porcupine fault zone near Matheson, Ontario; *in* Summary of Field Work and Other Activities 2000, Ontario Geological Survey, Open File Report 6032, p.8-1 to 8-6.
- 2001. Mineralogy of pyroxene, amphibole and mica in syenitic rocks of the Porcupine–Destor deformation zone near Matheson, Ontario; *in* Summary of Field Work and Other Activities 2001, Ontario Geological Survey, Open File Report 6070, p.11-1 to 11-9.
- Ploeger, F.R. 1978. Geology and ore control at the Ross Mine, Holtvre; Ontario Geological Survey, unpublished internal report, 58p.
- Prest, V.K. 1951. Township of Guibord, District of Cochrane, Ontario; Ontario Department of Mines, Map 1951-6, scale 1:12 000.
- 1953. Geology of Guibord Township, Cochrane District, Ontario; Ontario Department of Mines, Annual Report, 1951, v.60, pt.9, 56p.
- 1955. Township of Hislop, Cochrane District, Ontario; Ontario Department of Mines, Map 1955-5, scale 1:12 000.

- 1957. Geology of Hislop Township, Cochrane District, Ontario; Ontario Department of Mines, Annual Report, 1956, v.65, pt.5, 51p.
- Robert, F. 1997. A preliminary geological model for syenite-associated disseminated gold deposits in the Abitibi belt, Ontario and Quebec; *in* Current Research, Part C, Geological Survey of Canada, Paper 1997-C, p.201-210.
- Ropchan, J.C. 2000. Petrographic and geochemical studies of the alteration zones associated with gold mineralization at the Holloway Mine, southwestern Abitibi greenstone belt, Canada; unpublished MSc thesis, Ottawa–Carleton Geoscience Centre, University of Ottawa, Ottawa, Ontario, 141p.
- Ropchan, J.C., Nattress, S.D. and Fowler, A.D. 1999. Petrographic and geochemical studies of the alteration zones associated with gold mineralization at the Holloway Mine and down-dip extension of the Holt–McDermott deposit, southwestern Abitibi greenstone belt; *in* Summary of Field Work and Other Activities 1998, Ontario Geological Survey, Miscellaneous Paper 169, p.39-42.
- Rowins, S.M., Lalonde, A.E. and Cameron, E.M.I. 1991. Magmatic oxidation in the syenitic Murdock Creek intrusion, Kirkland Lake, Ontario: evidence from the ferromagnesian silicates; *Journal of Geology*, v.99, p.395-414.
- Sage, R.P. 1996. Kimberlites of the Lake Timiskaming structural zone; Ontario Geological Survey, Open File Report 5937, 435p.
- 2000. Kimberlites of the Lake Timiskaming structural zone: Supplement; Ontario Geological Survey, Open File Report 6018, 123p.
- Satterly, J. 1947. Township of Michaud, Cochrane District, Ontario; Ontario Department of Mines, Map 1947-3, scale 1:12 000.
- 1948. Geology of Michaud Township; Ontario Department of Mines, Annual Report, v.57, pt.4, 27p.
- 1949a. Township of Garrison, Cochrane District, Ontario; Ontario Department of Mines, Map 1949-1, scale 1:12 000.
- 1949b. Geology of Garrison Township; Ontario Department of Mines, Annual Report, v.48, pt.4, 33p.
- 1951a. Township of Harker, District of Cochrane, Ontario; Ontario Department of Mines, Map 1951-4, scale 1:12 000.
- 1951b. Geology of Harker Township; Ontario Department of Mines, Annual Report, v.60, pt.7, 47p.
- 1951c. Township of Munro, District of Cochrane, Ontario; Ontario Department of Mines, Map 1951-5, scale 1:12 000.
- 1952a. Geology of Munro Township; Ontario Department of Mines, Annual Report, v.60, pt.8, 60p.
- 1952b. Township of McCool, District of Cochrane, Ontario; Ontario Department of Mines, Map 1952-2, scale 1:12 000.
- 1953a. North part of the Township of Holloway, District of Cochrane, Ontario; Ontario Department of Mines, Map 1953-4, scale 1:12 000.
- 1953b. Geology of the north half of Holloway Township; Ontario Department of Mines, Annual Report, v.62, pt.7, 38p.



- Satterly, J. and Armstrong, H.S. 1947. Township of Beatty, District of Cochrane, Ontario; Ontario Department of Mines, Map 1947-2, scale 1:12 000.
- Siragusa, G.M. 1993. Gold mineralization in the Stock and Taylor townships area of the Abitibi greenstone belt; *in* Summary of Field Work and Other Activities 1993, Ontario Geological Survey, Miscellaneous Paper 162, p.74-78.
- Sproule, R.A., Leshner, C.M., Ayer, J.A. and Thurston, P.C. 2000. Temporal and spatial variations in komatiitic geochemistry in the Abitibi greenstone belt; *in* Summary of Field Work and Other Activities 2000, Ontario Geological Survey, Open File Report 6032, p.10-1 to 10-14.
- Thurston, P.C. 1991. Archean geology of Ontario: introduction; *in* Geology of Ontario, Ontario Geological Survey, Special Volume 4, Part 1, p.73-77.
- Troop, D.G. 1985. Preliminary report on geology and metasomatism at the Ross Mine and vicinity, District of Cochrane; *in* Summary of Field Work and Other Activities 1985, Ontario Geological Survey, Miscellaneous Paper 126, p.320-325.
- 1986. Multiple orebody types and vein morphologies, Ross Mine, District of Cochrane; *in* Summary of Field Work and Other Activities 1986, Ontario Geological Survey, Miscellaneous Paper 132, p.413-420.
- 1990a. Precambrian geology, Hislop and Guibord townships; Ontario Geological Survey, Open File Map 143, scale 1:20 000.
- 1990b. Precambrian geology, Michaud and Garrison townships; Ontario Geological Survey, Open File Map 144, scale 1:20 000.
- Vagners, U.J. 1985. Quaternary geology of the Matheson area, Cochrane District; Ontario Geological Survey, Preliminary Map P.2735, scale 1:50 000.
- Vagners, U.J. and Courtney, S.J. 1985. Quaternary geology, Lightning River area, District of Cochrane; Ontario Geological Survey, Preliminary Map P.2734, scale 1:50 000.
- Vaillancourt, C. 1999a. Geology of Sheraton Township, District of Cochrane; *in* Summary of Field Work and Other Activities 1998, Ontario Geological Survey, Miscellaneous Paper 169, p.59-64.
- 1999b. Precambrian geology of Sheraton Township; Ontario Geological Survey, Preliminary Map P.3387, scale 1:20 000.
- 1999c. Geological mapping west of Watabeag Lake, District of Cochrane; *in* Summary of Field Work and Other Activities 1999, Ontario Geological Survey, Open File Report 6000, p.7-1 to 7-9.
- 2000. New geological mapping and compilation in the Timmins west area – Bristol and Ogden Townships; *in* Summary of Field Work and Other Activities 2000, Ontario Geological Survey, Open File Report 6032, p.4-1 to 4-11.
- Vaillancourt, C., Sproule, R.A., MacDonald, C.A. and Hulbert, L.J. 2001. Potential for platinum group elements mineralization in mafic-ultramafic intrusions in Ontario; *in* Summary of Field Work and Other Activities 2001, Ontario Geological Survey, Open File Report 6070, p.38-1 to 38-10.
- Walker, R.G. 1992. Turbidites and submarine fans; *in* Facies models, response to sea level change, Geological Association of Canada, GEOText 1, p.239-263.
- Watson, G.P. and Kerrich, R. 1983. Macassa Mine, Kirkland Lake; *in* The geology of gold in Ontario, Ontario Geological Survey, Miscellaneous Paper 110, p.56-74.

- Wheller, G.E., Varne, R., Foden, J.D. and Abbott, M.J. 1987. Geochemistry of Quaternary volcanism in the Sunda–Banda Arc, Indonesia, and three-component genesis of island-arc basaltic magmas; *Journal of Volcanology and Geothermal Research*, v.32, p.137-160.
- Winkler, H.G.F. 1979. *Petrogenesis of metamorphic rocks*, 5th ed.; Springer-Verlag Inc., New York, 348p.
- Wood, P.C., Burrows, D.R., Thomas, A.V. and Spooner, E.T.C. 1986. The Hollinger–McIntyre Au-quartz vein system, Timmins, Ontario, Canada: geologic characteristics, fluid properties and light stable isotope geochemistry; *in Proceedings of Gold '86, an international symposium on the geology of gold*, Konsult International, Toronto, p.56-80.
- Workman, A.W. 1986. Geology of the McDermott gold deposit, Kirkland Lake area, northeastern Ontario, Canada; *in Proceedings of Gold '86, an international symposium on the geology of gold*, Konsult International, Toronto, p.184-190.
- Wyman, D. and Kerrich, R. 1988. Alkaline magmatism, major structures and gold deposits, implications for greenstone belt gold metallogeny; *Economic Geology*, v.83, p.454-461.
- Xie, Q., Kerrich, R. and Fan, J. 1993. HFSE/REE fractionations recorded in three komatiite-basalt sequences, Archean Abitibi greenstone belt: implications for multiple plume sources and depths; *Geochimica et Cosmochimica Acta*, v.57, p.4111-4118.

## **Appendix 1**

### **Geochemistry for the Kidd–Munro Assemblage in the Highway 101 Area**

**Appendix 1.** Geochemistry for the Kidd–Munro assemblage in the Highway 101 area.

Sample	97BRB0584	97BRB0586	97BRB0593	97BRB0644	97BRB0648	98BRB0654	98BRB0682	98BRB0695
Rock Type	Spinifex komatiite	Spinifex komatiite	Basalt	Spinifex komatiite	Basalt	Basalt	Massive basalt	Massive basalt
<b>Township</b>	Garrison	Holloway	Garrison	Guibord	Guibord	Munro	Michaud	Michaud
<b>Easting (m)</b>	578900	593100	575704	560023	579522	554684	570299	570020
<b>Northing (m)</b>	5374752	5375580	5376514	5376115	5375622	5377842	5375305	5374906
<b>SiO<sub>2</sub> (wt %)</b>	47.81	38.54	48.07	43.76	53.32	47.83	49.16	48.59
<b>Al<sub>2</sub>O<sub>3</sub></b>	7.89	8.61	12.24	9.32	13.13	13.25	13.53	14.83
<b>MnO</b>	0.17	0.16	0.26	0.21	0.22	0.28	0.22	0.25
<b>MgO</b>	18.83	26.75	6.68	19.68	5.17	4.72	6.19	6.11
<b>CaO</b>	8.72	0.93	8.03	8.26	7.37	7.56	7.46	13.69
<b>Na<sub>2</sub>O</b>	0.01	0.02	3.08	0.37	3.90	2.73	3.52	1.76
<b>K<sub>2</sub>O</b>	0.02	0.05	0.24	0.09	0.20	0.79	1.57	0.15
<b>P<sub>2</sub>O<sub>5</sub></b>	N.D.	N.D.	N.D.	0.03	0.08	0.14	0.16	0.05
<b>TiO<sub>2</sub></b>	0.5	0.52	1.38	0.47	1.33	1.53	1.51	0.92
<b>Fe<sub>2</sub>O<sub>3</sub></b>	11.28	14.81	16.7	12.72	13.08	13.36	14.92	12.92
<b>LOI</b>	5.36	9.32	2.59	5.23	2.64	8.41	1.83	1.66
<b>TOTAL</b>	100.59	99.71	99.27	100.14	100.44	100.60	100.07	100.93
<b>CO<sub>2</sub></b>	0.3	0.19	0.25	0.12	0.35	4.86	0.34	0.21
<b>S</b>	—	0.03	—	-0.01	0.01	0.09	0.01	-0.01
<b>As (ppm)</b>	-6	-6	-6	-6	-6	6	-6	-6
<b>Cr</b>	3000	3000	85	2727	17	127	-3	331
<b>Ni</b>	1100	1600	71	713	29	83	15	104
<b>Nb</b>	1.10	N.D.	3.96	0.62	4.92	4.17	16.90	2.49
<b>Rb</b>	N.D.	3.69	9.71	5.5	7	21.96	14.44	3.71
<b>Ta</b>	0.10	0.07	0.27	-0.1	-0.1	0.34	1.08	0.24
<b>Th</b>	0.13	N.D.	0.28	0.07	0.51	0.33	1.06	0.22
<b>U</b>	0.04	N.D.	0.08	0.03	0.08	0.08	0.28	0.08
<b>Hf</b>	—	0.2	—	—	—	1.15	9.78	1.27
<b>Y</b>	13	12	32	14	36	32	90	30
<b>Zr</b>	33	25	190	29	112	98	491	65
<b>Be</b>	—	—	—	N.D.	3	N.D.	N.D.	N.D.
<b>Co</b>	100	140	54	82	39	53	24	39
<b>Cu</b>	52	58	110	96	5	94	25	13
<b>Mo</b>	10	12	-8	-8	-8	—	—	—
<b>Sc</b>	28	32	44	30	39	38	30	34
<b>Sr</b>	9.8	20.5	103.2	31	154	124.8	67.0	174.4
<b>V</b>	170	200	360	198	361	—	—	—
<b>Zn</b>	90	79	140	98	90	122	198	79
<b>Au (ppb)</b>	—	-3	—	9	—	—	—	—
<b>Ba</b>	—	—	—	—	—	176	155	44
<b>Ag</b>	—	—	—	—	—	3	3	4
<b>La</b>	0.82	0.26	3.94	1.17	5.23	4.74	17.02	3.62
<b>Ce</b>	2.68	0.92	10.95	2.64	14.4	12.26	47.13	9.64
<b>Pr</b>	0.49	N.D.	1.76	0.45	2.27	2.02	7.55	1.57
<b>Nd</b>	2.84	1.06	9.42	2.46	11.59	10.26	39.65	8.49
<b>Sm</b>	1.09	0.51	3.31	0.9	3.67	3.33	12.11	2.81
<b>Eu</b>	0.31	N.D.	1.13	0.38	0.93	1.16	3.78	1.68
<b>Gd</b>	1.38	0.82	4.03	1.39	4.64	4.26	14.23	3.81
<b>Tb</b>	N.D.	N.D.	0.75	0.25	0.8	0.72	2.24	0.66
<b>Dy</b>	1.75	1.14	4.98	1.72	5.44	4.94	14.78	4.57
<b>Ho</b>	0.38	0.26	1.14	0.36	1.17	1.05	2.96	0.97
<b>Er</b>	1.06	0.76	3.31	1.09	3.44	2.90	8.32	2.73
<b>Tm</b>	0.15	0.12	0.50	0.16	0.49	0.40	1.16	0.38
<b>Yb</b>	1.06	0.68	3.32	1.06	3.24	2.50	7.55	2.44
<b>Lu</b>	0.16	0.09	0.50	0.17	0.52	0.34	1.19	0.35
<b>Cs</b>	0.24	8.98	0.52	1.4	0.86	0.73	1.96	0.30
<b>Mg#</b>	79.57	80.82	48.28	78.31	47.98	45.19	49.19	52.46

Notes: —, not analyzed; N.D., not detected; negative numbers = detection limit; UTM co-ordinates in NAD27, Zone 17.

Appendix 1. Continued

Sample	98BRB0710	98BRB0712	98BRB0714	98BRB0715	98BRB0718	98BRB0720	98BRB0776	98BRB0787
Rock Type	Variolitic basalt	Pillowed basalt	Contact felsic dike	Massive basalt	Felsic pods in variolites	Variolite	Variolite	Mafic flow
<b>Township</b>	Guibord	Guibord	Munro	Munro	Munro	Munro	Michaud	Guibord
<b>Easting (m)</b>	562647	558280	555306	555233	554687	554687	565362	566287
<b>Northing (m)</b>	5375355	5375541	5376758	5376746	5377423	5377423	5372992	5373263
<b>SiO<sub>2</sub> (wt %)</b>	46.08	45.66	81.17	51.44	79.22	66.43	69.97	49.15
<b>Al<sub>2</sub>O<sub>3</sub></b>	12.47	14.77	9.65	12.53	9.10	10.35	11.38	13.83
<b>MnO</b>	0.27	0.31	0.05	0.21	0.05	0.24	0.10	0.27
<b>MgO</b>	7.45	4.61	0.10	4.34	0.39	0.72	1.01	3.16
<b>CaO</b>	9.61	11.28	1.85	4.27	1.87	3.93	2.01	7.17
<b>Na<sub>2</sub>O</b>	1.83	1.62	2.54	2.64	3.58	3.97	2.32	5.21
<b>K<sub>2</sub>O</b>	0.47	0.30	1.59	0.02	1.09	0.15	1.72	0.05
<b>P<sub>2</sub>O<sub>5</sub></b>	0.12	0.15	0.03	0.20	0.04	0.13	0.19	0.19
<b>TiO<sub>2</sub></b>	1.61	1.67	0.26	2.03	0.31	0.65	0.96	2.28
<b>Fe<sub>2</sub>O<sub>3</sub></b>	18.81	17.33	0.52	16.97	1.70	9.00	6.67	14.44
<b>LOI</b>	2.28	2.39	2.40	7.04	2.65	4.58	3.61	5.35
<b>TOTAL</b>	101.00	100.09	100.16	101.69	100.00	100.15	99.94	101.10
<b>CO<sub>2</sub></b>	0.33	0.51	0.22	3.63	1.44	2.15	2.17	3.86
<b>S</b>	0.07	0.14	0.14	0.06	-0.01	0.09	0.09	0.28
<b>As (ppm)</b>	-6	-6	-6	-6	253	-6	-6	-6
<b>Cr</b>	163	139	-3	-3	3	-3	12	44
<b>Ni</b>	95	88	-5	17	-5	9	11	49
<b>Nb</b>	5.75	4.60	15.64	6.56	18.88	18.10	13.29	7.31
<b>Rb</b>	12.44	7.84	40.22	1.37	24.31	1.93	75.87	0.97
<b>Ta</b>	0.46	0.37	—	0.52	—	—	—	—
<b>Th</b>	0.55	0.27	1.70	0.42	2.00	1.43	1.06	0.57
<b>U</b>	0.16	0.06	0.41	0.10	0.47	0.34	0.22	0.15
<b>Hf</b>	2.37	1.45	7.76	2.54	10.88	—	4.64	1.59
<b>Y</b>	32	35	46.87	60	62.02	70.11	264.16	65.59
<b>Zr</b>	111	107	124.29	156	173.30	289.30	172.60	46.33
<b>Be</b>	N.D.	3	—	N.D.	—	—	N.D.	4
<b>Co</b>	53	55	25	36	N.D.	N.D.	17	43
<b>Cu</b>	143	104	51	51	16	7	52	52
<b>Mo</b>	—	—	N.D.	—	N.D.	N.D.	N.D.	N.D.
<b>Sc</b>	26	43	16	33	6	6	18	43
<b>Sr</b>	161.3	255.6	68.2	97.3	60.9	111.8	110	187
<b>V</b>	—	—	134	—	N.D.	6	55	400
<b>Zn</b>	139	126	96	132	164	34	91	162
<b>Au (ppb)</b>	—	—	—	—	—	—	—	—
<b>Ba</b>	138	111	258	58	120	49	183	76
<b>Ag</b>	5	4	—	3	—	—	—	—
<b>La</b>	6.81	4.46	11.90	7.18	15.40	23.09	11.30	8.55
<b>Ce</b>	18.84	12.34	38.89	20.19	43.84	59.88	30.99	22.79
<b>Pr</b>	2.96	2.04	6.51	3.36	7.19	9.45	4.99	3.72
<b>Nd</b>	14.62	10.81	31.36	17.80	35.69	47.32	25.92	19.85
<b>Sm</b>	4.38	3.54	9.08	5.19	10.52	13.61	8.12	6.92
<b>Eu</b>	1.44	1.23	1.60	1.30	1.30	3.24	1.81	1.98
<b>Gd</b>	4.82	4.60	7.76	4.77	8.04	13.42	8.02	9.04
<b>Tb</b>	0.79	0.78	1.26	0.70	1.30	2.01	1.19	1.58
<b>Dy</b>	5.02	5.29	8.32	4.34	9.21	12.66	6.91	10.46
<b>Ho</b>	1.03	1.15	1.85	0.87	2.37	2.68	1.52	2.29
<b>Er</b>	2.81	3.29	5.80	2.66	8.28	8.14	4.24	6.40
<b>Tm</b>	0.39	0.47	0.93	0.39	1.42	1.24	0.65	0.94
<b>Yb</b>	2.39	3.02	6.33	2.75	10.23	8.52	4.50	5.95
<b>Lu</b>	0.35	0.46	0.98	0.45	1.68	1.41	0.72	0.82
<b>Cs</b>	1.19	0.58	1.29	0.29	0.58	0.13	8.92	0.24
<b>Mg#</b>	48.03	38.30	30.97	37.37	34.87	15.73	26.11	33.80

Notes: —, not analyzed; N.D., not detected; negative numbers = detection limit; UTM co-ordinates in NAD27, Zone 17.

Appendix 1. Continued

Sample	Calc-Alkalic Rocks						
	97BRB0549	97BRB0550	97BRB0551	97BRB0552	97BRB0577	97BRB0589	97BRB0590
Rock Type	Inter. FP	Inter. FP	Andesite tuff	Inter. flow	Inter. flow	Dacite flow	Inter. tuff
Township	Rand	Rand	Holloway	Frecheville	Holloway	Garrison	Garrison
Easting (m)	580648	578813	596378	598240	593884	576054	576054
Northing (m)	5378153	5376884	5376161	5376869	5375721	5376586	5376586
SiO <sub>2</sub> (wt %)	64.69	66.49	53.64	59.99	52.76	62.99	58.52
Al <sub>2</sub> O <sub>3</sub>	14.12	14.79	15.67	13.35	15.07	15	14.96
MnO	0.02	0.07	0.11	0.13	0.17	0.02	0.15
MgO	2.18	1.1	3.99	2.3	4.89	0.34	3.34
CaO	4.37	3.43	6.64	4.57	5.89	5.28	5.3
Na <sub>2</sub> O	2.84	1.61	2.74	4.93	2.17	2.44	2.94
K <sub>2</sub> O	1.28	2.63	0.72	1.04	0.89	7.32	1.64
P <sub>2</sub> O <sub>5</sub>	0.08	0.09	0.03	0.15	0.16	0.07	0.07
TiO <sub>2</sub>	0.72	0.8	0.93	1.18	1.28	0.81	0.87
Fe <sub>2</sub> O <sub>3</sub>	6.52	5.52	9.28	8.46	11.69	3	8.52
LOI	1.84	2.16	5.09	2.28	3.8	1.4	2.21
TOTAL	98.66	98.69	98.84	98.38	98.77	98.67	98.52
CO <sub>2</sub>	0.25	0.35	1.6	0.39	0.28	1.3	0.21
S	—	—	—	—	—	—	—
As (ppm)	-6	-6	-6	-6	-6	27	11
Cr	21	28	39	4	120	28	85
Ni	23	18	69	12	73	31	65
Nb	13.39	15.72	7.03	10.37	14.58	12.10	12.79
Rb	41.81	90.14	24.52	26.71	20.61	185.84	64.98
Ta	0.91	1.16	0.52	0.92	0.84	0.89	17.50
Th	4.58	6.04	1.32	2.11	1.41	2.99	2.44
U	1.12	1.40	0.28	0.48	0.32	0.70	0.54
Hf	—	—	—	—	—	—	—
Y	25	27	24	28	38	30	32
Zr	200	220	120	180	200	200	190
Be	—	—	—	—	—	—	—
Co	18	9	30	18	38	32	28
Cu	450	7	38	22	70	12	28
Mo	-8	-8	-8	-8	-8	10	-8
Sc	10	10	22	15	21	11	17
Sr	514.7	179.9	165.0	161.0	284.7	105.1	253.2
V	110	82	160	120	170	79	120
Zn	21	42	100	97	140	11	52
Au (ppb)	—	—	—	—	—	—	—
Ba	—	—	—	—	—	—	—
Ag	—	—	—	—	—	—	—
La	37.36	35.76	13.61	22.75	23.22	38.44	24.10
Ce	87.67	79.10	30.87	51.67	57.06	83.88	55.16
Pr	9.21	9.34	3.93	6.40	7.63	9.98	7.00
Nd	35.27	35.96	16.72	26.06	33.12	39.88	29.04
Sm	6.25	6.63	3.84	5.33	7.47	7.65	6.00
Eu	1.30	1.54	1.08	1.36	1.88	2.08	1.48
Gd	4.75	5.27	3.68	4.68	6.96	6.44	5.26
Tb	0.70	0.77	0.58	0.71	1.12	0.95	0.86
Dy	4.13	4.67	3.72	4.36	6.68	5.66	5.28
Ho	0.85	0.89	0.79	0.90	1.36	1.07	1.10
Er	2.38	2.50	2.19	2.59	3.66	2.87	3.13
Tm	0.35	0.35	0.31	0.37	0.53	0.40	0.47
Yb	2.36	2.23	2.01	2.41	3.21	2.63	3.05
Lu	0.37	0.33	0.30	0.38	0.44	0.36	0.44
Cs	0.73	2.31	1.14	0.57	0.30	0.97	1.58
Mg#	43.83	31.74	50.08	38.81	49.39	20.91	47.77

Notes: Inter., Intermediate; —, not analyzed; N.D., not detected; negative numbers = detection limit; UTM co-ordinates in NAD27, Zone 17.

Appendix 1. Continued

Calc-Alkalic Rocks						
Sample	97BRB0599	97BRB0611	97BRB0613	97BRB0628	97BRB0629	97BRB0623
Rock Type	Intermediate tuff	Intermediate flow	Intermediate tuff	Intermediate tuff	Dacite flow	Altered basalt
<b>Township</b>	Stoughton	Lamplugh	Lamplugh	Harker	Harker	Stoughton
<b>Easting (m)</b>	603055	589288	586673	591226	591231	601683
<b>Northing (m)</b>	5377838	5378304	5377449	5375782	5375909	5377412
<b>SiO<sub>2</sub> (wt %)</b>	53.58	57.34	60.18	54.05	59.09	45.84
<b>Al<sub>2</sub>O<sub>3</sub></b>	15.48	14.25	15.56	15.94	14.67	13.34
<b>MnO</b>	0.22	0.15	0.12	0.1	0.12	0.30
<b>MgO</b>	3.06	3.8	2.99	4.36	3.05	3.83
<b>CaO</b>	6.71	4.67	3.06	2.8	6.38	8.80
<b>Na<sub>2</sub>O</b>	1.91	3.85	3.27	4.18	3.09	1.61
<b>K<sub>2</sub>O</b>	1.99	0.27	2.7	2.22	0.31	0.90
<b>P<sub>2</sub>O<sub>5</sub></b>	0.13	0.19	0.09	0.07	0.05	0.21
<b>TiO<sub>2</sub></b>	1.36	1.31	0.92	0.91	0.83	1.21
<b>Fe<sub>2</sub>O<sub>3</sub></b>	6.31	9.85	6.7	8.96	8.36	11.14
<b>LOI</b>	8.18	2.93	2.75	5.25	2.74	12.79
<b>TOTAL</b>	98.93	98.61	98.34	98.84	98.69	99.97
<b>CO<sub>2</sub></b>	4.8	0.16	0.23	0.21	0.32	10.50
<b>S</b>	—	—	—	—	—	0.07
<b>As (ppm)</b>	-6	-6	-6	-6	-6	10
<b>Cr</b>	120	24	29	90	120	32
<b>Ni</b>	68	46	38	59	58	41
<b>Nb</b>	11.71	12.59	16.35	12.67	11.53	6.14
<b>Rb</b>	62.92	15.06	90.67	57.24	12.04	30
<b>Ta</b>	0.60	1.82	0.98	0.79	0.72	6
<b>Th</b>	1.16	1.35	3.92	2.46	2.20	0.75
<b>U</b>	0.26	0.28	0.92	0.55	0.51	0.15
<b>Hf</b>	—	—	—	—	—	—
<b>Y</b>	31	31	37	31	28	31
<b>Zr</b>	150	170	250	180	170	111
<b>Be</b>	—	—	—	—	—	N.D.
<b>Co</b>	35	31	24	23	21	32
<b>Cu</b>	97	40	33	18	40	49
<b>Mo</b>	-8	-8	-8	-8	-8	N.D.
<b>Sc</b>	23	19	14	17	16	24
<b>Sr</b>	114.7	246.1	215.5	202.3	231.1	148
<b>V</b>	190	180	110	130	130	232
<b>Zn</b>	87	110	260	93	86	96
<b>Au (ppb)</b>	—	—	—	—	—	5
<b>Ba</b>	—	—	—	—	—	—
<b>Ag</b>	—	—	—	—	—	—
<b>La</b>	16.82	24.76	33.58	24.20	19.64	15.23
<b>Ce</b>	42.63	61.66	73.44	55.08	45.30	37.34
<b>Pr</b>	5.81	8.05	8.96	6.93	5.74	4.99
<b>Nd</b>	25.60	34.56	36.21	28.39	24.06	21.69
<b>Sm</b>	5.78	7.18	7.81	6.37	5.47	4.59
<b>Eu</b>	1.24	1.88	1.65	1.43	1.36	1.24
<b>Gd</b>	4.95	6.00	6.77	5.64	4.71	4.02
<b>Tb</b>	0.68	0.93	1.04	0.89	0.75	0.52
<b>Dy</b>	3.90	5.40	6.22	5.59	4.58	2.91
<b>Ho</b>	0.75	1.03	1.23	1.12	0.93	0.52
<b>Er</b>	2.08	2.65	3.33	3.15	2.66	1.57
<b>Tm</b>	0.31	0.33	0.48	0.47	0.37	0.22
<b>Yb</b>	2.00	1.83	3.03	2.96	2.33	1.43
<b>Lu</b>	0.30	0.23	0.46	0.45	0.35	0.23
<b>Cs</b>	0.80	0.19	1.08	0.44	0.36	0.73
<b>Mg#</b>	53.09	47.37	51.01	53.17	45.98	44.51

Notes: —, not analyzed; N.D., not detected; negative numbers = detection limit; UTM co-ordinates in NAD27, Zone 17.

Appendix 1. Continued

Ghost Range and Gabbroic Intrusions					
Sample	97BRB0546	97BRB0554	97BRB0555	97BRB0626	97BRB0632
Rock Type	Pegmatitic gabbro	Peridotite	Gabbronorite	Gabbro	Gabbro schist
Township	Harker	Harker	Harker	Harker	Harker
Easting (m)	586816	585488	585598	591235	591738
Northing (m)	5376536	5376265	5376290	5375461	5375518
SiO <sub>2</sub> (wt %)	51.42	37.01	47.45	49.22	48.98
Al <sub>2</sub> O <sub>3</sub>	12.2	3.83	15.86	14.97	15.21
MnO	0.25	0.17	0.11	0.14	0.19
MgO	3.06	30.98	11.57	9.86	8.6
CaO	6.67	3.08	15.17	8.15	6.09
Na <sub>2</sub> O	2.83	0	1.22	3.49	4.95
K <sub>2</sub> O	0.64	0.05	0.43	0.4	0
P <sub>2</sub> O <sub>5</sub>	0.03	N.D.	N.D.	N.D.	N.D.
TiO <sub>2</sub>	1.79	0.2	0.21	0.47	0.57
Fe <sub>2</sub> O <sub>3</sub>	17.73	13.95	5.46	9.23	9.88
LOI	2.27	10.31	3.31	3.19	4.19
TOTAL	98.89	99.58	100.79	99.12	98.66
CO <sub>2</sub>	0.74	0.3	0.25	0.16	1.1
S	-0.01	-0.01	-0.01	-0.01	0.13
As (ppm)	-6	-6	-6	-6	-6
Cr	4	2900	1200	590	140
Ni	17	1100	180	100	87
Nb	4.93	0.52	N.D.	1.26	1.58
Rb	16.78	1.50	11.31	19.55	2.08
Ta	0.30	0.06	0.06	0.10	0.11
Th	0.88	0.12	0.12	0.30	0.36
U	0.22	N.D.	0.03	0.08	0.08
Hf	3.06	0.44	0.52	1.03	1.03
Y	31	7	8	14	16
Zr	100	18	22	40	48
Be	—	—	—	—	—
Co	47	120	31	37	38
Cu	8	14	14	28	97
Mo	-8	13	9	-8	-8
Sc	35	12	26	30	32
Sr	185.3	5.7	166.5	274.2	218.2
V	290	74	110	160	190
Zn	69	77	37	69	110
Au (ppb)	-3	-3	-3	4	9
Ba	—	—	—	—	—
Ag	—	—	—	—	—
La	10.28	1.09	1.26	2.66	3.47
Ce	23.06	2.52	3.15	6.72	8.36
Pr	3.17	0.34	0.46	0.99	1.22
Nd	15.06	1.61	2.30	4.90	5.66
Sm	4.16	0.43	0.69	1.46	1.64
Eu	1.42	N.D.	0.25	0.57	0.74
Gd	4.57	0.53	0.75	1.72	1.98
Tb	0.77	N.D.	N.D.	0.30	0.34
Dy	5.01	0.60	0.92	1.93	2.26
Ho	1.07	N.D.	N.D.	0.42	0.47
Er	3.06	0.37	0.54	1.18	1.31
Tm	0.44	0.05	0.08	0.18	0.20
Yb	2.83	0.36	0.50	1.09	1.22
Lu	0.44	0.06	0.07	0.16	0.18
Cs	0.70	0.32	0.21	0.63	0.26
Mg#	28.71	83.82	83.18	71.37	67.01

Notes: —, not analyzed; N.D., not detected; negative numbers = detection limit; UTM co-ordinates in NAD27, Zone 17.



## **Appendix 2**

### **Geochemistry for the Tisdale Assemblage in the Highway 101 Area**

**Appendix 2.** Geochemistry for the Tisdale assemblage in the Highway 101 area.

Sample	98BRB0659	98BRB0706	98BRB0734	98BRB0743	98BRB0765	99BRB0810	99BRB0811	99BRB0820
Rock Type	Massive basalt	Massive basalt	Spinifex komatiite	Mafic flow	Spinifex komatiite	Massive basalt	Mafic flow breccia	Leucogabbro
<b>Township</b>	Michaud	Guibord	Guibord	Michaud	Guibord	Hislop	Hislop	Hislop
<b>Easting (m)</b>	566690	557195	559508	562969	554856	549392	548789	550021
<b>Northing (m)</b>	5368781	5372632	5368222	5370693	5370924	5374634	5375162	5372695
<b>SiO<sub>2</sub> (wt %)</b>	43.28	52.17	40.83	50.78	37.20	50.67	52.33	50.64
<b>Al<sub>2</sub>O<sub>3</sub></b>	13.61	15.19	7.36	17.31	9.20	14.67	14.42	13.34
<b>MnO</b>	0.29	0.25	0.19	0.17	0.21	0.21	0.20	0.12
<b>MgO</b>	5.47	5.26	23.64	9.91	24.08	5.37	6.43	7.06
<b>CaO</b>	9.15	11.75	6.87	8.09	4.74	8.47	6.34	4.54
<b>Na<sub>2</sub>O</b>	1.86	1.96	0.43	1.44	0.10	3.61	5.24	3.62
<b>K<sub>2</sub>O</b>	0.99	0.12	0.06	0.09	0.05	0.36	0.19	0.18
<b>P<sub>2</sub>O<sub>5</sub></b>	0.38	0.08	0.02	0.04	0.03	0.07	0.07	0.14
<b>TiO<sub>2</sub></b>	3.15	1.32	0.38	0.44	0.62	1.08	0.95	1.36
<b>Fe<sub>2</sub>O<sub>3</sub></b>	20.41	11.92	11.80	11.43	13.24	13.87	12.44	13.12
<b>LOI</b>	1.74	0.55	7.86	2.06	10.35	2.68	2.37	6.82
<b>TOTAL</b>	100.33	100.57	99.44	101.76	99.82	101.06	100.98	100.94
<b>CO<sub>2</sub></b>	0.27	0.18	0.32	0.16	1.75	—	—	—
<b>S</b>	0.13	0.48	0.12	0.01	0.01	—	—	—
<b>As (ppm)</b>	-3.5	-3.5	-3.5	-3.5	28	-3.5	-3.5	5.6
<b>Cr</b>	90	111	>3000	185	2415	46	123	85
<b>Ni</b>	66	82	1129	164	612	46	109	72
<b>Nb</b>	11.87	2.35	0.34	1.37	1.05	2.26	2.09	6.60
<b>Rb</b>	45.89	1.84	3.02	3.60	4.03	8.74	2.67	4.03
<b>Ta</b>	0.79	0.24	—	—	—	0.22	0.20	0.48
<b>Th</b>	2.83	0.26	0.05	0.23	0.07	0.24	0.22	2.37
<b>U</b>	0.52	0.13	N.D.	0.05	0.02	0.07	0.06	0.60
<b>Hf</b>	2.98	1.32	—	0.52	0.79	1.84	1.72	3.52
<b>Y</b>	30	27	9.92	18.44	10.93	29.22	28.00	35.42
<b>Zr</b>	111	63	23.85	17.45	25.36	65.28	56.46	132.21
<b>Be</b>	-3	-3	—	-3	-3	-3	-3	-3
<b>Co</b>	49	44	30	47	79	41	41	39
<b>Cu</b>	81	82	34	71	99	159	102	230
<b>Mo</b>	—	—	-8	-8	-8	-8	-8	-8
<b>Sc</b>	38	42	15	49	32	38	42	33
<b>Sr</b>	216.9	115.0	24.8	53	59	105	113	98
<b>V</b>	—	—	126	209	220	330	281	279
<b>Zn</b>	116	95	143	101	96	99	110	107
<b>Ba</b>	290	77	34	77	40	86	38	42
<b>La</b>	16.41	3.48	0.51	1.73	0.74	2.92	2.68	13.45
<b>Ce</b>	35.26	9.24	1.44	4.31	2.77	7.29	6.73	26.10
<b>Pr</b>	4.58	1.49	0.26	0.67	0.54	1.39	1.32	4.05
<b>Nd</b>	19.26	7.86	1.56	3.27	3.06	7.70	7.30	18.50
<b>Sm</b>	4.43	2.62	0.71	1.03	1.16	2.59	2.49	4.76
<b>Eu</b>	1.30	0.98	0.26	0.35	0.46	0.86	0.76	1.48
<b>Gd</b>	4.47	3.34	1.19	1.50	1.66	3.22	3.03	5.00
<b>Tb</b>	0.72	0.58	0.22	0.28	0.28	0.62	0.57	0.88
<b>Dy</b>	4.69	4.02	1.55	2.30	1.86	4.54	4.19	6.10
<b>Ho</b>	0.98	0.88	0.34	0.59	0.38	1.02	1.00	1.28
<b>Er</b>	2.86	2.49	0.97	2.01	1.02	3.03	2.95	3.61
<b>Tm</b>	0.40	0.38	0.14	0.32	0.14	0.53	0.52	0.63
<b>Yb</b>	2.64	2.40	0.92	2.27	0.91	2.92	2.79	3.34
<b>Lu</b>	0.42	0.36	0.15	0.37	0.14	0.45	0.43	0.50
<b>Cs</b>	0.91	0.23	2.62	0.48	1.94	1.24	0.50	0.90
<b>Mg#</b>	38.47	50.73	82.38	66.92	80.93	47.46	54.67	55.67

Notes: —, not analyzed; N.D., not detected; negative numbers = detection limit; UTM co-ordinates in NAD27, Zone 17.

Appendix 2. Continued

Sample	99BRB0822	99BRB0823	99BRB0824	99BRB0834	99BRB0839	99BRB0841	99BRB0844	99BRB0845	99BRB0849
Rock Type	Felsic tuff	Felsic tuff	Massive basalt	Mafic tuff	Massive basalt	Quartz porphyry	Massive mafic flow	Variolitic basalt	Carbonate breccia
<b>Township</b>	Hislop	Hislop	Hislop	Hislop	Hislop	Hislop	Hislop	Hislop	Hislop
<b>Easting (m)</b>	549900	549900	550988	546014	551767	553511	551776	552497	552634
<b>Northing (m)</b>	5371330	5371330	5373501	5373532	5371337	5372810	5371465	5371498	5371354
<b>SiO<sub>2</sub> (wt %)</b>	70.97	71.14	52.28	51.53	52.58	51.55	51.53	60.67	27.93
<b>Al<sub>2</sub>O<sub>3</sub></b>	15.06	15.09	13.63	13.47	14.38	15.18	13.56	13.40	2.45
<b>MnO</b>	0.02	0.02	0.21	0.16	0.19	0.16	0.18	0.13	0.19
<b>MgO</b>	0.45	0.43	4.65	5.87	5.90	4.79	3.27	0.60	12.08
<b>CaO</b>	1.41	1.23	5.54	7.64	4.55	6.99	3.80	2.43	19.84
<b>Na<sub>2</sub>O</b>	6.12	6.29	4.14	3.93	5.94	4.19	5.59	10.81	0.05
<b>K<sub>2</sub>O</b>	1.68	1.66	0.27	0.85	0.27	0.14	0.16	0.11	1.62
<b>P<sub>2</sub>O<sub>5</sub></b>	0.06	0.06	0.09	0.25	0.07	0.06	0.11	0.14	N.D.
<b>TiO<sub>2</sub></b>	0.19	0.19	1.28	0.91	0.98	0.98	1.42	0.76	0.11
<b>Fe<sub>2</sub>O<sub>3</sub></b>	1.54	1.47	15.65	7.85	13.30	8.24	16.52	9.94	4.93
<b>LOI</b>	2.22	2.00	3.50	8.02	2.85	7.98	4.82	1.44	30.00
<b>TOTAL</b>	99.72	99.58	101.24	100.48	101.01	100.26	100.96	100.43	99.20
<b>CO<sub>2</sub></b>	—	—	—	—	—	—	—	—	—
<b>S</b>	—	—	—	—	—	—	—	—	—
<b>As (ppm)</b>	-3.5	-3.5	4.42	6.23	7.78	5.55	25.71	5.98	42.11
<b>Cr</b>	12	16	26	249	48	127	14	78	>500
<b>Ni</b>	-5	-5	35	77	49	114	28	11	305
<b>Nb</b>	7.42	7.74	3.05	4.33	2.06	2.10	3.36	19.77	0.43
<b>Rb</b>	65.02	63.61	6.26	13.01	5.59	4.47	2.94	1.60	28.05
<b>Ta</b>	0.54	0.54	0.25	0.32	0.19	0.19	0.30	1.73	0.08
<b>Th</b>	4.03	4.34	0.48	3.68	0.24	0.22	0.41	2.88	0.36
<b>U</b>	1.82	1.86	0.12	0.72	0.07	0.07	0.11	4.25	0.56
<b>Hf</b>	3.22	3.50	2.34	3.43	1.74	1.62	2.89	18.18	0.41
<b>Y</b>	8.17	8.77	32.96	20.45	25.39	17.16	42.93	177.44	6.30
<b>Zr</b>	116.88	118.44	80.87	135.02	60.18	53.78	100.77	637.14	14.82
<b>Be</b>	-3	-3	-3	-3	-3	-3	-3	14	3
<b>Co</b>	-5	-5	42	27	39	39	43	5	23
<b>Cu</b>	-5	6	91	62	161	98	167	8	20
<b>Mo</b>	-8	-8	-8	-8	-8	-8	-8	-8	312
<b>Sc</b>	1	1	35	21	39	40	37	16	6
<b>Sr</b>	162.2	168.9	54	207	89	331.3	79	71	442.3
<b>V</b>	16	16	364	174	288	294	357	338	175
<b>Zn</b>	31	33	119	101	108	87	105	165	59
<b>Ba</b>	199	222	101	330	157	118	57	79	101
<b>La</b>	13.60	12.25	4.72	27.79	2.67	2.92	5.33	40.32	4.59
<b>Ce</b>	29.76	28.25	9.94	52.18	5.73	7.49	11.58	82.62	7.74
<b>Pr</b>	3.14	2.91	1.94	8.46	1.21	1.13	2.32	14.20	0.87
<b>Nd</b>	11.46	10.82	9.65	35.86	6.63	5.76	12.41	70.86	3.45
<b>Sm</b>	1.94	1.88	3.21	6.62	2.26	1.84	3.99	19.87	0.72
<b>Eu</b>	0.54	0.49	1.02	1.73	0.67	0.76	1.22	4.53	0.26
<b>Gd</b>	1.55	1.66	3.78	5.27	2.90	2.09	4.84	21.86	0.79
<b>Tb</b>	0.25	0.24	0.72	0.72	0.54	0.40	0.88	4.06	0.13
<b>Dy</b>	1.20	1.34	5.16	3.70	4.02	2.73	6.58	28.34	0.78
<b>Ho</b>	0.24	0.26	1.18	0.71	0.89	0.59	1.47	6.43	0.16
<b>Er</b>	0.65	0.67	3.37	1.86	2.66	1.65	4.39	19.24	0.46
<b>Tm</b>	0.13	0.12	0.58	0.32	0.48	0.29	0.78	3.45	0.07
<b>Yb</b>	0.78	0.75	3.35	1.70	2.75	1.62	4.44	19.49	0.40
<b>Lu</b>	0.12	0.12	0.53	0.26	0.41	0.27	0.69	3.00	0.07
<b>Cs</b>	1.76	1.56	0.99	0.25	1.85	0.18	1.57	0.13	0.40
<b>Mg#</b>	40.54	40.57	40.94	63.57	3.89	57.56	7.76	58.69	6.68

Notes: —, not analyzed; N.D., not detected; negative numbers = detection limit; UTM co-ordinates in NAD27, Zone 17.

## **Appendix 3**

### **Geochemistry for the Kinojevis Assemblage in the Highway 101 Area**

**Appendix 3.** Geochemistry for the Kinojevis assemblage in the Highway 101 area.

Sample	97BRB0540	97BRB0542	97BRB0543	97BRB0568	97BRB0596	97BRB0607	97BRB0609	98BRB0683
Rock Type	Basalt	Basalt	Basalt	Rhyolite	Plagioclase- phyric basalt	Basalt	Plagioclase- phyric basalt	Hornfels basalt
Township	Marriott	Marriott	Marriott	Harker	Marriott	Marriott	Harker	Harker
Easting (m)	609365	606638	603574	588538	605781	604961	588027	588044
Northing (m)	5375536	5375203	5375575	5367045	5375882	5376154	5371966	5373082
<b>SiO<sub>2</sub> (wt %)</b>	48.74	48.81	49.93	74.39	48.96	45.16	48.77	51.73
<b>Al<sub>2</sub>O<sub>3</sub></b>	13.84	13.63	14.53	11.34	13.42	14	14.68	11.58
<b>MnO</b>	0.22	0.19	0.19	0.03	0.21	0.21	0.18	0.25
<b>MgO</b>	7.27	5.41	7.82	0.44	7.62	5.99	8.91	2.21
<b>CaO</b>	10.51	8.14	8.81	0.55	9.77	3.64	10.65	4.74
<b>Na<sub>2</sub>O</b>	2.5	3.42	3.02	6.53	1.41	3.73	1.93	3.69
<b>K<sub>2</sub>O</b>	0.21	N.D.	N.D.	N.D.	2.19	0.01	0.52	0.41
<b>P<sub>2</sub>O<sub>5</sub></b>	N.D.	0.02	N.D.	N.D.	N.D.	0.11	N.D.	0.82
<b>TiO<sub>2</sub></b>	1.02	1.82	0.83	0.26	0.97	2.6	0.79	2.05
<b>Fe<sub>2</sub>O<sub>3</sub></b>	11.82	14.92	10.04	3.91	12.35	18.23	11.05	19.86
<b>LOI</b>	2.97	2.87	3.58	1.19	2.67	4.81	1.65	3.12
<b>TOTAL</b>	99.1	99.23	98.75	98.64	99.57	98.49	99.13	100.46
<b>CO<sub>2</sub></b>	0.73	0.19	0.21	0.64	0.44	1.3	0.26	0.24
<b>S</b>	—	—	—	—	—	—	—	0.23
<b>As (ppm)</b>	-6	-6	-6	-6	-6	7	-6	-3.5
<b>Cr</b>	330	82	290	17	250	50	380	54
<b>Ni</b>	110	58	100	9	74	75	120	63
<b>Nb</b>	3.21	4.42	4.15	27.93	2.31	4.70	2.35	5.15
<b>Rb</b>	10.73	2.11	-5	7.90	71.12	7.25	38.74	42.03
<b>Ta</b>	0.20	0.26	0.26	1.56	0.18	0.34	0.50	0.39
<b>Th</b>	0.26	0.38	0.40	3.06	0.20	0.39	0.23	0.11
<b>U</b>	0.07	0.10	0.11	0.76	0.05	0.11	0.07	0.03
<b>Hf</b>	—	—	—	—	—	—	—	0.77
<b>Y</b>	29	36	36	200	25	35	24	41
<b>Zr</b>	74	91	85	470	50	92	56	97
<b>Be</b>	—	—	—	—	—	—	—	4
<b>Co</b>	44	38	40	-5	40	47	44	49
<b>Cu</b>	120	110	93	-5	140	81	36	47
<b>Mo</b>	-8	-8	-8	15	-8	-8	-8	—
<b>Sc</b>	37	40	35	5	41	40	36	46
<b>Sr</b>	298.5	143.9	82.4	75.5	161.5	186.1	119.4	167.1
<b>V</b>	300	420	250	9	320	450	260	—
<b>Zn</b>	83	100	75	85	72	120	69	138
<b>Ba</b>	—	—	—	—	—	—	—	177
<b>La</b>	3.83	5.53	5.18	43.59	2.88	5.01	2.70	4.00
<b>Ce</b>	10.78	15.06	14.55	>250	7.69	14.23	7.82	11.69
<b>Pr</b>	1.69	2.32	2.26	17.12	1.24	2.30	1.26	2.09
<b>Nd</b>	9.14	12.47	11.93	83.74	6.76	12.25	6.74	12.01
<b>Sm</b>	2.94	3.92	3.73	22.02	2.35	4.09	2.33	4.12
<b>Eu</b>	0.98	1.38	0.96	3.37	0.76	1.35	0.71	1.75
<b>Gd</b>	3.58	4.79	4.50	16.59	2.95	5.01	2.75	5.62
<b>Tb</b>	0.64	0.86	0.81	2.44	0.52	0.87	0.50	0.97
<b>Dy</b>	4.18	5.65	5.44	16.32	3.60	5.92	3.51	6.48
<b>Ho</b>	0.91	1.25	1.24	3.89	0.81	1.30	0.81	1.40
<b>Er</b>	2.58	3.60	3.57	12.79	2.35	3.60	2.33	4.13
<b>Tm</b>	0.38	0.53	0.55	2.17	0.35	0.53	0.37	0.58
<b>Yb</b>	2.44	3.59	3.56	15.66	2.33	3.43	2.36	3.91
<b>Lu</b>	0.34	0.54	0.55	2.47	0.36	0.50	0.37	0.62
<b>Cs</b>	0.58	1.32	1.07	0.25	1.76	0.58	0.87	0.53
<b>Mg#</b>	58.93	45.83	64.51	20.80	59.01	43.40	65.30	20.61

Notes: —, not analyzed; N.D., not detected; negative numbers = detection limit; UTM co-ordinates in NAD27, Zone 17.

Appendix 3. Continued

Sample	98BRB0687	98BRB0688	98BRB0689	98BRB0696	98BRB0721	99BRB0793	99BRB798	99BRB0799	99BRB0802
Rock Type	Hornfels basalt	Pillowed basalt	Intermediate lapilli tuff	Massive basalt	Massive basalt	Massive basalt	Massive basalt	Pillowed basalt	Massive basalt
Township	Garrison	Garrison	Michaud	Michaud	Guibord	Guibord	Hislop	Hislop	Hislop
Easting (m)	577026	575827	571510	571890	559210	553650	545093	544539	550447
Northing (m)	5369777	5368293	5368575	5368090	5367999	5370571	5367850	5368523	5371268
SiO <sub>2</sub> (wt %)	53.96	53.03	64.55	54.19	48.60	48.99	49.26	52.72	50.63
Al <sub>2</sub> O <sub>3</sub>	12.96	15.36	16.40	13.10	14.45	14.53	13.88	13.31	14.00
MnO	0.25	0.14	0.04	0.20	0.20	0.21	0.25	0.24	0.21
MgO	3.17	6.86	1.76	3.15	6.14	7.01	4.97	4.35	6.89
CaO	6.02	8.57	2.43	5.49	7.51	6.92	7.68	8.38	5.25
Na <sub>2</sub> O	4.03	2.41	4.43	4.86	3.55	3.08	2.58	3.47	3.33
K <sub>2</sub> O	0.34	1.07	1.97	0.18	1.26	0.65	0.59	0.53	0.08
P <sub>2</sub> O <sub>5</sub>	0.42	0.07	0.12	0.39	0.14	0.07	0.35	0.34	0.08
TiO <sub>2</sub>	1.71	0.73	0.29	1.99	1.45	1.20	2.78	2.89	1.18
Fe <sub>2</sub> O <sub>3</sub>	17.60	8.85	3.24	13.35	14.48	14.93	17.58	13.34	15.00
LOI	0.14	2.79	3.73	3.26	2.60	3.33	1.12	0.85	4.55
TOTAL	100.60	99.88	98.96	100.16	100.38	100.92	101.04	100.42	101.20
CO <sub>2</sub>	0.14	0.34	0.99	1.28	3.10	—	—	—	—
S	0.15	0.10	0.05	0.19	0.04	—	—	—	—
As (ppm)	-3.5	-3.5	-3.5	-3.5	-3.5	-3.5	-3.5	-3.5	4.27
Cr	7	351	14	23	117	113	23	60	76
Ni	20	120	13	30	91	92	48	50	86
Nb	7.25	2.22	6.36	5.28	6.51	2.32	5.23	4.80	2.28
Rb	9.66	24.55	7.72	3.11	41.79	15.12	21.48	18.53	2.19
Ta	0.53	0.22	0.57	0.41	—	0.20	0.39	0.34	0.21
Th	0.72	0.46	0.64	0.45	1.58	0.23	0.50	0.37	0.25
U	0.16	0.13	0.18	0.12	0.41	0.07	0.13	0.11	0.07
Hf	2.85	1.64	2.80	2.47	—	1.65	3.44	3.05	1.90
Y	71	18	6	49	32.19	26.30	44.45	42.63	25.91
Zr	165	63	99	118	111.92	60.73	130.96	117.13	61.85
Be	-3	-3	—	-3	—	-3	3	3	-3
Co	25	48	6	33	6	48	46	47	47
Cu	44	122	9	93	18	148	49	36	63
Mo	—	—	—	—	-8	-8	-8	-8	-8
Sc	35	30	21.1	36	16	39	39	41	41
Sr	77.6	211.1	182.2	54.4	286.6	230	108	111	158
V	—	—	287	—	15	343	424	444	318
Zn	132	76	43	116	710	125	164	138	136
Ba	148	193	719	64	311	445	121	229	53
La	8.90	4.32	7.13	5.81	10.87	3.21	6.49	5.79	3.02
Ce	24.54	10.50	19.87	17.22	24.92	7.66	16.53	13.30	7.01
Pr	4.08	1.55	3.32	2.92	3.49	1.43	2.88	2.62	1.36
Nd	22.01	7.38	16.69	15.85	15.74	7.76	16.03	14.33	7.20
Sm	7.35	2.15	4.73	5.36	4.09	2.57	5.22	4.65	2.51
Eu	2.50	0.67	1.45	1.27	1.27	0.92	1.80	1.84	0.83
Gd	9.51	2.40	5.28	6.80	4.76	3.13	6.08	5.72	2.99
Tb	1.62	0.42	0.86	1.18	0.81	0.56	1.10	1.01	0.55
Dy	11.04	2.70	5.24	7.75	5.46	4.15	7.45	6.99	4.16
Ho	2.45	0.57	1.12	1.64	1.16	0.93	1.62	1.48	0.93
Er	7.08	1.63	2.86	4.64	3.51	2.72	4.66	4.26	2.68
Tm	1.04	0.23	0.43	0.64	0.52	0.43	0.78	0.72	0.46
Yb	6.72	1.51	2.88	4.11	3.37	2.39	4.30	4.05	2.60
Lu	1.05	0.23	0.39	0.56	0.51	0.39	0.67	0.63	0.40
Cs	0.43	0.26	1.24	0.87	0.90	0.88	0.72	0.34	0.20
Mg#	29.59	64.40	55.90	35.51	49.73	52.28	39.75	43.21	51.73

Notes: —, not analyzed; N.D., not detected; negative numbers = detection limit; UTM co-ordinates in NAD27, Zone 17.

Appendix 3. Continued

Sample	99BRB0807	99BRB0809	99BRB0825	99BRB0830	74J768	98BRB0J01	98BRB0J28	98BRBLH17
Rock Type	Intermediate crystal tuff	Intermediate tuff	Pillowed basalt	Massive basalt	Massive basalt	Variolitic flow	Massive felsic flow	Massive basalt
Township	Hislop	Hislop	Hislop	Hislop	Hislop	Holloway	Holloway	Holloway
Easting (m)	545350	545350	550958	550009	550225	593871	594489	595080
Northing (m)	5369183	5369183	5371100	5366430	5371478	5368116	5369395	5368676
SiO <sub>2</sub> (wt %)	56.62	64.89	49.52	46.93	49.37	60.60	75.92	47.77
Al <sub>2</sub> O <sub>3</sub>	16.27	14.72	14.67	15.36	13.58	11.75	10.66	14.00
MnO	0.11	0.07	0.20	0.20	0.21	0.17	0.03	0.20
MgO	6.03	3.51	6.28	7.92	9.61	1.93	0.22	8.08
CaO	6.39	4.37	6.55	8.90	7.99	5.23	1.72	9.54
Na <sub>2</sub> O	3.24	4.14	3.76	1.90	2.20	4.29	5.92	2.22
K <sub>2</sub> O	0.81	0.38	0.09	0.74	0.47	0.17	0.19	0.57
P <sub>2</sub> O <sub>5</sub>	0.15	0.23	0.06	0.08	0.05	0.52	0.02	0.06
TiO <sub>2</sub>	0.77	1.07	0.88	1.12	0.84	2.04	0.17	1.12
Fe <sub>2</sub> O <sub>3</sub>	7.21	4.86	11.35	14.44	12.90	11.87	3.66	13.83
LOI	3.02	2.04	7.36	3.53	3.97	1.56	1.70	3.16
TOTAL	100.62	100.28	100.72	101.12	101.19	100.13	100.21	100.55
CO <sub>2</sub>	—	—	—	—	—	0.41	1.34	0.28
S	—	—	—	—	—	0.45	0.09	0.02
As (ppm)	-3.5	-3.5	-3.5	-3.5	-3.5	-3.5	-3.5	-3.5
Cr	215	152	101	118	157	26	25	310
Ni	91	54	142	144	141	17	7	88
Nb	4.36	8.14	1.83	3.23	1.62	8.37	27.93	1.83
Rb	24.86	11.34	2.26	22.85	13.08	6.98	3.74	19.44
Ta	0.35	0.64	0.17	0.26	0.15	—	—	—
Th	1.96	4.14	0.20	0.34	0.17	0.60	2.78	0.14
U	0.48	0.96	0.07	0.09	0.06	0.16	0.82	0.04
Hf	2.97	5.96	1.43	2.06	1.35	3.87	12.30	1.00
Y	17.42	25.56	22.81	29.07	19.64	64.03	236.17	18.88
Zr	116.16	227.24	48.88	70.78	46.35	139.87	376.97	32.93
Be	-3	-3	-3	-3	-3	-3	-3	-3
Co	24	18	44	56	47	26	N.D.	46
Cu	5	25	137	95	101	33	N.D.	87
Mo	-8	-8	-8	-8	-8	-8	24	-8
Sc	20	14	42	31	40	37	2	47
Sr	296.5	289.7	92	126	85	103	25	125
V	156	150	278	293	264	143	25	389
Zn	126	62	108	124	106	83	27	90
Ba	284	175	42	111	92	113	36	155
La	13.06	24.10	2.61	4.36	2.26	9.18	30.67	1.96
Ce	30.30	56.96	5.83	8.74	5.14	25.45	82.65	5.46
Pr	3.90	7.06	1.18	1.78	1.01	4.21	12.38	0.92
Nd	17.32	30.51	6.17	9.06	5.53	22.27	57.07	4.87
Sm	3.57	6.01	2.11	2.91	1.84	7.38	15.10	1.65
Eu	1.06	1.46	0.78	0.90	0.69	2.76	2.28	0.67
Gd	3.18	5.26	2.68	3.31	2.30	9.38	13.85	2.27
Tb	0.50	0.79	0.49	0.65	0.42	1.57	2.30	0.40
Dy	2.80	4.31	3.66	4.53	3.12	9.88	15.53	2.69
Ho	0.58	0.90	0.83	1.04	0.69	2.14	3.53	0.61
Er	1.57	2.34	2.43	2.91	2.05	5.92	11.34	1.80
Tm	0.26	0.39	0.41	0.51	0.36	0.83	1.87	0.27
Yb	1.46	2.36	2.28	2.90	1.96	5.28	13.94	1.74
Lu	0.25	0.35	0.36	0.46	0.31	0.81	2.25	0.29
Cs	0.66	0.37	0.62	0.70	1.40	0.65	0.06	0.54
Mg#	66.12	62.76	56.35	56.14	63.48	27.50	12.30	57.68

Notes: —, not analyzed; N.D., not detected; negative numbers = detection limit; UTM co-ordinates in NAD27, Zone 17.

## **Appendix 4**

### **Geochemistry for Metasedimentary Rocks in the Highway 101 Area**



**Appendix 4.** Geochemistry for metasedimentary rocks in the Highway 101 area.

Sample	Porcupine Assemblage			Kinojevis Assemblage		Timiskaming Assemblage	
	98BRB0650	98BRB0708	98BRB0756	97BRB0580	98BRB0656	97BRB0544	97BRB0570
Rock Type	Wacke	Siltstone	Mudstone	Wacke	Black wacke	Sandstone	Sandstone
<b>Township</b>	Guibord	Guibord Hill	Guibord	Harker	Garrison	Harker	Garrison
<b>Easting (m)</b>	554559	557076	558984	585946	577222	591310	579719
<b>Northing (m)</b>	5375969	5372666	5374994	5371210	5367670	5374349	5374433
<b>SiO<sub>2</sub> (wt %)</b>	65.14	61.61	59.16	58.02	61.89	58.66	66.4
<b>Al<sub>2</sub>O<sub>3</sub></b>	15.02	17.48	17.99	19.21	16.95	14.49	13.49
<b>MnO</b>	0.06	0.07	0.02	0.05	0.07	0.07	0.04
<b>MgO</b>	2.90	2.43	4.06	4.26	2.90	5.05	2.07
<b>CaO</b>	1.89	2.46	0.56	0.96	2.76	2.69	1.61
<b>Na<sub>2</sub>O</b>	3.75	4.30	2.04	1.47	4.16	3.61	5.67
<b>K<sub>2</sub>O</b>	2.04	2.77	4.15	4.88	2.89	1.77	0.81
<b>P<sub>2</sub>O<sub>5</sub></b>	0.16	0.17	0.19	0.15	0.17	0.08	0.01
<b>TiO<sub>2</sub></b>	0.57	0.65	0.71	0.70	0.66	0.67	0.53
<b>Fe<sub>2</sub>O<sub>3</sub></b>	5.58	5.47	7.32	6.99	6.33	6.72	4.32
<b>LOI</b>	2.78	1.66	3.85	3.17	1.15	4.6	2.56
<b>TOTAL</b>	99.89	99.07	100.05	99.86	99.93	98.41	97.51
<b>CO<sub>2</sub></b>	0.78	0.28	0.43	0.17	0.27	1.7	1.2
<b>S</b>	0.25	N.D.	0.08	0.17	0.12	0.17	0.16
<b>As (ppm)</b>	19	N.D.	33	10	12	33	-6
<b>Cr</b>	217	178	258	230	188	280	130
<b>Ni</b>	91	9	136	123	95	100	57
<b>Nb</b>	5.49	7.09	4.44	6.38	6.98	5.79	3.00
<b>Rb</b>	66.95	106.67	145.19	146.00	117.32	49.82	39.44
<b>Ta</b>	—	—	—	N.D.	—	0.34	1.98
<b>Th</b>	5.04	5.51	6.43	7.59	5.49	5.10	3.27
<b>U</b>	1.46	1.51	1.78	2.23	1.50	1.39	0.79
<b>Hf</b>	3.05	3.32	3.43	—	3.30	3.72	2.67
<b>Y</b>	11.72	12.62	14.12	22	13.74	18	14
<b>Zr</b>	49.26	55.98	125.01	132	57.00	150	110
<b>Be</b>	ND	ND	N.D.	N.D.	N.D.	N.D.	N.D.
<b>Co</b>	23	N.D.	28	28	25	26	13
<b>Cu</b>	66	N.D.	81	52	53	42	19
<b>Mo</b>	9	N.D.	N.D.	10	9	-8	-8
<b>Sc</b>	13	2	20	21	16	1	9
<b>Sr</b>	377.6	462.7	142	145.00	403.9	325.0	304.1
<b>V</b>	114	22	156	156	131	130	77
<b>Zn</b>	89	45	266	96	103	98	64
<b>Ba</b>	554	477	1142	—	481	4	6
<b>La</b>	23.33	31.47	29.80	34.60	30.34	29.35	25.54
<b>Ce</b>	50.76	66.63	64.03	70.23	61.87	63.95	53.24
<b>Pr</b>	6.26	8.35	7.96	8.28	7.60	7.76	6.30
<b>Nd</b>	22.75	30.88	31.10	31.46	28.11	31.18	24.70
<b>Sm</b>	3.98	5.23	5.53	5.88	4.69	5.65	4.35
<b>Eu</b>	1.04	1.43	1.23	1.08	1.16	1.15	1.12
<b>Gd</b>	2.83	3.36	3.82	4.61	3.22	3.86	3.05
<b>Tb</b>	0.40	0.44	0.46	0.62	0.43	0.52	0.41
<b>Dy</b>	2.34	2.52	2.60	3.71	2.61	3.03	2.35
<b>Ho</b>	0.42	0.45	0.47	0.68	0.49	0.56	0.45
<b>Er</b>	1.24	1.31	1.39	2.02	1.41	1.59	1.34
<b>Tm</b>	0.17	0.18	0.20	0.27	0.20	0.21	0.18
<b>Yb</b>	1.14	1.09	1.32	1.81	1.24	1.37	1.23
<b>Lu</b>	0.18	0.17	0.22	0.28	0.19	0.22	0.19
<b>Cs</b>	3.92	11.77	5.88	5.18	9.52	0.80	1.16

Notes: —, not analyzed; N.D., not detected; negative numbers = detection limit; UTM co-ordinates in NAD27, Zone 17.

## Appendix 4. Continued

Sample	Timiskaming Assemblage						
	97BRB0571	97BRB0574	97BRB0578	97BRB0595	97BRB0606	97BRB0616	98BRB0663
Rock Type	Argillite	Sandstone	Wacke	Wacke	Wacke	Sandstone	Wacke
<b>Township</b>	Garrison	Holloway	Harker	Holloway	Marriott	Harker	Michaud
<b>Easting (m)</b>	579719	592588	585312	592700	608920	583408	571598
<b>Northing (m)</b>	5374433	5374753	5374984	5374972	5375787	5373985	5369875
<b>SiO<sub>2</sub> (wt %)</b>	57.79	62.23	61.21	61.77	64.39	66.8	62.61
<b>Al<sub>2</sub>O<sub>3</sub></b>	16.8	14.86	16.98	14.51	12.31	13.03	13.20
<b>MnO</b>	0.05	0.03	0.04	0.05	0.08	0.04	0.06
<b>MgO</b>	3.77	2.75	2.9	2.41	2.88	1.9	2.28
<b>CaO</b>	1.58	1.33	1.64	2.82	2.71	2.5	2.48
<b>Na<sub>2</sub>O</b>	4.25	4.76	0.69	6.9	3.63	8.12	1.64
<b>K<sub>2</sub>O</b>	1.84	0.95	4.88	0.02	1.27	N.D.	3.63
<b>P<sub>2</sub>O<sub>5</sub></b>	0.07	0.04	N.D.	N.D.	0.01	0.01	0.14
<b>TiO<sub>2</sub></b>	0.82	0.55	0.26	0.56	0.5	0.55	0.47
<b>Fe<sub>2</sub>O<sub>3</sub></b>	6.54	5.82	3.91	4.54	4.99	4.22	9.09
<b>LOI</b>	4.12	3.79	5.51	4.8	5.78	2.21	4.33
<b>TOTAL</b>	97.63	97.11	98.02	98.38	98.55	99.38	99.93
<b>CO<sub>2</sub></b>	1.1	1.8	2.3	3.9	4.2	1.7	1.88
<b>S</b>	0.05	0.3	-0.01	0.23	0.1	0.01	0.04
<b>As (ppm)</b>	-6	38	-6	-6	29	-6	N.D.
<b>Cr</b>	270	190	19	130	200	130	140
<b>Ni</b>	110	79	21	77	95	59	61
<b>Nb</b>	4.47	3.62	3.07	3.82	4.22	4.61	4.13
<b>Rb</b>	62.14	42.02	163.03	16.68	48.26	N.D.	126.17
<b>Ta</b>	0.45	0.28	0.23	0.26	0.64	0.21	—
<b>Th</b>	4.46	5.78	1.85	2.66	3.37	3.22	3.25
<b>U</b>	1.20	1.54	0.65	0.84	1.01	1.38	0.82
<b>Hf</b>	4.02	3.5	4.21	2.54	2.52	2.88	2.20
<b>Y</b>	21	15	11	17	16	15	8.96
<b>Zr</b>	150	140	130	98	98	120	37.26
<b>Be</b>	N.D.	N.D.	N.D.	N.D.	N.D.	N.D.	N.D.
<b>Co</b>	23	18	-5	17	19	15	14
<b>Cu</b>	24	56	-5	41	37	12	50
<b>Mo</b>	-8	-8	-8	-8	-8	-8	N.D.
<b>Sc</b>	16	12	4	10	12	9	11
<b>Sr</b>	239.5	308.7	155.7	191.5	438.5	372.6	135.4
<b>V</b>	130	96	32	75	90	88	98
<b>Zn</b>	110	89	59	90	53	53	63
<b>Ba</b>	3	-3	-3	5	8	-3	1204
<b>La</b>	31.21	30.36	10.29	19.00	18.62	20.74	19.80
<b>Ce</b>	68.18	63.39	25.32	43.03	49.10	46.80	41.46
<b>Pr</b>	8.46	7.42	3.32	5.47	4.72	5.70	5.26
<b>Nd</b>	34.72	27.98	14.11	22.45	19.10	23.13	19.93
<b>Sm</b>	6.28	4.67	2.68	4.31	3.63	4.33	3.58
<b>Eu</b>	1.62	1.18	0.62	1.18	0.95	1.14	0.73
<b>Gd</b>	4.27	2.88	1.88	2.86	2.66	3.03	2.47
<b>Tb</b>	0.54	0.35	N.D.	0.35	0.34	0.39	0.32
<b>Dy</b>	2.99	1.84	1.51	1.96	2.03	2.23	1.75
<b>Ho</b>	0.54	0.32	0.29	0.37	0.38	0.41	0.32
<b>Er</b>	1.58	0.97	0.82	1.13	1.12	1.18	0.98
<b>Tm</b>	0.23	0.15	0.12	0.17	0.17	0.17	0.14
<b>Yb</b>	1.59	0.99	0.78	1.21	1.17	1.06	0.90
<b>Lu</b>	0.24	0.16	0.12	0.19	0.19	0.16	0.14
<b>Cs</b>	2.00	1.55	3.16	0.66	0.97	N.D.	2.36

Notes: —, not analyzed; N.D., not detected; negative numbers = detection limit; UTM co-ordinates in NAD27, Zone 17.

## Appendix 4. Continued

Sample	Timiskaming Assemblage						
	98BRB0664	98BRB0725	98BRB0728	98BRB0730	99BRB0815	99BRB0827	99BRB0847
Rock Type	Wacke	Sandstone	Mudstone	Wacke	Siltstone	Siltstone	Altered siltstone
<b>Township</b>	Michaud	Guibord	Guibord	Guibord	Hislop	Hislop	Hislop
<b>Easting (m)</b>	571640	559584	559584	559584	550823	550548	552833
<b>Northing (m)</b>	5369758	5367924	5367924	5367924	5372790	5373311	5369574
<b>SiO<sub>2</sub> (wt %)</b>	63.49	67.79	43.38	62.37	61.23	63.54	46.28
<b>Al<sub>2</sub>O<sub>3</sub></b>	15.39	14.58	22.73	15.41	16.72	15.99	12.17
<b>MnO</b>	0.04	0.05	0.09	0.05	0.07	0.06	0.12
<b>MgO</b>	3.85	1.38	5.01	3.20	2.49	2.35	5.55
<b>CaO</b>	1.48	2.37	2.23	0.94	1.81	2.09	7.85
<b>Na<sub>2</sub>O</b>	5.39	4.17	3.58	6.99	3.18	1.98	0.92
<b>K<sub>2</sub>O</b>	1.20	1.75	3.34	0.09	3.11	3.57	4.44
<b>P<sub>2</sub>O<sub>5</sub></b>	0.12	0.11	0.27	0.12	0.17	0.19	0.32
<b>TiO<sub>2</sub></b>	0.64	0.52	1.00	0.74	0.62	0.53	0.45
<b>Fe<sub>2</sub>O<sub>3</sub></b>	4.79	4.13	11.92	6.13	5.49	4.32	6.73
<b>LOI</b>	3.53	3.36	6.12	2.46	4.67	5.33	14.75
<b>TOTAL</b>	99.92	100.21	99.67	98.50	99.56	99.95	99.58
<b>CO<sub>2</sub></b>	1.03	0.11	1.72	1.50	—	—	—
<b>S</b>	0.05	0.12	0.22	0.11	—	—	—
<b>As (ppm)</b>	N.D.	N.D.	N.D.	N.D.	26.37	7.92	16.90
<b>Cr</b>	124	138	247	150	185	148	307
<b>Ni</b>	97	91	71	156	81.00	61.00	61.00
<b>Nb</b>	5.35	3.06	8.06	5.70	5.31	4.56	3.40
<b>Rb</b>	29.91	46.04	102.58	1.05	98.90	97.96	116.64
<b>Ta</b>	—	—	—	—	0.42	0.36	0.25
<b>Th</b>	3.16	2.91	6.15	3.40	5.26	4.20	4.68
<b>U</b>	0.90	0.79	1.57	0.92	1.47	1.26	1.14
<b>Hf</b>	2.75	—	—	—	3.61	3.37	2.81
<b>Y</b>	11.33	11.11	22.55	16.04	15.56	12.68	17.72
<b>Zr</b>	46.35	95.66	172.27	120.17	136.52	133.25	110.91
<b>Be</b>	N.D.	N.D.	N.D.	N.D.	-3	-3	-3
<b>Co</b>	23	54	20	40	20.00	16.00	26.00
<b>Cu</b>	40	201	50	46	66.00	32.00	70.00
<b>Mo</b>	9	N.D.	N.D.	N.D.	-8	-8	-8
<b>Sc</b>	12	43	11	30	14	11	18
<b>Sr</b>	166.2	136.7	66.9	60.7	333.6	154.3	476.1
<b>V</b>	102	382	94	227	116	93	151
<b>Zn</b>	112	147	94	163	85	66	104
<b>Ba</b>	231	326	603	43	561	566	1968
<b>La</b>	23.77	22.46	38.97	19.98	30.53	26.07	29.24
<b>Ce</b>	51.64	47.74	82.76	43.37	66.62	58.44	62.86
<b>Pr</b>	6.59	6.00	10.36	5.72	7.58	6.66	7.53
<b>Nd</b>	25.68	23.54	40.80	22.97	29.92	26.64	30.69
<b>Sm</b>	4.86	4.24	7.59	4.47	5.08	4.44	5.72
<b>Eu</b>	1.22	1.12	1.91	1.16	1.32	1.02	1.86
<b>Gd</b>	3.45	3.00	5.38	3.64	4.07	3.43	4.82
<b>Tb</b>	0.42	0.35	0.67	0.49	0.53	0.49	0.67
<b>Dy</b>	2.31	2.15	4.22	3.00	2.70	2.27	3.03
<b>Ho</b>	0.41	0.40	0.79	0.56	0.51	0.44	0.58
<b>Er</b>	1.22	1.20	2.46	1.59	1.40	1.10	1.48
<b>Tm</b>	0.17	0.17	0.34	0.21	0.23	0.17	0.26
<b>Yb</b>	1.18	1.15	2.27	1.38	1.31	1.08	1.49
<b>Lu</b>	0.17	0.19	0.36	0.21	0.22	0.18	0.23
<b>Cs</b>	2.10	1.31	2.47	0.04	2.97	4.07	5.16

Notes: —, not analyzed; N.D., not detected; negative numbers = detection limit; UTM co-ordinates in NAD27, Zone 17.

## **Appendix 5**

### **Geochemistry for Alkalic Intrusive and Extrusive Rocks in the Highway 101 Area**

**Appendix 5.** Geochemistry for alkalic intrusive and extrusive rocks in the Highway 101 area.

Sample	97BRB0558	97BRB0564	97BRB0582	97BRB0587	97BRB0603	97BRB0604	97BRB0617	97BRB0620	97BRB0635
Rock Type	Syenite	Basalt-andesite	Alkalic flow-intrusion?	Alkalic flow	Granite dike	Monzonite dike	Gabbro	Albitite	Basalt
<b>Township</b>	Harker	Harker	Harker	Garrison	Garrison	Garrison	Harker	Harker	Harker
<b>Easting (m)</b>	590398	585056	584114	578581	577526	577526	583408	583881	585586
<b>Northing (m)</b>	5367399	5374316	5375992	5373688	5369611	5369611	5373984	5373987	5374439
<b>SiO<sub>2</sub> (wt %)</b>	64.92	52.04	49.66	65.25	67.4	53.65	46.12	65.01	52.55
<b>Al<sub>2</sub>O<sub>3</sub></b>	17.87	11.55	13.57	14.47	15.03	14.26	13.21	18.2	10.95
<b>MnO</b>	N.D.	0.22	0.09	0.04	0.04	0.11	0.14	N.D.	0.18
<b>MgO</b>	0.1	3.45	8.39	1.67	0.51	5.69	10.41	0.11	3.11
<b>CaO</b>	0.16	5.78	5.56	1.55	1.42	5.44	8.19	0.53	4.37
<b>Na<sub>2</sub>O</b>	9.02	5.97	2.35	7.06	5.32	3.68	4.53	11.53	7.23
<b>K<sub>2</sub>O</b>	2.84	N.D.	4.12	1.23	4.56	3.83	0.92	0	0.08
<b>P<sub>2</sub>O<sub>5</sub></b>	N.D.	0.29	0.5	N.D.	N.D.	0.29	0.33	N.D.	0.32
<b>TiO<sub>2</sub></b>	0.11	1.96	0.76	0.45	0.22	0.76	0.67	0.09	2.01
<b>Fe<sub>2</sub>O<sub>3</sub></b>	1.52	17.14	9.76	3.91	2.05	7.63	8.84	0.97	17.24
<b>LOI</b>	0.6	0.2	3.56	2.75	1.06	3.28	5.70	0.79	0.4
<b>TOTAL</b>	97.14	98.6	98.32	98.38	97.61	98.62	99.06	97.23	98.44
<b>CO<sub>2</sub></b>	0.16	0.24	0.63	2	0.56	1.6	3.05	0.51	0.62
<b>S</b>	0.01	0.41	-0.01	0.23	0.01	0.02	0.03	0.48	0.39
<b>As (ppm)</b>	-6	-6	8	-6	-6	-6	-6	-6	-6
<b>Cr</b>	6	8	360	82	19	280	651	7	12
<b>Ni</b>	6	29	110	53	10	54	284	-5	28
<b>Nb</b>	2.21	6.98	7.97	1.65	8.48	7.66	4.72	3.44	7.22
<b>Rb</b>	32.01	14.95	97.72	27.88	150.17	114.17	19	3.55	15.91
<b>Ta</b>	0.23	0.44	0.64	0.18	0.47	0.55	N.D.	0.14	0.45
<b>Th</b>	6.51	0.59	7.24	2.86	16.11	4.47	6.24	26.82	0.62
<b>U</b>	2.64	0.22	2.18	0.83	3.05	1.58	1.07	8.44	2.68
<b>Hf</b>	3.8	2.37	4.8	2.5	4.62	3.91	—	7.9	3.62
<b>Y</b>	8	53	23	14	9	19	18	10	53
<b>Zr</b>	120	130	170	100	160	140	114	370	120
<b>Be</b>	N.D.	N.D.	N.D.	N.D.	N.D.	N.D.	N.D.	N.D.	N.D.
<b>Co</b>	-5	29	37	15	-5	27	41	-5	28
<b>Cu</b>	-5	45	9	17	-5	44	98	150	45
<b>Mo</b>	-8	18	-8	-8	-8	-8	N.D.	-8	-8
<b>Sc</b>	-1	36	26	8	3	17	22	-1	37
<b>Sr</b>	558.3	148.9	460.4	262.6	1051.6	584.7	660	216.5	213.3
<b>V</b>	18	170	190	69	30	140	169	8	210
<b>Zn</b>	11	110	110	54	40	94	81	8	160
<b>Au (ppb)</b>	4	5	-3	—	6	-3	4	10	10
<b>Ba</b>	—	—	—	-3	—	—	—	—	—
<b>Ag</b>	—	—	—	—	—	—	—	—	—
<b>La</b>	9.66	7.47	58.36	18.98	51.04	32.21	50.4	30.54	17.83
<b>Ce</b>	15.15	21.86	>250	41.24	122.64	70.04	106.14	48.88	37.88
<b>Pr</b>	1.48	3.57	16.33	5.08	9.97	8.94	12.78	4.52	4.91
<b>Nd</b>	5.03	19.62	66.21	19.86	35.76	37.47	49.86	14.49	22.75
<b>Sm</b>	0.88	6.41	11.61	3.48	5.45	7.25	8.56	2.20	6.39
<b>Eu</b>	N.D.	2.12	2.64	0.90	0.90	1.88	1.79	0.51	2.21
<b>Gd</b>	0.73	7.93	7.62	2.15	3.32	5.23	6.03	1.27	7.59
<b>Tb</b>	N.D.	1.37	0.94	N.D.	0.38	0.67	0.7	N.D.	1.31
<b>Dy</b>	0.78	9.19	5.03	1.40	1.98	3.56	3.98	1.17	8.67
<b>Ho</b>	N.D.	2.03	0.85	0.27	0.29	0.64	0.62	0.25	1.89
<b>Er</b>	0.60	5.70	2.32	0.83	0.82	1.73	1.9	0.90	5.44
<b>Tm</b>	0.10	0.82	0.29	0.12	0.10	0.23	0.22	0.16	0.80
<b>Yb</b>	0.83	5.39	1.86	0.85	0.69	1.47	1.52	1.30	5.18
<b>Lu</b>	0.12	0.81	0.27	0.14	0.11	0.22	0.22	0.20	0.78
<b>Cs</b>	0.22	0.97	0.99	0.30	3.09	1.48	1	N.D.	0.44
<b>Mg#</b>	13.31	31.96	66.73	49.91	36.73	63.50	73.32	20.92	29.62

Notes: —, not analyzed; N.D., not detected; negative numbers = detection limit; UTM co-ordinates in NAD27, Zone 17.

Appendix 5. Continued

Sample	97BRB0640	97BRB0646	98BRB0655	98BRB0658	98BRB0660	98BRB0667	98BRB0668	98BRB0670
Rock Type	Gabbro	Hornblende	Granite	Diorite	Hornblende-lamprophyre	Altered albitite	Albitite	Quartz monzonite
<b>Township</b>	Garrison	Harker	Garrison	Michaud	Michaud	Michaud	Michaud	Michaud
<b>Easting (m)</b>	580539	589932	577429	570725	566690	567915	567915	568026
<b>Northing (m)</b>	5373586	5366992	5369867	5374750	5368523	5369329	5369329	5369032
<b>SiO<sub>2</sub> (wt %)</b>	47.79	45.01	66.54	51.28	46.99	66.18	65.50	64.81
<b>Al<sub>2</sub>O<sub>3</sub></b>	13.55	11.41	16.11	13.93	8.81	15.83	16.01	15.46
<b>MnO</b>	0.16	0.21	0.04	0.20	0.12	0.04	0.05	0.05
<b>MgO</b>	6.21	10.17	0.76	5.13	17.29	0.77	0.76	0.75
<b>CaO</b>	8.34	9.65	1.72	7.52	5.41	1.67	1.72	1.67
<b>Na<sub>2</sub>O</b>	5.44	2.69	5.60	4.09	2.27	5.32	9.38	6.48
<b>K<sub>2</sub>O</b>	2.42	0.63	4.44	0.17	4.24	4.44	0.23	4.05
<b>P<sub>2</sub>O<sub>5</sub></b>	0.39	0.04	0.11	0.10	0.50	0.10	0.18	0.11
<b>TiO<sub>2</sub></b>	0.62	1.98	0.23	1.07	0.43	0.21	0.26	0.22
<b>Fe<sub>2</sub>O<sub>3</sub></b>	9.05	15.36	1.99	14.49	7.20	1.94	1.53	2.22
<b>LOI</b>	4.14	1.64	1.06	2.48	5.59	2.78	1.87	1.63
<b>TOTAL</b>	98.11	98.79	98.60	100.46	98.85	99.28	97.49	97.45
<b>CO<sub>2</sub></b>	3.1	0.2	0.78	0.27	1.88	1.03	0.11	1.72
<b>S</b>	0.47	-0.01	0.25	0.12	0.04	0.05	0.12	0.22
<b>As (ppm)</b>	-6	-6	-6	-6	-6	-6	-6	-6
<b>Cr</b>	150	380	2	20	1557	27	22	21
<b>Ni</b>	54	140	8	33	585	9	7	6
<b>Nb</b>	4.72	4.64	6.65	3.10	3.96	2.64	3.61	11.06
<b>Rb</b>	106.21	12.93	126.09	3.36	166.30	104.25	163.58	239.99
<b>Ta</b>	0.24	0.24	0.83	1.53	0.57	0.29	0.17	0.83
<b>Th</b>	7.58	1.56	9.79	0.74	9.02	4.01	4.42	8.91
<b>U</b>	2.40	0.32	3.59	0.19	3.35	1.61	0.60	1.06
<b>Hf</b>	3.43	3.06	4.10	2.36	3.06	2.90	2.82	5.26
<b>Y</b>	21	41	8	25	17	8	11	9
<b>Zr</b>	130	94	167	86	123	112	122	126
<b>Be</b>	N.D.	N.D.	N.D.	N.D.	N.D.	N.D.	N.D.	N.D.
<b>Co</b>	30	51	N.D.	46	48	N.D.	N.D.	N.D.
<b>Cu</b>	49	38	N.D.	70	6	29	N.D.	7
<b>Mo</b>	-8	-8	N.D.	N.D.	N.D.	N.D.	N.D.	N.D.
<b>Sc</b>	23	58	5.6	36.3	23.6	4.7	28.5	21.0
<b>Sr</b>	1073.1	340.5	1158.8	89.0	269.0	532.9	1906.8	>3000
<b>V</b>	200	440	40	306	178	54	224	339
<b>Zn</b>	83	110	49	85	84	37	22	33
<b>Au (ppb)</b>	11	5	—	—	—	—	—	—
<b>Ba</b>	—	—	1654	65	2013	1239	2519	1595
<b>Ag</b>	—	—	2	3	3	2	2	2
<b>La</b>	38.64	13.92	42.70	7.18	48.22	23.94	133.94	>250
<b>Ce</b>	85.55	38.99	81.92	17.04	110.44	45.89	>250	>250
<b>Pr</b>	10.81	6.31	9.39	2.40	13.99	5.38	38.26	51.67
<b>Nd</b>	46.63	32.09	32.96	11.04	57.86	19.18	157.79	194.30
<b>Sm</b>	9.87	8.63	5.26	2.94	10.14	3.05	26.33	33.53
<b>Eu</b>	2.39	2.26	1.62	0.95	2.82	1.04	6.07	8.84
<b>Gd</b>	7.14	8.20	3.83	3.52	7.28	2.17	16.64	24.57
<b>Tb</b>	0.89	1.24	0.47	0.60	0.92	0.28	1.90	3.02
<b>Dy</b>	4.75	7.50	1.89	3.80	3.42	1.14	6.43	10.46
<b>Ho</b>	0.81	1.57	0.33	0.86	0.58	0.19	1.05	1.61
<b>Er</b>	2.04	4.23	0.73	2.42	1.24	0.53	2.31	3.26
<b>Tm</b>	0.28	0.61	0.10	0.35	0.17	0.08	0.28	0.38
<b>Yb</b>	1.75	3.70	0.76	2.30	1.22	0.64	1.92	2.58
<b>Lu</b>	0.27	0.56	0.12	0.35	0.15	0.10	0.28	0.35
<b>Cs</b>	14.37	0.16	2.23	0.55	11.18	0.73	4.75	14.64
<b>Mg#</b>	61.55	60.71	47.12	45.24	84.86	48.08	53.68	44.08

Notes: —, not analyzed; N.D., not detected; negative numbers = detection limit; UTM co-ordinates in NAD27, Zone 17.

Appendix 5. Continued

Sample	98BRB0672	98BRB0673	98BRB0675	98BRB0678	98BRB0684	98BRB0697	98BRB0700	98BRB0735	98BRB0740
Rock Type	Syenite	Hornblende syenite	Diorite- lamprophyre	Diorite	Hornblendite	Granite	Intermineral dike	Granite	Granite
Township	Michaud	Michaud	Michaud	Michaud	Harker	Guibord	Holloway	Guibord	Guibord
Easting (m)	570101	570101	569608	569097	588044	559617	592488	562614	561914
Northing (m)	5371093	5371093	5371245	5372033	5373082	5370796	5374873	5367953	5368464
<b>SiO<sub>2</sub> (wt %)</b>	62.00	47.04	44.34	45.86	38.19	66.08	30.32	69.78	70.11
<b>Al<sub>2</sub>O<sub>3</sub></b>	18.20	15.89	10.51	14.19	9.93	15.89	10.46	14.58	15.55
<b>MnO</b>	0.04	0.18	0.18	0.22	0.26	0.04	0.20	0.02	0.02
<b>MgO</b>	0.49	2.72	9.36	4.25	10.57	1.03	8.34	0.36	0.55
<b>CaO</b>	1.37	7.19	11.25	9.41	12.22	2.14	13.39	1.14	1.55
<b>Na<sub>2</sub>O</b>	4.55	5.28	2.69	2.26	2.06	5.63	3.07	5.98	5.72
<b>K<sub>2</sub>O</b>	9.07	4.55	4.12	6.35	0.99	3.49	1.28	3.98	3.54
<b>P<sub>2</sub>O<sub>5</sub></b>	0.04	0.47	1.00	0.86	0.34	0.13	0.36	0.08	0.09
<b>TiO<sub>2</sub></b>	0.20	0.83	0.85	1.40	2.91	0.26	0.65	0.18	0.23
<b>Fe<sub>2</sub>O<sub>3</sub></b>	1.63	7.19	9.10	10.68	20.79	2.03	8.85	1.09	1.31
<b>LOI</b>	0.75	5.92	4.96	1.83	0.82	1.71	21.58	1.28	0.73
<b>TOTAL</b>	98.34	97.26	98.36	97.31	99.08	98.43	98.50	98.47	99.40
<b>CO<sub>2</sub></b>	1.50	0.32	0.22	0.24	1.44	2.15	0.28	0.24	0.99
<b>S</b>	0.11	0.12	0.14	0.04	N.D.	0.09	N.D.	0.04	0.05
<b>As (ppm)</b>	-6	-6	-6	-6	-6	-6	46	-6	-6
<b>Cr</b>	14	48	430	21	160	29	299	18	9
<b>Ni</b>	9	28	145	18	116	12	106	12	12
<b>Nb</b>	9.15	2.72	2.67	5.06	2.07	4.35	13.12	4.55	4.08
<b>Rb</b>	6.73	56.94	4.20	89.76	68.76	198.92	40.80	64.92	103.30
<b>Ta</b>	0.54	0.30	0.32	0.40	0.28	0.32	0.68	—	—
<b>Th</b>	0.97	2.49	5.72	7.06	5.34	5.53	3.04	5.49	6.11
<b>U</b>	0.19	0.88	2.21	2.14	2.45	1.78	0.43	1.83	2.03
<b>Hf</b>	5.12	2.02	3.98	3.56	3.55	3.06	1.45	—	—
<b>Y</b>	5	31	26	30	76	7	31	3.45	3.52
<b>Zr</b>	111	203	143	225	151	134	82	98.62	127.06
<b>Be</b>	N.D.	N.D.	N.D.	N.D.	N.D.	N.D.	—	N.D.	N.D.
<b>Co</b>	N.D.	18	41	31	68	N.D.	35	92	N.D.
<b>Cu</b>	9	75	19	118	247	N.D.	79	19	191
<b>Mo</b>	N.D.	N.D.	N.D.	N.D.	N.D.	N.D.	—	N.D.	N.D.
<b>Sc</b>	76.0	5.5	4.6	5.1	4.8	4.2	20.5	28	2
<b>Sr</b>	669.3	370.2	1371.2	933.2	1155.8	>3000	1193.4	468.1	1235.9
<b>V</b>	>350	58	27	54	45	68	169	198	19
<b>Zn</b>	42	142	161	287	167	47	125	82	20
<b>Au (ppb)</b>	—	—	—	—	—	—	—	—	—
<b>Ba</b>	2303	3992	2305	4007	528	1559	322	1695	1458
<b>Ag</b>	2	3	3	4	4	2	3	—	—
<b>La</b>	36.64	11.60	21.37	34.64	24.44	34.78	55.21	25.98	30.03
<b>Ce</b>	103.97	24.39	46.98	64.62	48.02	72.30	113.48	48.04	56.45
<b>Pr</b>	16.28	3.11	5.93	7.63	5.58	8.52	14.79	5.50	6.28
<b>Nd</b>	76.87	12.00	21.85	26.89	19.59	30.55	57.10	19.37	21.93
<b>Sm</b>	18.20	2.31	3.77	4.25	3.30	4.82	9.18	2.82	3.16
<b>Eu</b>	4.83	0.80	1.48	1.41	1.10	1.83	2.31	0.62	0.73
<b>Gd</b>	16.93	1.64	2.91	3.00	2.32	3.69	7.26	1.52	1.69
<b>Tb</b>	2.64	0.22	0.37	0.37	0.29	0.47	0.97	0.15	0.17
<b>Dy</b>	13.85	0.90	1.36	1.35	1.16	1.96	4.34	0.88	0.90
<b>Ho</b>	3.03	0.17	0.26	0.25	0.22	0.33	0.87	0.10	0.11
<b>Er</b>	7.63	0.41	0.77	0.58	0.60	0.86	2.20	0.36	0.34
<b>Tm</b>	1.08	0.07	0.11	0.09	0.09	0.13	0.31	0.03	0.03
<b>Yb</b>	6.69	0.41	0.74	0.60	0.68	0.94	2.13	0.27	0.24
<b>Lu</b>	0.96	0.06	0.13	0.09	0.11	0.13	0.27	0.04	0.03
<b>Cs</b>	0.09	1.10	0.10	3.05	0.42	2.75	1.70	0.38	2.08
<b>Mg#</b>	41.23	46.89	70.59	48.15	54.26	54.21	68.74	43.52	49.49

Notes: —, not analyzed; N.D., not detected; negative numbers = detection limit; UTM co-ordinates in NAD27, Zone 17.

Appendix 5. Continued

Sample	98BRB0748	98BRB0749	98BRB0758	98BRB0760	98BRB0763	98BRB0777	98BRB0779	98BRB0782
Rock Type	Hornblende	Lamprophyre	Mafic flow	Monzonite	Alkalic mafic flow	Syenite	Bleached syenite	Alkalic breccia
<b>Township</b>	Guibord	Guibord	Guibord	Guibord	Guibord	Michaud	Michaud	Guibord
<b>Easting (m)</b>	558780	558780	560341	560206	560206	566915	566915	560341
<b>Northing (m)</b>	5375197	5375197	5374580	5374096	5374096	5370432	5370432	5374580
<b>SiO<sub>2</sub> (wt %)</b>	37.71	43.91	48.50	49.67	53.96	64.89	65.75	54.76
<b>Al<sub>2</sub>O<sub>3</sub></b>	8.36	9.11	14.91	15.64	14.19	17.16	17.96	19.23
<b>MnO</b>	0.55	0.15	0.16	0.24	0.17	0.03	0.04	0.13
<b>MgO</b>	6.86	19.96	5.37	3.44	6.02	0.42	0.11	2.45
<b>CaO</b>	12.86	7.93	8.68	8.34	8.75	0.62	0.55	3.50
<b>Na<sub>2</sub>O</b>	1.02	1.59	2.98	4.44	3.26	7.96	9.29	2.37
<b>K<sub>2</sub>O</b>	2.36	1.61	4.41	2.92	2.63	4.56	2.86	8.27
<b>P<sub>2</sub>O<sub>5</sub></b>	0.59	0.06	0.92	0.63	0.07	0.05	0.09	0.20
<b>TiO<sub>2</sub></b>	5.01	0.52	1.03	1.38	0.73	0.18	0.11	0.66
<b>Fe<sub>2</sub>O<sub>3</sub></b>	23.85	11.02	9.17	10.19	8.25	1.45	1.42	5.07
<b>LOI</b>	0.4	2.56	2.37	2.38	2	0.75	0.67	2.73
<b>TOTAL</b>	99.57	98.42	98.50	99.27	100.03	98.07	98.85	99.37
<b>CO<sub>2</sub></b>	0.25	0.23	1.19	0.28	0.83	0.46	0.45	0.90
<b>S</b>	0.33	0.45	0.04	0.05	N.D.	0.05	0.08	0.06
<b>As (ppm)</b>	12	7	10	-6	N.D.	-6	-6	6
<b>Cr</b>	226	1973	45	34	155	14	11	68
<b>Ni</b>	214	921	27	107	75	8	N.D.	44
<b>Nb</b>	46.50	1.51	10.64	13.78	2.28	4.39	5.28	18.06
<b>Rb</b>	124.58	58.05	160.30	53.32	103.61	84.03	55.26	240.95
<b>Ta</b>	—	—	—	—	—	—	—	—
<b>Th</b>	15.65	1.03	17.39	16.61	0.52	2.93	20.18	23.75
<b>U</b>	2.68	0.26	4.08	3.09	0.13	1.08	2.75	5.94
<b>Hf</b>	11.58	1.23	6.22	8.46	1.31	1.86	2.25	7.66
<b>Y</b>	94.84	13.27	39.41	54.03	18.24	7.34	12.35	40.33
<b>Zr</b>	428.82	47.28	266.45	331.73	43.96	69.01	74.10	346.94
<b>Be</b>	7	N.D.	5	N.D.	N.D.	N.D.	4	5
<b>Co</b>	116	75	30	48	40	N.D.	N.D.	12
<b>Cu</b>	231	73	117	51	8	11	31	60
<b>Mo</b>	N.D.	N.D.	N.D.	8	N.D.	11	13	10
<b>Sc</b>	68	27	23	34	33	2	1	6
<b>Sr</b>	1166	174	2544	166	704	707	211	1972
<b>V</b>	690	195	265	222	235	36	57	151
<b>Zn</b>	379	57	128	70	59	28	41	121
<b>Au (ppb)</b>	—	—	—	—	—	—	—	—
<b>Ba</b>	1581	194	2438	2101	922	1490	718	3447
<b>Ag</b>	—	—	—	—	—	—	—	—
<b>La</b>	235.55	5.54	122.39	141.20	4.94	19.13	>250	120.87
<b>Ce</b>	>250	10.60	>250	>250	11.63	45.55	>250	>250
<b>Pr</b>	53.16	1.30	32.53	38.73	1.65	5.62	35.60	27.57
<b>Nd</b>	191.53	5.64	130.15	158.04	7.68	20.91	105.79	101.81
<b>Sm</b>	31.58	1.47	23.40	29.92	2.18	3.70	11.73	18.13
<b>Eu</b>	8.15	0.51	5.40	7.24	0.71	0.81	2.39	3.10
<b>Gd</b>	22.97	1.80	15.70	20.72	2.61	2.26	5.94	11.84
<b>Tb</b>	3.06	0.30	1.68	2.32	0.43	0.26	0.52	1.44
<b>Dy</b>	17.52	1.99	8.55	11.84	2.75	1.32	2.81	7.36
<b>Ho</b>	3.12	0.44	1.23	1.78	0.60	0.22	0.31	1.15
<b>Er</b>	8.62	1.24	3.26	4.64	1.73	0.61	1.20	3.21
<b>Tm</b>	1.07	0.18	0.35	0.51	0.25	0.07	0.12	0.39
<b>Yb</b>	6.30	1.20	2.13	3.20	1.61	0.45	0.68	2.32
<b>Lu</b>	0.91	0.20	0.31	0.48	0.25	0.07	0.10	0.33
<b>Cs</b>	5.05	11.00	8.85	0.42	0.87	0.52	0.40	2.11
<b>Mg#</b>	40.16	80.87	57.74	44.06	63.00	40.33	15.31	53.00

Notes: —, not analyzed; N.D., not detected; negative numbers = detection limit; UTM co-ordinates in NAD27, Zone 17.



Appendix 5. Continued

Sample	99BRB0797	99BRB0801	99BRB0803	99BRB0806	99BRB0842	99BRB0846	99BRB0848	HISLOP
Rock Type	Quartz syenite	Hornblende syenite	Feldspar porphyry	Intermediate flow	Alkalic flow breccia	Hornblende syenite	Mauve syenite	Alkalic flow breccia
Township	Hislop	Hislop	Hislop	Hislop	Hislop	Hislop	Hislop	Hislop
Easting (m)	544099	545617	552911	552911	552126	550823	552634	552079
Northing (m)	5366966	5366989	5369572	5369572	5366443	5372790	5371354	5366399
SiO <sub>2</sub> (wt %)	65.12	63.27	60.27	47.68	57.14	49.37	62.86	56.86
Al <sub>2</sub> O <sub>3</sub>	17.31	17.15	16.46	12.48	16.52	16.52	21.13	15.96
MnO	0.05	0.07	0.15	0.22	0.10	0.13	N.D.	0.11
MgO	1.05	1.71	4.62	8.93	4.02	4.29	0.21	3.90
CaO	2.41	2.54	2.34	8.05	2.35	5.44	0.06	3.39
Na <sub>2</sub> O	6.86	8.53	3.80	4.92	4.80	3.46	7.75	4.45
K <sub>2</sub> O	2.45	0.75	3.05	0.17	4.07	4.83	4.89	2.98
P <sub>2</sub> O <sub>5</sub>	0.10	0.12	0.14	0.37	0.27	0.47	0.01	0.28
TiO <sub>2</sub>	0.25	0.36	0.35	0.73	0.58	0.69	0.08	0.57
Fe <sub>2</sub> O <sub>3</sub>	2.36	3.41	3.86	9.92	6.39	8.30	1.06	6.59
LOI	1.34	1.35	4.30	6.05	3.53	6.04	1.29	4.42
TOTAL	99.30	99.26	99.34	99.52	99.77	99.54	99.34	99.51
CO <sub>2</sub>	—	—	—	—	—	—	—	1.79
S	—	—	—	—	—	—	—	N.D.
As (ppm)	-3.5	-3.5	13.85	37.58	6.91	7.79	-3.5	12
Cr	20	26	80	365	115	78	28	104
Ni	11	16	42	93	35	31	50	32
Nb	4.63	4.78	5.93	3.12	5.62	7.27	3.47	5.70
Rb	50.05	18.97	67.77	1.99	69.49	136.78	66.59	83.01
Ta	0.29	0.34	0.36	0.22	0.36	0.46	0.24	0.40
Th	2.38	3.10	2.51	3.81	10.59	10.05	17.90	9.31
U	0.70	0.78	0.72	1.21	2.53	2.49	5.03	2.51
Hf	2.75	3.23	2.78	2.46	4.10	4.90	7.16	4.16
Y	6.74	8.48	8.72	21.22	17.04	30.32	5.64	17
Zr	107.64	126.03	107.81	95.09	166.89	204.51	365.95	159
Be	-3	-3	-3	3	-3	3	4	N.D.
Co	5	8	8	36	19	24	-5	19
Cu	-5	-5	110	15	21	57	31	24
Mo	-8	-8	-8	-8	-8	-8	-8	—
Sc	3	5	6	26	13	14	N.D.	14
Sr	916.5	880.5	96	406.0	1128.8	1856.7	565.9	990.3
V	42	66	82	204	134	185	99	—
Zn	52	62	216	117	88	129	26	80
Au (ppb)	—	—	—	—	—	—	—	—
Ba	1192	529	318	2826	3035	1961	830	1811
Ag	—	—	—	—	—	—	—	3
La	14.56	20.37	19.85	25.56	52.92	79.09	6.85	51.93
Ce	31.70	44.29	39.69	52.70	107.14	169.45	16.07	100.56
Pr	3.48	4.70	5.12	7.05	11.56	19.85	1.61	11.64
Nd	13.66	18.92	20.05	30.42	44.19	79.82	5.72	44.02
Sm	2.33	3.16	3.39	5.88	7.37	13.69	0.90	7.38
Eu	0.84	0.90	0.90	2.12	2.37	3.56	0.41	1.69
Gd	1.71	2.24	2.43	5.05	5.33	10.15	0.69	4.69
Tb	0.23	0.31	0.33	0.70	0.69	1.31	0.12	0.58
Dy	1.06	1.41	1.57	3.69	3.02	5.55	0.63	3.33
Ho	0.20	0.26	0.31	0.75	0.59	0.99	0.14	0.55
Er	0.56	0.75	0.86	1.96	1.54	2.53	0.51	1.70
Tm	0.10	0.14	0.14	0.32	0.24	0.40	0.10	0.22
Yb	0.67	0.85	0.88	1.93	1.71	2.42	0.69	1.51
Lu	0.10	0.13	0.14	0.29	0.24	0.35	0.13	0.23
Cs	0.23	0.27	1.82	0.26	1.39	4.92	0.36	1.76
Mg#	50.94	53.92	73.63	67.75	59.48	54.67	31.61	58.00

Notes: —, not analyzed; N.D., not detected; negative numbers = detection limit; UTM co-ordinates in NAD27, Zone 17.

# Metric Conversion Table

Conversion from SI to Imperial			Conversion from Imperial to SI		
<i>SI Unit</i>	<i>Multiplied by</i>	<i>Gives</i>	<i>Imperial Unit</i>	<i>Multiplied by</i>	<i>Gives</i>
<b>LENGTH</b>					
1 mm	0.039 37	inches	1 inch	<b>25.4</b>	mm
1 cm	0.393 70	inches	1 inch	<b>2.54</b>	cm
1 m	3.280 84	feet	1 foot	<b>0.304 8</b>	m
1 m	0.049 709	chains	1 chain	20.116 8	m
1 km	0.621 371	miles (statute)	1 mile (statute)	<b>1.609 344</b>	km
<b>AREA</b>					
1 cm <sup>2</sup>	0.155 0	square inches	1 square inch	<b>6.451 6</b>	cm <sup>2</sup>
1 m <sup>2</sup>	10.763 9	square feet	1 square foot	<b>0.092 903 04</b>	m <sup>2</sup>
1 km <sup>2</sup>	0.386 10	square miles	1 square mile	2.589 988	km <sup>2</sup>
1 ha	2.471 054	acres	1 acre	0.404 685 6	ha
<b>VOLUME</b>					
1 cm <sup>3</sup>	0.061 023	cubic inches	1 cubic inch	<b>16.387 064</b>	cm <sup>3</sup>
1 m <sup>3</sup>	35.314 7	cubic feet	1 cubic foot	0.028 316 85	m <sup>3</sup>
1 m <sup>3</sup>	1.307 951	cubic yards	1 cubic yard	0.764 554 86	m <sup>3</sup>
<b>CAPACITY</b>					
1 L	1.759 755	pints	1 pint	0.568 261	L
1 L	0.879 877	quarts	1 quart	1.136 522	L
1 L	0.219 969	gallons	1 gallon	<b>4.546 090</b>	L
<b>MASS</b>					
1 g	0.035 273 962	ounces (avdp)	1 ounce (avdp)	28.349 523	g
1 g	0.032 150 747	ounces (troy)	1 ounce (troy)	<b>31.103 476 8</b>	g
1 kg	2.204 622 6	pounds (avdp)	1 pound (avdp)	<b>0.453 592 37</b>	kg
1 kg	0.001 102 3	tons (short)	1 ton (short)	<b>907.184 74</b>	kg
1 t	1.102 311 3	tons (short)	1 ton (short)	<b>0.907 184 74</b>	t
1 kg	0.000 984 21	tons (long)	1 ton (long)	<b>1016.046 908 8</b>	kg
1 t	0.984 206 5	tons (long)	1 ton (long)	<b>1.016 046 90</b>	t
<b>CONCENTRATION</b>					
1 g/t	0.029 166 6	ounce (troy)/ ton (short)	1 ounce (troy)/ ton (short)	34.285 714 2	g/t
1 g/t	0.583 333 33	pennyweights/ ton (short)	1 pennyweight/ ton (short)	1.714 285 7	g/t

## OTHER USEFUL CONVERSION FACTORS

	<i>Multiplied by</i>	
1 ounce (troy) per ton (short)	31.103 477	grams per ton (short)
1 gram per ton (short)	0.032 151	ounces (troy) per ton (short)
1 ounce (troy) per ton (short)	20.0	pennyweights per ton (short)
1 pennyweight per ton (short)	0.05	ounces (troy) per ton (short)

*Note: Conversion factors which are in bold type are exact. The conversion factors have been taken from or have been derived from factors given in the Metric Practice Guide for the Canadian Mining and Metallurgical Industries, published by the Mining Association of Canada in co-operation with the Coal Association of Canada.*



**ISSN 0826-9580**  
**ISBN 0-7794-3278-9**

